Development of Smart Thickening Fluid based Ultra Resistant Adaptive Kinematic Soft Human Armour (SURAKSHA)

A Thesis Submitted

In Partial Fulfilment of the Requirements

for the Degree of

DOCTOR OF PHILOSOPHY

By

Suman Kumar

DEPARTMENT OF CIVIL ENGINEERING

INDIAN INSTITUTE OF TECHNOLOGY GUWAHATI

GUWAHATI – 781039

July 2022

CERTIFICATE

This is to certify that the work contained in the thesis entitled *"**Development of Smart Thickening Fluid based Ultra Resistant Adaptive Kinematic Soft Human Armour (SURAKSHA)**"* is the result of investigations carried out by **Mr. Suman Kumar** under my supervision and is an authentic record of the results obtained from the research work carried out at the Department of Civil Engineering, Indian Institute of Technology Guwahati, India for the award of degree of Doctor of Philosophy. This work has not been submitted elsewhere for a degree.

Thesis Supervisor

Dr. Hrishikesh Sharma

Associate Professor

Department of Civil Engineering

Indian Institute of Technology Guwahati, India

Guwahati

July 2022

DECLARATION

I, Suman Kumar, a PhD Scholar of Indian Institute of Technology Guwahati declare that the content of this thesis titled *"**Development of Smart Thickening Fluid based Ultra Resistant Adaptive Kinematic Soft Human Armour (SURAKSHA)**"* submitted here is a partial fulfilment for the requirement of awarding the Degree for **Doctor of Philosophy** and is submitted to Indian Institute of Technology Guwahati, India. This thesis contains the documentation of the research work carried out by me at the institute in a period of **July 2016 to July 2022** under the supervision of ***Dr. Hrishikesh Sharma,*** Associate Professor, Department of Civil Engineering, Indian Institute of Technology Guwahati, India. This work has not been submitted elsewhere for any degree or diploma of any institute or university to the best of my knowledge and belief.

In keeping with the general practice of reporting scientific observations, due acknowledgements have been made wherever the work described is based on the findings of other observations.

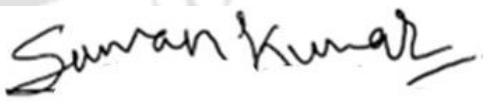

Guwahati **SUMAN KUMAR**

July 2022

Roll No. 166104039

ACKNOWLEDGEMENT

This is to acknowledge all who has directly or indirectly supported me in any way through the course of my PhD work, without whose support, it would have been difficult to complete this thesis.

I would like to express my sincere gratitude to my supervisor **Dr. Hrishikesh Sharma,** Associate Professor, Department of Civil Engineering, IIT Guwahati for his constant support throughout my PhD journey. His invaluable guidance, constant effort and encouragement has always been a great motivation to carry out and continue my research work. Besides, the lessons I have learned from him through the course of my research work will always help me in my future endeavors.

I am also thankful to my doctoral committee members Prof. Konjengbam Darun Kumar Singh, Prof. Vinayak Kulkarni (Department of Mechanical Engineering), Prof. Bulu Pradhan for their invaluable guidance and suggestions from time to time that helped me shape my research work better.

I am also thankful to **Prof. Anugrah Singh, Department of Chemical Engineering, and Mr. Ajith Prabhu, PhD scholar in the Department of Chemical Engineering** for their constant support and suggestions which helped me to further pursue my research work in better direction. I am immensely thankful to **Mr. Sanchit Saxena**, Research Scholar, Department of Civil Engineering for his continuous and helpful support.

I am thankful to my friends and Trainee Teachers of NIT Meghalaya – Kumar Abhinav, Dr. Rubi Chakraborty, Dr. Nur Alom, Avilash Sahoo, Ramyani Chakrabarty, Supratim Kaushik and Sambit Majumder for their constant emotional support in this journey. I am also thankful to Saurav Suman (Trainee Teacher, Department of Mechanical Engineering, NIT Mizoram) for his enormous support in very difficult times of my life. I am also thankful to Umesh Sharma for his constant support through this journey.

I am extremely thankful to my spouse **Mrs. Himanshu Kumari** and my lovely daughter **Ms Avani Yadav** for their wonderful love, support, and togetherness in this very difficult journey.

I am extremely thankful to my parents – **Shri Sitaram Singh Yadav** and **Smt. Lilawati Devi**, my elder and younger brothers, my sisters for their love, support, encouragement and

tremendous belief in me all the time. I am also thankful to my In-laws for their constant love, support, believe and providing motivation throughout this journey.

Last, but not least, I am thankful and indebted to the Lord Shiva for the blessings and strength that led me continue my life and research work.

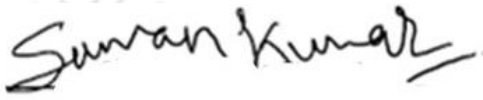

Suman Kumar

Dedicated

To

Lord Shiva

&

My Grandfather & Grandmother

Late Shri Panmukh Singh & Late Srimati Lakhrajiya Devi

ABSTRACT

With the progress of great development occurring in society, day by day a greater number of threats arises against humanity. The history of the conflicts between two parties is not new. In the present era, the form of war has been changing constantly, and it has taken various shapes such as guerilla warfare, insurgency, and similar. With the rapid development in technology, arms and ammunition have modernized. This increases the threat to the personnel who is directly participating in the conflict. The main objective during combat situation is survivability of the engaged personnel. Due to the rapid development in the lethality of bullets, there is an immense demand for the development of enhanced protective suit which can safeguard against these threats and are simultaneously flexible and light. **This thesis presents the design and development of liquid ballistic body armour to counter extreme threats arising from the bullet (direct and indirect effect) from standard arms and ammunition (as per National Institute of Justice (NIJ) specifications).** The effect of inter-yarn friction on the ballistic performance of the fabric is analyzed. The fabric consisting of varying yarn density (fabric sett) is considered to select optimum yarn density. From the numerical modelling, the ballistic performance of the fabric is optimized as a function of coefficient of friction and a critical coefficient of friction is obtained. The modelling of Shear Thickening Fluid (STF) treated Kevlar is presented and the ballistic performance of the STF treated fabric is evaluated. The numerical model of (STF) treated fabric utilizes the friction-based models and is implemented by adopting very high coefficients of inter-yarn friction. The present study shows that there is enhancement of ballistic performance due to increasing coefficient of friction up to a critical coefficient of friction for a specific fabric sett. Beyond critical level, no appreciable improvement in the ballistic performance of the fabric is observed. There is a decrease in the ballistic performance beyond critical friction level. After that, the Multi Material – Arbitrary Lagrangian Eulerian (MM-ALE) approach of modelling STF treated fabric is found to be an efficient option as compared to the friction-based model to evaluate the ballistic performance of the STF treated fabric. The different configurations of STF treated fabric are evaluated and optimum configuration is arrived to completely stop the projectile conforming to Ballistic Rating (BR) I, II A, II and III A as per NIJ standards. After that, the ballistic performance of STF encapsulated in bubble wrap configuration is analyzed and evaluated. The STF encapsulated bubble wrap configuration consists of STF filled in bubbles and these bubbles are either uniformly or randomly placed to prepare a layer of bubbles. The numerical strategies for modelling of STF encapsulated bubble wrap configuration is proposed and presented in this

thesis. In this study uniformly placed cylindrical bubbles of diameter 5 mm and height 5 mm is investigated and presented. This new configuration is found to be more efficient as compared to STF treated fabric in terms of ballistic performance against projectiles of different ballistic rating. The STF encapsulated bubble wrap is investigated under the impact of projectile of BR I, II A, II, and III A as per NIJ standards. The optimum configuration is arrived to completely stop the projectile conforming to BR I, II A, II and III A as per NIJ standards. Based on the outcome of the investigation a design guidelines and methodology are proposed in this thesis.

TABLE OF CONTENTS

LIST OF FIGURES

LIST OF TABLES

LIST OF EQUATION

Equation

LIST OF ABBREVIATIONS

MM-ALE	Multi-material Arbitrary Lagrangian Eulerian
STF	Shear thickening fluid
μ_s	Static coefficient of friction
μ_d	Dynamic coefficient of friction
C	Exponential decay factor
σ'_{ij}	Deviatoric stress
μ	Dynamic viscosity
ε'_{ij}	Deviatoric strain
RK	Power law fitting parameters
RN	Power law fitting parameters
$\bar{\gamma}'$	Shear strain rate

1 Introduction

1.1 General

Human civilization always lives in a great sense of threat that comprise of war and anti-social activities, which is the outcome of conflicts between multiple entities. These activities result in fatalities to associated military and civil personnel. Terrorist attack in India is not unknown, and these activities are so high that India remains in the top 10 list of these activities according to the Global Terrorism Database. Figure 1-1 shows year wise terrorist activities and corresponding fatalities in India.

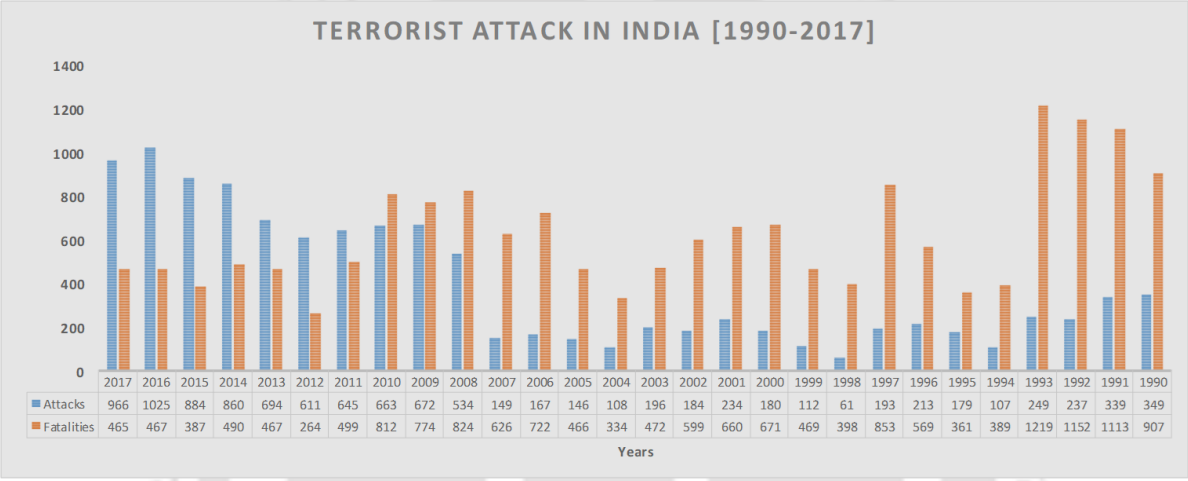

	2017	2016	2015	2014	2013	2012	2011	2010	2009	2008	2007	2006	2005	2004	2003	2002	2001	2000	1999	1998	1997	1996	1995	1994	1993	1992	1991	1990
Attacks	966	1025	884	860	694	611	645	663	672	534	149	167	146	108	196	184	234	180	112	61	193	213	179	107	249	237	339	349
Fatalities	465	467	387	490	467	264	499	812	774	824	626	722	466	334	472	599	660	671	469	398	853	569	361	389	1219	1152	1113	907

Source: Global Terrorism Database (START)

Figure 1-1 Terrorist attack in India [1990-2017]

With the rapid development in technology of war, different tactics, military operations, arms and ammunition are modernizing at a fast pace. This increases the threat to the personnel who are facing the combat situation. There is a high risk to survivability of the personnel engaged in countering these activities. The most common defense approach of survivability is the onion approach, also known as ‘survivability onion’. The onion approach shown in Figure 1-2 emphasizes on the layered level of survivability to maximize personal protection, and each layer is having a specific purpose (Hazell, 2016). Due to the modernization of arms and ammunition, the threat of penetration, and the probability of hit during combat situation has increased immensely.

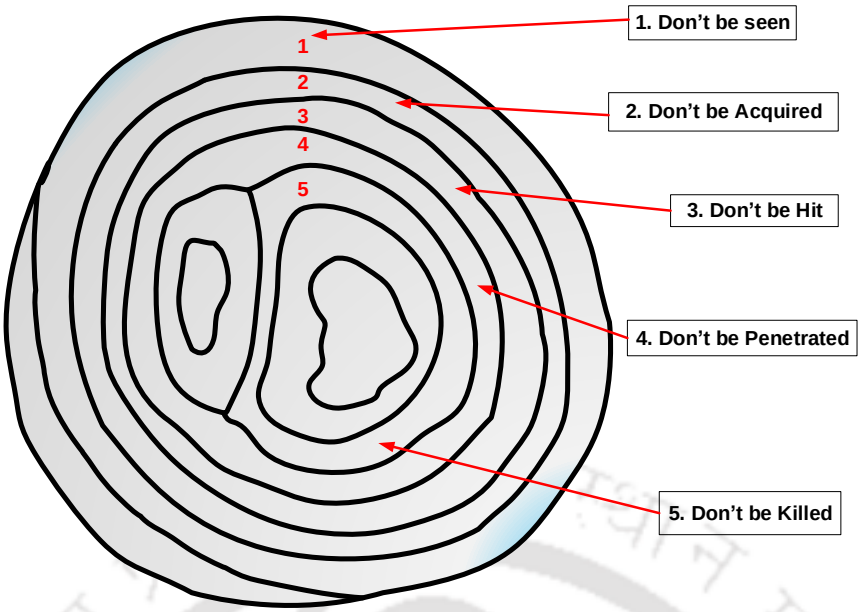

Figure 1-2 Multi-layer onion survivability diagram (Hazell, 2016)

The use of body armour during combat situation is not new to humankind. The body armour has significantly reduced the fatalities to the military personnel during combat and war (Horsfall, 2012; Larsen et al., 2011). The primary function of body armour is to provide protection from ballistic threat, however, modern military operations, technology-driven war tactics, and current on-street weapons and ammunition necessitates the development of advanced ballistic protection body armour system that is damage resistant, flexible, lightweight, and of high energy absorbing capacity (David et al., 2009). For protection against handgun bullets, it is common practice to use a pack of layered fabrics, loosely held or stitched together to form a comfortable wrap around the torso. For knife and spike attack, additional, or different packs are used which contain various "stiffer" materials like laminated fabrics, or metallic elements. For high-velocity rifle rounds, including armour-piercing (AP) ammunition, a Hard Armour Plate (HAP) is commonly added to the front of the system to work in conjunction with the soft armour pack and prevent perforation and severe blunt trauma (Crouch, 2019). The typical sub-systems and material groups used in a body armour system are as shown in Figure 1-3.

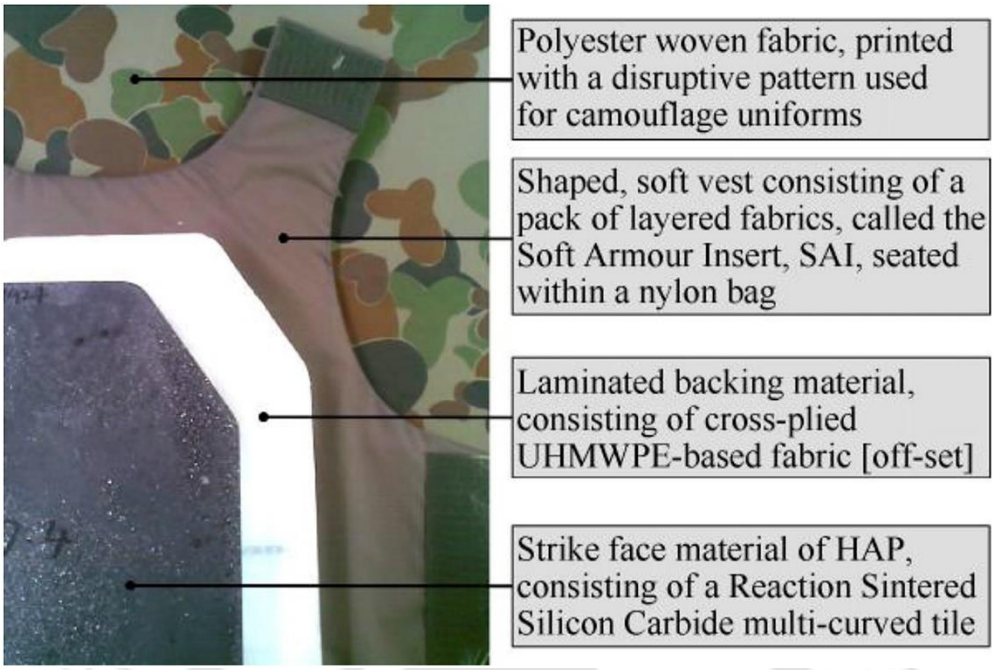

Figure 1-3 Material grouping in conventional body armour (Crouch, 2019)

To develop lightweight and flexible body armour with intended ballistic resistance, the various material subgroup needs to be investigated under different test conditions as per test standards (NIJ 0108.01, 1985; NIJ Standard-0101.06, 2008). The threat considered for the present study is ballistic rating III A (Armour Piercing Rifle) according to (NIJ Standard-0101.06, 2008).

1.2 Motivation

In nature there are outstanding examples of species which depicts great protection from predators through various mechanisms comprising of great energy absorbing capacity as well as maintaining high flexibility to survive in the respective surroundings (Funk et al., 2015; Liu et al., 2016; Meng et al., 2016; Ortiz & Boyce, 2008; Wegst et al., 2015; Wu et al., 2019). The motivation for advanced ballistic body armour system comes from biological composite fiber structure exoskeleton of lobster (Homarus Americanus). Homarus americanus, known as American lobster, is fully covered by its exoskeleton composed of **rigid cuticles** and **soft membranes**. These soft membranes are mainly located at the joints and abdomen to connect the rigid cuticles and greatly contribute to the **agility** of the lobster in swimming and preying (Wu et al., 2019). The research carried by (Wu et al., 2019) shows that there is unique multi-layered structure in this membrane, achieved through the ordered arrangement of chitin fibers,

which plays a crucial role in dissipating energy during rupture and making this membrane robust and damage tolerant.

1.3 **Threats: Ballistic impact**

In order to design and develop ballistic armour it is necessary to understand ballistic threats and standardize it as per the requirement of different agencies. As the body is quite well protected against blunt impacts, with the most sensitive organs lying beneath the skull or the rib cage. (Horsfall, 2012) observed that most of the armour system has to be designed to exhibit penetration resistance and does not have to absorb energy. For soft body armour, there is a concern that injuries can be caused by non- penetrating projectiles, creating a Behind Armour Blunt Trauma (BABT) (Cannon, 2001). Whilst this is a possible dangerous mechanism, the incidence of serious BABT is very low in soft body armour. Its occurrence is confined to a small number of unusual cases in which the armour has been stuck close to its edge, or a very high-energy impact has been sustained. There is some concern that the pursuit of thinner and more flexible armour may lead to a situation in which the bullet is retained by the armour, but the armour is so flexible that it penetrates the body by a penciling injury mechanism. The Kinetic Energy Density (KED) is one of the best single measure of penetration capability. KED is defined as the energy at impact divided by the projected cross-sectional area of the projectile. In addition to the KED, the velocity of the projectile is also important, as the contact load is typically related to the square of the impact velocity. The impact energy need not be absorbed by the armour, but it is necessary to spread the impact load so that the wearer is not injured. Therefore, the incident kinetic energy will also be a factor in armour design. The KED, velocity, and kinetic energy of most common bullets from small ammunitions is shown in Figure 1-4 and given in Table 1-1 and Table 1-2.

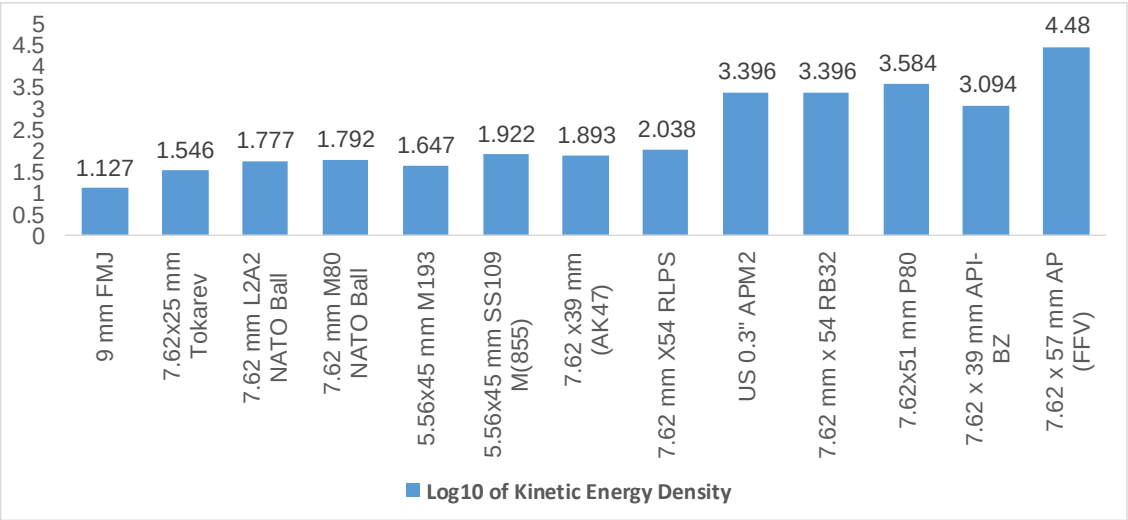

Figure 1-4 Kinetic Energy Density of common bullets (small arms and ammunitions) (Crouch, 2019)

Table 1-1 Ballistic threats from common arms and ammunitions (Horsfall, 2012)

Threats	**Velocity (m/s)**	**Kinetic Energy (J)**	**Presented area (mm^2)**	**KED (J/mm^2)**	**Armour Material**
Handgun	450	1032	65 (initial)	16	Textile
(.357" Magnum)			254 (final)	4	
1.1 g (17 grain) fragment	450	111	24	4.5	Textile
Bowie Knife	8	42	0.25	160	Special Textile
Assault rifle (AK 47)	720	2050	24	85	Composite Plate
HV rifle (SA80)	940	1805	75	24	Ceramic Plate

Table 1-2 Ballistic threats (NIJ Selection and Application Guide-0101.06, 2014)

		Test Variables		Performance Requirements		
Armor Type	**Test Ammunition**	**Nominal Bullet Mass**	**Suggested Barrel Length**	**Required Bullet Velocity**	**Required Hits Per Armor Specimen**	**Permitted Penetrations**
I	22 LRHV Lead 38 Special	2.6 gm	15 to 16.5 cm	320 ± 12 m/s	5	0
	RN Lead	10.2 gm	15 to 16.5 cm	259 ± 15 m/s	5	
II A	357 Magnum JSP 9 mm	10.2 gm	10 to 12 cm	381 ± 15 m/s	5	0
	FMJ	8.0 gm	10 to 12 cm	332 ± 12 m/s	5	
II	357 Magnum JSP 9 mm	10.2 gm	15 to 16.5 cm	425 ± 15 m/s	5	0
	FMJ	8.0 gm	10 to 12 cm	358 ± 12 m/s	5	
III A	44 Magnum Lead SWC	15.55 gm	14 to 16 cm	426 ± 15 m/s	5	0
	Gas Checked 9 mm FMJ	8.0 gm	24 to 26 cm	426 ± 15 m/s	5	
III	7.62 mm 308 Winchester	9.7 gm	56 cm	838 ± 15 m/s	5	0
	FMJ					
IV	30-06 AP	10.8 gm	56 cm	868 ± 15 m/s	1	0

Thus, the high penetrative capability and the high kinetic energy of bullets require both a resistant armour to achieve energy transfer from the projectile and an ability to spread the contact loads to a much greater extent (Horsfall, 2012).

1.4 Current trends in the development of liquid body armour: Lightweight and flexible Ballistic Armour

The work in the field of light weight bullet proof Armour started way back in in 1972. It was reported by (Silvia et al., 1972) that two experimental Buoyant, Anti-Fragment, Bulletproof Vests were developed, which give low-velocity protection against mortar shell bursts and secondary pieces spall, as well as protection against 30-caliber small-arms fire and emergency, inherent buoyancy. Each model included a carrier with front and back panels containing a 30-caliber ball, a body-armour plate, a combination of felt and/or woven ballistic nylon materials, and layers of buoyant, unicellular polyethylene foam. These vests were created to replace a standard ensemble worn by Navy personnel in Southeast Asia to protect them from shrapnel and rifle fire wounds and act as a floatation device in the event of a drowning. A 40-pound ceramic body vest was worn over a Navy MAE WEST and under a lightweight flak vest in the ensemble. In-house physiological stress tests on the vests revealed that there was no significant difference in the amount of stress between the new models and the regular ensemble. The experimental vests, on the other hand, were clearly favored by the test subjects because of their smaller weight and reduced size, which boosted relative comfort. In 1973, this work was put into implementation by (Montanarelli et al., 1973). The goal of this 12-month project was to design a non-obtrusive, lightweight external garment top coat or sport coat for use by public officials to combat the 0.38 caliber particular danger. The ballistic characteristics of a number of prospective protective materials were tested. The PRD-49-IV material outperformed all other materials tested, and it was used to create an acceptable exterior garment. Several types of ballistic projectiles with threat severity equal to or less than that of the 0.38 caliber special were fired at panels of candidate materials in the ballistic penetration tests. The test conditions complied with the criteria of the National Bureau of Justice (NIJ) Standards. In animals wearing protective panels, blunt trauma effects were detected. The damage resistant, flexible, lightweight, and high energy absorbing capacity features of the advanced ballistic protection body armour systems makes it indispensable for modern military operations and actions. Many organizations across the globe are working on the development of ballistic suit having features

mentioned above viz. U.S. Army Research giant **RDECOM**, **SOCOM**, British defense technology giant **BAE** (Gill, 2010), Polish research institute **MORATEX.**

The U.S. Army Research, Development and Engineering Command, known as **RDECOM**, is working on the development of lightweight, flexible body armour **Tactical Assault Light Operator Suit (TALOS)** (Matthew, 2016)**. TALOS** is an advanced infantry suit having high strength with improved ballistic protection. TALOS is currently being developed using **Shear Thickening Fluid (STF). Magnetorheological (MR) Fluids** will also be explored for development of liquid body armour. In this armour, the liquid will transform into solid in milliseconds when acted upon by high pressure in case of STF and through a magnetic field or electric field generated in case of MR fluids.

A similar type of ballistic armour is in developing phase by British defense company **BAE.** As per BAE, latest tests on ballistic armour made of STF provide the first evidence that liquid armour could effectively protect soldiers from bullets or shrapnel. Two tests have been carried out, one using a large gas gun, and the other one using a ball-bearing metal bullets with speed over 300 meters per second. In BAE study, the test material comprises of 31 layers of untreated Kevlar and ten layers of Kevlar treated with STF (Gill, 2010)**.**

Polish company **MORATEX** is also working on the liquid body armour based on STF. In 2014, Iran put its claim of making an armour built with STF.

The U.S. Army had planned to commission similar type of ballistic shirt by 2019. The target of this newly developed ballistic shirt is to reduce the weight of ballistic suit by 14 -26 percent with enhanced protection from the current weapons threat. The mass of the previous armour with Insert Plate (IP) is 31 pounds. The recently developed ballistic shirt is shown in Figure 1-5.

Figure 1-5 Status of the Ballistic shirt developed by the U.S. Army in 2019 (Matthew, 2016)

In order to develop a lightweight and flexible ballistic body armour, there is need to review the available potential materials for ballistic applications such as high-performance fabric, auxetic materials (to efficiently absorb impact energy due to negative Poisson's ratio effect), auxetic metal composite foams, (Ibrahim, 2012; Ren et al., 2018), ceramic plates (to defeat high kinetic energy density bullet) (Lane, 2005). This has been covered in the next chapter (Chapter 2) of this thesis which presents the review on ballistic performance of high-performance fabric and enhancement of fabric performance through impregnation to shear thickening fluid. Furthermore, Chapter 2 also presents the available knowledge on the ballistic performance of STF encapsulated configuration. The encapsulated STF could have potential to absorb and disperse more kinetic energy due to confinement effect. Based on the above discussion the research gaps have been identified and presented in the following section.

1.5 Research gap

The development of light-weight and flexible body armour which is damage resistant and high energy absorbing capacity along with providing great comfort to the wearer is the current demand posed by security agencies across the globe. In order to achieve the required demand following research gaps have been identified in the process of developing ballistic body armour which will be light and flexible as well:

- In all the researches done in this field, the Kevlar fibers and other high strength fibers are individually used for resisting the ballistic impacts. The use of STF with Kevlar fibers is limited to small scale impact like a knife attack or small bullet impacts. The weight of the bullet proof jacket is not reduced significantly as compared to the existing technologies in this field. A major thrust in development of armour can be focused in reducing the weight

and improving the flexibility of the jackets as per NIJ standards (NIJ Selection and Application Guide-0101.06, 2014).

- The full potential of STF has not been utilized as an armour material till now. STF can alone be used to absorb energy as the energy absorbing capacity is the most important function of this family of materials. STF can be utilized as an effective energy absorbing material in order to protect from ballistic impacts. Impetus will be placed on development of armour using STF with varied compositions to improve the efficiency of the armour in resting ballistic impacts.
- The basic constituent of STF and its and its configurations needs to be analyzed and investigated under realistic threat scenarios as per NIJ standards (NIJ Selection and Application Guide-0101.06, 2014) in such a way that it will leads us to design and develop liquid ballistic armour meeting the criteria of lightweight and flexible ballistic body armour.

Based on these research gaps, the objective has been framed. This will extend the current state of the art in exploring the full potential of STF and designing a lightweight and flexible ballistic body armour. The basic constituent material for the proposed study is as shown in Figure 1-6.

Figure 1-6 Basic constituent of liquid ballistic armour (1) Shear Thickening Fluid, (2) Ballistic Fabric, and (3) Schematic of STF filled Bubbles (Challenge, 2020).

1.6 Objective

The objective of this thesis is to develop the methodology for the design and development of light-weight and flexible **Smart thickening fluid based Ultra Resistant Adaptive Kinematic Soft Human Armour (SURAKSHA)** to sustain ballistic threats. The design and development methodology of two types of liquid human armour having

specification as per NIJ standards and performance criteria given in Table 1-2 is presented in this thesis as follows:

- **SURAKSHA A:** STF impregnated multi-layer high performance fabric liquid armour system conforming to BR I, IIA, II, IIIA.
- **SURAKSHA B:** STF encapsulated bubble wrap configuration based high performance liquid armour conforming to BR I, IIA, II, IIIA.

1.7 Work plan and Methodology

In order to achieve the proposed objective, the following tasks and methodologies have been performed and presented in this thesis:

1. The ballistic performance evaluation of body armour based on STF impregnated high performance fabric through friction based numerical models.
2. The impact characterization of STF using Multi-Material ALE based on user defined varying viscosity modelling.
3. The performance evaluation of ballistic armour based on STF impregnated high performance fabric through Multi-material Arbitrary-Lagrange-Eulerian (MM-ALE) based user defined numerical viscosity numerical models.
4. The ballistic performance characterization of confined STF encapsulated in uniformly and randomly distributed high-performance fiber bubble wrap using MM-ALE based user defined viscosity models.
5. The design and development methodologies for the development of the said **Smart thickening fluid based Ultra Resistant Adaptive Kinematic Soft Human Armour (SURAKSHA)** is formulated on the basis of results from computational models of STF treated fabric system and STF encapsulated bubble wrap configuration.

The tasks discussed above is achieved through work plan shown in Figure 1-7. The work plan shows the methodology adopted to obtain the design configuration of liquid ballistic armour. The experimental data are obtained from literature and only simulation is accrued out in this study.

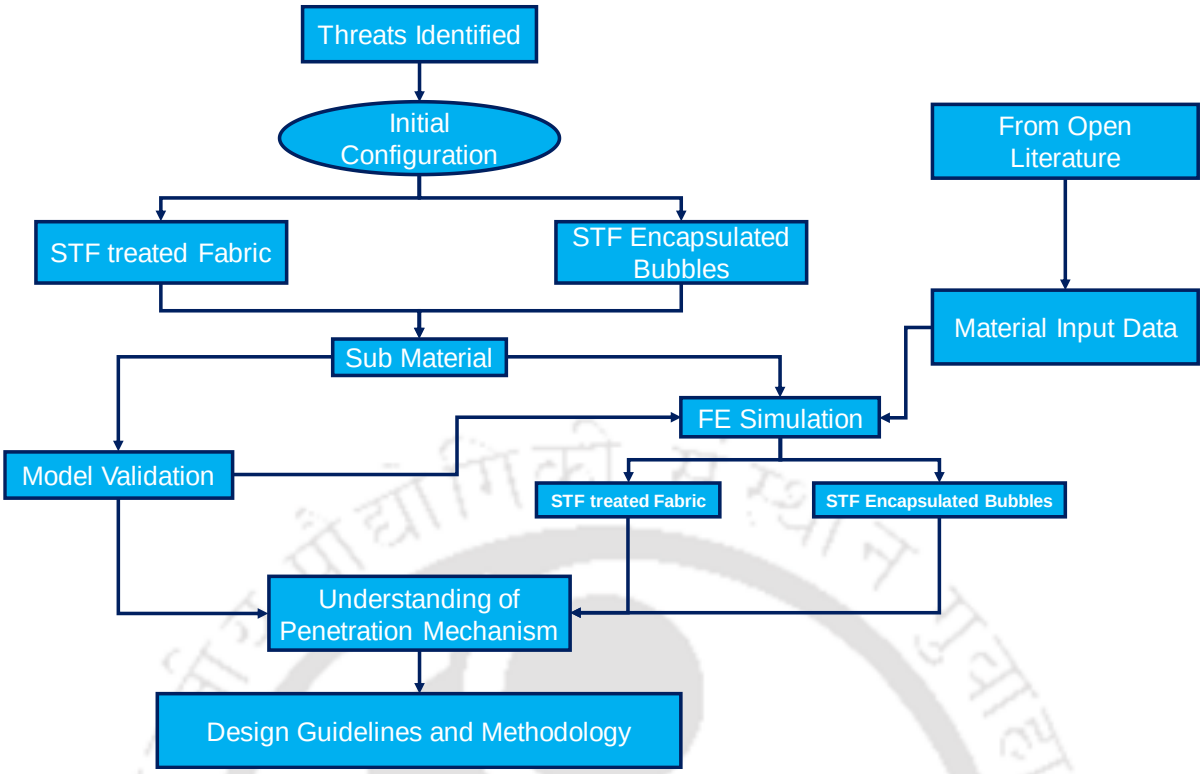

Figure 1-7 Workplan to achieve proposed objective of this study

1.8 Organization of this thesis

The thesis presents the outcome of the research carried out for the attainment of the proposed objective of design and development of light-weight and flexible **Smart thickening fluid based Ultra Resistant Adaptive Kinematic Soft Human Armour (SURAKSHA)** to sustain ballistic threats. The current chapter describes about the challenges faced in the field of ballistic armour development and presents the outline for obtaining a light-weight and flexible armour. Chapter 2 presents a comprehensive literature review in the field of ballistic armour development. Further, it highlights the key findings and limitations of the study reported in open literature. Based on the limitations of widely used numerical models of STF treated fabric in the earlier studies, this thesis presents the investigation on the effect of inter-yarn friction on ballistic penetration and performance of the fabric in subsequent chapters. After that, Chapter 3 presents the modelling of fabric using commercially available package LS-DYNA. The model described in Chapter 3 is based on friction-based models and it covers modelling of neat fabric. This chapter shows that behavior of neat fabric is captured well within agreement to the experimental results and provides comprehensive insight about ballistic impact behavior upon varying inter-yarn co-efficient of friction. Chapter 4 presents the modelling of STF treated fabric based on multi-scale friction-based models. This chapter highlights the behavior of STF

treated multi ply fabric system and on later stage presents the limitations of the friction-based models. Chapter 5 gives details about the modelling of STF using user defined MM-ALE approach. Further, this chapter also presents the impact characterization of a rigid spherical ball impacting on different STF samples. The impact characterization will provide an insight in understanding the resisting mechanism of the STF during impact. Based on the model of fabric and STF presents in Chapter 3, 4 and 5, Chapter 6 presents the fluid structure interaction between STF and fabric. This chapter also presents the application of ALE model for the ballistic impact characterization of STF treated fabric. Further, the findings of the STF treated fabric, highlights the need of different configuration to harness the smart behavior of STF fluid. After that, Chapter 7 presents a new configuration to harness the smart behavior of STF by encapsulating STF in bubble wrap configurations. The findings present in this chapter shows the potential of STF encapsulated configuration to resist projectile efficiently. Chapter 8 presents the design guidelines and methodologies for the development of liquid based ballistic body armour. This chapter contains the design formulation for both configuration of SURAKSHA. Chapter 9 presents the conclusion, and future work; and research outcome from the present thesis.

2 Literature Review

2.1 Introduction

The success of military tactics and strategies largely depends upon the deployed technologies and personnel on the ground. The body armour during combat and military action proves to be an efficient device to safeguard the deployed personnel on the ground from the penetrations, reduces wounds and fatalities, and hence strengthens the success of military tactics and strategies. The design and development of body armour evolves through the contemporary warfare tactics and strategies. Further, the selection of the constituent material is one of the critical steps and depends on the modern military operations and threats from the current arms and ammunitions. The armour may be classified depending on the energy dissipation mechanism and the constituent materials, such as hard (application of metals and ceramics) and soft amour (application of fabrics and composites). There is advantages and disadvantages of both type of body armour. For instance, the employment of immense number of high-explosive artillery shells during the First World War resulted in a high rate of wounds from flying shell fragments. Some special-purpose troops were given experimental torso armour comprised of steel and fiber layers that were bulletproof, but the armour was too heavy for general usage. Hence, there is need of the development of damage resistant lightweight and flexible body armour which will be providing more mobility and comfort to the wearer.

In order to design and develop the lightweight and flexible ballistic body armour the current practices, corresponding theory and mechanism should be known. This chapter briefly describes the theory and practices in the field of lightweight and flexible ballistic body armour. Finally, this chapter will provide the detailed modelling approach of the ballistic events in LS-DYNA®.

2.2 Earlier Development of Bullet proof armor using Ceramic and metals

During world war II, the shell fragments were responsible for 80% of all casualties, and 70% of all wounds were to the torso. Further, both the military and business conglomerates have realized the need of lightweight, flexible, and effective body armour which should effectively protect the torso of the wearer. They proposed the design and development of a novel lightweight body armour where the vests composed of resin-bonded fiberglass, steel, aluminum, and heavy nylon doth were worn by ground soldiers and bomber crews. Further, the army and navy of the United States developed semi-flexible vests composed of plates and

basket-weave nylon. These jackets were effective against mortar and artillery shrapnel, but not against armour-piercing projectiles. After 1967, titanium plates in body armour provided further protection. During the Vietnam War, hovering helicopter pilots and crews needed stronger protection from heavy ground fire. As a result, in 1960s, steel with dual hardness and ceramic plastic composites were invented. Dual-hardness Steel armour provided 50 percent better ballistic protection than aluminum armour of comparable weight, as well as the ability to absorb numerous impacts better than shatter-able ceramic armour. A very hard front face is metallurgically connected to a robust crack-resistant rear face. The front face shatters the steel core of an oncoming armour-piercing bullet, while the ductile rear face absorbs the kinetic energy. The plates can be rolled to the desired thickness to defend against a given threat. Hard ceramic plates are reinforced with woven glass roving connected with an elastic glue (or other plastic backing) to make ceramic composite armour much lighter. The bullet is abruptly slowed by the hardness of the ceramic, which dissipates the projectile's kinetic energy as it shatters the ceramic. A bulletproof vest's ceramic tiles, on the other hand, must be changed because they shatter with every collision.

The major drawback of ceramic based armour is the shattering of ceramic plates upon hitting of high round of the projectile. The contemporary researchers identified this limitation and they further carried research to develop shatter-resistant composite of ceramic plates and metals such as Cermets. Cermets are a new ceramic-metal composite material that is five times more crack- and shatter-resistant than traditional ceramics. Cermets are made by penetrating molten-reactive metals through chemically treated boron carbide, boron, or boron fibers or powders. Cermet characteristics are still being investigated, and structural models of material reactions are being developed. Researchers are continuing to enhance the cermet-formation process in order to develop less expensive, commercially viable production methods so that Cermets can be used more widely. (Anderson, 1992) stated that Cermet body armour may become the most effective type of bulletproof vest on the market in the near future. Extending the previous research in the field, (Bajaj & Sriram, 1997) presented the understanding of the mechanism of ballistic penetration of high-performance materials. Further, this work paved the way for the selection of newer materials for better protection and satisfying the requirements of both the wearer and the technologist. This study brought together the findings of a flurry of recent research in the subject of ballistic protection, from material selection to modelling, with a focus on evaluation methods and mechanisms.

The performance of ceramic was enhanced using various technologies and materials along with it. One such work was done by (O'Donnell, 1992), who developed an equation that allowed the computation of the elastic deformation energy of a Kevlar plate employed as a backing for ceramic armour and further strengthen the understanding of the plate profile at maximum deflection. Based on the calculations for two low weight ceramic armour, it was reported that the energy of deformation of the composite backing accounts for 30 to 60 percent of the projectile's initial kinetic energy. In his research, Kevlar came first into the picture that was later extended in developing the latest bullet proof armors. Mathematically and empirically, the influence of the adhesive layer used to connect ceramic tiles to a metallic plate on the ballistic behavior of ceramic/metal mixed armour was investigated by (Zaera et al., 2000). The study considered two types of adhesives, polyurethane (soft adhesive) and rubber-modified epoxy resin (stiff adhesive), as well as varying thicknesses. Using a commercial finite difference code, numerical simulations of low caliber projectiles impacting on alumina tiles supported by an aluminum plate were also performed and reported. Further, the adhesive's impact through full-scale testing was determined. An engineering model was devised to provide a preliminary design tool that considered the adhesive's influence. The experimental comparison of fragmentation of the adjacent tiles is shown in Figure 2-1.

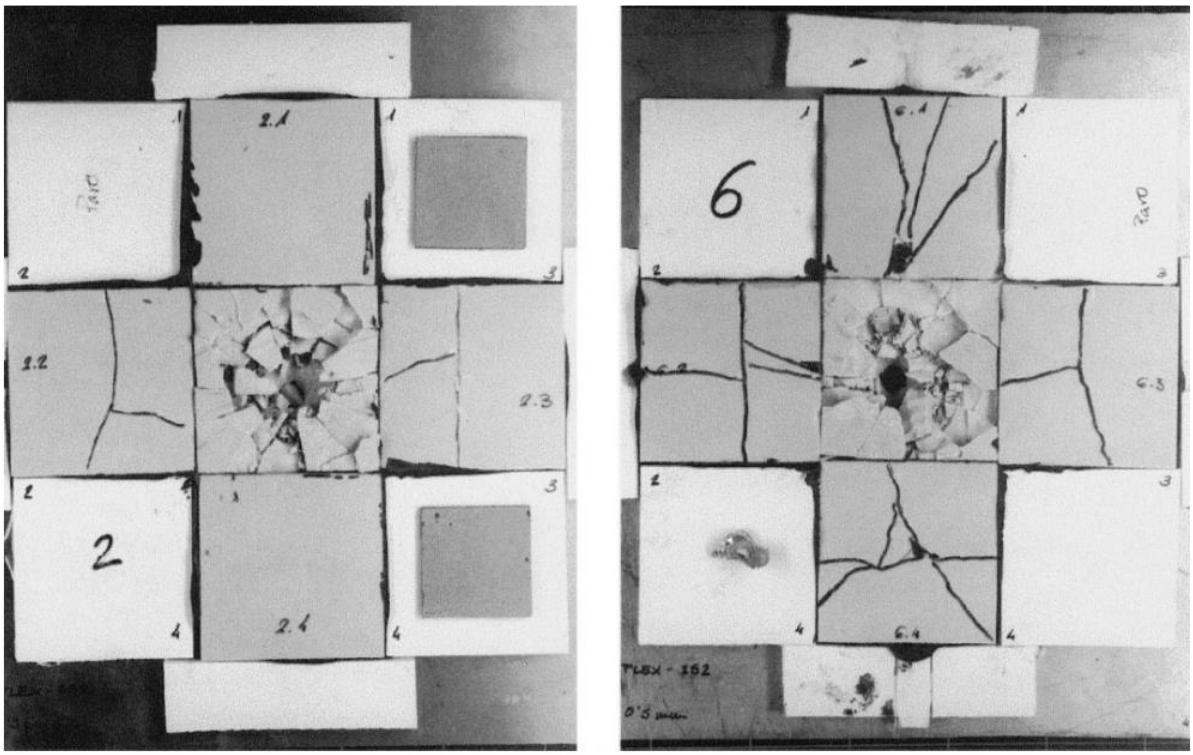

Figure 2-1 Comparison of the degree of fragmentation of the adjacent tiles for a polyurethane adhesive layer of thicknesses of 1.5 mm (left) and 0.5 mm (right) (Zaera et al., 2000)

Ceramic armors were researched ahead with different additive features. The study by (Nayak et al., 2013) presents the investigation on ballistic impact response of Zirconia Toughened Alumina (ZTA) ceramic front and aramid laminated composite backing against 7.62 mm Armour Piercing (AP) rounds. The ballistic impact of steel core 7.62 mm AP bullets with different impact velocities were targeted to evaluate the V50 Ballistic Limit (BL) of the ceramic-faced and stand-alone composite laminates. The study found that in comparison to stand-alone ceramic front layers, the addition of a ceramic front layer resulted in a significant increase in BL. The study about the absorption of the energy has been presented and draws the conclusion that during penetration, the impact energy was absorbed largely by ceramic fracture, projectile deformation and fracture, and elastic-plastic deformation of the flexible backing composite layer. It was observed that the ceramic tile breaking was restricted to the impact area and did not spread to the entire surface, with projectile fracturing above BL and blunting on impact below BL. Further, it has been reported with Twaron-PP as the backing, the ceramic-faced composites had a higher BL than a Twaron-epoxy laminate of the same thickness. This combination of ceramic-composite laminates demonstrated improved multi-hit resistance, making it appropriate for light armour.

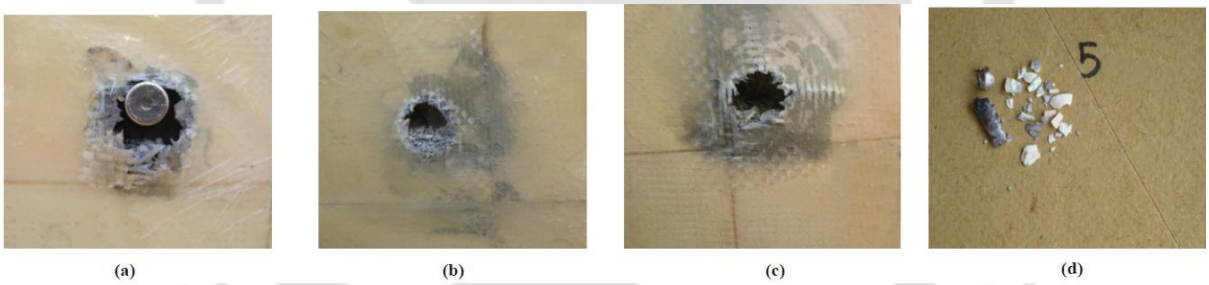

Figure 2-2 Front face of post impacted ceramic faced composite laminates (a) below ballistic limit, (b) around ballistic limit, (c) above ballistic limit, and (d) broken ceramic tile and projectile. (Nayak et al., 2013)

2.3 Development of high-performance fabric-based armor

There was always a demand to replace cermet formed armors with much lighter and flexible armour. On the other side, it was also observed that there is extensive application of high-performance fiber-based fabric to mitigate ballistic impact of lower ballistic rating according to NIJ standard of BR I and II such as (Bazhenov, 1997; Cunniff & Auerbach, 2002). With the vision of this, (Wang & Chou, 1997) investigated the penetrating resistance of fiberglass reinforced plastic plates under ballistic impact using a combination of experimental and semi-empirical methods, with ballistic tests utilizing 7.62 mm armour-piercing bullets. The

methodology included a slow penetration test by utilizing a produced bullet profile to compare the damage process and energy absorbing properties of the composites under the two different loading situations. It was reported that the quantity of energy absorbed by the materials for the two different loading circumstances was found to be very similar even after changes in failure processes. It was suggested that the slow penetration test can be used to determine the target's ballistic limit from the standpoint of energy absorption. Also, a semi-empirical model to characterize the resistive force at each penetration stage was created, from which the energy absorption could be computed and the projectile's remaining velocity could be approximated.

The impact process in effect requires two things from the fabric or yarns in order to impart resistance: firstly, they should not break, so they should be strong (or tough); and, secondly, the imposed load and the resulting stress waves need to move quickly from the impact point. This has led to the combined performance factor U* (Cunniff, 1999), which states that the performance of the fabric is the product of the specific yarn toughness and the longitudinal wave speed of the yarn. Ballistic helmets, vests, blankets, and add-on automobile armour are among the principal fiber reinforced ballistic items. High strength and high modulus fibers have revolutionized the design of lightweight armour. Modelling of the ballistic properties of multi-layer fiber reinforced armour is in the development stage, and structural models that can be used to describe the penetration of such armour by deformable projectiles, as well as to design new armour, are not yet available in plenty. (Jacobs & Dingenen, 2001) devised a simplified model for calculating the performance of Dyneema® armour against deformable bullets and FSPs. The fact that the number of input values in this model is so less is crucial. In this simplified model only two materials-related criteria are necessary to calculate the performance of Dyneema® unidirectional-based armour. The experimental results and penetration of soft ballistic package consisting Dyneema® against 9 mm Parabellum bullet is shown in Figure 2-3.

Figure 2-3 Penetration due to 9 mm Parabellum bullet in a soft ballistic package (Jacobs & Dingenen, 2001)

Furthermore, many different materials are utilized in the field of protective gear to provide cut, tear, and puncture resistance where high degrees of stiffness and shear resistance are needed. (Messiry, 2014) investigated the cutting phenomena in protective materials using typical cut test procedures in his work. The Multi-layer pads, highly preformed woven nets, and tri-axial fabrics were utilized by (Messiry, 2014) as supporting layers to improve the puncher resistance of protective fabric. The results show that when a silk stuffed cushion is supported on a high tenacity polyester net, the specific puncture load is the highest. Further, the study reported that the Para-aramid tri-axial weave fabric (TWF) with multi-layer silk fabric is superior to para-aramid plain weave fabric. The test results showing cut behavior of different padded samples are depicted in Figure 2-4.

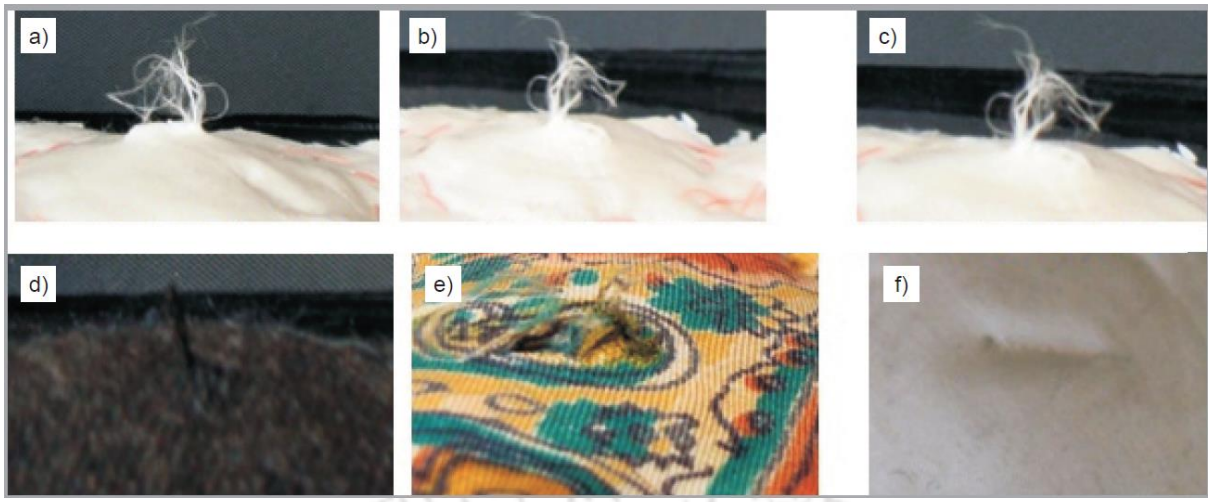

Figure 2-4 Cut behaviour of padded samples (a) multi-layer 100% silk pad (b) multi-layer 100% silk pad (c) multi-layer 100% silk pad (d) multi-layer 100% wool pad (e) multi-layer 100% silk pad (f) multi-layer 100% silk fabric. (Messiry, 2014)

But there are some limitations in using neat fabric to design ballistic armour is the requirement of very high number of fabric layer (even more than 31 layers) (Srivastava et al., 2012). Due to very high number of neat fabrics layers, the developed armour becomes bulky. There has been extensive study carried in order to enhance the ballistic performance of high-performance fabric (from this onwards it will be termed as ballistic fabric instead of high-performance fabric) in order to reduce the number of required neat fabric layer.

Kevlar® 49 fabrics were widely utilized in ballistic systems, aerospace, fabric reinforced composite materials, and other sectors due to their exceptional properties such as high elastic modulus and strong impact resistance. The multi-scale mechanical behaviors of Kevlar® 49 in the forms of fiber, yarn, and fabric exposed to uniaxial tension was investigated by (Zhu et al., 2016). Their study revealed that the material mechanical properties were influenced by the structural size scale and sample gauge length. A statistical analysis was used to quantify the degree of variability in the tensile strengths of fiber and yarn with different gauge lengths. The tensile strengths decrease with increasing gauge length and structural size scale from fiber to yarn, and then to fabric, and followed the Weibull distribution. Furthermore, the constitutive models of fiber and yarn was used, respectively, which incorporated the Weibull distribution in tensile strength. User-defined subroutines (UMAT) in ANSYS was constructed to simulate the tensile behaviors of single yarn and fabric. It was reported that the probabilistic method proposed is accurately simulating the multi-scale tensile behaviors of Kevlar® 49.

If the yarns are loosely woven, there is a greater tendency for projectiles to part the yarns and penetrate without fully loading them: **a process known as windowing**. It has been shown that thin armour are less efficient than thick armour, but they are much better at stopping projectiles in short distances. The requirement for high cover factors (the ratio of the projected area of the individual yarns to the area covered by the yarns when woven into fabric) is only for the layers in contact with the projectile, so it may be beneficial to have high cover factor fabric towards the impact face and coarser weave fabric to the rear. Ballistic performance is usually improved by using a finer yarn with greater tightness of the weave and optimizing weave style.

For bullets having a KED of above 30 Jmm^{-2}, ballistic fabric systems become overly bulky. The contact loads tend to be sufficient to cause the shear failure of the fibers and capture of the projectile occurs only after numerous layers have been perforated. For a KED of 30–45 Jmm^{-2} it is possible to protected by the use of polymer matrix composites. It has been shown that at low KED flexibility is a key factor in projectile capture, while at higher KED shear strength within the material becomes dominant (Walker, 2001).

2.4 Numerical modelling of high-performance fabric

There are several well developed modelling approach exists in the open literature and these approaches are documented in the literature such as review article by (Tabiei & Nilakantan, 2008). These approaches are highlighted from the literature such as analytical (used for simple physical problem), semiempirical and empirical (analysis of data obtained through experimental work and useful for small number of parameters involved in the analysis with limited accuracy), and numerical (this approach can handle any complexity involved in the modelling of the high-performance fabric including contact definition between yarns, filaments etc.). The strategies of modelling high performance fabric depend upon the objective of the study and subsequently, on the scale of the fabric model. The plain weave fabric is composed of weaved yarns. These yarns are comprised of several threads/ filament having diameter approximately 12 μm. The filaments in the yarn consists of fiber having length scale of nanometer range. Furthermore, based on scale of the model, the model of the fabric may be divided into four scale: (1) macroscale (2) mesoscale (3) microscale, and (4) nanoscale. The graphical representation of the fabric model at different scale is as shown in Figure 2-2.

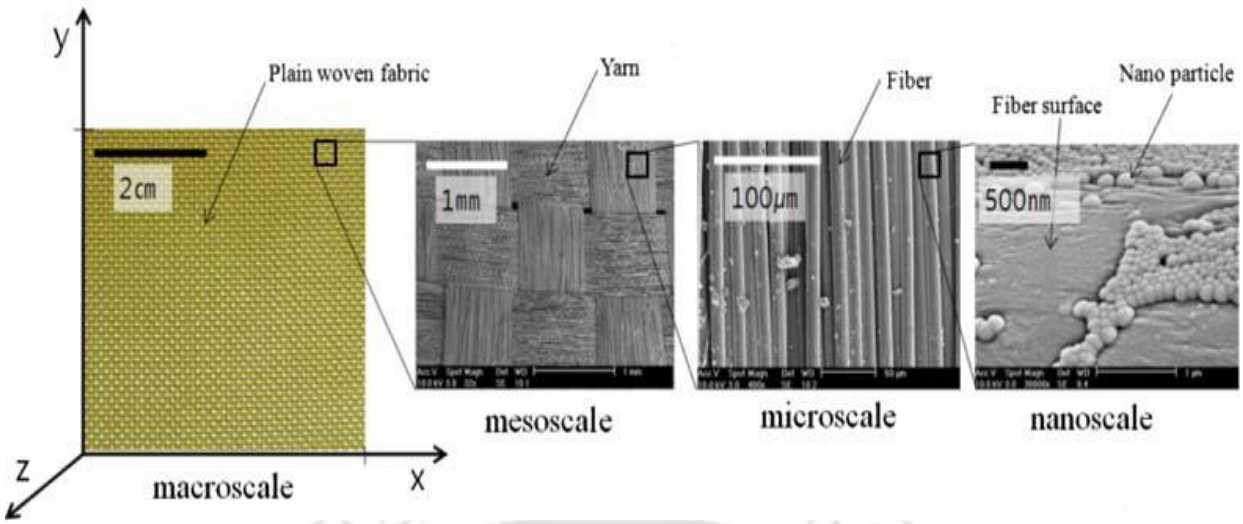

Figure 2-2 Multi-scale modelling approach of the high-performance fabric (Lee & Kim, 2012)

A numerical code was designed by (Roylance et al., 1995) to understand the complex behavior of woven fabric panels subjected to ballistic impact. The code developed by (Roylance et al., 1995) can be used to model by considering different-layer of fabric panels, multiple projectile geometries, and fabric flaws such as yarn slippage at crossovers and clamps. Few years back, (Chu et al., 2016) used the explicit nonlinear FEA code to simulate a numerical ballistic impact on a single-ply of plain-woven fabric Kevlar KM2® that was clamped at four edges, with varied yarn material parameters such as yarn density and longitudinal young's modulus. The parametric studies revealed that yarn density had no major impact on cloth ballistic performance.

To understand the behavior of Kevlar fiber, models were developed by many researchers. (Cheng et al., 2005) described the transverse mechanical behavior of Kevlar® KM2 single fibers under compression using a phenomenological continuum model. The developed model could be used to simulate the mechanical properties of fabrics made of Kevlar® KM2 fibers numerically. It has been shown that the model matches experimental results on the transverse behavior of Kevlar® KM2 single fibers in compression quite well. In recent years, modelling of high-performance ballistic fabrics has gradually shifted from continuum and yarn length scales to the sub-yarn length scale, allowing for the establishment of relationships between fabric penetration resistance and various fiber-level phenomena such as fibre-fibre friction, fiber twist, transverse fiber properties, and the stochastic nature of fibers. Special numerical approaches such as the digital-element method and bespoke computational codes are used in most sub-yarn modelling schemes. These methods and tools for sub-yarn

fabric modelling are not generally available to the academic and industrial research communities due to their current condition. (Grujicic et al., 2012) by utilizing traditional finite element method developed a tool to do sub-yarn numerical analysis of the penetrating resistance of Kevlar® KM2 ballistic fabric. The purpose was to show that results could be obtained that were comparable to those obtained using the digital-element method.

Further, yarns are used to make woven fabrics, and each yarn is made up of coiled fibers. The microstructure of the fibers and the geometrical design of the yarns have a big impact on the mechanical response of woven fabrics. All of these factors influence the fabric's mechanical characteristics and reactivity under various loading conditions, such as tension, bending, and shear. Shear deformation is an important deformation mechanism in woven fabrics, and it is significantly influenced by material qualities and geometrical patterns. The shearing mechanism has a direct impact on the woven fabric's performance by allowing for high flexibility under various loads. As a result, a systematic strategy to investigate the impact of material constants and fabric architecture on fabric mechanical response, particularly during shear deformation, is required. (Keefe & Erol, 2014) modelled the woven fabric at the yarn level. The study target was to explore crimp interchange, yarn-yarn sliding, and locking processes. The woven fabric is modelled at the yarn level under different loading situations (tensile and shear).

Further, (Priyanka et al., 2019) characterized the Kevlar fibers and Kevlar fiber reinforced polymer (KFRP) composites to define the scope of future research in terms of its applicability with optimum design in today's high-tech environment. In diverse applications such as defense, industrial, marine, and aerospace, appropriate characterization was critical for improving material qualities. The focus of this review work was on the mechanical impact and deformation behavior of Kevlar fiber and KFRP composites. Kevlar fibers were used as high-performance reinforcement in polymer textile composites because of their high fracture toughness and high strength to weight ratio. The effect of different parameters such as fabric weaving pattern, matrix material, composite fabrication techniques, working and loading conditions were discussed in detail by researchers using different modelling approaches such as homogeneous isotropic and orthotropic material models, as well as the effect of different parameters such as fabric weaving pattern, matrix material, and composite fabrication techniques, working and loading conditions. KFRP composites had a high ratio of longitudinal tensile to compression strength because to the anisotropic nature of Kevlar fibers, and the compression strength was shown to rose significantly following fiber surface treatment.

2.5 Shear Thickening Fluid (STF) and its development

STF is being used extensively in the field of defense due to its very suitable property of providing flexibility along with the strength and that is a very rare combination. Along with this, it is reversible in nature. It thickens on application of the perturbation and then back to normal state. The reason given for this is due to the formation of 'hydro-clusters' formed by the silica nanoparticles that cause a jamming condition on the application of any strain rate (Boersma et al., 1992). It is also important to understand the procedure for synthesis of STFs. The following methods/ techniques are commonly used:

- The most typical method is by adding the silica nanoparticles to polyethylene glycol (PEG) with a speed of 800 rpm and stirring for around 12 hrs. Later, the suspension solution is put in sonication for 2 hrs. to ensure uniform distribution and no particle aggregation (Yu et al., 2012).

- Acoustic cavitation technique is one of the techniques used to disperse the nanoparticles into the liquid polymers by applying alternate acoustic pressure and using the cavities created in the liquid (Hassan et al., 2010).

- Sonochemical method is also used for the synthesis of STF. Ethanol is used to mix the PEG and silica nanoparticles and irradiated with high intensity ultrasonic horn at a particular temperature. The sonochemcial method has resulted in the production of the improved rheological properties and it is used to develop STF/ethanol solution in a single step (Hassan et al., 2010).

The modification of STF is also done to vary the different aspects. One way of doing this is by using the surface modifiers. Silane coupling agent is one such surface agent that works on by increasing the inter particle friction. (Clements & Mahfuz, 2007) reported improved adhesion properties between fluids and fabrics, which will increase energy dissipation capabilities. Some of the silane coupling agents used in for research are methyl trimethoxy silane and vinyl triethoxy silane (Joselin & Wilson, 2014). The other modification is done by the use of PMMA (PolyMethyl Metacrylate) as the nano particles. It helps in solving the problem of abrading of the fibers when the standard STF is used with the fabrics. This is due to the soft nature of the PMMA. But overall, based on the experiments performed, the performance of the STF is less as compared to the standard STF (silica dispersion). Further,

Wagner et al., 2007 clearly reported that the hardness of the particle plays an important role in the performance of the STF. The other possible modification was done (Ge et al., 2017) by adding silicon carbide nanowires to silica based STF, and the rheological properties showed that the initial and maximum viscosity are significantly improved due to addition of SiC nanowires. At the same time, the viscosity of STF is enhanced with increasing of the content of SiC nanowires.

The effect of temperature on the performance of the STF is studied and reported in the literature. The behavior of STF along with the temperature was also studied by (Tian et al., 2015) In their research, they prepared STF from ethylene glycol and fumed silica, with 20 percent –26 percent weight fractions. The shear rate dependence of viscosity was investigated by using three typical temperatures, ranging from 20°C to 60°C. It was reported that the high temperatures increased the critical shear rate and decreased the shear thickening ratio, according to the temperature testing.

Zhao et al., 2018 experimentally studied the dynamic performance of a self-developed shear thickening fluid (STF) damper, and proposed a mechanical model using nonlinear fitting. An intelligent STF damper was designed and built. (Wei et al., 2018) developed a dynamic model of an STF-filled damper that may been used in controlled engineering applications. Shear stressed at the phase transition of the STF material was used as an internal variable for this purpose.

2.6 Application of STF in Ballistic Protection Armors

The application of STF along with the ballistic fabric is the most investigated method of enhancement of ballistic performance (Fahool & Sabet, 2016; Gürgen et al., 2017; Lee & Kim, 2012; Lee et al., 2003, Joselin & Wilson, 2014; Lee, Kim, & Kim, 2009; Wang et al., 2021; Wang et al., 2020)). The shear thickening fluid is a non-Newtonian fluid with shows smart rheometric behavior at critical shear rate. Many researchers have identified the potential application of STF to improve the ballistic performance of fabric. In most of the experiments, it has been tried to improve the performance of the conventional Kevlar fiber body armor. The reason is to make the jacket much lighter, with higher strength and flexibility. The first study on the application of STF to enhance the ballistic performance was reported by (Lee et al., 2003). They investigated ballistic performance on a sample size of 4.76 cm x 4.76 cm and reported that the impregnated fabric enhances more ballistic performances than the staking of STF filled pouch in between fabric layer. They performed tests on the Kevlar fiber impregnated

with the STF. In the experiment, helium filled gas gun was used for ballistic testing. The penetration v/s velocity graph was also plotted to understand the behavior which appeared to be linear. Along with this, a study on the energy dissipation after the impact was also done. This resulted in observation that the maximum energy was absorbed by the Kevlar impregnated with the STF. The next study performed was to understand the effect of different layer composition using 4 layers of STF and 8 ml of STF such as STF(8ml) K K K K, K K K STF K and similar. In such composition, the best result was displayed by the composition of 4 layers of STF impregnated with the 8 ml STF. The outcomes from the testes performed showed that the impregnated fabrics have less pull-out than the un-impregnated ones. The energy absorption in the impregnated target was likely provided by the first layer of Kevlar, although the backing layers may still have provided a critical secondary role during the impact event. The various configuration of high-performance fabric and STF studied is shown in Figure 2-3.

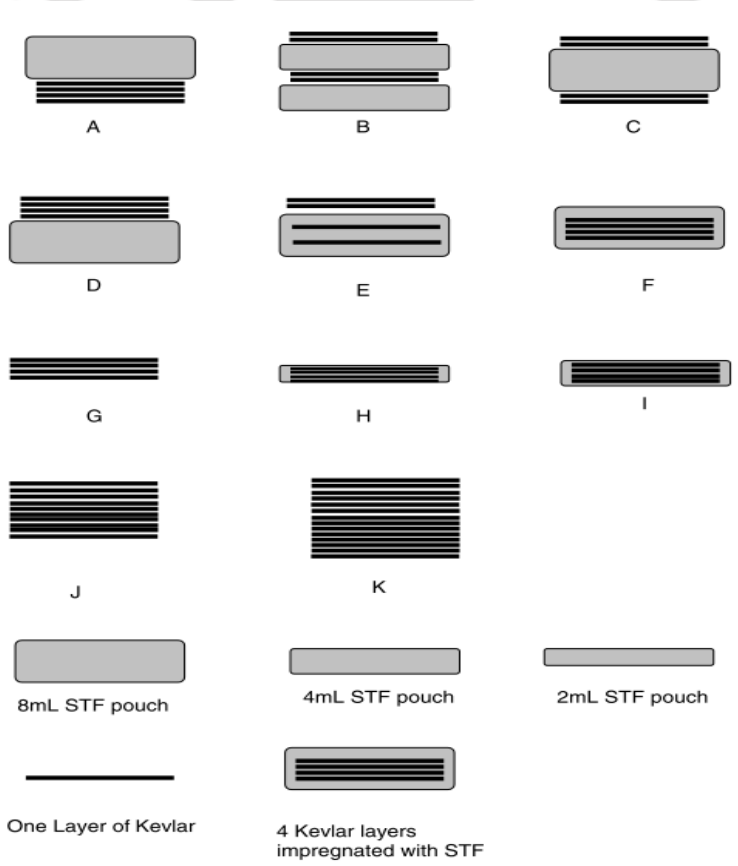

Figure 2-3 Various schematic of studied configuration of fabric treated with STF (Lee et al., 2003)

One such work is done by (Joselin & Wilson, 2014) to study the effect of various compositions on the Kevlar fiber. The tests performed on the Kevlar coated with the STF were divided as

quasi-static and impact loading. This is done in order to understand the behavior of the fiber, their interaction along with the different compositions. The cases were:

- 4 layers Kevlar fabric
- 4 layers Kevlar fabric impregnated with STF
- 4 layers Kevlar fabric impregnated with STF+VITES and
- 4. layers Kevlar fabric impregnated with STF+MTMS.

The quasi-static load test results showed that functionalized/modified were much better than the other two with the scale of 3-4 times and STF+VITES gave the best result. Overall, the functionalized STF based Kevlar fabrics provides more protection, yet it is much thinner and more flexible. The performance enhancement provided by the STF may be due to an increase in the yarn pull out force upon transition of the STF to its rigid state. (Li et al., 2013) proposed a new armour material based on nanocomposites made of Kevlar cloth and slipped thickener made form STF. The STF was synthesized using colloidal silica particles using the Stover synthesis method and then used to prepare suspensions in polyethylene glycol 200 solvent. Finally, the Kevlar material was treated with a suspension and the resulting nanocomposite was named STF-Kevlar. The results showed that the silica particles could been determined as monodisperse spherical particles. Based on the results, on comparing the target properties of multi-layer STF-Kevlar nanocomposites with those of pure Kevlar fabrics showed that STF-Kevlar nanocomposites had improved barrier properties and were more flexible and comfortable. Further, the study briefly describes the mechanisms that could improve the barrier properties of STF-Kevlar. The STF impregnated fabric after experiments by (Li et. al., 2013) is shown in Figure 2-4.

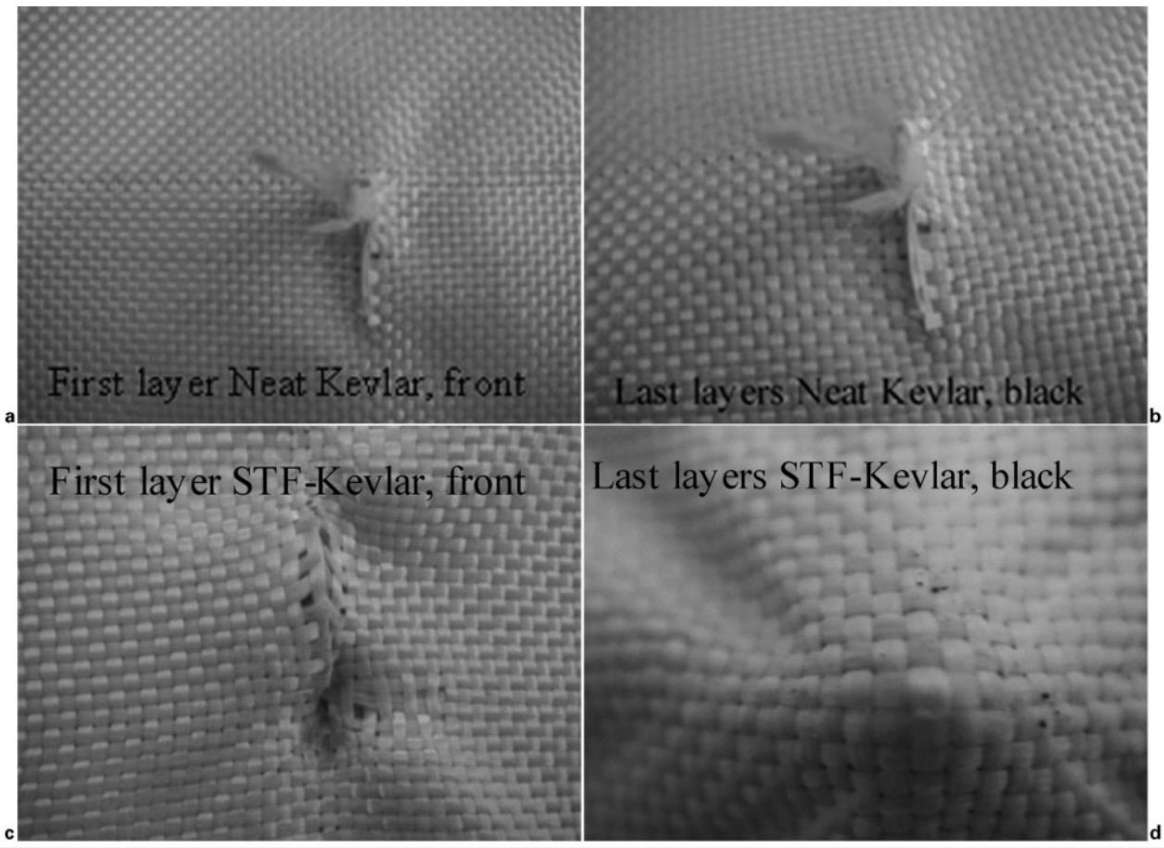

Figure 2-4 Photographs of neat Kevlar and STF–Kevlar nanocomposites after first testing(Li et al., 2013)

Further, Gürgen et al., 2017 created and investigated Multi-phase STFs by varying the amount of silicon carbide (SIC) additives added to silica and polyethylene glycol (PEG) based solutions. Lead core bullets were used with an impact speed of 330 m/s to made ballistic impacts on multi-phase STF treated fabrics. According to the findings, multi-phase STFs improved the ballistic performance of high-performance textiles when compared to single-phase STFs, but fabric mass efficiency suffers under high-velocity impact conditions. Taking his study forward, (Gürgen, 2020) mixed the additional carbide particles into a single-phase STF to create a multi-phase STF, and high-performance textiles were treated with this smart fluid for even better protection. Based on the results from the experiments, the principal effect of the STF was discovered to be an increase in fabric friction. Further in order to verify the experimental observation they a numerical model was made by incorporating the frictional effect of the STF treatments. In terms of target deformations and projectile residual velocities, their numerical findings show a good fit with the experimental results, yielding a correlation index of 0.9691.

In order to understand the mechanical property and energy absorption of the STF impregnated Kevlar (STF/Kevlar) fabric at high strain rate, (Cao et al., 2017) utilized a Split Hopkinson Pressure Bar (SHPB) device to examine the anti-impact mechanism. It was reported that the dynamic mechanical performance of the STF/Kevlar composite was heavily influenced by the volume percentage of STF, the quantity of fabric specimens, and the impact velocity. Further, it was highlighted that when the number of fabric specimens was increased from two to eight layers, the energy transfer rate dropped from 0. 85 to 0. 01. Overall, it was shown that the multilayer Kevlar fabrics impregnated with a high-volume fraction of STF is the best choice for soft body armor. Over that, mechanical property of STF for soft body armor were also investigated by (Wang et al., 2021). In their research, the effect of the temperature on the STF was also considered. It was kept within limits while preparation of sample as well as during testing. By plotting the graph between force and displacement, the graph was divided in three zones namely free diffusion phase (Zone I), viscous flow phase (Zone II), thickening phase (Zone III) and the possible reasons for such behaviors were explained. Along with this, boundary and interface tests were also performed to understand the behavior. In the pull-out, the extent of change in force was observed in the STF from constant value of 1.5 N without thickening to 150 N maximum after thickening. This leads to a very important conclusion that mechanical property of STF is greatly improved due to the thickening of STF.

In the latest development in this direction, (Arora et al., 2020) created traditional soft armour panels using multiple layers of orthotropic high-performance fabrics by stitching symmetrically atop each other. The study investigated the idea of angular stacking of tidy and STF-impregnated woven fabric plies so that the panel responds to an impact in a quasi-isotropic rather than orthotropic manner. Seven sets of 3-, 4-, and 5-layered panels were created by stacking them in varied angular orientations, stitched from plain and STF impregnated p-aramid and ultra-high molecular weight polyethylene (UHMWPE) woven textiles. Based on experimental findings it was observed that the more angular orientations of fabrics within a panel, the better the energy absorbing ability was discovered. It was reported that the favorable effect of angular stacking was more obvious in STF impregnated fabric panels (19% to 58%) than in neat fabric panels, showing the synergistic effect of stressed wave propagation in various directions and secondary yarn engagement through shear thickening. An optimal angular orientation for panels with 3 and 4 layers of fabric plies was proposed which was [0/30/60] and [0/22. 5/45/67. 5], respectively.

2.6.1.1 Numerical Modelling of STF impregnated high-performance fabric

The behavior of STF treated fabric should be properly understood for the design and development of the effective body armour. In order to understand the behavior of STF treated fabric (Majumdar et al., 2013) presented the deformation and energy absorption modes of STF treated and untreated Kevlar woven fabrics when it was hit. They found that only the primary yarns, which were engaged by the impactor contributed in load sharing and thus energy absorption in untreated Kevlar textiles. The yarns slipped at the griped, generating large loops, while the rest of the fabric remains undamaged due to the high stressed per yarn. It was further stated that the energy absorption was modest due to the participation of only a few strands. STF treated fabrics, on the other handed, were turned into a solid-like material during impact. The altered STF functions as a bridging matrix, transforming the fabric's network of yarns into a single structure (Majumdar et al., 2013). Further, it was highlighted that unlike untreated fabrics, the entire fabric contributes in load carrying and energy absorption rather than just the core strands. The rupture of fibers and yarns, rather than their sliding, causes the STF-treated structure to collapse.

Experimental investigation was carried out under different test conditions. The high velocity impact response of composite laminated plates using a nitrogen gas pistol (Ramadhan et al., 2013). A sandwich construction made of Kevlar-29 fiber/epoxy resin and tested with varied stacking sequences of 6061-t6 Al plates was used. Further, to achieve complete perforation of the target, the impact testing was conducted utilizing a cylindrical shape 7. 62 mm diameter steel bullet at a range of velocities (180–400 m/s). Further, a numerical parametric study of ballistic impact caused by the same conditions in experimental work to predict the ballistic limit velocity, energy absorbed by the target were conducted. The comparison between simulation and experimental work using ANSYS AUTODYN 3d v. 12 software, as well as to investigate the effects of projectile shape with different (4, 8 and 12 mm) thicknesses on ballistic limit velocity was also performed. It was reported that the Al backed stacking sequence plate was the best structure to resisted impact loading. Similar kind of work was done by Park et al., (2015) who numerically investigated the high velocity impact energy absorption capabilities of neat and STF impregnated Kevlar fabric, considering the muzzle velocity of current rifles with high performance bullets. The primary energy absorption mechanism of STF impregnated fabric during impact was considered and a numerical investigation of the impact energy absorption characteristics have been reported in the study using the commercial tool LS-DYNA. The friction was assumed between the impact projectile,

fabric, and yarns within the fabric during impact, which was considered as the major factor behind the energy absorption mechanism, with experimentally obtained static and dynamic friction coefficients yielding analysis results in good visual agreement with experimental results. Furthermore, Mirrahimi et al., (2017) conducted numerical investigation on the impact of an ogival tip projectile on a multi-layered plain-woven High Modulus Poly-Propylene (HMPP) fabric impregnated with STFs made up of fumed silica nanoparticles suspended in polyethylene glycol (peg) using LS-DYNA. It was similarly concluded that the friction is main factor in the ballistic performance of the STF treated fabric. Extending the researches above in this direction, (Khodadadi et al., 2017) evaluated the high-velocity impact performance of a composite material made of woven Kevlar fabric impregnated with colloidal STF. It was highlighted that the specific involvement of the STF in the high-velocity defeat process was unknown, and assumed that the enhanced frictional interaction between yarns in impregnated textiles have been the cause of improved performance. The fabric was modelled using LS-DYNA to characterize the frictional behavior of the STF impregnated fabric, utilizing the experimental data of yarn pull-out experiments. Similar conclusion like other researchers were drawn reported that the enhanced friction was responsible for the improved performance of STF impregnated Kevlar fabric. The predicted deformation through numerical modelling by (Khodadadi et. al., 2017) is shown in Figure 2-5.

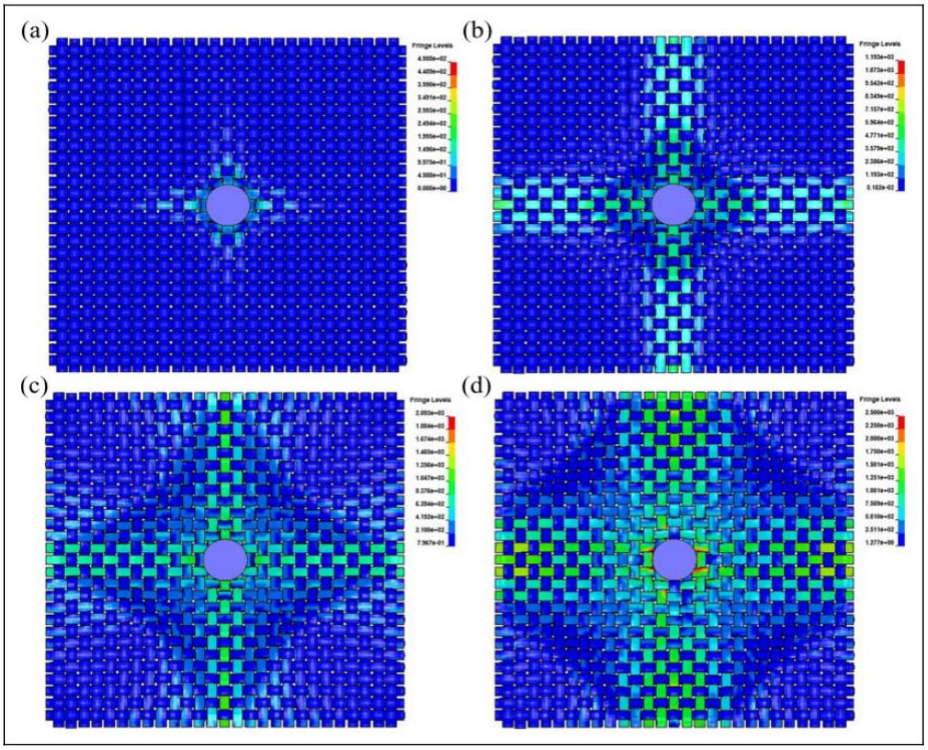

Figure 2-5 Predicted deformation characteristics of STF fabric for various impacts (Khodadadi et al., 2017)

The impact resistance capabilities of woven High Modulus PolyPropylene (HMPP) textiles impregnated with Shear Thickening Fluid (STF) comprised of fumed silica nanoparticles suspended in polyethylene glycol was varied out by researchers (Hasanzadeh et al., 2017) experimentally. Numerical modelling was done using LS-DYNA to model the impact of an ogival tip bullet on four-layered textiles. The friction between the yarns and their crossovers, as well as the friction between the projectile and the fabric during impact was considered while evaluating the effect of STF impregnation on fabric. The research emphasizes that the frictional characteristics is the main contributing factor in the enhancement of the ballistic performance of the fabric.

The challenges of replacing the rigid ballistic inserts with more flexible material without damaging the armor's strength was investigated (Sen et al., 2019a) and (Sen et al., 2019b). It was highlighted that the STF is a promising substance in this context. The research attempted to examine the possibilities of STF in such applications statistically. Two Kevlar-STF composite targets comprised of Kevlar-STF-Kevlar sandwich composite and STF impregnated Kevlar were manufactured this purpose. The composite's ballistic response using the coupled Eulerian–Lagrangian (CEL) method was investigated. In the study, the Kevlar®

yarn was represented using a Lagrangian membrane element in the CEL method, and STF was incorporated in a Eulerian mesh.

2.7 STF encapsulated in uniform and random bubble wrap

The search of an effective configuration which can perform efficiently under ballistic impact is an ongoing process. The STF encapsulated bubble wrap configuration could be a promising configuration. In this configuration, STF is encapsulated within bubbles made of high-performance flexible material having minimal bending and torsional stiffness. This configuration is light-weight, flexible and perform better than its counterpart. (Zhang et al., 2017) investigated encapsulation of STF for easy handling and re-processing. The encapsulated STF was supposed to be impact-resistant material. Double- walled macroscopic STF capsules were synthesized using a convenient process by instilling diluted STF droplets into reaction solution. The STF capsules show good shear thickening response to dynamic impact in comparison to quasi-static compression (154 times higher absorbed nominal strain energy). (Liu et al., 2019) encapsulated STF using orifice coagulation bath method, in an attempt to improve the combination of STF and the matrix as well as strengthen the flexibility and stability of the STF composites. (Huo et al., 2020) prepared a graded buffer composite by using STF capsules, Poly-Urethane (PU) foam, and low-melting point PET fabric or spacer fabric with improved energy absorption performance. These studies emphasize the STF encapsulation for the better alternative energy absorbent composites. The encapsulation will not only provide better ballistic impact performance but it will also provide better stability to the fluid itself. **There is need to extensively characterize STF encapsulated configuration under ballistic impact and the same is developed in this thesis.**

2.7.1 Modelling of Shear Thickening Fluid

The numerical analysis of incompressible non-Newtonian fluid flowed through a symmetric abrupt expansion is proposed by (Ternik et al., 2006) and the same was used to determine the critical value of the Reynolds number. To account for the shear-thickening behaviour of the corn-starch and watered mixture, a quadratic model was used. It was validated using the results from the Newtonian fluid flow in a range of Reynolds numbers. In addition, it was compared to the results from Quadratic model to those produced using the Power law. (Aradian & Cates, 2005) proposed a STF model with a tendency to combine the inhomogeneous, shear-banded flowed and sluggish fluid microstructure relaxational dynamics.

Periodic regimes (oscillating bands, travelling bands, and more complex oscillations) and spatiotemporal rheochaos result from the interaction of these components were compared. Even though the steady-state flowed curve was monotonous, these events might arise due to constitutive nonlinearity rather than inertia. In a low-dimensional truncation, where sharply defined shear bands could not emerge, the model also reveals rheochaos.

Johnson et al., 2017 studied to predict the shear thickening behavior in order to avoid the wear and tear in the industries. A strategy was provided regarding how to model these processes used a particle-scale numerical approach. A micromechanical model was created that could simulate interparticle stresses for particles immersed in a fluid by combining the discrete element method (DEM) with the lattice Boltzmann method (LBM). It was demonstrated the potential of method as a researched tool by a comparison of simulation findings to experimental results. A parametric study to explore the impacts of solid fraction, particle-particle, and particle-wall contact stiffness was conducted. DEM-LBM model was proposed which shows that increasing boundary stiffness directly raises the maximum shear stressed of the shear thickening regime when the wall stiffness was varied in a systematic way. It was shown that, according to traditional soil mechanics principles, the key mechanism causing shear thickening was particle medium dilatation. (Arora et al., 2017) predicted the rheology of the STF over a wide range of shear rate at different temperatures using phenomenological and artificial neural network (ANN) models. The rheological behavior of STF was investigated with 65 percent (w/w) silica nanoparticles with polyethylene glycol (PEG) as the dispersion medium at various temperatures. The STF viscosity for all zones in both models was investigated, with good match between experimental and predicted viscosity for both training and testing data sets. (Gürgen & Sofuoğlu, 2020) studied the effect of STF in machining tools and developed a mode to predict the behavior of shear thickening fluid. The STF was integrated into standard cutting tools for turning operations, resulting in a unique tool. The non-Newtonian rheology of STF helps to the vibration dampening capabilities of cutting tools, minimizing chatter vibrations during machining operations, based on the improved design. As a result, STF integrated cutting tools improve the stability of operations, resulting in better workpiece surface quality.They examined the rheology of multi-phase STF using an intelligent model in this studied. Intelligent modelling was particularly efficient, according to the results, due to its parameter-free approached and good fitting capacity.

2.8 Modelling in LS-DYNA

There are several platforms to perform numerical modelling of ballistic events such as LS-DYNA, ABAQUS, ANSYS AUTODYN and similar. This section will briefly review about modelling approach using a commercially available program LS-DYNA developed by Livermore Software Technology (LSTC). Based on official website of the developer LS-DYNA is a general-purpose finite element program capable of simulating complex real-world problems. It is used by the automobile, aerospace, construction, military, manufacturing, and bioengineering industries. The code is developed mainly for highly non-linear, transient dynamic finite element analysis using explicit time integration. There is several studies conducted using LS-DYNA program in various field such as (Barauskas & Abraitienė, 2007; Chatla, 2012; Klöppel et al., 2013; Souli et al., 2008; Vesenjak et al., 2008) and shows the robustness of the program.

Different numerical studies about the protection of fiber reinforced concrete pieces under blast loads and fragments was taken up (Ågårdh, 1997). An accurate FE model of the behavior of such elements when subjected to transient dynamic loads was developed. More and more people concerned about industrial accidents and/or terrorism are interested in modelling structures' response to blast loads. Two most common approaches available today are: an ALE model (*ALE) with a Lagrangian-Eulerian coupling (*constrained Lagrange in solid) or a pure Lagrangian approached in which the propagation calculation was replaced by an analytical loading of the structure. Because only the structure was modelled, the Lagrangian technique allows for a significantly smaller model. This technique is now accessible in LS-DYNA (*load_blast), and was based on the empirical model provided in the (TM 5 855, 1986) us army manual (CONWEP). It was, however, confined to the treatment of hemispherical charge explosions on the ground or spherical charge explosions in the air without ground interaction. The interaction of the shockwave with the earth caused blast reinforcement in several circumstances. CRIL technology had created a new user-loading model (evolution from *load blast) to took into consideration new abacuses for TNT and reflecting coefficients, ground effects, and Mach stem in ordered to produce a more exact blast load evaluation with a pure Lagrangian approached (Blanc et al., 2005). The (TM 5 1300, 1990) us army handbook describes empirical models for major evolutions. This method is solely based on Lagrangian approach. As such, this novel user-loading often results in a more exact and conservative load while maintaining a fair model size.

The fluid-structure interaction was investigated using different techniques in LS-DYNA (Vesenjak et al., 2008). The experimental observations of a fluid sloshing problem in a simple container box was compared to different formulations (Lagrange, Euler, ALE, and SPH). It was concluded that the ALE and SHP approaches in LS-DYNA could also best represent the fluid motioned, according to computational simulations. (Arriaga et al., 2010) studied the Perzynas model, which was sensitive to the rate of viscous-plastic deformation. LS-DYNA MAT_24 material model was used to evaluate the dependence on yield stress, and MAT_19 to evaluate the dependence on yield stressed and modulus of elasticity. It was in good agreement.

The modelling of massive deformation processes and highlighted the numerical issues caused by element distortions limit the application of a Lagrangian description of motioned (Souli et al., 2008) studies. The multi-material Eulerian formulation was an alternate technique in which the material flowed through a mesh that was fixed in space and each element was allowed to include a mixture of different materials. This method totally avoids element distortions and could been paired with a Lagrangian description of motioned for parts of the model used a Eulerian-Lagrangian coupling algorithm. Numerical issues abound in the Eulerian formulation. With the passage of mass between elements, there were issues of dissipation and dispersion. Furthermore, the Eulerian mesh may require a large number of elements to enclose the entire location where the material had been placed throughout the simulated event. The multi-material arbitrary Lagrangian-Eulerian (ALE) formulation excels in this situation. The mass flux between elements could been decreased and the mesh size could be kept smaller than in a Eulerian model by translating, rotating, and deforming the multi-material mesh in a controlled manner. The research presents a new fluid structure coupling algorithm based on the penalty method. Further, LS-DYNA had become an effective tool for evaluating massive deformation processes, such as bird attacked events, forging operations, penetration problems, and airbag simulations, thanked to its coupling method and increased multi-material ale capabilities.

The dynamic mechanical behavior of aluminum alloy such as the 7075-t6 was investigated by researchers (Zhang et al., 2015). Various load rates through dynamic tensile testing with a comprehensive electronic tester, high speed testing system, and Hopkinson tensile strength (SHTB) was implemented. The results indicated that the stiffening effect of the 7075-t6 aluminum alloy was significant. By changing the cure time of the Johnson Cook base model, the new Johnson Cook (JC) model made from a 7075-t6 aluminum alloy was obtained.

Numerical simulations of tensile tests at various speeds using the Johnson Cook base model for the 7075-t6 aluminum alloy was performed. (Khodadadi et al., 2017) studied and presents the rapid impact resistance of a composite material made from a woven Kevlar fabric impregnated with colloidal shear thickening fluids (STFs).

2.9 Discussion and Limitation of the State of Art

In this Chapter, detailed literature review related to the theory, and development of light-weight ballistic body armour was presented. The literature begun with the general practices in the development of the ballistic armour and presented how ceramic based armour is developed to reduce the weight of the armour with its contemporary material steel. The ceramic based armour show best ballistic performance and have light-weight but they are not flexible enough to provide the comfort to the wearer. Moreover, to make ceramic based armour wearable, traditionally high-performance based fabric is used to make torso where ceramic based plates were inserted. With progress, it was felt that instead of using ceramic plate as an insert there could be any potential system which could replace ceramic pates. Further, different studies have been conducted to enhance the ballistic performance of the fabric. Meanwhile numerous theories were proposed related to understanding the behavior of ballistic impact and performance of the high-performance fabric. Mainly, these theories highlight about the dissipation of kinetic energy of the projectile. These theories emphasized that the energy dissipation will be more if the strain wave will travel longer before failure. In view of this, many research articles were published where researchers emphasized on enhancing the inter-yarn friction of the fabric. There was a believe that high inter-yarn friction will stop the slippage between yarns and more strain wave could travel longer within the armour system. In this regard, the first proposal was to utilize some agents which can enhance the inter-yarn friction of the fabric. Initially a dilatant powder was investigated and suggested by many researchers. In 2003, the use of non-Newtonian dilatant fluid impregnated with high performance fabric was proposed. Several experimental studies were carried and reported but they were not sufficient to make a guideline in the design of the ballistic armour using STF impregnated high performance fabric. Further, many researchers proposed to use simulation-based technique to design STF impregnated ballistic armour. One of its kind is friction-based modelling of STF impregnated fabric. But this technique involves complex procedure such as determination of inter-yarn friction through utilizing semi-empirical based methods where one needs to find an experiment results from pull-out test and then through numerical simulation inter-yarn friction

should be determined. Further, the way of harnessing the potential of the STF is highlighted in the literature. The manufacturing of STF based encapsulated tubes/bubbles is studied and presented in the literature. But the application of STF encapsulated bubbles in ballistic impact scenario is limited. Further, there were no design guidelines and methodologies are available in the open literature related to the development of light-weight and flexible armour. In this thesis these untouched scopes will be explored and presented.

3 Ballistic performance evaluation of the high-performance fabric due to inter-yarn friction

3.1 Introduction

The high-performance fiber-based fabric such as S-glass® (glass), Kevlar® (aramid), Spectra® (high molecular weight polyethylene), Zylon® (PBO), and M5® (PIPD) is the obvious choice in the development of soft ballistic armour due to its high strength to weight ratio. An extensive study carried on the ballistic impact characterization and understanding of penetration mechanism in the ballistic fabric is presented in literature (Barauskas & Abraitienė, 2007; Bazhenov, 1997; Briscoe & Motamedi, 1990; Cunnif, 1992; Duan et al., 2005; Duan et al., 2006; Kirkwood et al., 2004; Kirkwood et al., 2004; Nilakantan & Gillespie, 2012; Zeng et al., 2005; Zeng et al., 2006). The ballistic impact performance and penetration mechanism depend upon fabric architecture, mechanical properties of the fiber, and boundary conditions applied in the testing methods. Also, there have been experimental and numerical studies reported in the literature where their findings suggest a significant improvement in the ballistic performance of the fabric through impregnation in the non-Newtonian dilatant fluid. The non-Newtonian dilatant fluid is widely known as Shear Thickening Fluid (STF). The STF shows the sudden increase in the resistance through enhanced dynamic viscosity above a critical shear rate.

The numerical investigation of neat and STF impregnated fabric systems under impact is based on frictional effects between inter-yarn and between projectile and fabric (Gürgen, 2020; Hasanzadeh et al., 2017; Lee & Kim, 2012; Park et al., 2015). The effect of STF was assumed to be due to the enhancement of the inter-yarn friction in the modelling approach by many researchers of STF impregnated. Many researchers have modelled the effect of STF on fabric by enhancing frictional co-efficient in the inter-yarns. In order to study the ballistic performance of the STF fabric, it is essential to perfectly model the fabric, which should capture the effects of parameters to the ballistic impact. There are many multi-scale methods proposed to model the fabrics. The membrane or micromechanical model has been proposed by (Tanov & Tabiei, 2002), (Ivanov & Tabiei, 2004) and; (Ivanov & Tabiet, 2002). There are limitations of the developed micromechanical model of the fabric based on continuum theory. They are not able to capture the behavior due to fiber-fiber interaction, filament-filament interaction, and yarn-yarn interaction. So, the micromechanical model cannot be used to study the effect of friction on the ballistic performance of high-performance fabrics. In order to mitigate the limitation of micromechanical or membrane level modelling, researchers have proposed yarn level modelling, also known as mesoscale modelling. A 3D finite element analysis model was created by (Duan et al., 2006) using LS-DYNA to simulate the transverse impact of a rigid right circular cylinder onto a square patch of plain-woven Kevlar

fabric. The fabric model had a resolution at yarn level, and relative motion between yarns was allowed. The friction between yarns was implemented through frictional contact between yarns and between the fabric and the projectile. The effects of inter-yarn friction on the ballistic performance of woven fabric armour were investigated by (Zeng et al., 2006). The parametric studies show that the ballistic response of woven fabric is very sensitive to yarn friction when the friction coefficient is low but insensitive beyond a certain level. Moreover, their study showed that very high inter-yarn friction can lead to premature yarn rupture, thus reducing the ability of the fabric to absorb impact energy. (Rao et al., 2009) studied the impact of a rigid sphere onto a high-strength plain-weave Kevlar KM2® fabric and carried out the numerical analysis in LS–DYNA. The influence of friction and material properties on ballistic performance was considered. In the study, yarns were modelled as continua with modulus and strength dominating along the length. The study showed that the ballistic performance depends upon friction, elastic modulus, and strength of the yarns. The friction improves the ballistic performance by maintaining the integrity of the weave pattern; the material properties of the yarns have a significant influence on the effect of friction. (Grujicic et al., 2010) developed and implemented a mesoscale ballistic material model for a prototypical plain-woven single-ply flexible armour in a material user subroutine for use in commercial explicit finite element programs. The primary intent of the model was to attain computational efficiency when calculating the mechanical response of the multi-ply fabric-based flexible-armour material during its impact with various projectiles without significantly sacrificing the essential physical aspects of the fabric microstructure architecture and behavior. (Minh et al., 2012) proposed yarn level numerical model of ballistic impact on a two-dimensional Kevlar KM2® plain-woven fabric and validated through experiment. (Nilakantan et al., 2013) studied the effects of size and shape of the projectile on the impact response of a single-layer fully-clamped flexible woven fabric. A numerical finite element study on a yarn-level fabric model with a deterministic implementation of experimental mean yarn tensile strength and inter-yarn friction was carried out. There had been studies on micro-scale modelling or fiber-level modelling of the fabric. These require very high computation power in fiber-level modelling. In order to investigate the ballistic performance of the STF impregnated fabric, it is suggested to utilize the yarn level modelling of the fabric to reduce the requirement of high computational power. Furthermore, there has been very limited understanding of behavior of fabric at very high inter-yarn coefficients though there has been extensive numerical investigation carried and reported. In open literature, in best of authors review, very few studies are reported for the optimum ballistic behavior of fabric at varying coefficients of friction such as (Wang et al., 2016), (Zeng et al., 2006). (Nilakantan & Gillespie, 2012) reported that there is a decrease in the impact performance while increasing inter-yarn friction coefficients for four-sided clamped boundary condition while ballistic performance is increasing with increase in the inter-yarn coefficients for the two-sided fixed boundary condition.

The present study aims to provide insight into the understanding of ballistic performance of the fabric due to variation in the inter-yarn friction using numerical technique. As there is change in the inter-yarn friction due to STF treatment to the fabric, this study also tries to correlate the varying inter-yarn friction with practical application such as STF treated fabric.

3.2 Numerical modelling and validation

3.2.1 Geometric Modelling

The yarn level resolution (mesoscale modelling of the fabric) is used to model the entire fabric in the present investigation. The yarns are modelled as continua and can be modelled as planar 2D surfaces. To enhance accuracy, yarns can be modelled as 3D solid elements and a combination of shell and solid elements known as hybrid element analysis. (Nilakantan et al., 2010) has modelled yarn of the plain weave fabric using fully shell element, fully solid element (baseline), and hybrid element (multi-scale models consists of yarns as solid elements in region R1 near contact and premises of projectile, yarns of shell elements in region R2 and continuous fabric of shell element in region R3. There is a significant deviation in the numerical results of non-penetrating and penetrating projectile velocity between yarns modelled as fully solid element (baseline study), fully shell element, and hybrid element analysis (HEA). Also, as per the reported results, HEA overestimates the energy dissipation compared to yarns having a shell and solid element for penetrating projectile velocity.

The yarn model having six elements across their width produces close estimates of residual velocity to the baseline study compared to four elements across the width. The possible reason could be effectively representing yarn cross-section using six elements as compared to four elements. However, due to the very high computational requirement, the present study presents the modelling of yarn using 2D shell elements having four elements across the width. The four elements across the width are sufficient to capture fabric's behavior under the ballistic impact, and for the same, a validation with experimental results is presented. The experimental data are obtained from (Lee et al., 2009) and (Lee & Kim, 2012). The geometry of the mid surface has been modelled using the sinusoidal function. Many researchers reported that the equation for the mid surface of the yarn would follow sinusoidal characteristics and sufficiently represents the crimp of the yarn. LS-PrePost® is used to model the yarn geometry and mesh of plain weave fabric. The yarns per inch (fabric sett) and cross-over of the yarns in weft and warp directions have been modelled and kept the same for warp and weft. The schematic of yarn cross-over, modelling of yarn cross-section, and shell-based modelling of yarn is shown in Figure 3-1.

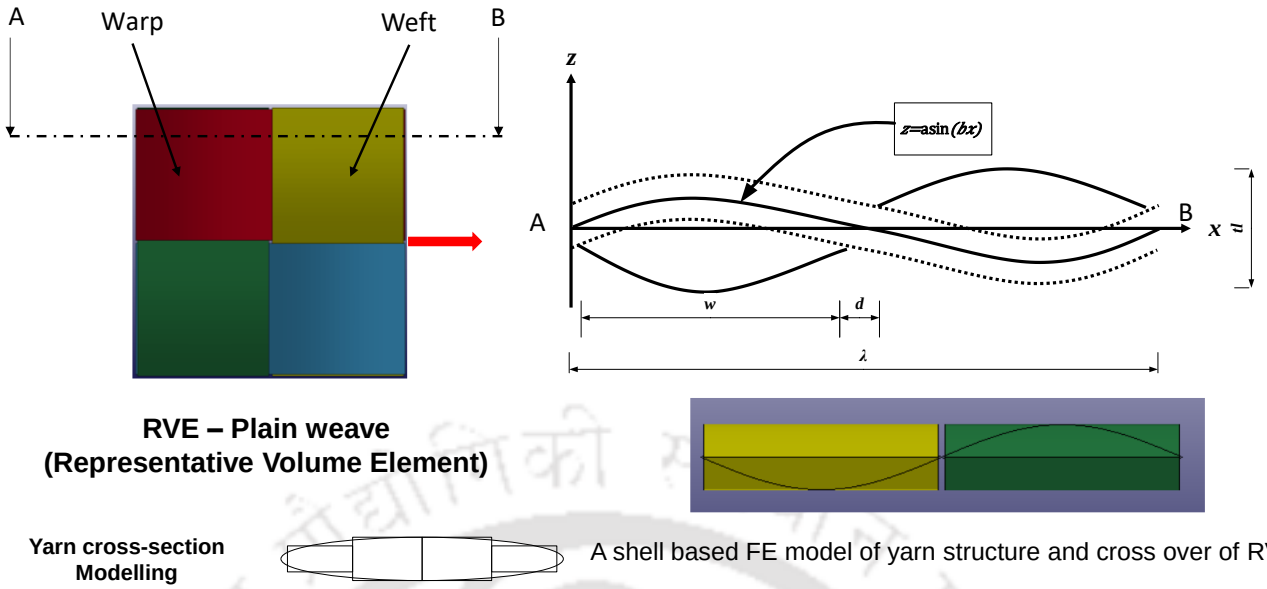

Figure 3-1 Representative volume element showing yarn crimp, and cross-section modelling of the yarns.

The geometrical parameter of the mesoscale model of a plain weave fabric shown in Figure 3-1 is summarized in Table 3-1 for different fabric sett. These geometrical parameters are theoretically designed and calculated using TexGen® (a dedicated python-based platform for fabric modelling). In the present study, the quarter model of the fabric has been used due to symmetry and save computational efforts. The fabric model and representative volume element designed using TexGen with different fabric sets are shown in Figure 3-2.

Table 3-1 Geometric properties of plain weave fabric.

Fabric sett	**Yarn density (n/inch)**	**λ (mm) (50.8/n)**	**b (2π/λ)**	**a (mm)**	**w (mm)**	**d (mm)**
25x25	25	2.03	3.09	0.11	1.0	0.02
30x30	30	1.69	3.71	0.11	0.8	0.02
35x35	35	1.45	4.32	0.11	0.7	0.02
40x40	40	1.27	4.95	0.11	0.6	0.02
45x45	45	1.12	5.56	0.11	0.5	0.02
31x31	**31**	**1.64**	**3.83**	**0.11**	**0.8**	**0.02**

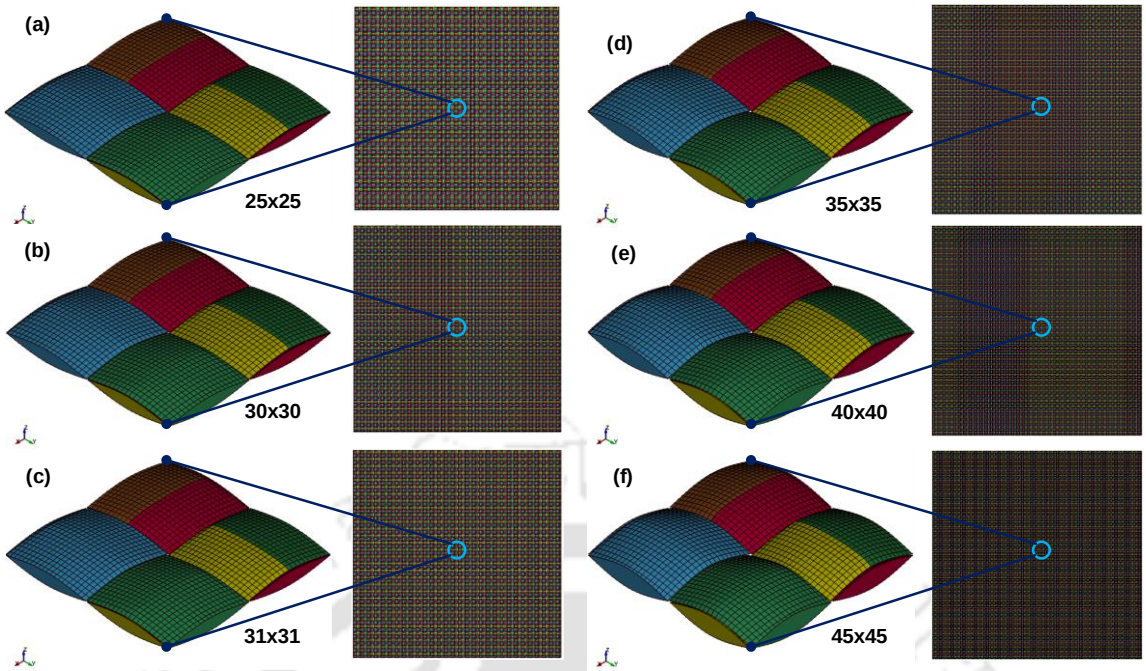

Figure 3-2 Representative volume element and quarter FE model of plain weave fabric of varying yarn density.

3.2.2 Material and Contact Modelling

In order to study the ballistic performance of the fabric, it is essential to characterize the fabric material mechanically. In this study, the mechanical properties of para-aramid-based Kevlar KM2® have been used. (Cheng et al., 2005) studied the mechanical properties of Kevlar KM2® at a single fiber level. The mechanical properties suggest that the Kevlar KM2® behaves as a linearly elastic and transversely isotropic material till failure. The constitutive relation in the modelling of Kevlar fiber is strain rate independent because the stress-strain curve is independent of the applied strain rate. The required number of material constants for a linear elastic and transversely isotropic material to describe its stress-strain response are five. In order to model the constitutive behavior, this study uses material model MAT_02_ORTHOTROPIC_ELASTIC in a commercial program LS-DYNA®. This material model represents linear elastic and transverse isotropic properties till failure criteria satisfies. The material properties utilized in this study is obtained from (Cheng et al., 2005) and presented in Table 3-2. The failure of the yarns is achieved using von-mises based failure criteria and implemented through defining maximum effective stress and failure strain in the MAT_ADD_EROSION card. The von-mises stress value is given in Table 3-2 as Tensile strength.

Table 3-2 Mechanical Properties of Kevlar KM2® (Cheng et al., 2005)

Fabric	Properties	Symbol	Value (Unit)
Kevlar KM2®	Young's Modulus	E11	84.62 (GPa)
		E22= E33	1.34 (GPa)
	Shear Modulus	G12=G13=G23	1.34 (GPa)
	Poisson's Ratio	υ12= υ13= υ23	0
	Density	P	1.44 (g/cc)
	Tensile Strength	Warp/weft	3.9 (GPa)
	Failure Strain	Warp/weft	4.5 (%)

The contact modelling between yarns crimp are implemented using contact card CONTACT_AUTOMATIC_SURFACE_TO_SURFACE. This contact type is the most recommended for the crashworthiness analysis. The effect of friction is implemented using coefficients of friction between inter-yarn. The friction between inter-yarns are modelled using Coulomb's friction model and implemented through CONTACT_AUTOMATIC_SURFACE_TO_SURFACE. The equation of Coulomb's friction model is given in **(3-1)**.

$$\mu = \mu_d + (\mu_s - \mu_d)e^{-C|v_{rel}|} \quad (3\text{-}1)$$

The magnitude of dry friction basically depends on the relative velocity of the surface in the contact and the above equation is implemented in the contact model. Further, the effect of inter-yarn friction on the ballistic performance of the fabric is studied through linearly varying static and dynamic coefficients of friction between inter-yarn from (0.1-0.6).

3.3 Validation of numerical model

The fabric model used in the present study is validated through experimental data from (Lee & Kim, 2012). The literature uses a plain weave fabric model at yarn level resolution. The numerical model of fabric contains a yarn density of 31 and a yarn cross-section of the lenticular shape. The geometric details about yarn crimp and other parameters are given in Table 3-1. The central line of the yarn crimp is assumed as sinusoidal and shown in Figure 3-1 and Figure 3-2. The modelling of fabric samples of size 101.6 x 101.6 mm^2 uses the benefit of symmetry, and a quarter symmetric model of size 50.8 x 50.8 mm^2 is developed. A plane-symmetric boundary

condition is applied to create a quarter model. These boundary conditions assume that there will be no out-of-the-plane motion at the symmetric plane, and hence one translational and two rotational degrees of freedom are restrained to the nodes in the symmetric plane. The yarn is discretized using quad shell elements. In order to approximately represent the lenticular yarn cross-section, a total of 4 shell elements is provided across the width of the yarn. The inter-yarn friction is implemented and the coefficients of friction for neat as well as STF treated fabric is provided to the contact model. The parameters of Coulomb's friction model such as coefficients of the friction and exponents for neat and STF treated fabric is given in Table 3-3 Parameters of Coulomb's friction model (Lee & Kim, 2012).

Table 3-3 Parameters of Coulomb's friction model (Lee & Kim, 2012)

Parameter	**Neat**	**Without STF-Effect**	**STF Effects**
μ_s	0.15	0.33	0.79
μ_d	0.12	0.41	0.87
C	1.23	0.21	0.82

A rigid spherical projectile of diameter 7.62 mm and mass 5.52 g is projected at designated orthogonal velocity towards the target. A quarter projectile is modelled, and its motion is restrained in all degrees of freedom except in the direction towards the target. In the experiment, the target fabric was clamped at two edge and two edge free and for the validation similar boundary conditions are applied at the edges. In order to validate computational model for the wide range of velocity numerical simulation are conducted for velocities varying from 82 to 389 m/s. The numerical results obtained from computational model is shown in Figure 3-3 and Figure 3-4 and compared with the experimental data from (Lee et al., 2012); and found in good agreement. The residual velocity and kinetic energy absorbed is deviating more for low velocity of projectile as compared to the results at high velocity of the projectile. The residual velocity and kinetic energy absorbed for the neat fabric case at different initial velocity of the projectile is shown in Figure 3-3 and Figure 3-4.

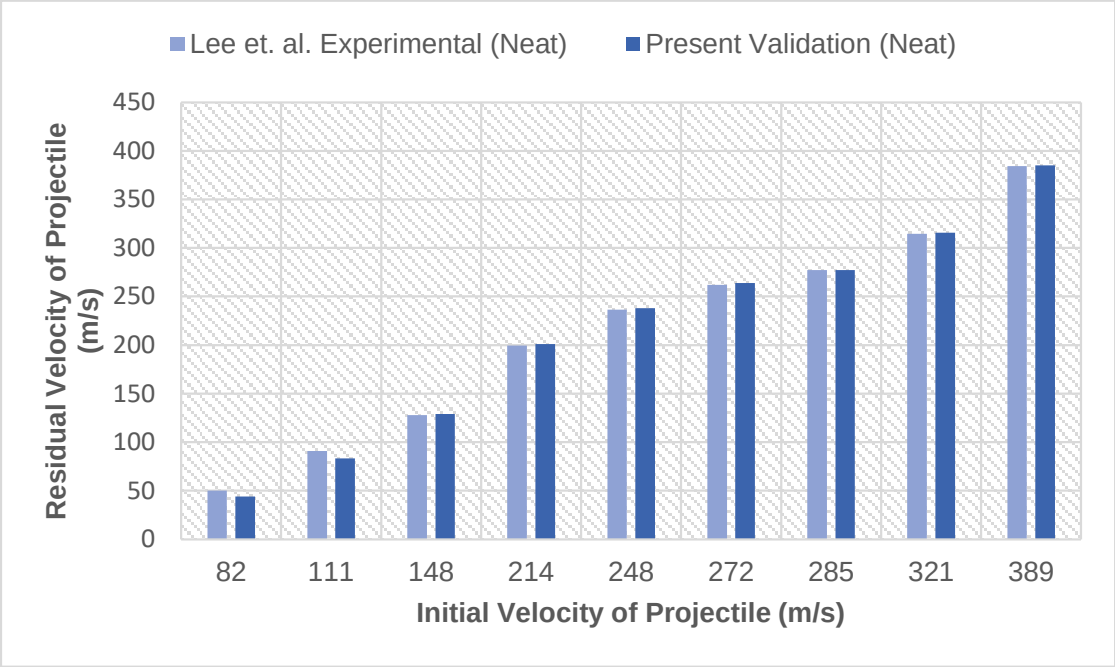

Figure 3-3 A graphic comparison of residual velocity of a projectile for neat fabric.

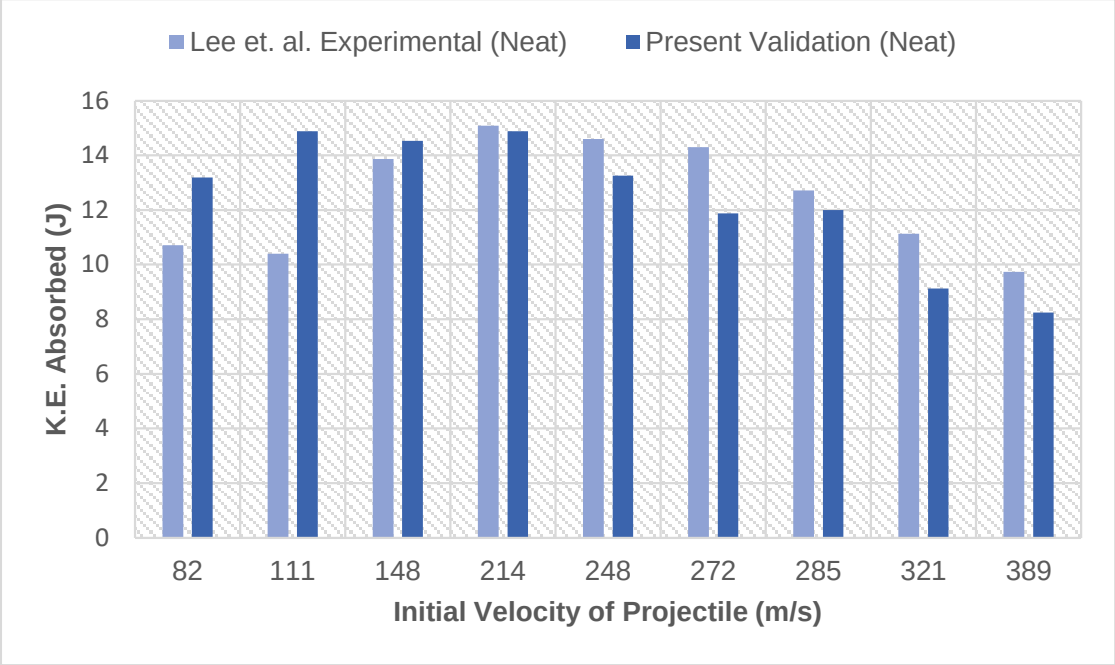

Figure 3-4 A graphic comparison of absorbed kinetic energy of a projectile for neat fabric.

The numerical validation is carried on different inter-yarn coefficients of friction. The inter-yarn coefficients of friction for this case is supposed to mimic the characteristics of STF treated fabric. The residual velocity and kinetic energy absorbed for three different case neat, without STF characteristic, and with STF characteristic is shown in Figure 3-5 and Figure 3-6

respectively. These figures show that at higher coefficients of friction the computational model is obtaining closer results as compared to the experimental results at projectile velocity 214 m/s.

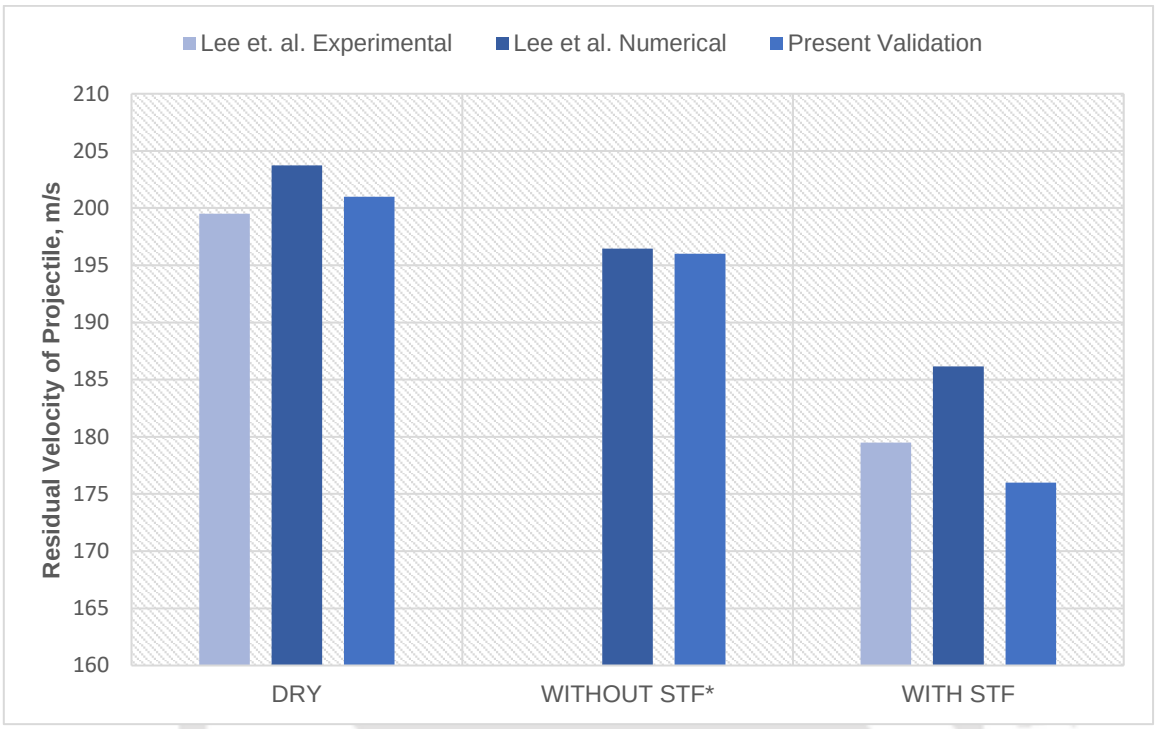

Figure 3-5 A graphic comparison of residual velocity of a projectile at 214 m/s for dry fabric and STF impregnated condition.

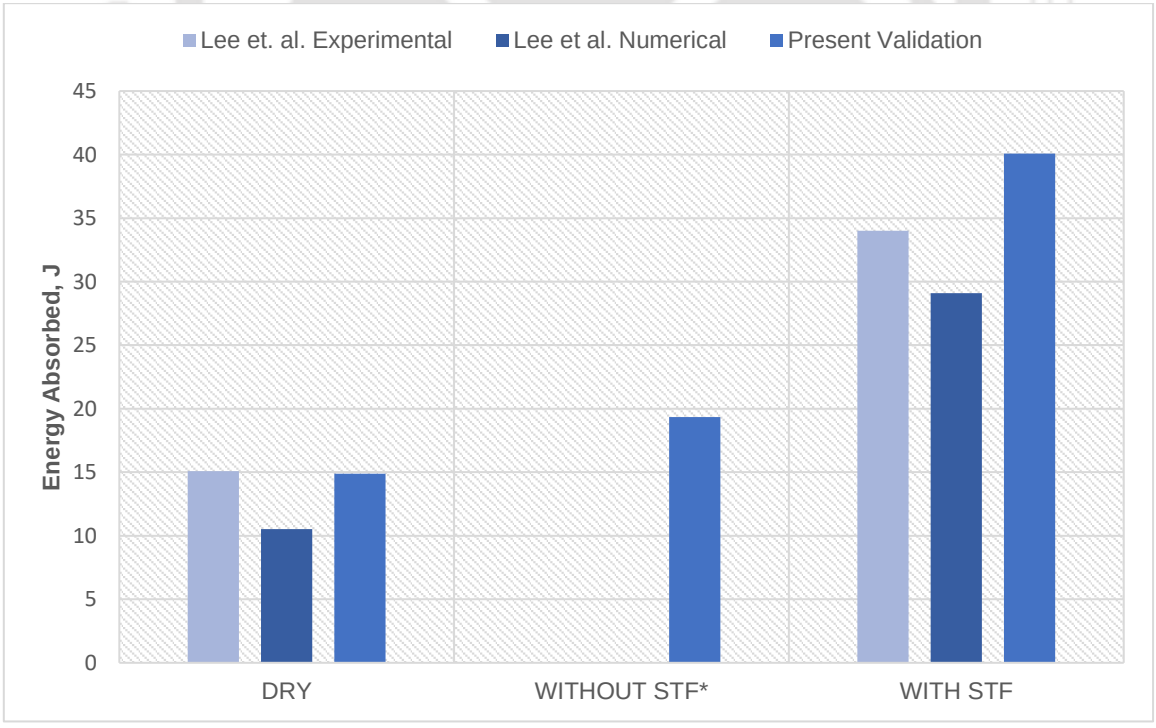

Figure 3-6 A graphic comparison of residual kinetic energy of a projectile at 214 m/s for dry fabric and STF impregnated condition.

The modelling approach discussed and validated in this section are applied on the single layer of fabric having varying fabric sett and coefficients of friction as discussed earlier.

3.4 Effect of inter-yarn coefficient of friction on ballistic performance of fabric

This section presents the numerical results obtained from the single layer mesoscale fabric model. The boundary conditions applied in this investigation is two sides fixed. The yarn density of the fabric is varying and their geometric parameters are given in Table 3-1. The validated numerical model of fabric considering effect of inter-yarn friction is further extended to study the effect of varying inter-yarn coefficient of friction. In present study, the coefficient of friction is in the range of (0-0.6). The aim of this study is to find out the optimum value of friction at which the ballistic performance is either not enhancing or start degrading. In present study the coefficient of friction varies in the range of (0-0.6).

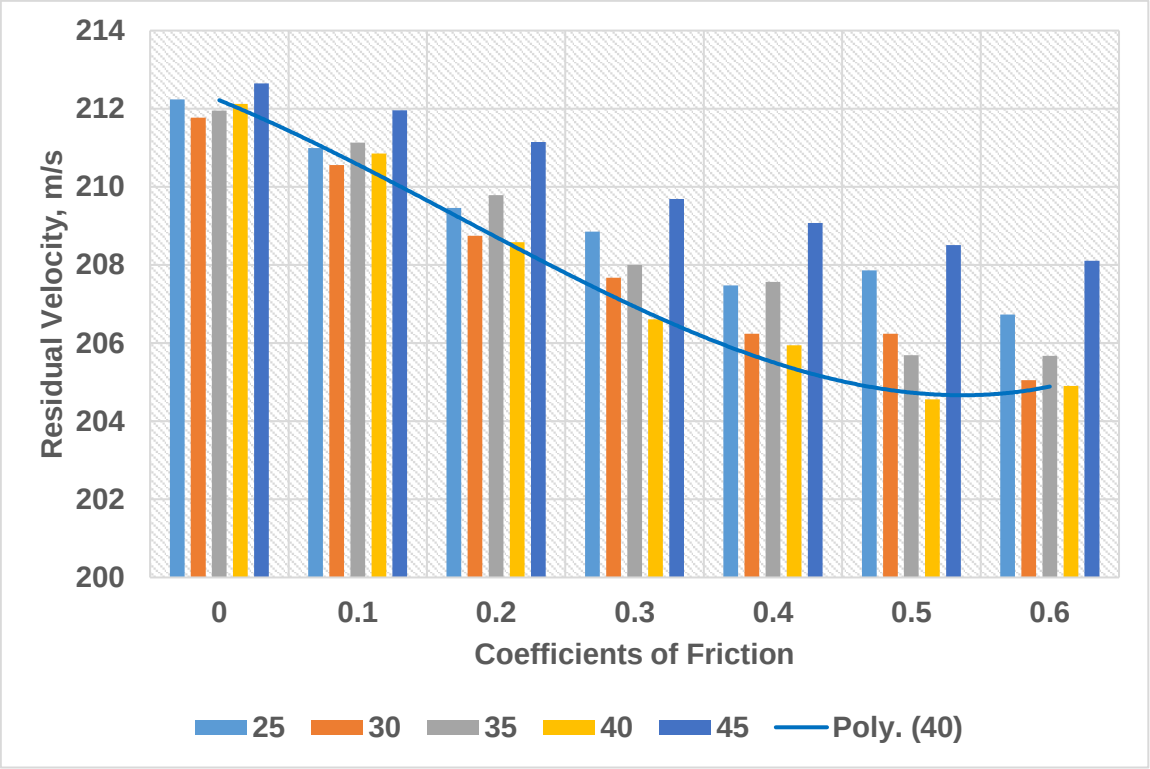

Figure 3-7 Residual velocity of a projectile at 214 m/s for different fabric sett and varying inter-yarn coefficients of friction.

The variation of residual velocity of the projectile for the different fabric sett and coefficients of the inter-yarn friction is compared and shown in Figure 3-7. From the comparison it is evident that the residual velocity is improving due to increase in the inter-yarn friction. However, the improvement in the residual velocity is not significantly observed after a critical inter-yarn friction coefficient. This observation is more or less true for all fabric sett.

There is more improvement in the ballistic performance of the fabric at lower level of friction coefficients as compared to the larger values of friction coefficients. The similar observation is made in the literature (Wang et al., 2016). The study in the literature shows that the ballistic limit is improve due to increase in the inter-yarn coefficients till a critical friction coefficient. Moreover, the study reports the loss of ballistic performance due to increase in the friction beyond the limiting value. A similar observation was reported by (Nilakantan & Gillespie, 2012). (Zeng et al., 2006) reported that there is premature failure of the yarn at very high inter-yarn friction. The premature failure of the yarns could be related to the stress wave propagation in the ballistic fabric and developed strain in the fiber. The energy absorption mechanism of the fabric described in (Hogg, 2006; Lane, 2005) suggest that the energy absorption will be more if more fabric yarns have deformation. The longitudinal stress wave propagation at high friction is restricted. The stress wave is not able to reach out to the maximum yarns before failure and due to this the involvement of the yarns in the dissipation of the energy is very less. The pull-out studies by (Kirkwood et al., 2004) demonstrate that for the efficient absorption of energy, the size of cross shaped pull out zone in the deformed state of the fabric should be high. At higher friction coefficients the size of the pull-out zone (deformation area of yarns) is more or less not increasing. The accumulation of stress in the fabric near vicinity of the projectile and fabric interaction is increasing at higher friction. Due to this, the ballistic performance is not improving while increasing yarn friction beyond a critical value. The residual kinetic energy of the projectile is also compared and similar observation is reported. The graphical representation of residual kinetic energy of the projectile is shown in Figure 3-8. The residual kinetic energy is improving up to a critical value of the inter-yarn friction coefficients. The reason can be attributed to the premature failure of the yarns due to decrease in the stress wave propagation in the fabric at higher friction.

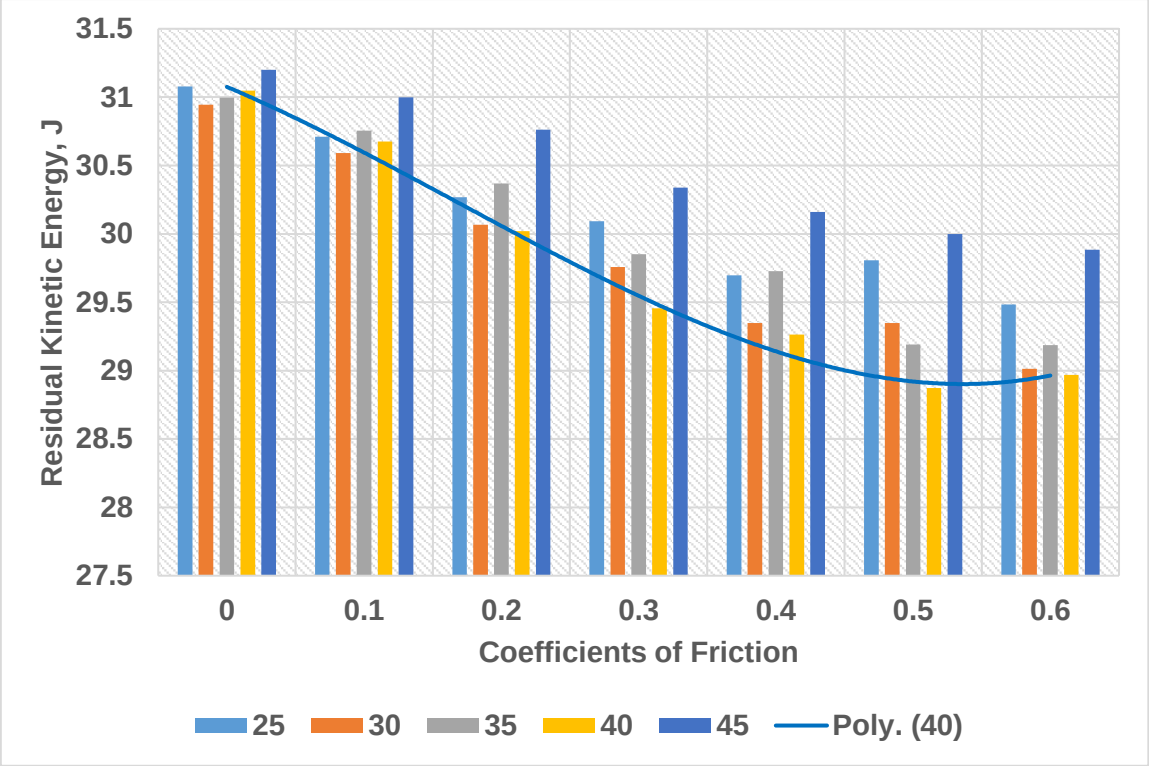

Figure 3-8 Residual kinetic energy of a projectile at 214 m/s for different fabric sett and varying inter-yarn coefficients of friction.

The contact force and frictional energy between yarns are not improving significantly at higher level of the friction. The fabric dissipate energy through propagation of stress wave to the network of yarns. The stress waves are not distributed uniformly to the maximum number of yarns of the fabric at higher friction coefficients. Due to less transfer of forces between yarn to yarn the contact force and frictional energy is not increasing further at higher friction. The comparison of frictional energy and contact force is shown in Figure 3-9 and Figure 3-10 respectively.

(a)

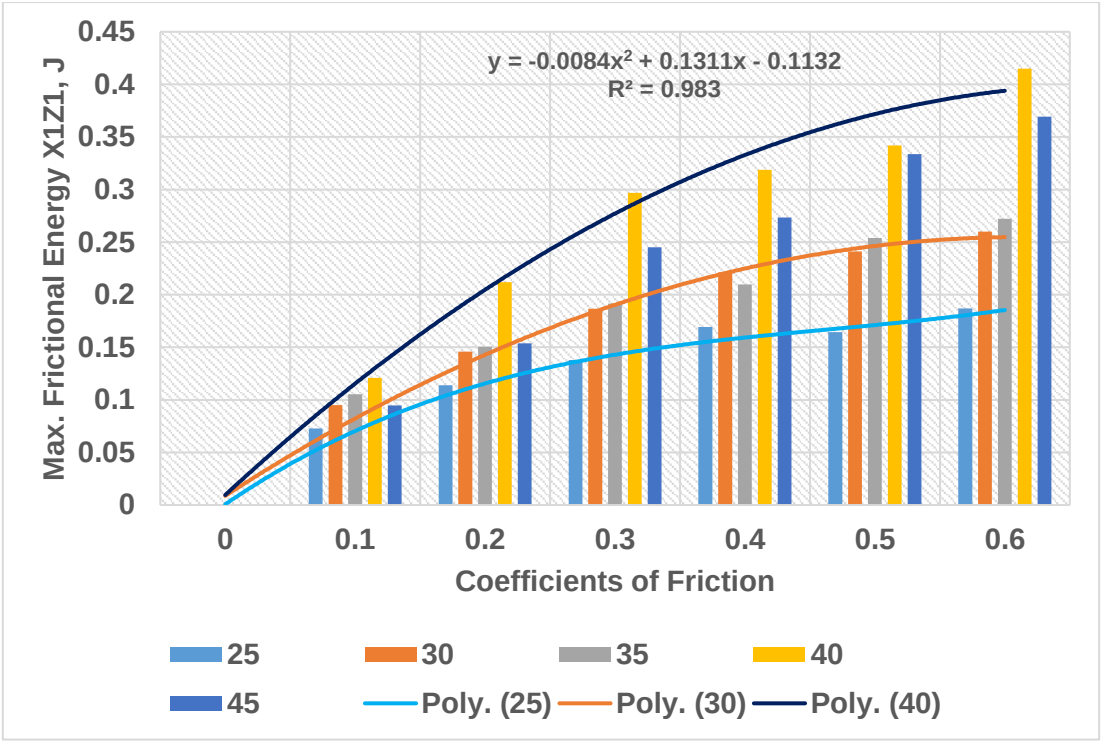

(b)

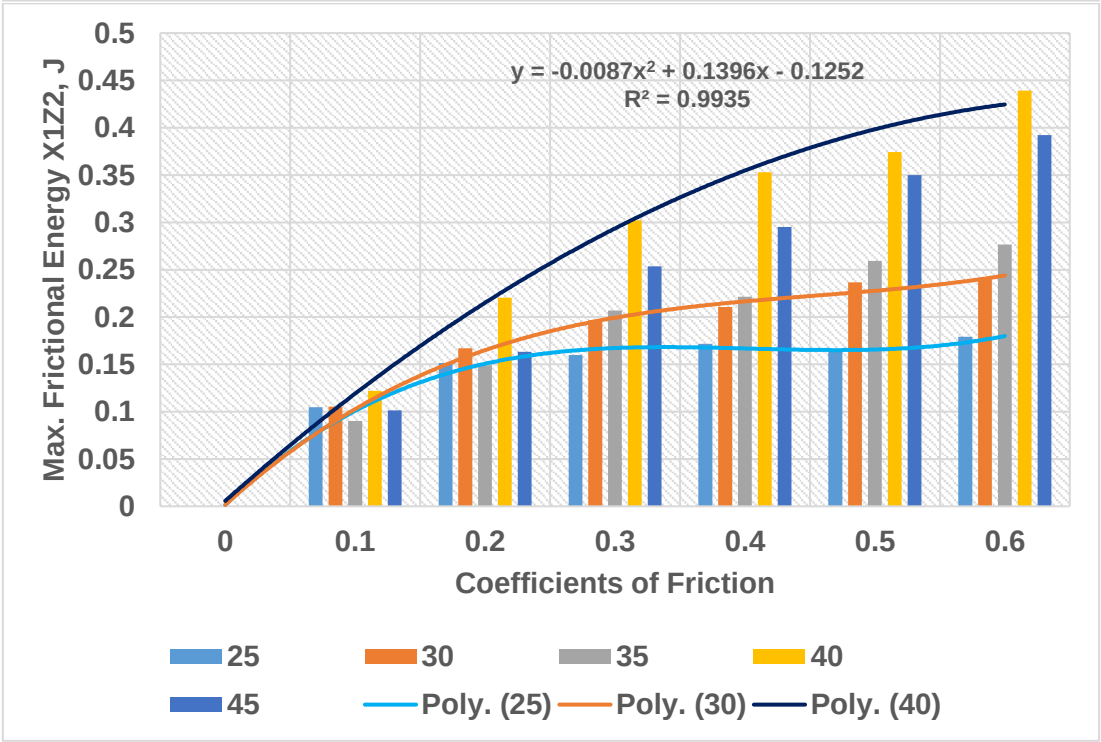

Figure 3-9 Peak frictional energy of (a) contact 1 and (b) contact 2 between warp and weft yarns for different fabric sett and varying inter-yarn coefficients of friction.

(a)

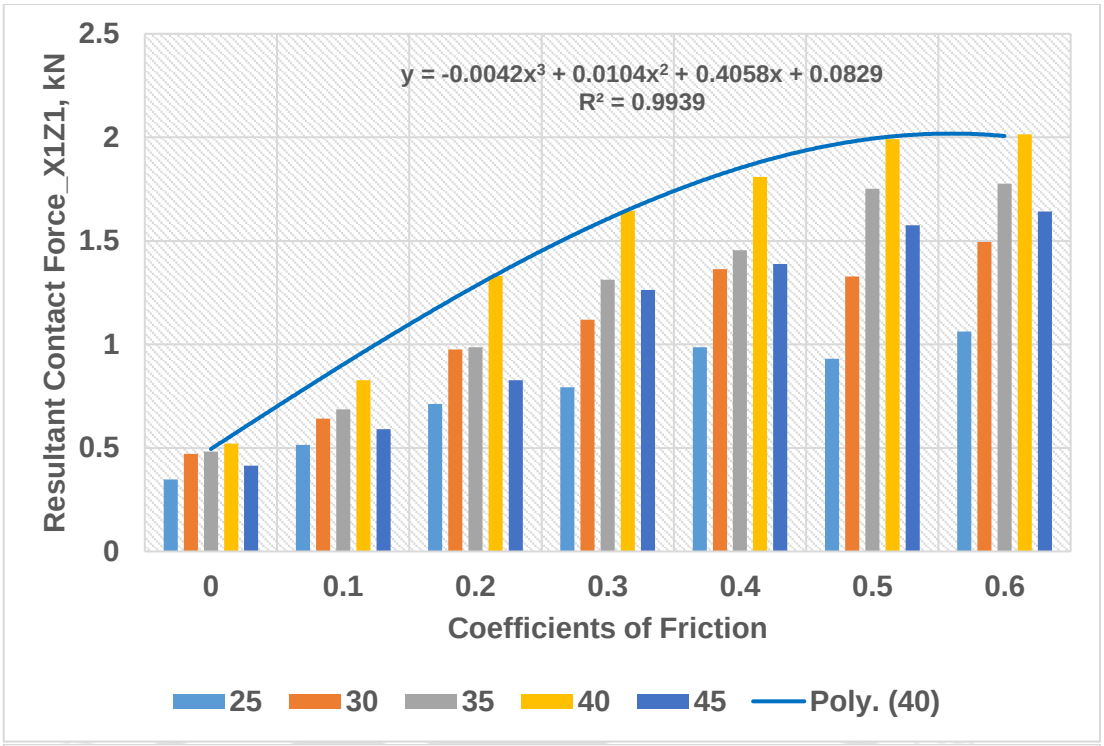

(b)

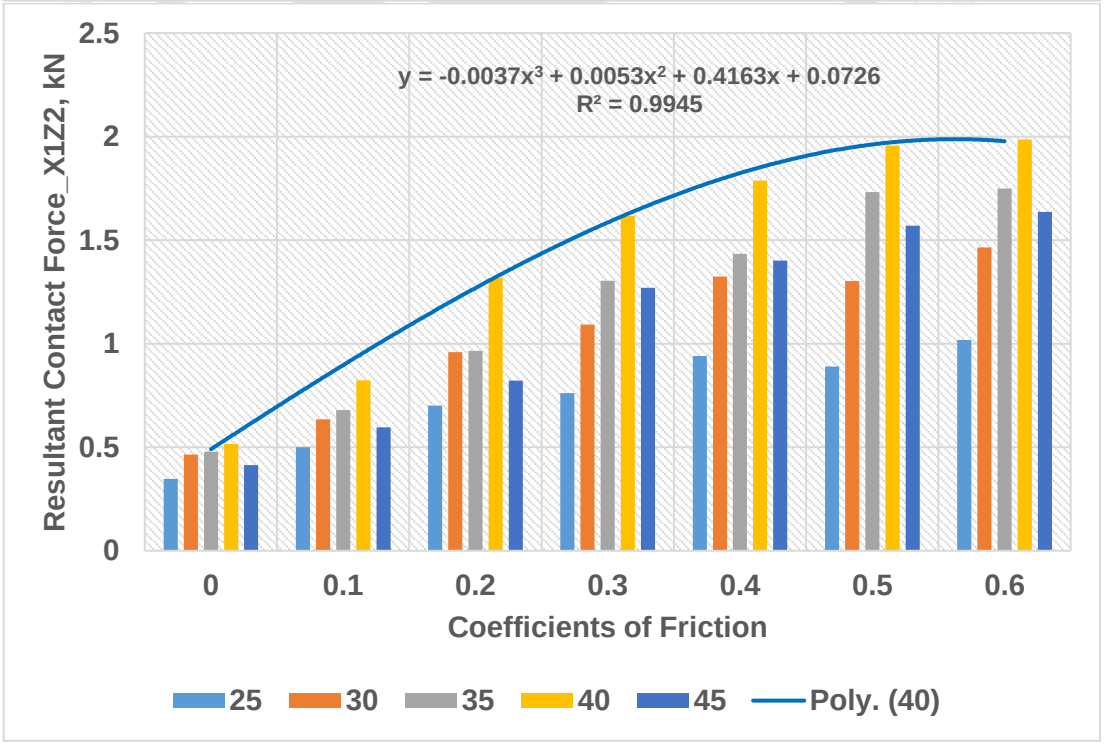

Figure 3-10 Peak resultant contact force of (a) contact 1 and (b) contact 2 between warp and weft yarns for different fabric sett and varying inter-yarn coefficients of friction.

3.5 Conclusions

The ballistic performance of the fabric is critical in the design of light-weight and flexible body armour as it is the main constituent in the armour system. There are several parameters which are controlling the ballistic performance of the fabric and inter-yarn friction

is one of them. Through alteration of friction by any means, the ballistic performance of the fabric can be further improved. Due to limited studies available in open literature related to the systematic study of the effect of inter-yarn friction on the ballistic performance of the fabric, this chapter presented a systematic study where the effect of inter-yarn friction on the ballistic performance of the fabric is investigated. The modelling of dry fabric which should consider the effect of inter-yarn friction is validated and further, the effect of inter-yarn friction on the ballistic performance of the fabric is evaluated and presented in this chapter. The computational model presented in this study is validated though experimental data and found to be in good agreement for further investigation. Through computational model of the fabric, it is shown that the ballistic performance of the fabric is improving with the increase in the inter-yarn friction. There is very limited influence of friction beyond a critical value. The ballistic performance of the fabric is not enhancing substantially due to increase in the inter-yarn friction. There has been premature failure of the yarns at higher friction and due to this there is very limited scope to utilize the treated fabric optimally. This Chapter fulfils the designated task to understand the frictional behavior of the STF along with the fibers to much more details. This work is the basics of the work to be done ahead in achieving our objectives. With limited understanding the effect of STF can be model using friction-based modelling of the fabric. At least the multi-layer modelling of STF impregnated fabric will provide the understanding of the ballistic behavior of the multi-layer fabric system impregnated with STF. Further, the yarn level modelling of fabric is used to investigate the effect of STF on the ballistic performance of the multi-layer of the fabric and presented next in Chapter 4.

4 Multi-scale friction based numerical modelling of STF impregnated ballistic fabric

4.1 Introduction

The structural parameters of woven fabrics play a crucial role in determining its impact resistance performance. Conventionally, treatment with Shear Thickening Fluid (STF) has been found to increase the impact energy absorption capacity of fabrics. (Lee et al., 2003) studied the ballistic penetration performance of a composite material composed of woven Kevlar fabric impregnated with a colloidal shear thickening fluid (silica particles of size 450 nm) dispersed in ethylene glycol. The impregnated Kevlar fabric yields a flexible, yet penetration resistant composite material. Fragment simulation projectile (FSP) is a novel composite material for ballistic application. They have demonstrated a significant enhancement in penetration measurements at ~244 m/s due to the addition of shear thickening fluid to the fabric, without any loss in material flexibility. (Tan et al., 2005) investigated the ballistic performance of Twaron® CT615 plain-woven fabric impregnated with a silica colloidal water suspension (SWS) of different particle concentrations in water. Ballistic limits and specific ballistic energy of single, double, quadruple and six ply fabric systems impregnated with 0, 20, 40 and 50 wt.% SWS particle concentration were compared to that of a neat untreated system. Results show that the systems with 40 wt.% SWS particle concentration yields the highest ballistic limit for single, double and quadruple ply systems, with the double ply system showing the greatest improvement. The ballistic limits of double ply systems with 40 wt.% SWS particle concentration is 70% higher than the ballistic limit of neat double ply systems. The improvement in ballistic resistance is attributed to the increase in projectile-fabric friction and inter-yarn friction arising from the silica particle and silica clusters formed. The double ply system with 40 wt.% SWS particle concentration showed the greatest improvement with a 100% increase in the specific ballistic energy over neat double ply systems. However, the specific ballistic energy for quadruple and six ply systems with SWS is lower compared to the neat systems. High-speed photography showed that these systems experience more localized deformation on impact and this may limit the frictional effects. It is also shown that SWS impregnated double ply systems can be incorporated into six ply configurations to significantly improve over- all ballistic performance. (Yeh et al., 2019) studied the preparation methodology and rheological properties of an STF. STF/Kevlar composites were made using ethanol as the cosolvent. The physical properties of the composites were determined by ballistic penetration,

drop tower, and yarn pull-out tests. The ballistic penetration was tested at a projectile velocity of 180 m/s. The ballistic penetration tests showed that adding the STF could obviously increase the energy dissipation. In addition, the weight of the composites may be reduced by 37% while their ballistic resistance is maintained. The knife drop-tower tests showed that adding the STF may improve the energy absorption by 20%. The yarn pull-out test demonstrated that the maximum pull-out force of the STF/Kevlar composites is 3.17 times that of neat Kevlar. The enhancements in the physical properties were apparently associated with the addition of the STF. (Majumdar et al., 2013) presented the design methodology for the optimal design of soft body armour materials by treating Kevlar (para-aramid) fabrics with silica nano-particle based shear thickening fluid (STF). The effect of silica concentration, padding pressure and diluent: STF ratio (solvent ratio) were studied on STF add-on% and impact energy absorption. According to (Majumder et. al., 2013), higher padding pressure enhances the impact energy absorption by the STF treated Kevlar fabrics although it does not influence the STF add-on% significantly. It was concluded in the study that higher STF add-on% is necessary but not the sufficient condition for improving the impact resistance performance of Kevlar fabrics. (Laha & Majumdar, 2016) studied five different weave structures with varying thread densities of p-aramid (Technora) yarns, followed by treatment with 60% w/w STF to develop soft armor materials. In untreated condition, plain woven fabrics showed the highest impact resistance, followed by 3/1 twill, 2/2 twill, 5 end satin and 2/2 matt. STF treatment improved the impact resistance performance in all the weave structures and thread densities except for the plain weave with the highest thread density. The ascending order of weaves in terms of enhancement in impact energy absorption after STF treatment was exactly opposite to the ascending order of weaves in terms of impact energy absorption before STF treatment. (Khodadadi et al., 2019) studied the response of fiber reinforced composite material composed of woven Kevlar fabric impregnated with a colloidal shear thickening fluid (STF) under high velocity impact loading. In the study, experimental investigation on effects of silica nanoparticle loading on energy absorption and ballistic limit was conducted. It was shown that by increasing Nano silica loading, the force required to pull the yarn out from the fabric impregnated by STF increases.

There have been many attempts made to understand the effect of STF impregnation to fabric through numerical simulation. The simulation was based on assumption that there is enhancement of performance of fabric because of sudden increase in inter-yarn friction due to smart rheological behavior of STF. In similar way, (Lee & Kim, 2012) explored the mechanism of enhanced energy absorption on impregnation of STF into fabric through a computational

analysis. A computational study was performed by considering the effect of STF impregnation on the ballistic performance of STF impregnated fabrics. The proposed computational model accounts for STF impregnation by employing the experimental results of yarn pull-out tests to characterize the frictional behavior of the STF impregnated fabric using commercially available code LS-DYNA. (Gürgen & Kuşhan, 2017) studied the multi-phase STFs by adding different amount of silicon carbide (SiC) additives into silica and polyethylene glycol (PEG) based suspensions. Ballistic impacts on multi-phase STF treated fabrics were carried out using lead core bullets with the impact speed of ~330 m/s. Based on the results, it was concluded that multi-phase STFs improve the ballistic performance of high-performance fabrics in comparison to single-phase STFs. However, the mass efficiency of fabrics has a loss of performance for high velocity impact conditions. (Hasanzadeh et al., 2017) carried the experimental and numerical investigation of the impact resistance properties of woven High Modulus PolyPropylene (HMPP) fabrics impregnated with Shear Thickening Fluids (STFs) composed of fumed silica nanoparticles suspended in PolyEthylene Glycol (PEG). Numerically the impact of ogival tip projectile on four layered fabrics using LS-DYNA was simulated. These numerical studies are focused on correlation between residual velocity to initial velocity and total energy absorbed. A design methodology for optimal design of ballistic protective gear using numerical study has not been presented.

In the current research, a methodology is being presented which provides the optimized performance of the developed ballistic system. In this research, the parameters considered are mechanical properties of fiber, textile structures such as linear density, fabric sett, inter-yarn friction and between fabric and projectile, multi-layer fabric system.

4.2 Numerical modelling

The numerical investigation on STF impregnated fabric system is based on frictional effects between inter-yarn and between projectile and fabric researchers (Gürgen, 2020; Hasanzadeh et al., 2017; Lee & Kim, 2012; Park et al., 2015). The effect of STF on fabric has been modelled through enhancement of frictional co-efficient in the inter-yarns. In order to study the ballistic performance of the STF fabric, it is very important to model the fabric itself. There are many multi-scale methods proposed to model the fabrics such as the membrane or micromechanical model (Tanov & Tabiei, 2002; Ivanov & Tabiei, 2004; Ivanov & Tabiet, 2002). At present, there are limitations of developed micromechanical model of the fabric which is based on continuum theory. Aspects such as fibre-fibre interaction, fibre-fibre friction,

filament-filament friction and interaction, yarn-yarn friction interaction are not addressed. So, the micromechanical model can't be used to study the effect of friction on the ballistic performance of high-performance fabrics. In order to mitigate the limitation of micromechanical or membrane level modelling researchers have proposed yarn level modelling which is also known as mesoscale modelling. A 3D finite element analysis model is created by (Duan et al., 2006) using LS-DYNA to simulate the transverse impact of a rigid right circular cylinder onto a square patch of plain-woven Kevlar fabric. The fabric is modelled to yarn level resolution and relative motion between yarns is allowed. A frictional contact is defined between yarns and between the fabric and the projectile. The effects of inter-yarn friction on the ballistic performance of woven fabric armour are investigated by (Zeng et al., 2006). Frictional sliding between yarns is implemented in a computational model of the fabric that takes the form of a network. Parametric studies have been carried out and it is shown that the ballistic response of woven fabric is very sensitive to yarn friction when the friction coefficient is low but insensitive beyond a certain level. It is also shown that very high inter-yarn friction can lead to premature yarn rupture, thus reducing the ability of the fabric to absorb impact energy. (Rao et al., 2009) studied impact of a rigid sphere onto a high-strength plain-weave Kevlar KM2® fabric and carried out the numerical analysis in LS–DYNA. The influence of friction and material properties on ballistic performance was considered. In the study, yarns were modelled as continua with modulus and strength dominating along the length. It was shown that the ballistic performance depends upon friction, elastic modulus and strength of the yarns. The friction improves the ballistic performance by maintaining the integrity of the weave pattern, material properties of the yarns have a significant influence on the effect of friction. (Grujicic et al., 2010) developed and implemented a mesoscale ballistic material model for a prototypical plain-woven single-ply flexible armor in a material user subroutine for the use in commercial explicit finite element programs. The main intent of the model was to attain computational efficiency when calculating the mechanical response of the multi-ply fabric-based flexible-armor material during its impact with various projectiles without significantly sacrificing the key physical aspects of the fabric microstructure, architecture, and behavior. (Minh et al., 2012) proposed yarn level numerical model of ballistic impact on a two-dimensional Kevlar KM2® plain-woven fabric and validated through experiment. (Nilakantan et al., 2013) studied the effects of projectile size and shape on the impact response of a single-layer fully-clamped flexible woven fabric. A numerical finite element study on yarn-level fabric model with a deterministic implementation of experimental mean yarn tensile strength and inter-yarn friction was done. The proposed study on micro-scale modelling or fiber-level

modelling of the fabric require very high computation power in fiber-level modelling. In order to investigate the ballistic performance of the STF impregnated fabric, it is suggested to utilize the yarn level modelling of the fabric to reduce the requirement of high computational power.

4.2.1 Geometric modelling

The meso-scale modelling of the fabric has been utilized in this study to optimize the ballistic performance of the STF impregnated fabric. In meso-scale, yarns are modelled as continua and for the same LS-PrePost (Yan & Ho, 2018) has been utilized to model the yarn geometry of plain weave fabric. The yarns per inch (fabric sett) and cross-over of the yarns in weft and warp direction has been modelled. The yarns can be modelled as planar surface or to enhance accuracy can be modelled as 3D yarns. The computational requirement will be very high when the yarns will be modelled using 3 dimensional solid elements. In present study 2D shell elements are utilized to reduce the computational requirements. The geometry of central surface has been modelled by using sinusoidal function. The open literatures such as (Bridgens & Gosling, 2008; Yurgartis et al., 1993) reported that the initial yarn crimp of plain weave fabric can be modelled using sinusoidal characteristics. The geometrical model described by (Lee et al., 2012) has been used to create the geometry of the yarns and subsequently entire fabric. The schematic of yarn has been shown in Figure 4-1.

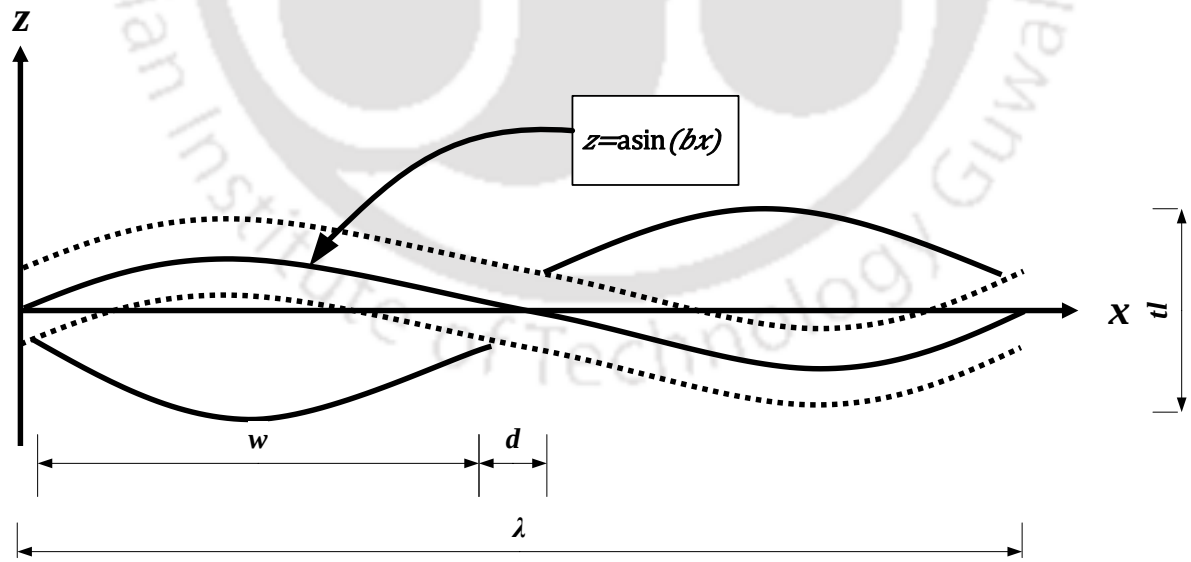

Figure 4-1 Schematic of sinusoidal yarn model

The geometrical modelling parameter has been adopted from (Lee et al., 2012) and shown in Table 4-1.

Table 4-1 Geometrical modelling parameter (Lee et al., 2012)

Parameters	***λ***	***w***	***d***	**a**	**b**	***tl***
Value (mm)	1.64	0.78	0.02	0.11	3.83	0.22

In order to develop the design methodologies for optimum performance level design of the ballistic armour consisting of STF impregnated fabric system multi-layer fabric system has been investigated for all possible conditions. The multi-layer fabric system has been modelled and shown in Figure 4-2.

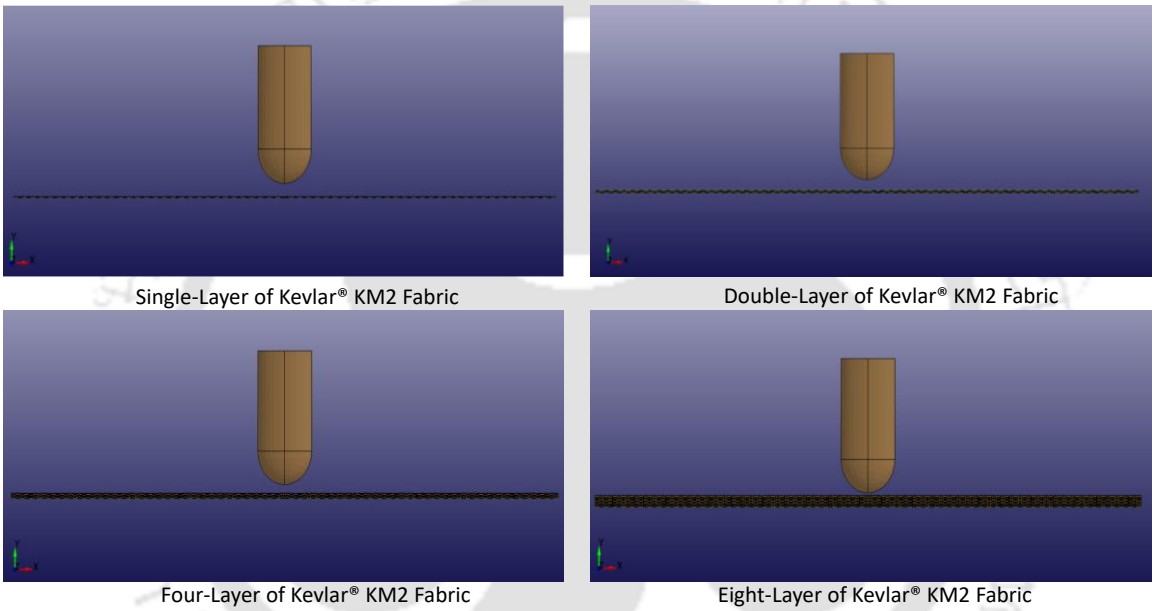

Figure 4-2 Multi-layer model of the fabric system of fabric sett 30 x 30

4.2.2 Material modelling

In order to study the ballistic performance of the fabric it is important to mechanically characterize the fabric. In the current study, para-aramid based Kevlar KM2® has been taken. (Cheng et al., 2005) studied the mechanical properties of Kevlar KM2® at single fiber level. The mechanical properties reported suggests that the Kevlar KM2® is transversely isotropic. For a linear elastic, and transversely isotropic material, five material constants are needed to describe its stress-strain response. In order to model the constitutive behavior in the current study, MAT_02 ORTHOTROPIC ELASTIC has been used. This material model represents transverse isotopic properties. For a linear, elastic, and transversely isotropic material, five

material constants are needed to describe its stress-strain response. The material properties utilized in this study is adopted from (Cheng et al., 2005) and shown in Table 4-2.

Table 4-2 Properties of Neat Kevlar KM2® Fabric (Cheng et al., 2005)

Fabrics	**Properties**	**Symbol**	**Values**
Kevlar KM2®	Young's Modulus	E11	84.62 GPa
		E22= E33	1.34 GPa
	Shear Modulus	G12=G13=G23	1.34 GPa
	Poisson's Ratio	υ12= υ13= υ23	0
	Density	ρ	1.44 g/cc
	Tensile Strength	Warp	3900 MPa
	Tensile Strain (%)	Warp	4.5

The failure criteria of the fiber is 3.9 GPa von-mises stress and strain of 4.5 % has been assigned in MAT_ADD_EROSION.

4.3 Modelling of STF effect on multi-layer fabric system impregnated with STF

In order to develop the optimal design methodologies, numerical investigation on STF impregnated multi-layer fabric system has been carried. Many researchers (Fahool & Sabet, 2016; Hasanzadeh et al., 2017; Khodadadi et al., 2018; Park et al., 2015) have stated the beneficial effect of STF through friction enhancement. In the current study, it has been found that the ballistic performance of the fabric is enhanced by incorporating friction between inter-yarns. The enhanced performance of the fabric is shown through the residual energy of the projectile. The projectile velocity for single layer fabric system is shown in Figure 4-3.

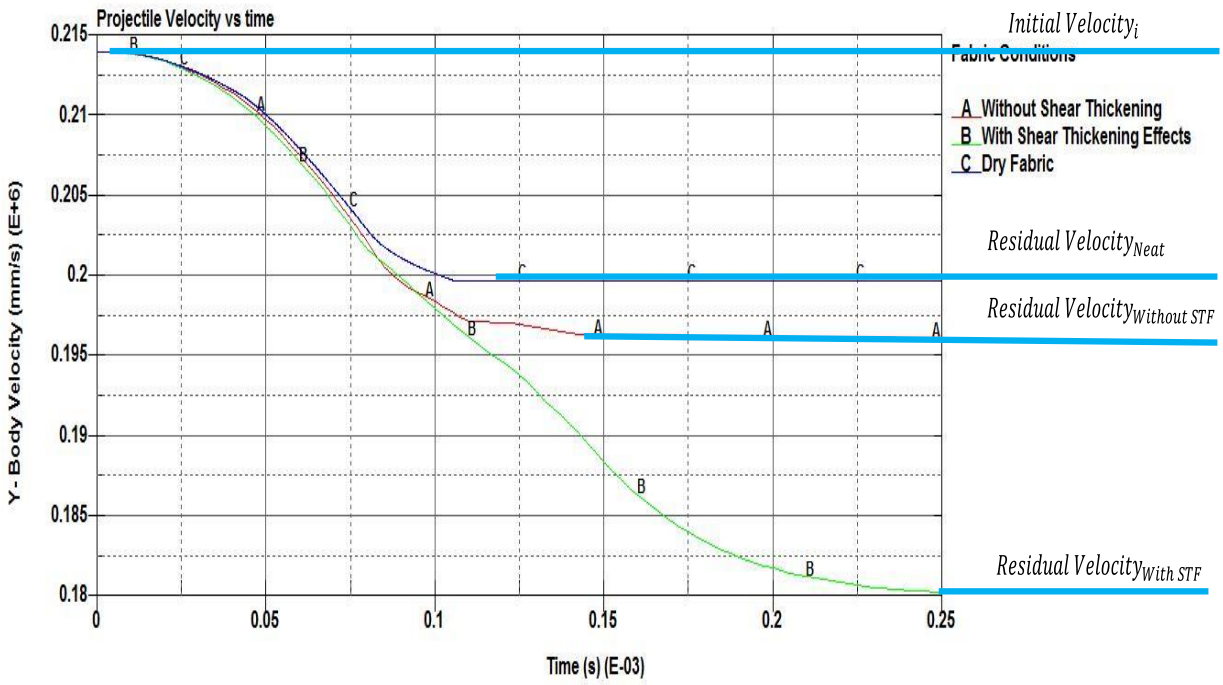

Figure 4-3 Projectile velocity of single layer dry and impregnated fabric with and without STF effects and fabric sett 30 x 30

Similar findings for the kinetic energy are observed. It is evident from the Figure 4-4 of single layer fabric system that there is enhancement in the absorption of the kinetic energy of the projectile. The enhancement in the kinetic energy is due to the consideration of STF into the modelling of the fabric system. The STF behavior is considered through friction between inter-yarns and projectile and it has been incorporated through *CONTACT_AUTOMATIC_SURFACE_TO_SURFACE in LS-DYNA. This formulation incorporates Coulomb's friction model between surfaces of yarns and projectile.

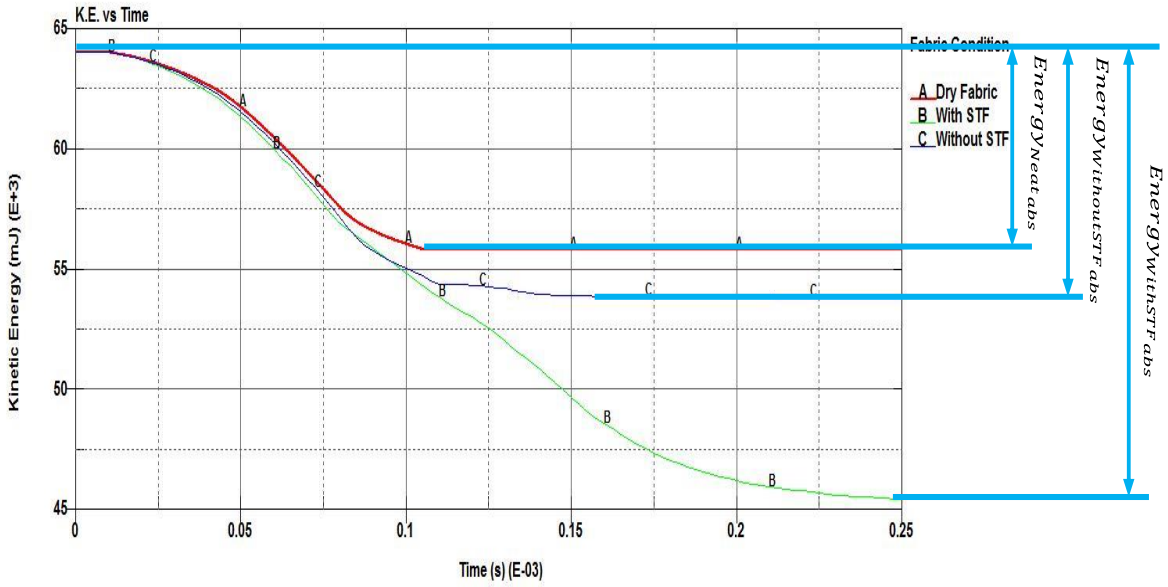

Figure 4-4 Kinetic energy of single layer dry and impregnated fabric with and without STF effects and fabric sett 30 x 30

The various stages of failure of single layer dry fabric system is shown in Figure 4-5. The von-mises stress in the fabric system shows the propagation of loading wave. It is evident from the failure stages that there is significant role of boundary condition on the prediction of the ballistic performances of the fabric system though ballistic impact phenomena is highly local in nature. In initial stages, there is star shape of the loading wave propagation and later on these loading waves will concentrate nearer to restrained boundary edges.

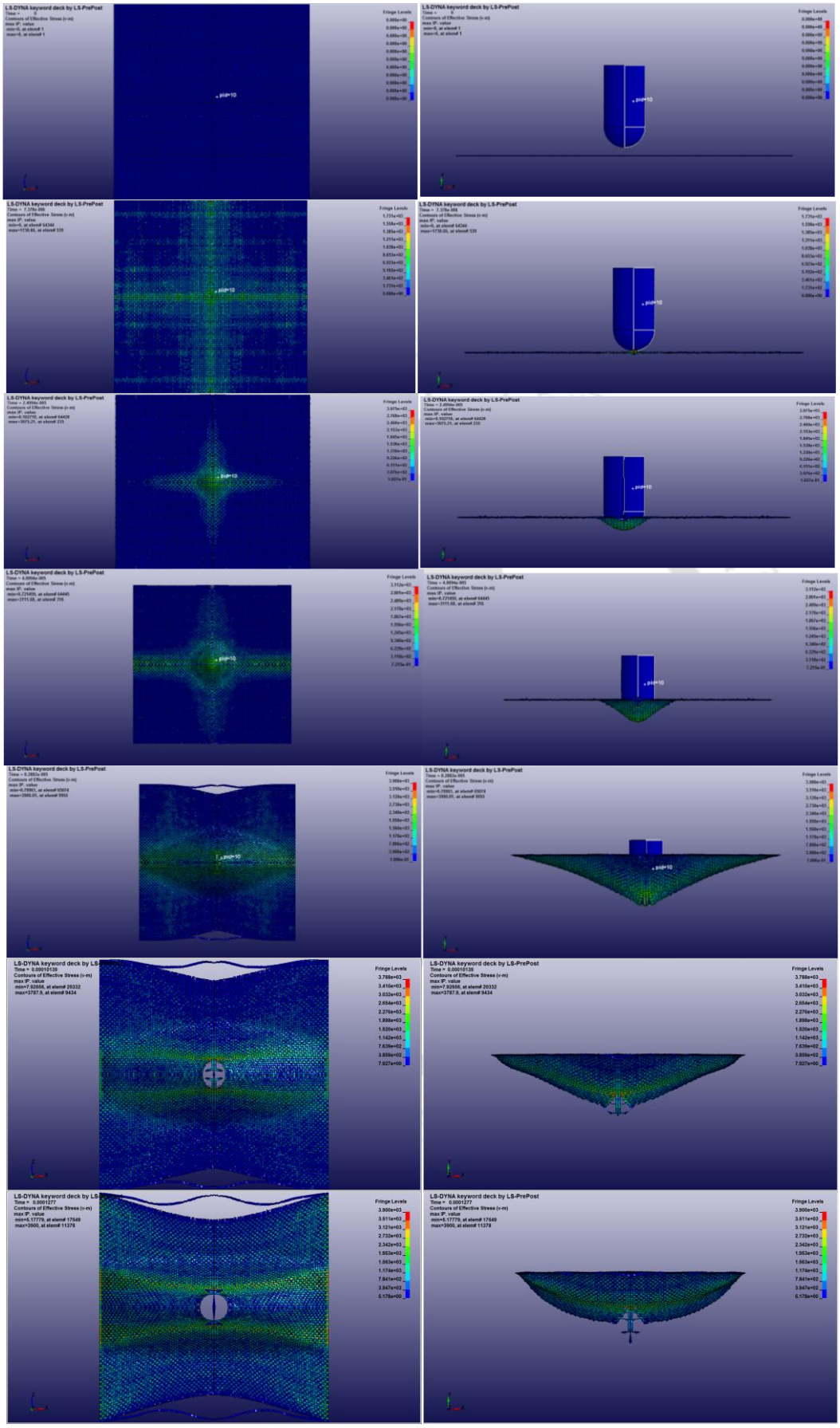

Figure 4-5 Failure stages of single layer dry Kevlar KM2® fabric of fabric sett 30 x 30

There is substantial improvement in the ballistic performance due to the application of STF into fabric system. It is evident from the trend-line shown in Figure 4-6. It shows the residual velocity of the projectile on single layer of fabric sett 30 x30.

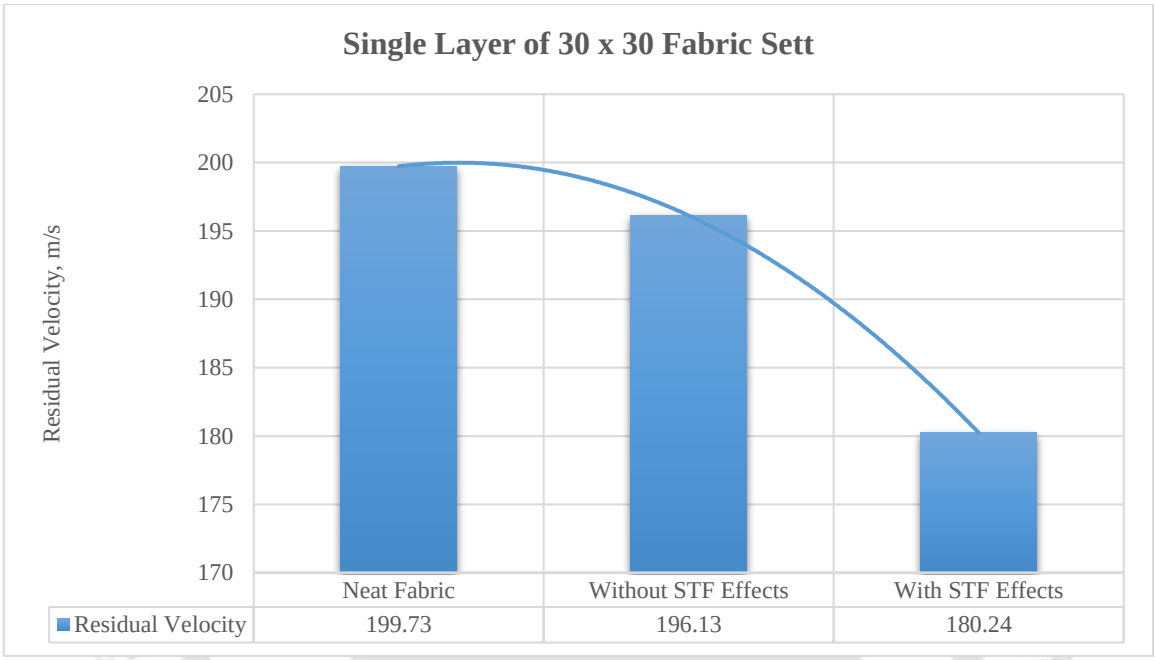

Figure 4-6 Residual velocity of single layer fabric system of having 30 x 30 fabric sett

Similarly, it is evident from the trend-line shown in Figure 4-7 that there is substantial improvement in the energy absorption of the STF treated fabric system having fabric sett 30x 30.

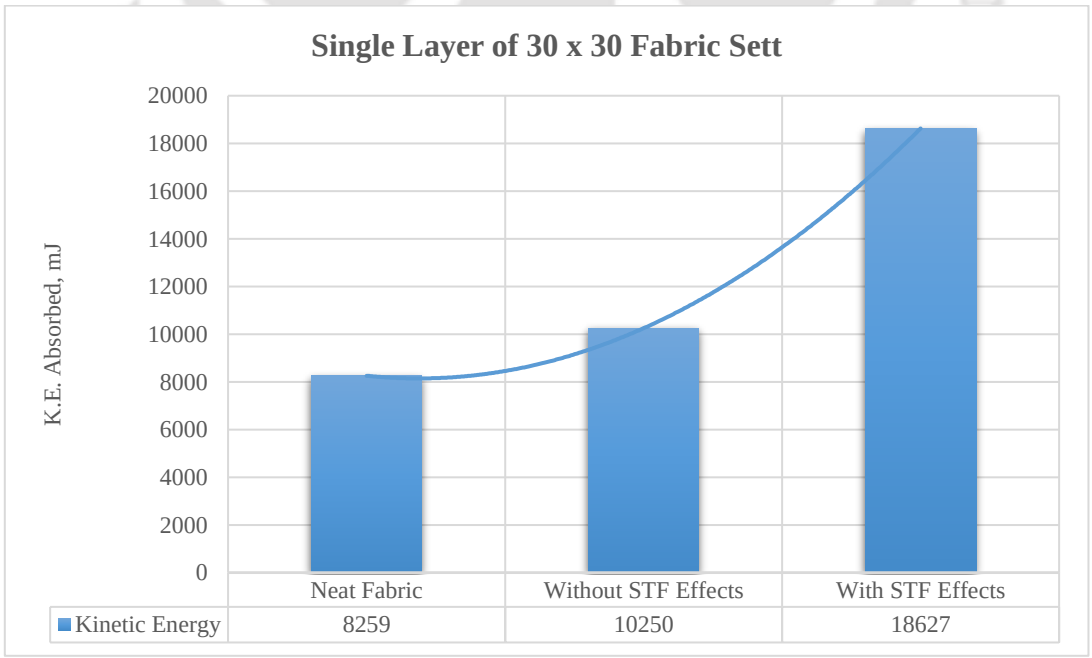

Figure 4-7 K.E. absorbed of single layer fabric system of having 30 x 30 fabric sett

The similar kind of investigation is carried on multi-layer fabric system of having fabric sett 30 x 30. It has been found that there is no significant improvement observed in the residual velocity of the projectile in double layer fabric system than single layer fabric system. However, there is significant improvement in the residual velocity of the projectile in quadruple layer fabric system than the double layer fabric system. The residual velocity of the projectile for multi-layer fabric system is shown in Figure 4-8.

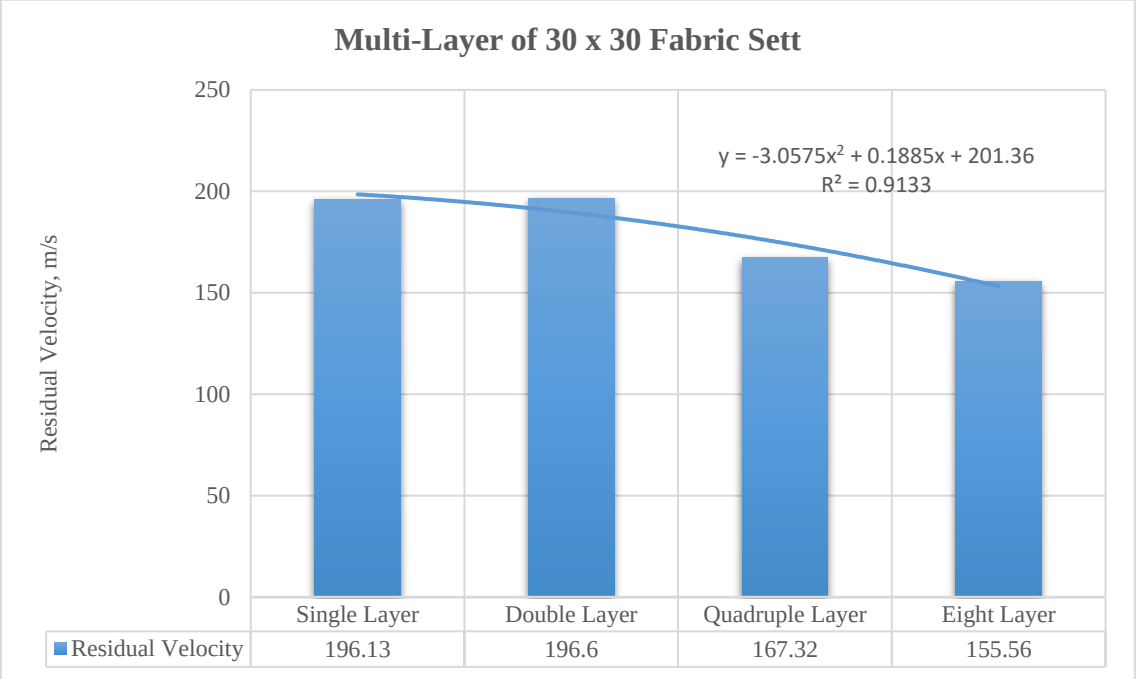

Figure 4-8 Residual velocity of Multi-layer fabric system of having 30 x 30 fabric sett and without STF Effects

The kinetic energy absorption by the multi-layer fabric system is shown in Figure 4-9. The similar observation can be made in case of energy absorption as the residual velocity of the projectile.

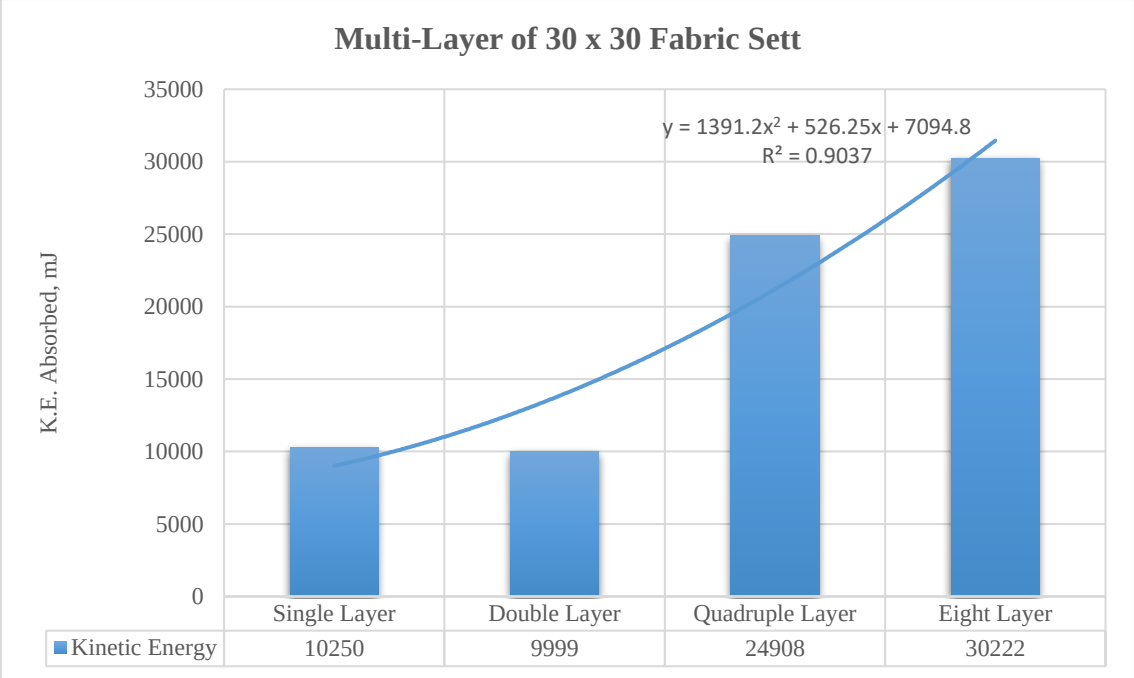

Figure 4-9 K.E. absorbed of Multi-layer fabric system of having 30 x 30 fabric sett and without STF Effects

Based upon results of single layer fabric multi-layer fabric system of fabric sett 31x31 has been investigated up-to eight layers of the fabric. A graphical representation of the residual velocity of the multi-layer STF impregnated system is shown in Figure 4-10.

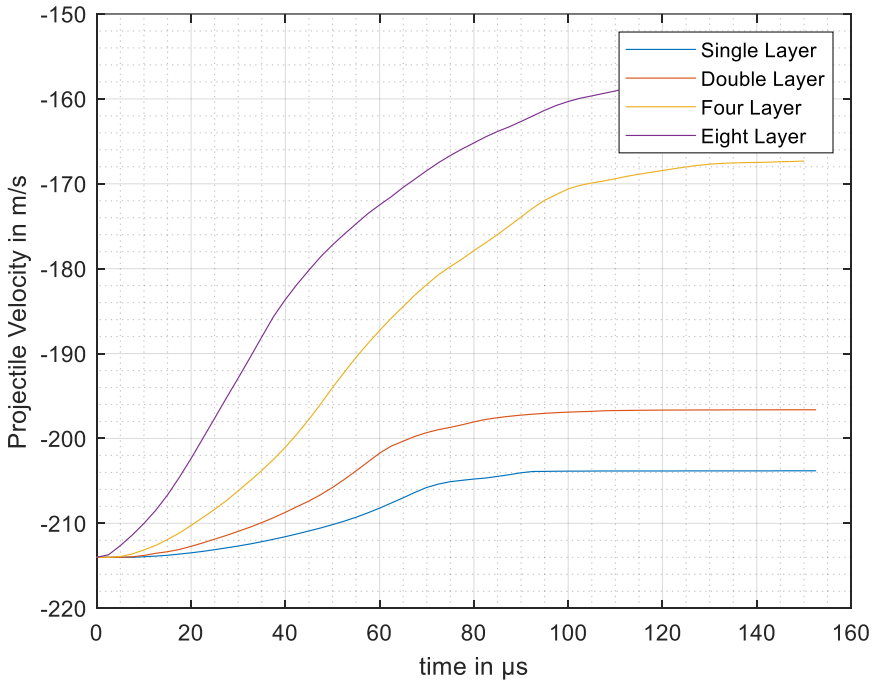

Figure 4-10 A graphical representation of residual velocity of multi-layer STF impregnated fabric system under ballistic impact

The kinetic energy dissipation over increase in the number of layers of multi-layer fabric system is observed and a graphical representation is shown in Figure 4-11.

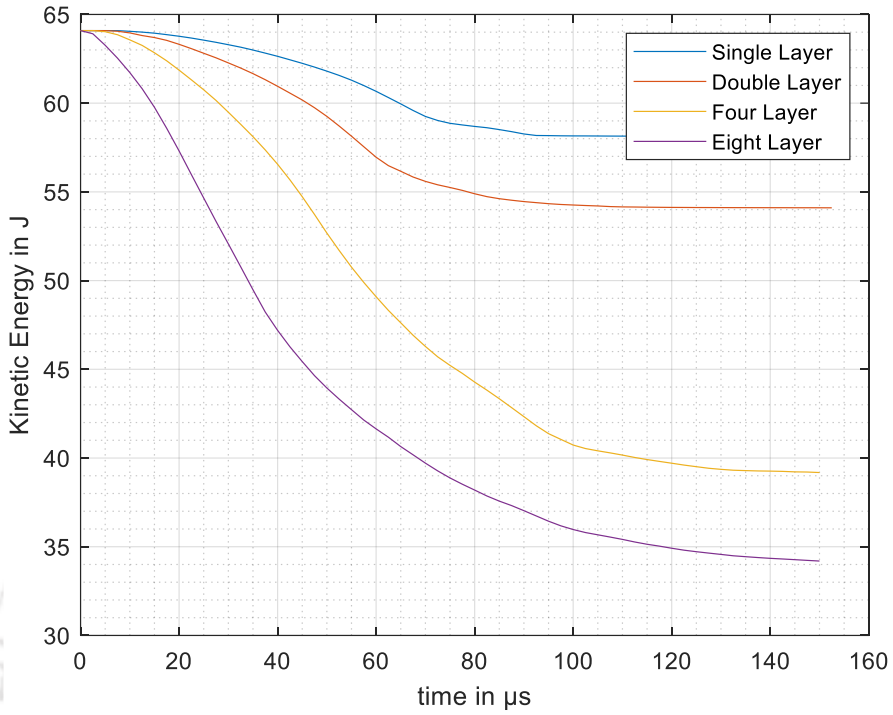

Figure 4-11 A graphical representation of kinetic energy dissipation through multi-layer fabric system under ballistic impact

Numerical models developed in this Chapter can be used to determine the optimum number of fabric layers to achieve better ballistic performance at a standard rating and can be implemented in the design of ballistic armour. Moreover, these models do not consider the STF effect directly. Instead friction is considered as a leading parameter. Hence, these models cannot provide any insight about STF effects on ballistic performance of STF treated fabric. The smart properties of shear thickening fluid are neglected in these models, and hence the sole purpose of the implementation of STF through fabric system is still not understood completely. The smart behavior of STF shows as liquid behavior at shear rates lower than critical value and solid behavior above critical shear rate. When STF impregnation is modelled by assuming improvement in the inter-yarn friction than it deviates from its smart behavior. In view of these findings, the next Chapters discusses about the development and implementation of numerical model based on modelling of STF as fluid and multi-material ALE technique is adopted in in LS-DYNA.

4.4 Conclusion

This Chapter presents the effect of STF on the ballistic performance of STF treated fabric. The current study shows the various limitation of the modelling approach which were highlighted in the earlier research. The main disadvantage of friction-based model is that it is using semi-empirical approach to compute inter-yarn coefficient of friction for STF treated case. The underlying problem in the approach is that pull-out test can be carried at a particular pull-out speed. However, the phenomena are extremely dynamic and it requires special attention to capture the effect of STF. The behaviour of STF significantly changes when the shear strain rate is changing and hence pull-out test limits the understanding of STF effect as it is done at constant speed and at fixed shear strain rate will be applied to the STF treated fabric. Furthermore, this technique is most suitable for a particular velocity range of 150-300 m/s but beyond this the results obtained from this modelling approach are not reliable. Hence, subsequent Chapter discusses a new approach to study the effect of STF on fabric. The modelling approach is based on MM-ALE approach. In MM-ALE approach, STF is modelled as fluid and fabric as solid and coupling between them is defined. The MM-ALE based STF treated fabric model is presented in Chapter 5 and chapter 6. However, the friction-based models can be used to study the multi-layer fabric system and the equations developed to calculate the residual velocity and kinetic energy can be applied to extrapolate for higher number of fabric layer in case of MM-ALE approach.

5 A user-defined MM-ALE based numerical modelling of shear thickening fluid under impact

5.1 Introduction

Shear Thickening Fluid (STF) is a dilatant fluid showing smart behavior under different applied shear strain rate. STF fluid shows sudden rise in viscosity when an external applied shear rate exceeds from a limit which is known as critical shear rate. This smart behavior of STF fluid is used for the development of liquid ballistic armour. The available literature regarding application of STF for the development of STF is comprehensively discussed in Chapter 2. STF is synthesized from dispersion of Nano-particles of silica and Newtonian fluid such as PolyEthylene Glycol (PEG). This synthesized homogenous colloidal solution shows non-Newtonian fluid behavior. The flow visualization of shear thickening fluid is extensively studied and presented by (Ge et al., 2017; Hassan et al., 2010; Prabhu & Singh, 2021; Wetzel et al., 2004). This flow visualization is attributed to two kind of possible mechanism of shear thickening viz

1) formation of hydro-clusters of colloidal Nano-particles of silica, and

2) Increase in contact forces between particles due to instabilities arises in the vicinity of nano-particles and shear thickening fluid after application of shear strain rate.

The realistic modelling of STF involves modelling of Nano-silica particles as rigid particles, Newtonian fluid such as PolyEthylene Glycol (PEG) and their interaction based on above mechanisms. This approach requires a very high computational power as it involves Nano-scale multi-phase modelling. The modelling of STF as single phase i.e. only fluid requires data of viscosity vs applied dynamic shear strain rate from rheometric experiments. The rheometric data of STF is obtained from (Prabhu & Singh, 2021). The subsequent section of this Chapter presents the modelling approach of STF using rheometric data obtained from experiments.

5.2 Numerical Modelling

In order to develop the model for STF as a fluid, baseline model is developed and various formulations in LS-DYNA is validated case in which a rigid ball impacts on a surface of water using experimental data reported in (Bisagni & Pigazzini, 2018). The developed model in which a rigid ball is impacting on water at different time is shown in the Figure 5-1. The

models consist of multi-material fluid and ALE. It has been formulated using 1-point ALE multi-material element. The material model for water is user-defined material card where viscosity vs strain rate data has been provided as an input and hence this general user-defined material card can be utilized to predict any kind of fluid including Non-Newtonian fluid. The linear polynomial EOS is considered for variation of pressure w.r.t temperature and volume. The surrounding domain is modelled as Vacuum and hence there will be no need of EOS. This methodology is computationally fast and efficient. The rigid ball is modelled using default formulation which is constant stress solid element and rigid material model.

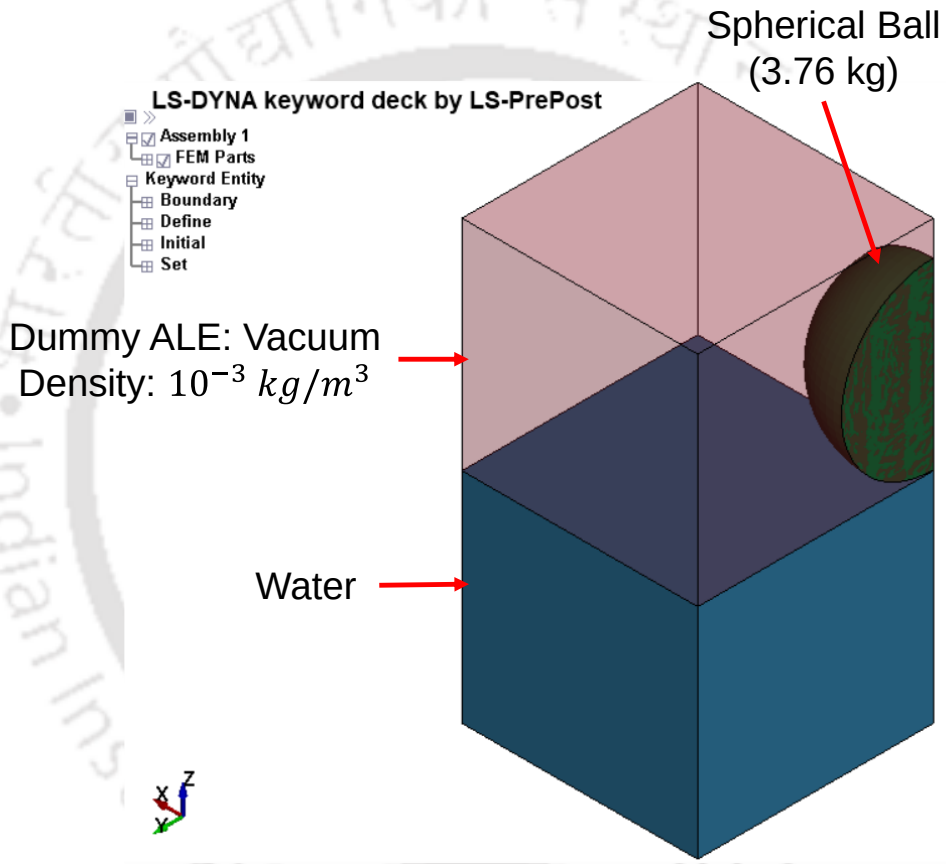

Figure 5-1 Multi-material ALE Quarter Model of rigid ball impacting on water

5.2.1 Constitutive modelling of fluid

LS-DYNA has robust capabilities of modelling the constitutive behaviour of fluid such as formulations covered by the following cards: *MAT_NULL, *MAT_ALE_VISCOUS, and *MAT_SPH_VISCOUS. The MAT_NULL card is the basic material card which can be used for the constitutive modelling of the fluid. This card can only be applied for ALE formulation as will not work purely for Lagrangian formulation. For implementing this card with solids or

thick shells, material must be used with an Equation-of-State (EOS). Pressure cutoff is negative in tension. A deviatoric viscous stress of the form is given in **(5-1**),

$$"\boldsymbol{\sigma}'" _{ij}" = 2\boldsymbol{\mu}" "\dot{\boldsymbol{\varepsilon}}'" _{ij} \quad (5\text{-}1)$$

This card can be applied for any kind of fluid which is having constant dynamic viscosity i.e. it is not varying w.r.t other parameter. Due to this limitation this card can be applied for water or Air, which is Newtonian fluid but it cannot be used for non-Newtonian fluid. The dynamic viscosity of non-Newtonian fluid is changing when an applied external strain rate is changing. First, the MAT_NULL card is applied to the validation case where rigid ball is impacting on water surface and then an improved version of material card is implemented where the variation of dynamic viscosity effect can be introduced in the modelling. The value of parameters for water in MAT_NULL and later card respectively is given in Table 5-1.

Table 5-1 Implemented material card of water in LS-DYNA

MAT	**Density (ρ),** $\frac{\mathbf{kg}}{mm^3}$	**Dynamic Viscosity, (Gpa.ms)**
Water	1E-6	1E-9 (USER INPUT CURVE)

The MAT_NULL card requires an EOS to correlate the hydrodynamic state of stress (normal compression). This EOS is generally calculating the variation of pressure when their will be change in volume or temperature of the fluid. The EOS_LINEAR_POLYNOMIAL is used to implement such variation in the modelling. The mathematical form of EOS_LINEAR_POLYNOMIAL is given in (**5-2**).

$$\boldsymbol{P = C\_0 + C\_1\,\mu + C\_2\,\mu\text{^}2 + C\_3\,\mu\text{^}3 + \llbracket(C\rrbracket \_4 + C\_5\,\mu + C\_6\,\mu\text{^}2)E} \quad (5\text{-}2)$$

$$\text{Where, } \mu = \frac{\rho}{\rho_0} - 1$$

The parameters of EOS_LINEAR_POLYNOMIAL for water is given in Table 5-2.

Table 5-2 EOS for water: EOS_LINEAR_POLYNOMIAL(Bisagni & Pigazzini, 2018)

Material	C_0 (MPa)	C_1 (MPa)	C_2 (MPa)	C_3 (MPa)	C_4	C_5	C_6
Water	0	2723	7727	14660	0	0	0

The material card MAT_ALE_VISCOUS is an improved version of the MAT_NULL card. In this material card variation of dynamic viscosity can be implemented either using power law of modelling variation of dynamic viscosity or viscosity can be defined using user defined curve. The empirical variable dynamic viscosity is typically modelled as a function of equivalent shear rate based on experimental data.

$$\boldsymbol{\mu\left(\dot{\bar{\gamma}}'\right) = RK \times \dot{\bar{\gamma}}'^{(RN-1)}, (\text{Power Law model})} \tag{5-3}$$

For an incompressible fluid (5-3 may be written equivalently as,

$$\boldsymbol{\mu\left(\dot{\bar{\varepsilon}}'\right) = RK \times \dot{\bar{\epsilon}}'^{(RN-1)}, (\text{Power Law model})} \tag{5-4}$$

The "overbar" denotes a scalar equivalence. The "dot'' denotes a time derivative or rate effect. The "prime" symbol denotes deviatoric or volume preserving components. The equivalent shear rate component may be related to the basic definition of (small-strain) strain rate component as follows:

$$\boldsymbol{\dot{\varepsilon}_{ij} = \frac{1}{2}\left(\frac{\partial u_i}{\partial x_i} + \frac{\partial u_j}{\partial x_i}\right) \Rightarrow \dot{\varepsilon}'_{ij} = \dot{\varepsilon}_{ij} - \delta_{ij}\left(\frac{\dot{\epsilon}_{kk}}{3}\right)} \tag{5-5}$$

Further the shear strain rate in terms of small strain rate is given by (5-6;

$$\boldsymbol{\dot{\gamma}_{ij} = 2\dot{\varepsilon}_{ij}} \tag{5-6}$$

Typically, the 2nd invariant of the deviatoric strain rate tensor is given by (5-7:

$$\boldsymbol{I_{2\dot{\bar{\varepsilon}}'} = \frac{1}{2}\left[\dot{\varepsilon}'_{ij}\dot{\varepsilon}'_{ij}\right]} \tag{5-7}$$

The equivalent (small-strain) deviatoric strain rate is defined as:

$$\dot{\varepsilon}' \equiv 2\sqrt{I_{2\dot{\varepsilon}'}} = \sqrt{2\left[\dot{\varepsilon}'_{ij}\dot{\varepsilon}'_{ij}\right]} = \sqrt{4\left[\dot{\varepsilon}'^{\,2}_{12} + \dot{\varepsilon}'^{\,2}_{23} + \dot{\varepsilon}'^{\,2}_{31}\right] + 2\left[\dot{\varepsilon}'^{\,2}_{11} + \dot{\varepsilon}'^{\,2}_{22} + \dot{\varepsilon}'^{\,2}_{32}\right]} \quad (5\text{-}8)$$

In non-Newtonian literatures, the equivalent shear rate is sometimes defined as

$$\dot{\bar{\gamma}} \equiv \sqrt{\frac{\dot{\gamma}_{ij}\,\dot{\gamma}_{ij}}{2}} = \sqrt{2\left[\dot{\varepsilon}'_{ij}\dot{\varepsilon}'_{ij}\right]} = \sqrt{4\left[\dot{\varepsilon}^2_{12} + \dot{\varepsilon}^2_{23} + \dot{\varepsilon}^2_{31}\right] + 2\left[\dot{\varepsilon}^2_{11} + \dot{\varepsilon}^2_{22} + \dot{\varepsilon}^2_{33}\right]} \quad (5\text{-}9)$$

The power law model can be used to model the STF characteristic in LS-DYNA but it requires acceptable estimation of power law model parameters. The acceptable estimation of these parameters may be difficult to achieve sometimes and it increases the complicacy of the simulation. There is another very efficient capability presents in LS-DYNA to implement STF characteristic by providing empirical dynamic viscosity vs shear strain rate data using user defined curve. In order to directly feed the empirical rheometric data, a user defined curve is required as provided by DEFINE_CURVE card. The empirical rheometric data of STF sample used in the modelling is as shown in Figure 5-3, Figure 5-4, and Figure 5-5. The values of material card are given in Table 5-3 and density of STF is given in Table 5-4.

Table 5-3 Implemented material card of STF MAT_ALE_VISCOUS in LS-DYNA

MAT	**Density (ρ), $\frac{kg}{mm^3}$**	**Dynamic Viscosity, (Gpa.ms)**
STF	Varying (Refer Table 5-4)	(USER INPUT CURVE) (Refer Figures showing dynamic viscosity vs shear rate) Figure 5-3, Figure 5-4, and Figure 5-5

The density and other critical properties of STF sample is given in Table 5-4. These values are directly fed in material card to predict the STF characteristic of samples.

Table 5-4 Properties of shear thickening fluid (STF) samples used in FE models (Prabhu & Singh, 2021)

STF	PEG	Wt.%	Gp	Gs	STF density (gm/cc)	Critical Viscosity (Pa.s)	Critical Shear Rate (1/s)
1	200	15	1.124	2.3	1.217	68.5	86.7
2	200	20	1.124	2.3	1.252	99.5	71.6
3	200	25	1.124	2.3	1.289	258	61.6
4	200	30	1.124	2.3	1.328	335	56.5
5	300	15	1.125	2.3	1.218	98	76.6
6	300	20	1.125	2.3	1.253	109.8	71.6
7	300	25	1.125	2.3	1.290	268	51.4
8	300	30	1.125	2.3	1.329	355	56.5
9	400	15	1.128	2.3	1.221	88.5	46.4
10	400	20	1.128	2.3	1.256	195	41.3
11	400	25	1.128	2.3	1.293	238	41.3
12	400	30	1.128	2.3	1.331	453	36.3

The MAT_ALE_VISCOUS is an improved version of MAT_NULL and hence it requires EOS to predict hydrostatic stress (normal compression). In order to define the hydrostatic stress only bulk modulus is considered and values are adopted from (Rizzo et al., 2020). The parameters of EOS_LINEAR_POLYNOMIAL for shear thickening fluid is given in Table 5-5.

Table 5-5 EOS for STF: EOS_LINEAR_POLYNOMIAL (Rizzo et al., 2020)

Material	C_0 **(MPa)**	C_1 **(MPa)**	C_2 **(MPa)**	C_3 **(MPa)**	C_4	C_5	C_6
Water	0	3000	0	0	0	0	0

The MAT_SPH_VISCOUS is another material card which can be used to simulate the STF characteristic in LS-DYNA. This material card is only applied to smooth particle hydrodynamics (SPH) nodes. This material card can also implement user defined dynamic viscosity of fluids and hence can be used where high stability in the simulation is required. Similar to previous material cards this material card also requires EOS to predict the hydrostatic stress in the fluid. Furthermore, for shear thinning behavior, this model utilizes Cross viscous model. The quarter model of STF and its domain is shown in Figure 5-2.

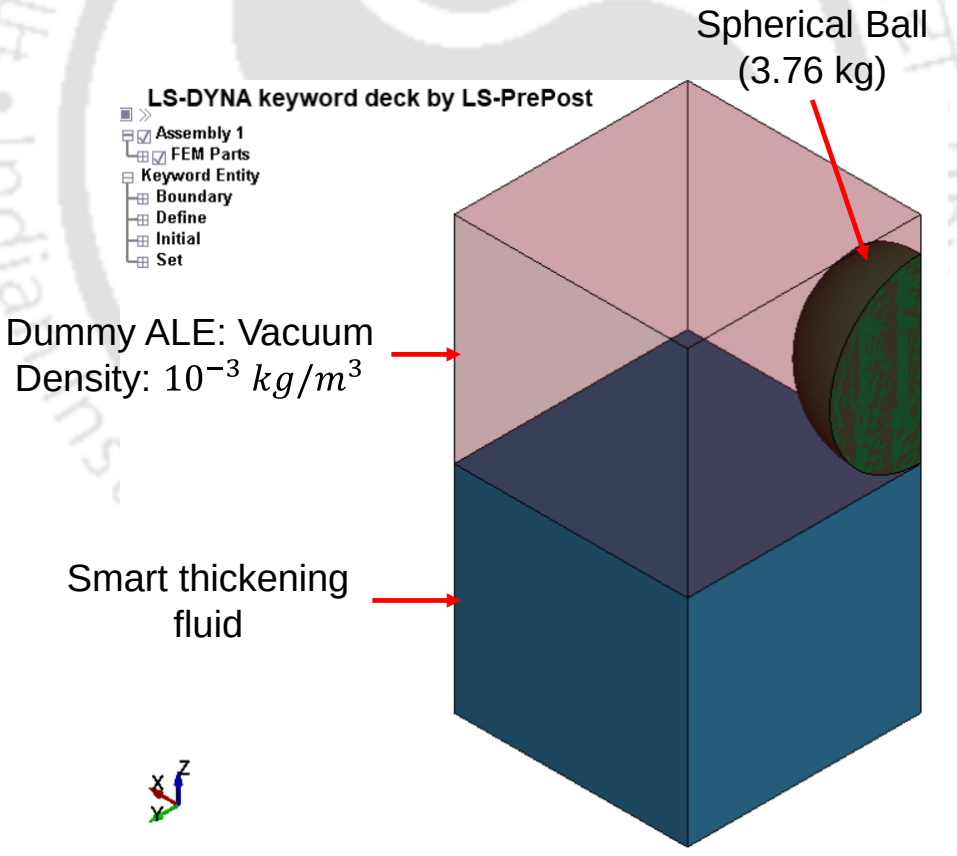

Figure 5-2 Multi-material ALE Quarter Model of rigid ball impacting on shear thickening fluid

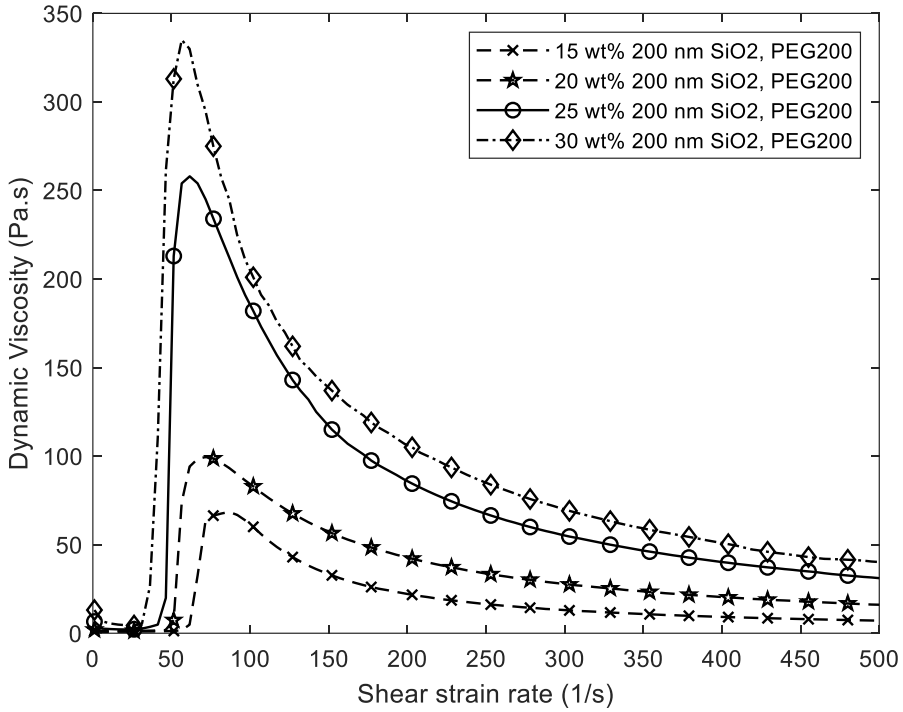

Figure 5-3 A graphical representation of variation of dynamic viscosity w.r.t. shear strain rate of STF samples having varying weight % fraction of 200 nm fumed silica and 200 molecular weight of Polyethylene Glycol

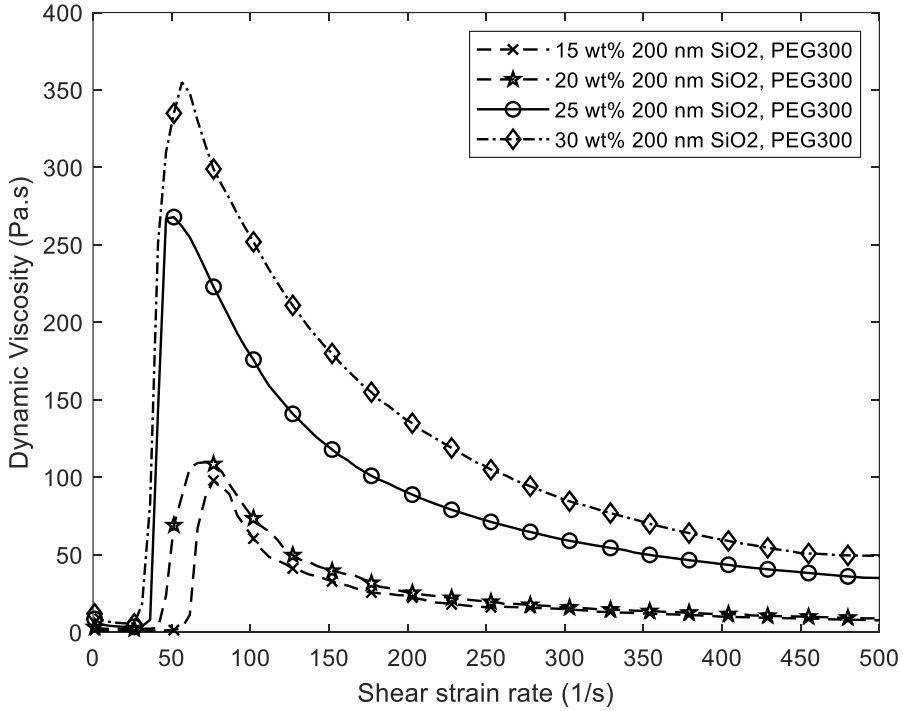

Figure 5-4 A graphical representation of variation of dynamic viscosity w.r.t. shear strain rate of STF samples having varying weight % fraction of 200 nm fumed silica and 300 molecular weight of Polyethylene Glycol

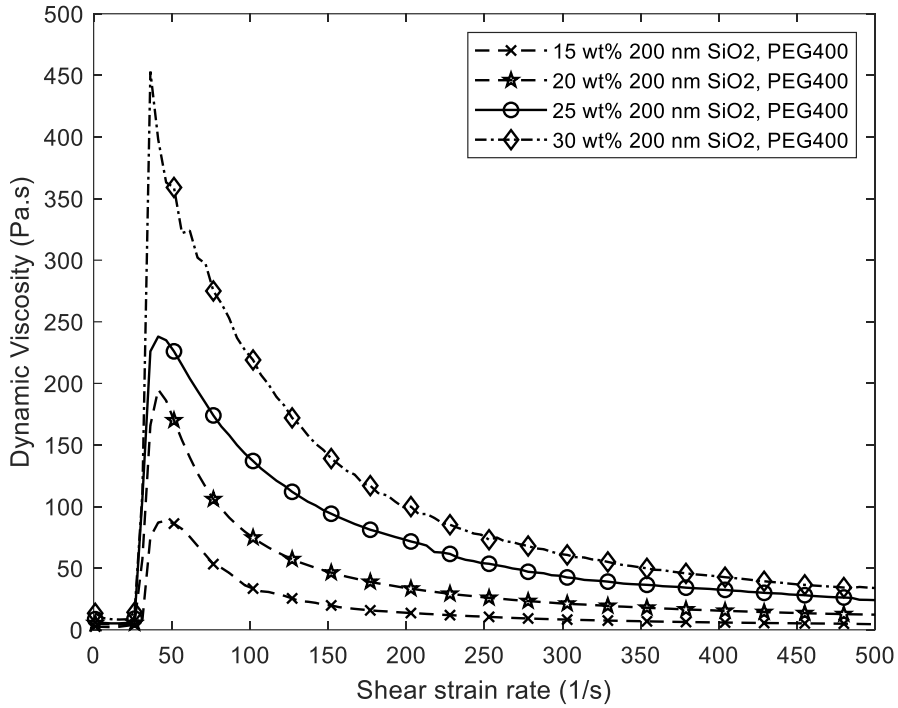

Figure 5-5 A graphical representation of variation of dynamic viscosity w.r.t. shear strain rate of STF samples having varying weight % fraction of 200 nm fumed silica and 400 molecular weight of Polyethylene Glycol

5.3 Coupling between fluid and rigid sphere

Fluid Structure Interaction (FSI) is implemented using coupling type penalty-based coupling formulation between fluid and solid in CONSTRAINED_LAGRANGE_IN_SOLID card. Since, the mesh of two domains are not uniform the number of coupling points are distributed over each coupled Lagrangian surface, the segment is set to be 3 for optimal performance and computation time. Higher values increase the computational time. The fluid only resists the normal compression and shear when it interacts with rigid body. The coupling direction is normal compression only and coefficient of friction between fluid and solid is set as 1×10^{20}. The infinite value of coefficient of friction is set to achieve no slip wall boundary condition between fluid and rigid body. All other values in the coupling are set as default values.

5.4 Results and Discussion

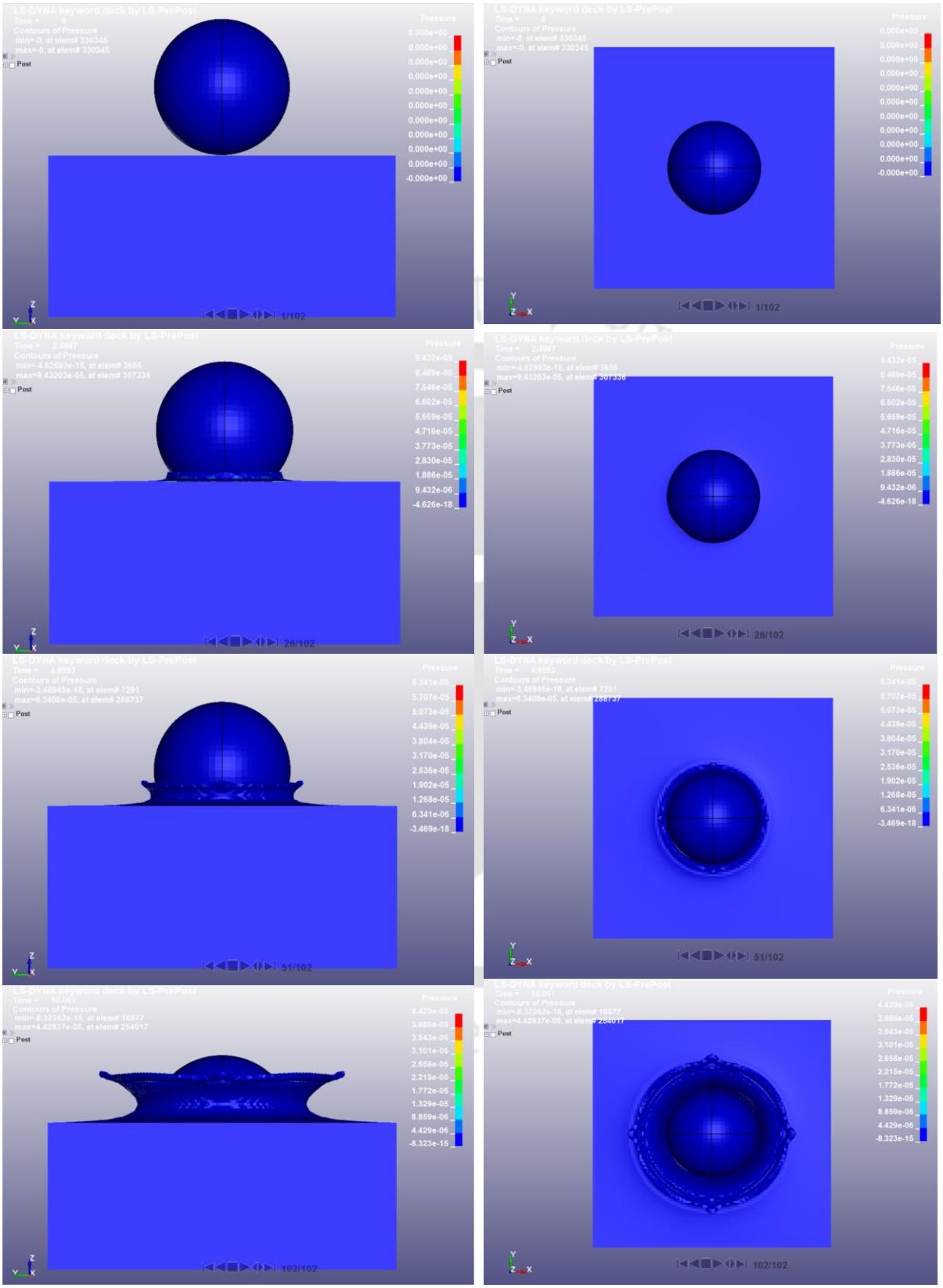

Figure 5-6 A pictorial representation of a rigid ball impacting on surface of water at different time frame.

The residual acceleration from the numerical simulation when compared with (Bisagni & Pigazzini, 2018) are in good agreement. The graphical representation of the residual acceleration is shown in Figure 11.

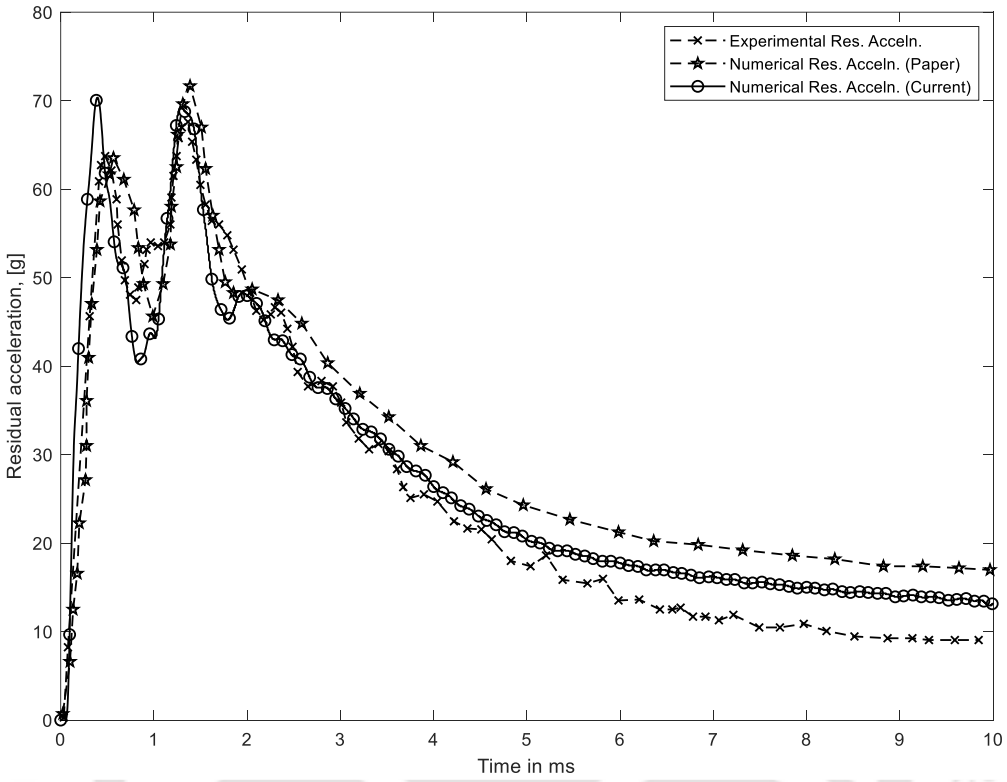

Figure 5-7 A graphical representation of comparison of residual acceleration from experiment, numerical results from the paper, and numerical simulation in this thesis from rigid ball impacting on the water

Further, similar modelling has been carried out by replacing water to shear thickening fluid. For simplicity only, bulk modulus of the shear thickening fluid is considered in the EOS card. The numerical simulation has been conducted to understand the impact performance using different developed shear thickening fluid under varying viscosity w.r.t shear strain rate, and sphere velocity. In order to perform numerical simulation of STF under impact, the user-defined viscous fluid material card requires viscosity data w.r.t shear strain rate. The properties of STF greatly varies based on the type of solid nanoparticles, medium in which it is blended like polyethylene glycol, filler materials. and the synthesising technique. The sonochemical method is the most suitable method to achieve best rheological properties of STF (Prabhu & Singh, 2021). The STF is further tested to get the rheological data using rheometer. The rheological data is provided as an input in the numerical model to simulate the STF fluid. The same modelling technique as detailed earlier is followed and STF is characterized numerically under impact.

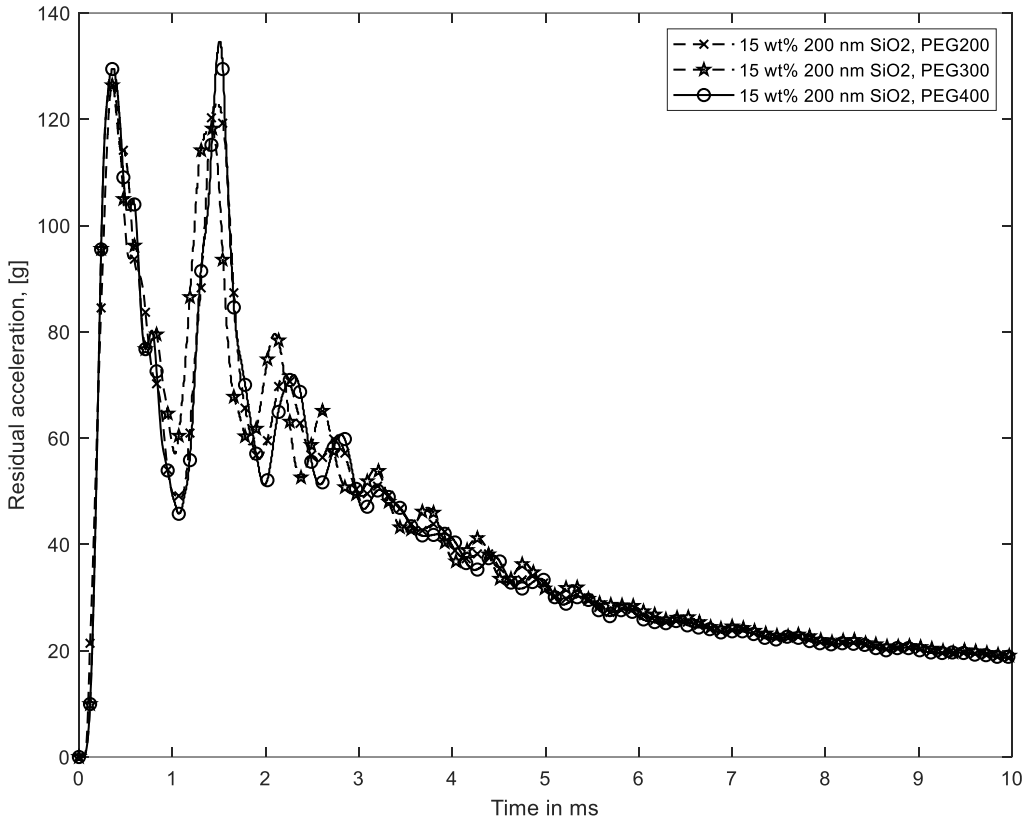

Figure 5-8 A graphical comparison of residual acceleration of STF sample having varying molecular weight of Polyethylene Glycol and 15 weight % fraction of 200 nm fumed silica under rigid sphere impact

The obtained residual acceleration data from numerical simulation is graphically shown in Figure 12 for 15 wt. % of 200 nm size fumed silica blended into PEG200, PEG300, and PEG400 (Polyethylene glycol: molecular weight 200, 300, and 400 respectively). The residual acceleration of the rigid sphere is considered because it gives and indirect estimation of the force experienced by sphere during impact. It can be inferred that higher the retarding acceleration, better will be the impact performance. It is observed from the figure that the behavior of residual acceleration of STF of 15 wt. % of 200 nm size fumed silica blended into PEG200, PEG300, and PEG400 is similar, and it does not depend significantly upon different types of PEG. The reason for such impact behavior is due to the similar rheological properties of STF for different polyethylene glycol and same weight % of fumed silica. The critical viscosity at critical strain rate obtained from the experiment for 15 wt. % of 200 nm size fumed silica blended into PEG200, PEG300, and PEG400 is 68.5 Pa.s, 98 Pa.s, and 88.5 Pa.s respectively. The variation in the critical viscosity of the STF from 15 wt. % of 200 nm size fumed silica blended into PEG200, PEG300, and PEG400 is not significant and hence their impact characteristics are similar.

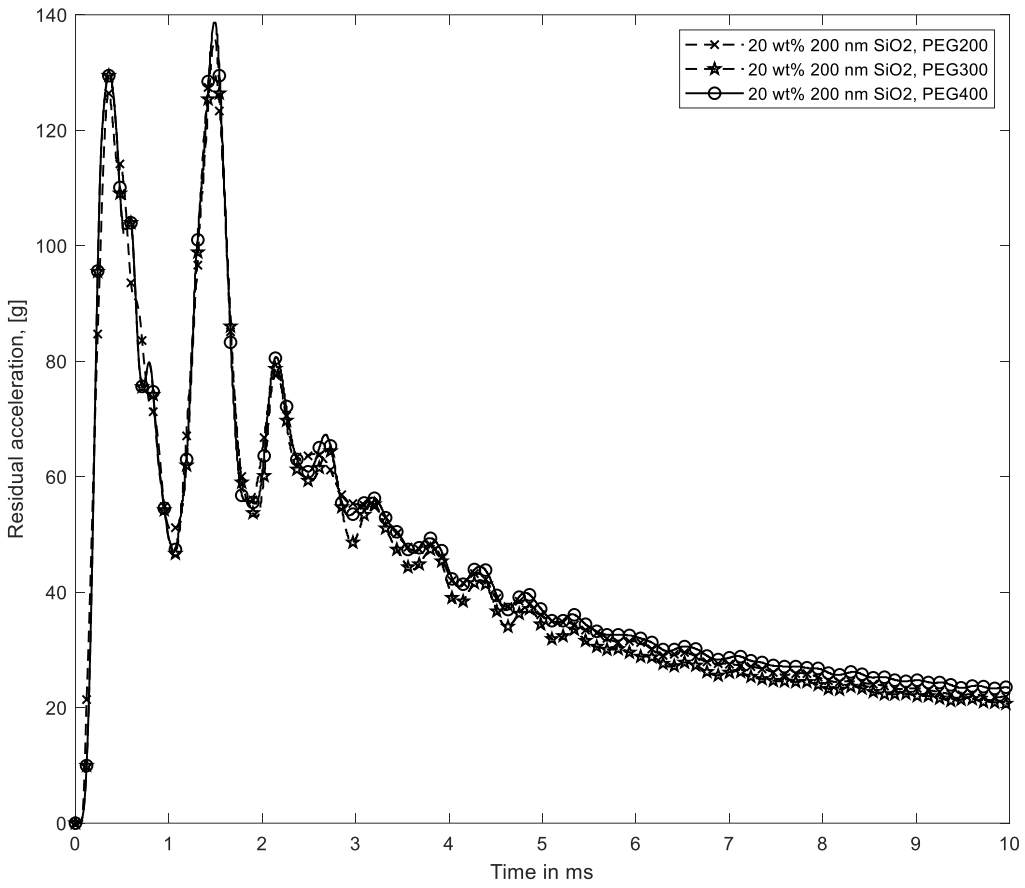

Figure 5-9 A graphical comparison of residual acceleration of STF sample having varying molecular weight of Polyethylene Glycol and 20 weight % fraction of 200 nm fumed silica under rigid sphere impact

The obtained residual acceleration data from numerical simulation is graphically shown in Figure 13 for 20 wt. % of 200 nm size fumed silica blended into PEG200, PEG300, and PEG400 (Polyethylene glycol: molecular weight 200, 300, and 400 respectively). It is observed from the figure that the behavior of residual acceleration of STF of 20 wt. % of 200 nm size fumed silica blended into PEG200, PEG300, and PEG400 is similar and more or less does not depend upon different types of PEG. The reason for such impact behavior is due to similar rheological properties of STF for different polyethylene glycol and same weight % of fumed silica. The critical viscosity at critical strain rate obtained from the experiment for 20 wt. % of 200 nm size fumed silica blended into PEG200, PEG300, and PEG400 is 99.5 Pa.s, 109.8 Pa.s, and 195 Pa.s respectively. The variation in the critical viscosity of the STF from 20 wt. % of 200 nm size fumed silica blended into PEG200, PEG300, and PEG400 is not significant and hence their impact characteristics are similar.

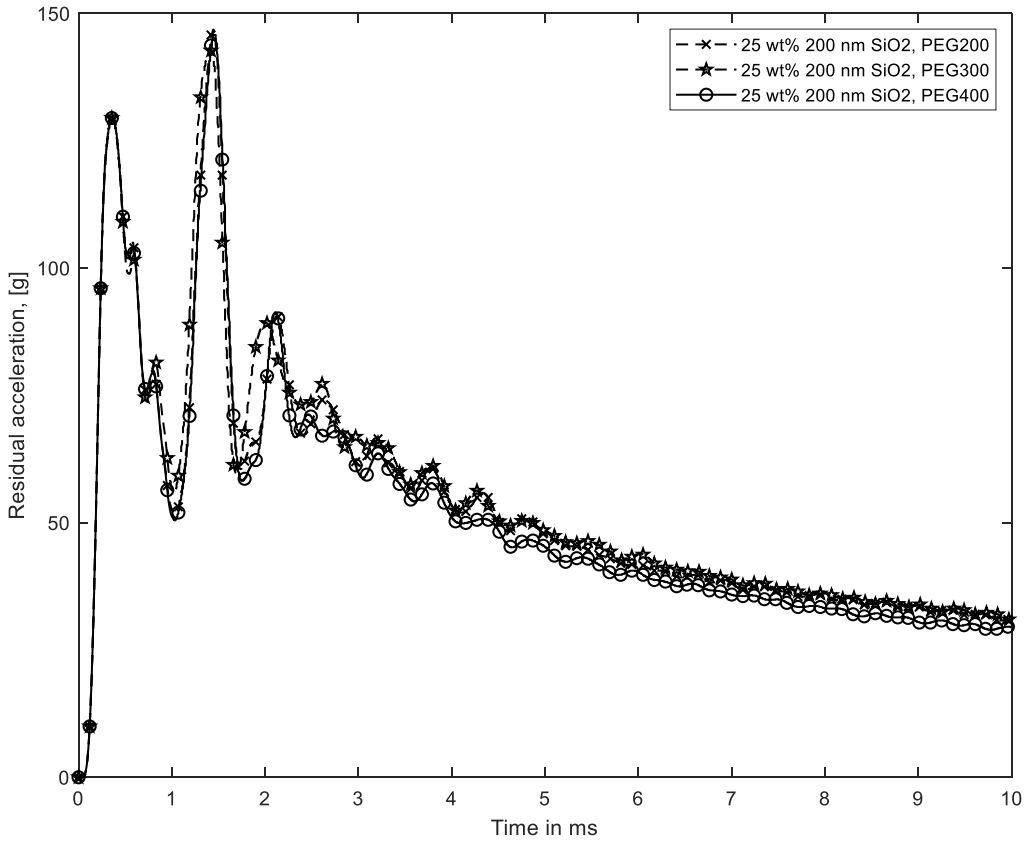

Figure 5-10 A graphical comparison of residual acceleration of STF sample having varying molecular weight of Polyethylene Glycol and 25 weight % fraction of 200 nm fumed silica under rigid sphere impact

The obtained residual acceleration data from numerical simulation is graphically shown in Figure 14 for 25 wt. % of 200 nm size fumed silica blended into PEG200, PEG300, and PEG400 (Polyethylene glycol: molecular weight 200, 300, and 400 respectively). It is observed from the figure that the behavior of residual acceleration of STF of 25 wt. % of 200 nm size fumed silica blended into PEG200, PEG300, and PEG400 is similar and more or less does not depend upon different types of PEG. The reason for such impact behavior is due to similar rheological properties of STF for different polyethylene glycol and same weight % of fumed silica. The critical viscosity at critical strain rate obtained from the experiment for 25 wt. % of 200 nm size fumed silica blended into PEG200, PEG300, and PEG400 is 258 Pa.s, 268 Pa.s, and 238 Pa.s respectively. The variation in the critical viscosity of the STF from 25 wt. % of 200 nm size fumed silica blended into PEG200, PEG300, and PEG400 is not significant and hence their impact characteristics are similar.

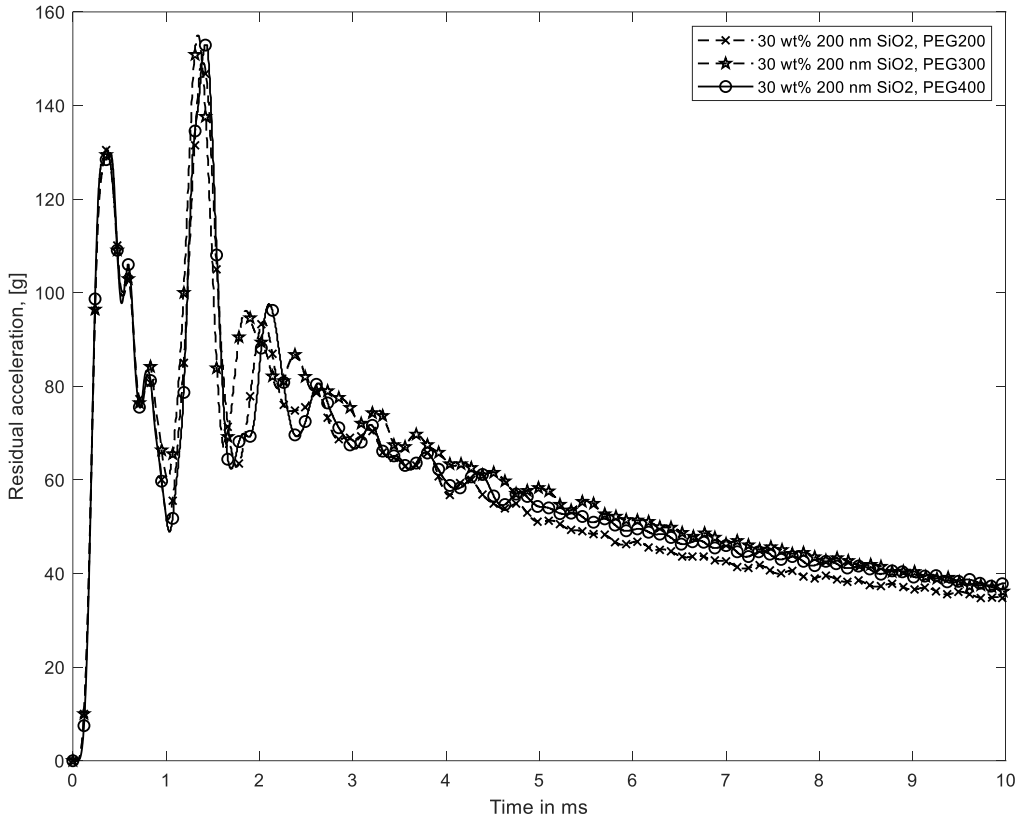

Figure 5-11 A graphical comparison of residual acceleration of STF sample having varying molecular weight of Polyethylene Glycol and 30 weight % fraction of 200nm fumed silica under rigid sphere impact

The obtained residual acceleration data from numerical simulation is graphically shown in Figure 15 for 30 wt. % of 200 nm size fumed silica blended into PEG200, PEG300, and PEG400 (Polyethylene glycol: molecular weight 200, 300, and 400 respectively). It is observed from the figure that the behavior of residual acceleration of STF of 30 wt. % of 200 nm size fumed silica blended into PEG200, PEG300, and PEG400 is similar and more or less does not depend upon different types of PEG. The reason for such impact behavior is due to similar rheological properties of STF for different polyethylene glycol and same weight % of fumed silica. The critical viscosity at critical strain rate obtained from the experiment for 30 wt. % of 200 nm size fumed silica blended into PEG200, PEG300, and PEG400 is 335 Pa.s, 355 Pa.s, and 453 Pa.s respectively. The variation in the critical viscosity of the STF from 30 wt. % of 200 nm size fumed silica blended into PEG200, PEG300, and PEG400 is not significant and hence their impact characteristics are similar.

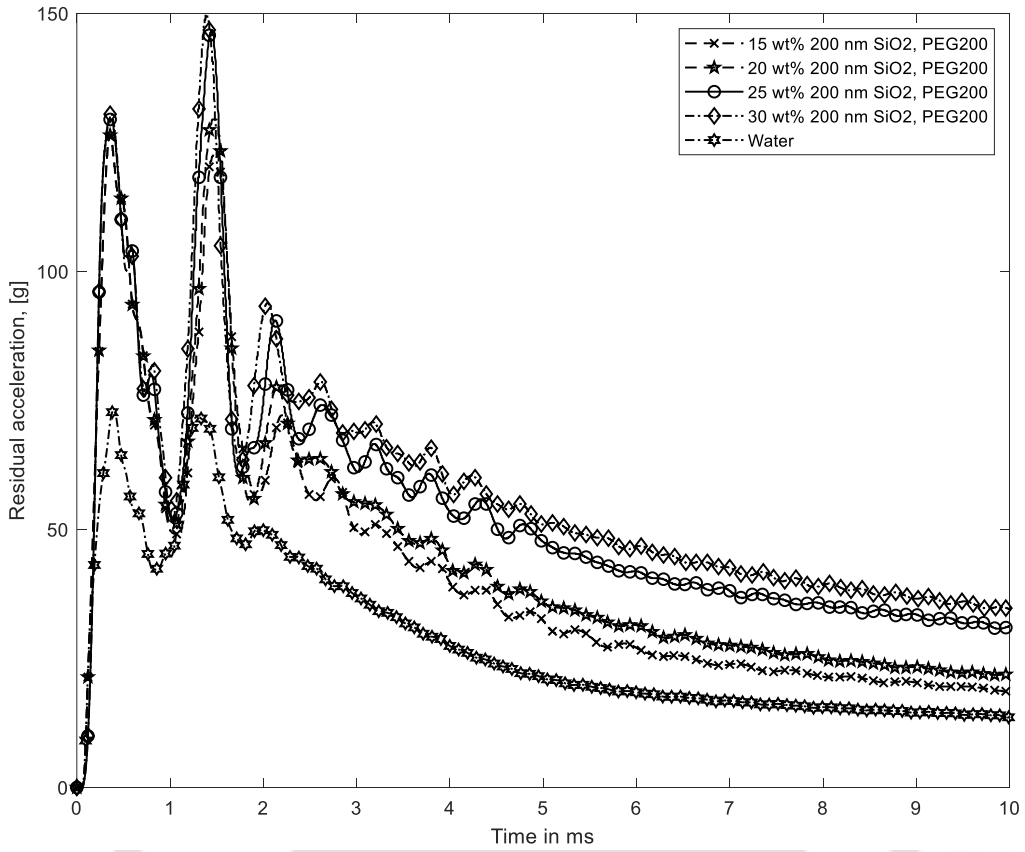

Figure 5-12 A graphical comparison of residual acceleration of Water and STF samples having varying weight % fraction of 200 nm fumed silica and 200 molecular weight of Polyethylene Glycol under rigid sphere impact

The impact characteristic of STF comprised of different weight percentage of 200 nm size silica and PEG200 is obtained numerically and its graphical representation is shown in Figure 16. From the figure it is observed that the residual acceleration values are approximately twice for all STF as compared to standard validated water model. Also, impact characteristics of STF having quantity of 200 nm fumed silica of 25% and 30 % of weight fraction is similar and better as compared to 200 nm fumed silica of 25% and 30 % of weight fraction in the same media. The reason is that it is at its critical viscosity. The critical viscosity for 15 wt %, 20 wt %, 25 wt%, and 30 wt % and PEG 200 is 68.5 Pa.s, 99.5 Pa.s, 258 Pa.s, and 335 Pa.s. The critical viscosity of 15 wt %, and 20 wt% lies in the same range while the critical viscosity of STF comprised of 25 wt%, and 30 wt% may be falling in the same category.

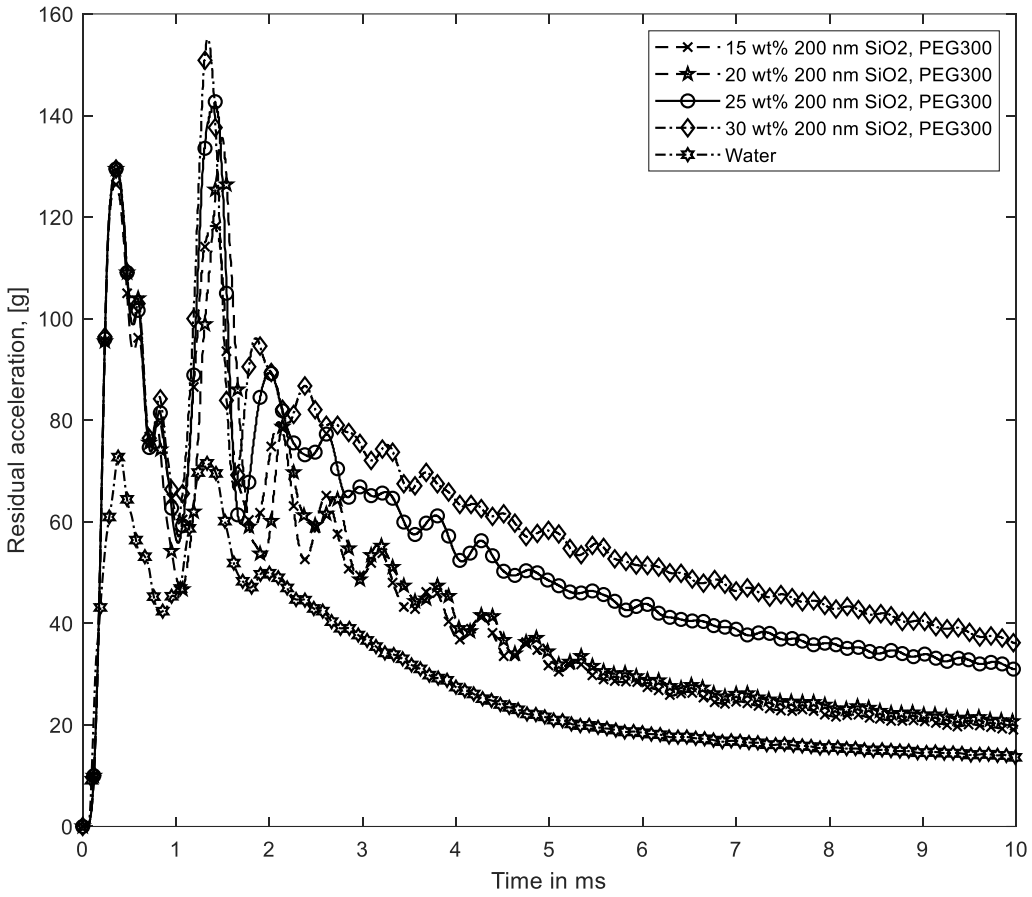

Figure 5-13 A graphical comparison of residual acceleration of Water and STF samples having varying weight % fraction of 200 nm fumed silica and 300 molecular weight of Polyethylene Glycol under rigid sphere impact

The similar observation was found for the PEG 300. The impact characteristic of STF comprised of different weight percentage of 300 nm size silica and PEG300 is obtained numerically and its graphical representation is shown in Figure 17. From the figure, it is observed that the residual acceleration values are approximately twice for all STF as compared to standard validated water model. Also, impact characteristics of STF having quantity of 300 nm fumed silica of 25% and 30 % of weight fraction is similar and better as compared to 300 nm fumed silica of 25% and 30 % of weight fraction in the same media. The reason is the critical viscosity of the STF. The critical viscosity for 15 wt %, 20 wt %, 25 wt%, and 30 wt % and PEG 300 is 98 Pa.s, 109.8 Pa.s, 268 Pa.s, and 355 Pa.s. The critical viscosity of 15 wt %, and 20 wt% lies in the same range while the critical viscosity of STF comprised of 25 wt%, and 30 wt% may be falling in the same category.

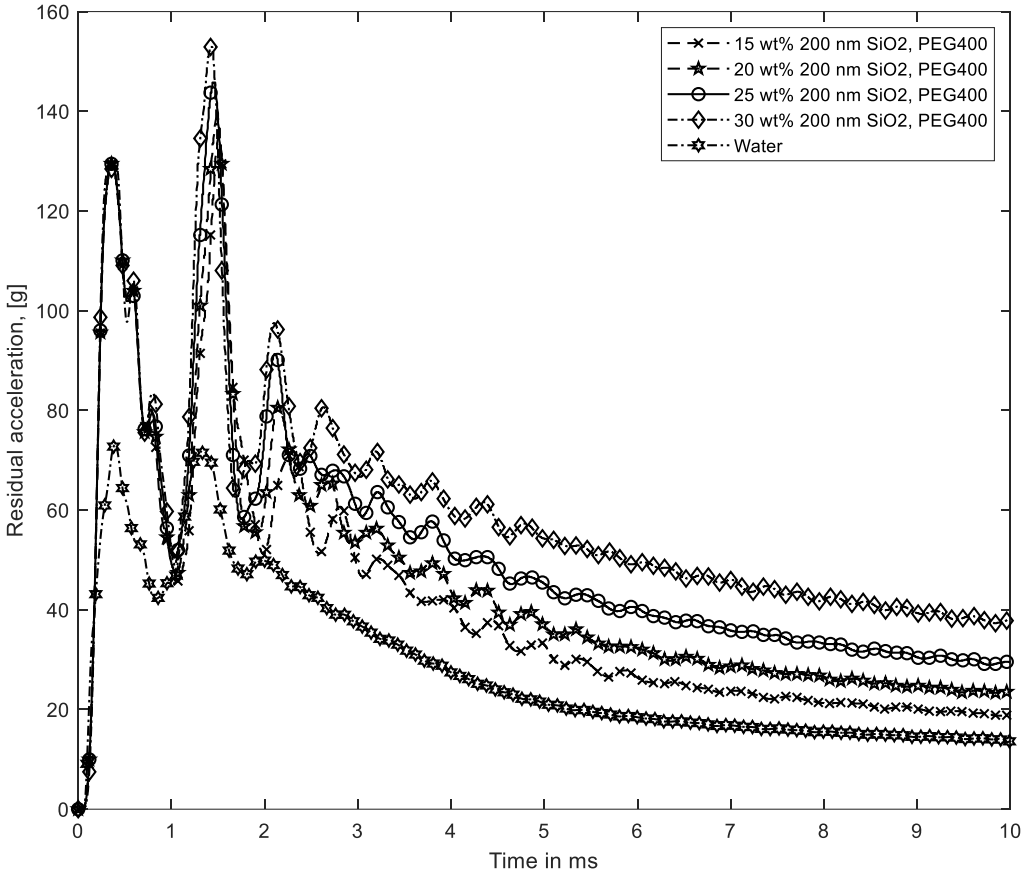

Figure 5-14 A graphical comparison of residual acceleration of Water and STF samples having varying weight % fraction of 200 nm fumed silica and 400 molecular weight of Polyethylene Glycol under rigid sphere impact

The impact characteristic of STF comprised of different weight percentage of 400 nm size silica and PEG400 is obtained numerically and its graphical representation is shown in Figure 18. From the figure, it is observed that the residual acceleration values are approximately twice for all STF as compared to standard validated water model. Also, impact characteristics of STF having quantity of 400 nm fumed silica of 25% and 30 % of weight fraction is similar and better as compared to 400 nm fumed silica of 25% and 30 % of weight fraction in the same media. The is its critical viscosity. The critical viscosity for 15 wt %, 20 wt %, 25 wt%, and 30 wt % and PEG 400 is 68.5 Pa.s, 99.5 Pa.s, 258 Pa.s, and 335 Pa.s. The critical viscosity of 15 wt %, and 20 wt% lies in the same range while the critical viscosity of STF comprised of 25 wt%, and 30 wt% may be falling in the same category.

5.5 Conclusion

In this chapter MM-ALE based modelling approach of Shear Thickening Fluid is developed. The LS-DYNA has robust capabilities to simulate the shear thickening fluid, and

for this various material cards in MM-ALE modelling approach are investigated. The modelling approach adopted in this research is of macro-level modelling of STF where STF is treated as one phase material. The rheology of STF is experimentally determined and implemented in the model. Based on the variation of nano-silica particle and polyethylene glycol a total of 12 different samples of STF is implemented in the modelling of STF. The de-acceleration of sphere for STF sample having same weight percent of silica particle and different polyethylene glycol is more or less same. Also, the residual velocity is same for all STF samples having same weight percent of nano-silica and different polyethylene glycol. There is decrease in the residual velocity where weight percent of the silica particle is increasing in the STF sample. The MM-ALE based approach overcomes the limitations of friction-based models. The model proposed in this Chapter will be used to integrate with neat fabric. The integrated MM-ALE approach will be used to the ballistic performance of the fabric impregnated with STF and presented in Chapter 6.

6 Multi-scale MM-ALE based numerical modelling of STF impregnated fabric under ballistic impact

6.1 Introduction

The light weight and flexible armour whose performance match as per NIJ standards is presented in this Chapter. The most common method to develop flexible armour is to utilize high performance ballistic fabric such as Kevlar® KM2. Further the performance of these neat fabric can be enhanced after shear thickening fluid treatment. The advantages of such method are discussed and highlighted in Section 2.3 of Chapter 2. Many researchers show the benefits of treating fabric to STF fluid such as significant improvement in the ballistic performance without or insignificant compromising in the flexibility (Arora et al., 2020; Laha & Majumdar, 2016; Majumdar et al., 2013; Wetzel et al., 2004). The enhancement technique is studied extensively by researchers using experimental as well as numerical technique. The numerical technique employed is based on modelling approach of fabric as well as STF fluid. Generally, modelling of fabric involves multi-scale modelling approach where a fabric can be modelled from continuous to fiber level modelling by utilizing the principle of mechanics of materials. The scale of fabric varies depending upon accuracy and efficiency requirements from fiber level to micro-mechanical modelling. Fiber level modelling is more accurate as compared to filament level; filament level is more accurate as compared to yarn level; and yarn level is more accurate as compared to micro-mechanical level but the improved accuracy comes at the cost of high computational power which may be proven to be inefficient for higher resolution modelling approach. Furthermore, interaction of various constituents of fabric will be interacting with each other and the interactions such as yarn-yarn interaction, filament-filament interaction, and fiber-fiber interaction should be considered. It is well established that the performance of ballistic fabric depends upon these interactions (Briscoe & Motamedi, 1992; Dong & Sun, 2009; Duan et al., 2005; Ha-Minh et al., 2012; Nilakantan et al., 2010; Wang et al., 2016; Zeng et al., 2006). Since, micromechanical models does not account for these interactions, and hence this approach will be not used for evaluation of ballistic performance of the fabric. Furthermore, fiber and filament level modelling require very high computational cost as compared to yarn-level modelling and produces slightly improved results. Based on these facts, yarn level models (also known as meso-scale models) of fabric produce acceptable results with economical computational cost and considering of yarn-yarn interaction effect. The yarn level modelling provides great opportunities to model the effect of STF fluid

interaction to the fabric. Many researchers implemented the mechanism of STF fluid interaction in STF treated fabric through incorporating altered inter-yarns friction (Gürgen, 2020; Gürgen et al., 2017; Khodadadi et al., 2018; Lee & Kim, 2012; Mirrahimi et al., 2017). It was proposed that STF significantly improves the inter-yarn friction and subsequently, the ballistic performance of the fabric. The inter-yarn friction is determined for STF treated fabric using pull out test following similar procedure for neat fabric. The results from the pull-out test is simulated using meso-scale modelling of the fabric. The inter-yarn friction is implemented based on coulomb's friction model as discussed in Section 3.3 of Chapter 3. The process of determining inter-yarn friction based on pull-out test and coulomb's friction model is known as semi-empirical approach. The modelling of STF treated fabric based on inter-yarn friction is vastly applied to study the ballistic performance of the fabric but this approach has limitations. The inter-yarn friction model requires coefficients of friction between yarns of treated fabric and it is very difficult to achieve at various pull-out speed. There will be always limited scope to implement friction-based model at different pull-out speed and hence there will be always chance to ignore the effect of STF at different strain rate. The friction-based models do not provide insight regarding STF effect on ballistic performance of the fabric. The only advantage of friction-based models is that they are computationally very fast and efficient too but they fail to properly simulate the ballistic impact of STF treated fabric. The proper modelling of STF is required to account the STF effect on the fabric. There is limited literature available which discusses this approach. (Sen et al., 2019) describes coupled Eulerian-Lagrangian approach to model the ballistic impact behaviour of STF treated fabric. The STF is modelled as fluid using Eulerian approach while fabric is modelled as Lagrangian approach and the coupling between both is defined to simulate fluid structure interaction. It has been shown that the numerical model produces results in good agreement with the experimental results. The outcome of the developed model based on CEL approach is that it successfully replicates impact behavior of STF treated fabric.

In the current research, Fluid Structure Interaction (FSI) approach will be used in which the model considers the interaction of STF to the fabric through modelling STF as a Eulerian domain and fabric as Lagrangian domain and their mutual interaction is far superior, better and realistic modelling approach than modified friction-based models. In order to model FSI problem a commercial package LS-DYNA is used. The arbitrary-Lagrangian-Eulerian approach which is synonymous to the CEL approach is applied to model the fluid structure interaction. The proposed model is applied to study the impact behavior of STF treated fabric

as per NIJ standards. The four ballistic rating is considered for the present investigation and reported in this Chapter.

6.2 Numerical Modelling

The numerical model of fluid structure interaction consists of modelling of fabric, shear thickening fluid and their mutual interaction through strong coupling between them. The modelling strategy is based on multi-material arbitrary Lagrangian Eulerian (MM-ALE). In MM-ALE approach shear thickening fluid is formulated using Eulerian approach while high-performance fabric is formulated using Lagrangian approach. An additional card is used to define the coupling between Eulerian and Lagrangian domain. The additional vacuum domain is also modelled to retain STF domain otherwise it will be deleted in the simulation when it crosses the boundary of the domain.

6.2.1 Modelling of threat: Projectile

The projectile configuration used for the validation is adopted from (Lee & Kim, 2012). The other projectiles for the study use different projectile which conforms to the NIJ standard and the parameters implemented in simulation is presented in Table 6-1. All the projectiles are considered to be hemi-elliptical and the material is lead having varying mass and velocity.

Table 6-1 Bullet specification used in FE models

Rating	**Bullet diameter (mm)**	**Bullet Length (mm)**	**Bullet weight (gm)**	**Material**	**Shape**	**Bullet Velocity (m/s)**	**Characteristic Strain rate (1/s)**
I	5.72	9.83	2.6	Lead	Hemi-elliptical	332	58041.96
II A	9.03	10.54	8	Lead	Hemi-elliptical	344	38095.24
II	9.03	10.54	8	Lead	Hemi-elliptical	370	40974.53
III A	9.03	10.54	8	Lead	Hemi-elliptical	441	48837.21

6.2.2 Modelling of fabric

The modelling of the fabric adopted is meso-scale (yarn level models) based models. The modelling strategies at yarn level has been discussed in Chapter 3. The inter-yarn friction coefficients for neat fabric is implemented and defined in CONTACT_CARD. The co-efficient of friction for STF treated fabric in MM_ALE approach is adopted as discussed in the previous Chapters. The co-efficient of inter-yarn friction is same as given in Table 3-3 Parameters of Coulomb's friction model (Lee & Kim, 2012) For the validation of MM-ALE based model the experimental results by (Lee & Kim, 2012) is used in this study. The boundary condition of neat fabric is two side fixed and two side free. The size and fabric type are same as discussed in Chapter 2. Further, the current study is extended for projectile confirming to NIJ standard. The boundary condition of fabric for later case is circular clamped and hence all the node beyond the circle will be constrained DOF in all direction. The STF effect is implemented using MM-ALE approach which is discussed in Sub-section 6.2.3 and 6.2.4.

6.2.3 Modelling of STF: MM-ALE Technique

The modelling of STF behavior in LS DYNA is implemented using MM_ALE technique and the procedure for the modelling is same as described in Chapter 5. Further, the model is validated using rheometric data from (Lee et al., 2009). The rheometric data of STF sample for the validation is as shown in Figure 6-1. Further, the order of characteristic strain rate in case of ballistic impact is $10^4\ s^{-1}$ (see Table 6-1) and the STF data corresponds to maximum strain rate of 500 s^{-1}. Since, the STF data is limited up to 500 s^{-1} strain rate, it is assumed that the dynamic viscosity will be constant beyond the maximum strain rate.

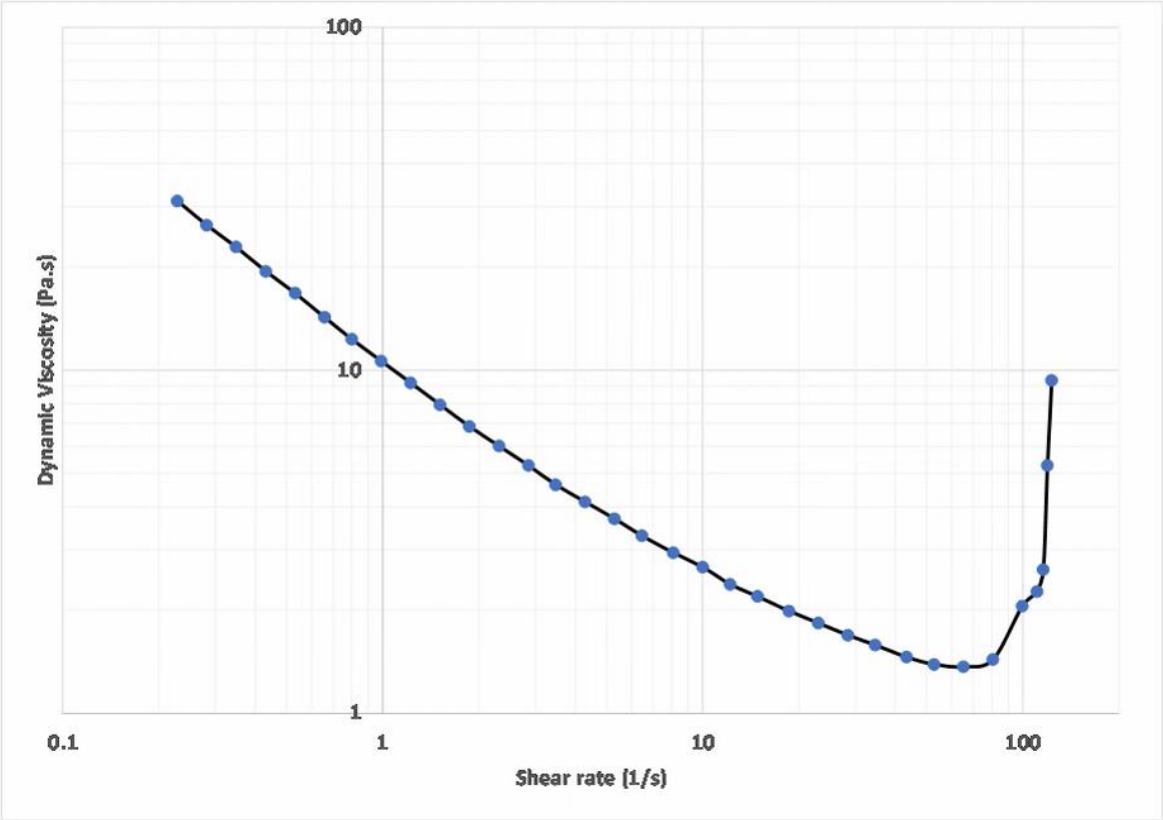

Figure 6-1 A graphic representation of Rheological data of STF sample 500nm SCS (65 % by weight) (Lee et al., 2009)

6.2.4 Modelling of coupling between fluid and lagrangian domain

The strong coupling between fluid and lagrangian domain is defined using CONSTRAINED_LAGRANGE_IN_SOLID card in LS-DYNA. The method and procedure described in Section 5.3 of Chapter 5 has been adopted. The developed model to study the effect of STF on neat fabric is as shown in Figure 6-2 and the same model is used for validation as shown in Figure 6-3.

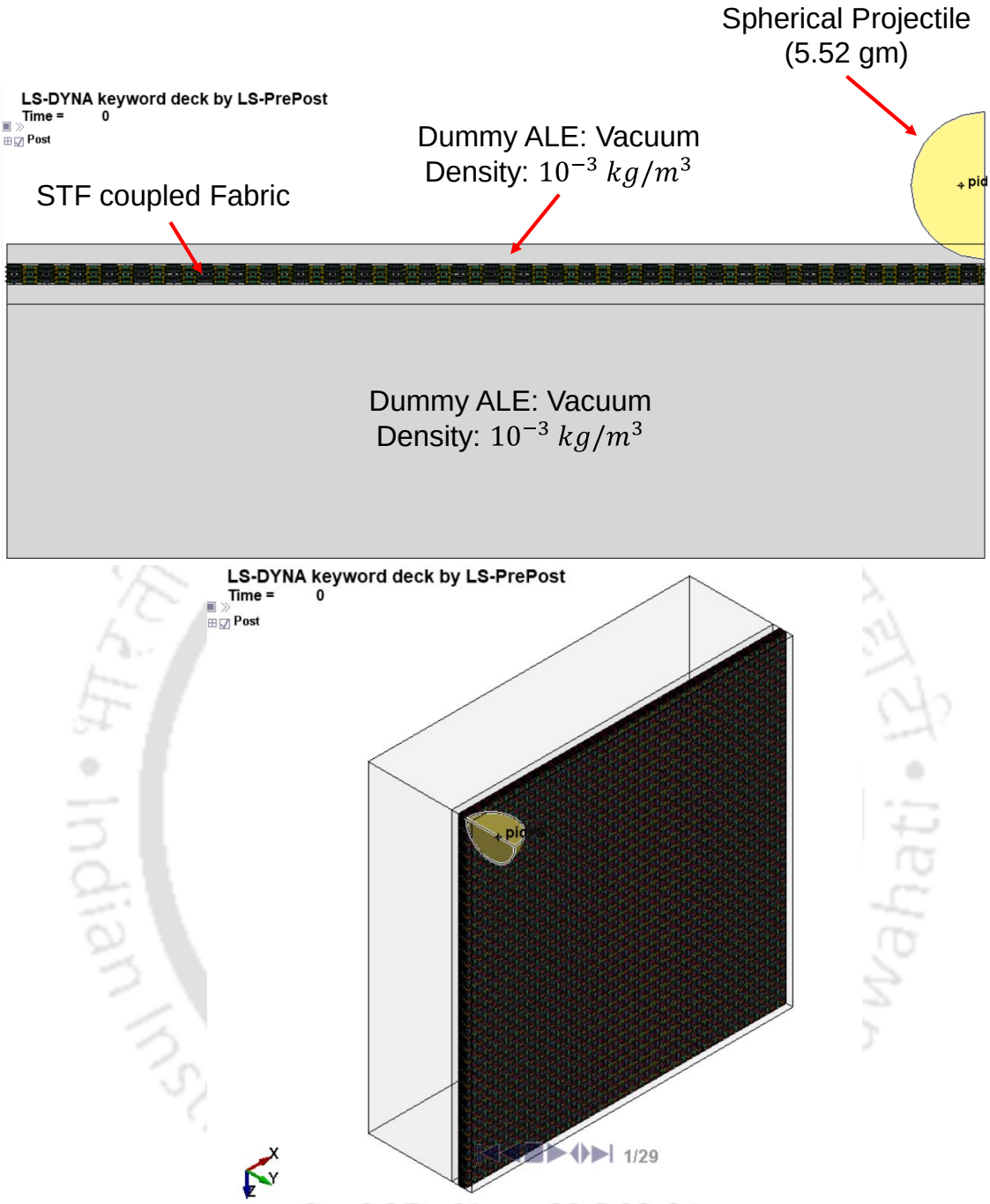

Figure 6-2 A graphical representation of MM-ALE based quarter FE model of STF impregnated to fabric having boundary Conditions: Two edges Fixed and Two Edges Free; Sample Size: 101.6 x 101.6 mm.

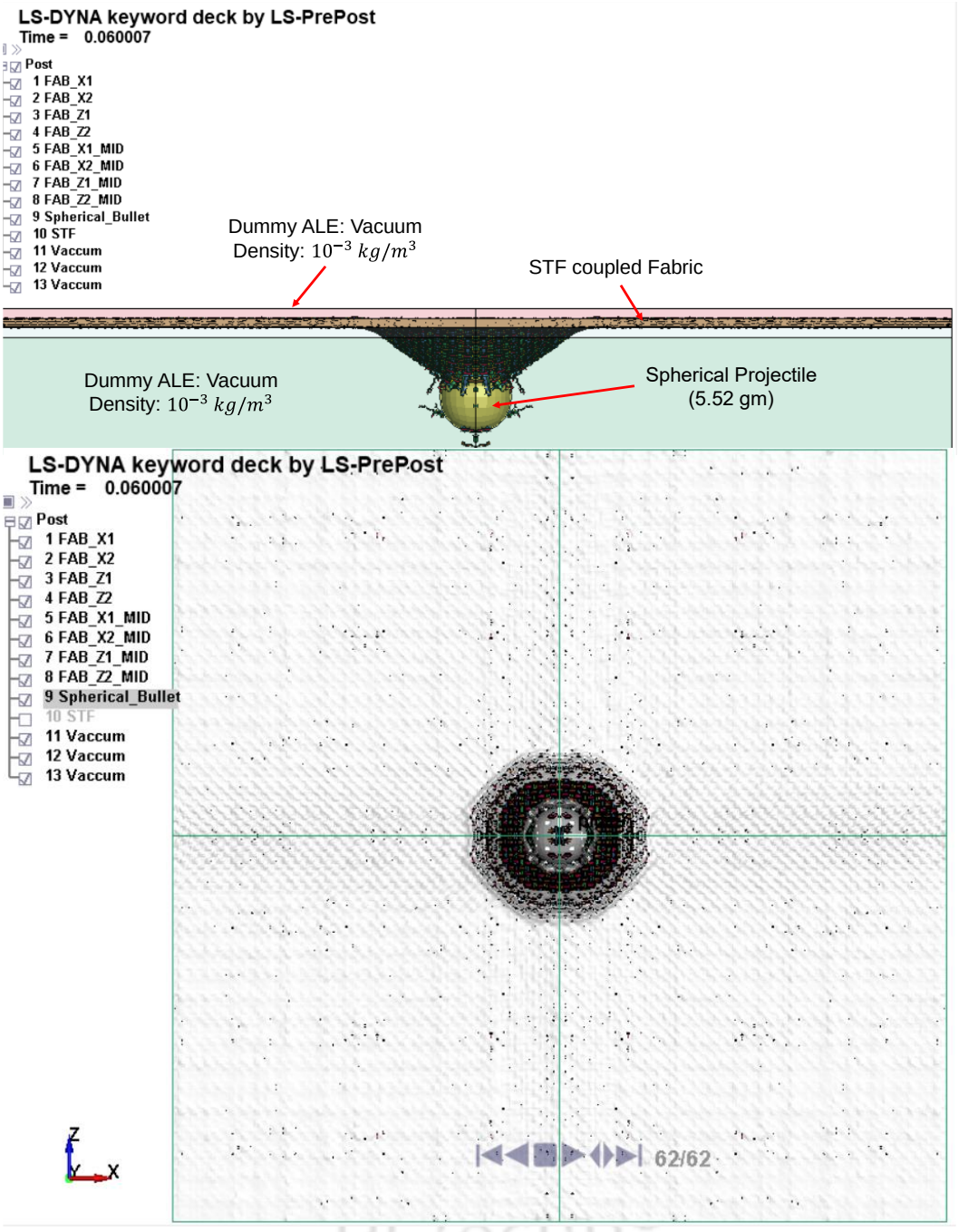

Figure 6-3 A graphical representation of MM-ALE based FE model of STF impregnated to fabric interacting with projectile having boundary Conditions: Two edges Fixed and Two Edges Free; Sample Size: 101.6 x 101.6 mm.

6.3 Results and discussion

This section presents the results obtained from numerical modelling of different configurations for instance dry fabric, STF treated fabric based on friction models of fabric and MM-ALE based models. The computational model details of friction and MM-ALE based

models are shown in Table 6-2. he double precision mechanical solver is used to solve the defined computational model in an available commercial package LS-DYNA® having SMP (Symmetric Multi-Processing) license and on a CPU consisting of single count processor of Ryzen™ 9 3900x, 12 cores and RAM 32 GB DDR4 3200 Mhz.

Table 6-2 Comparison of model complexity between friction-based model and MM ALE model (4 layers of fabric)

Element Type	**Friction-based Model**	**MM-ALE based Model**
Nodes	661010	1867710
Shells	517584	517584
Solids	378	1154080
Rigid Elements	378	378
Deformable Elements	517584	1671286
Total Elements	517962	1671664

The results obtained from friction-based model and MM-ALE based model is compared and found that MM-ALE model is more efficient as compared to friction-based models. Moreover, MM-ALE method only requires empirical rheometric data can be obtained from experiment for the design of STF treated ballistic armour. The MM-ALE method is used to predict the behavior of multi-layer fabric system under projectile impact and results for different sample of STF is compared to characterize the STF sample.

6.3.1 Modelling of high-performance neat fabric

The finite element model of the neat fabric is shown in Figure 6-4. The model accurately represents the ballistic behavior of the neat fabric. The accurate simulation of ballistic behavior of neat fabric is very important as the same model will be used to integrate into STF fluid using MM-ALE method. The numerical results of neat fabric at various projectile velocity is shown in Figure 3-3. It is very important for a model to accurately capture the ballistic behavior of neat fabric at different velocity and the model is accurately simulating ballistic performance of neat fabric at different initial velocity of projectile.

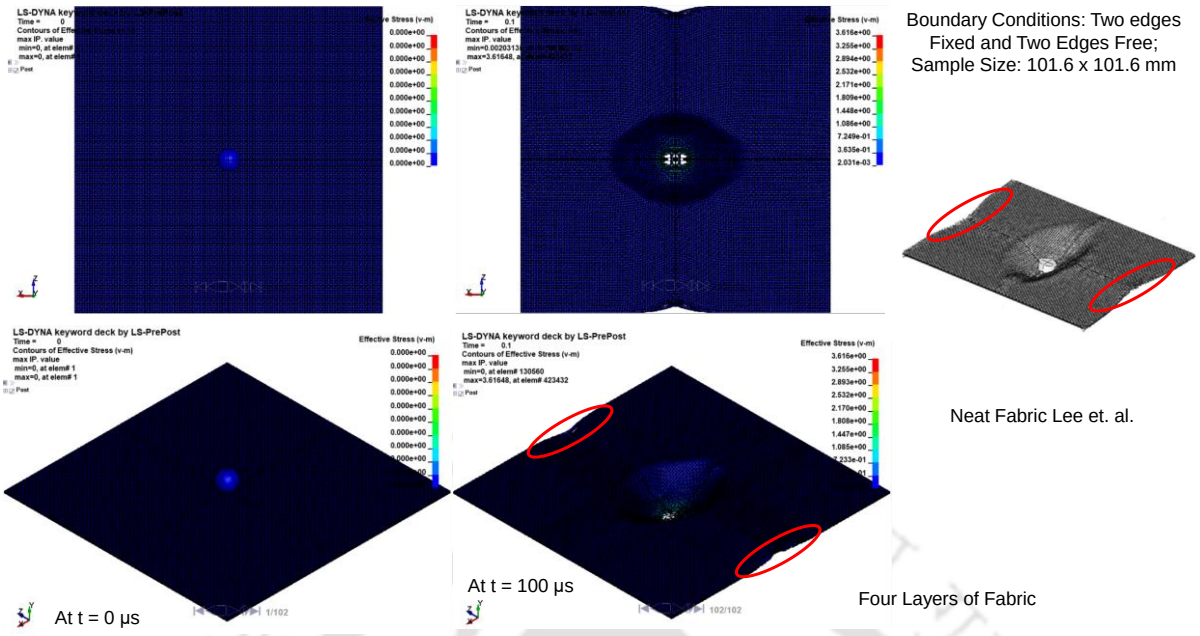

Figure 6-4 A graphic representation of model validation of neat fabric

6.3.2 Multi-Material-ALE based modelling of STF impregnated fabric

Many researchers proposed that STF behavior can be captured by altering inter-yarn friction of the fabric (Gürgen, 2020; Gürgen et al., 2017; Khodadadi et al., 2018; Lee & Kim, 2012; Mirrahimi et al., 2017). The inter-yarn friction coefficients have been calculated using semi-empirical approach. The semi-empirical approach provides coefficients of inter-yarn friction in two steps

1) Pull out test on STF treated fabric gives experimental relations between pull-out force and displacement

2) The same pull-out test is validated numerically by altering inter-yarn frictions.

The validated pull-out test provides inter-yarn friction coefficients for STF treated fabric which is used later to study the ballistic behavior of STF treated fabric. The whole process is complex and there may be possibility of not achieving the desired outcome. Moreover, there are limitations due to the varying speed at which pull-out test is carried. Hence, this process not widely used for different velocities of the projectile. The STF treated fabric is modelled using friction-based model and is presented here for comparative purpose. The finite element model of STF treated fabric using friction-based model is shown in Figure 6-5.

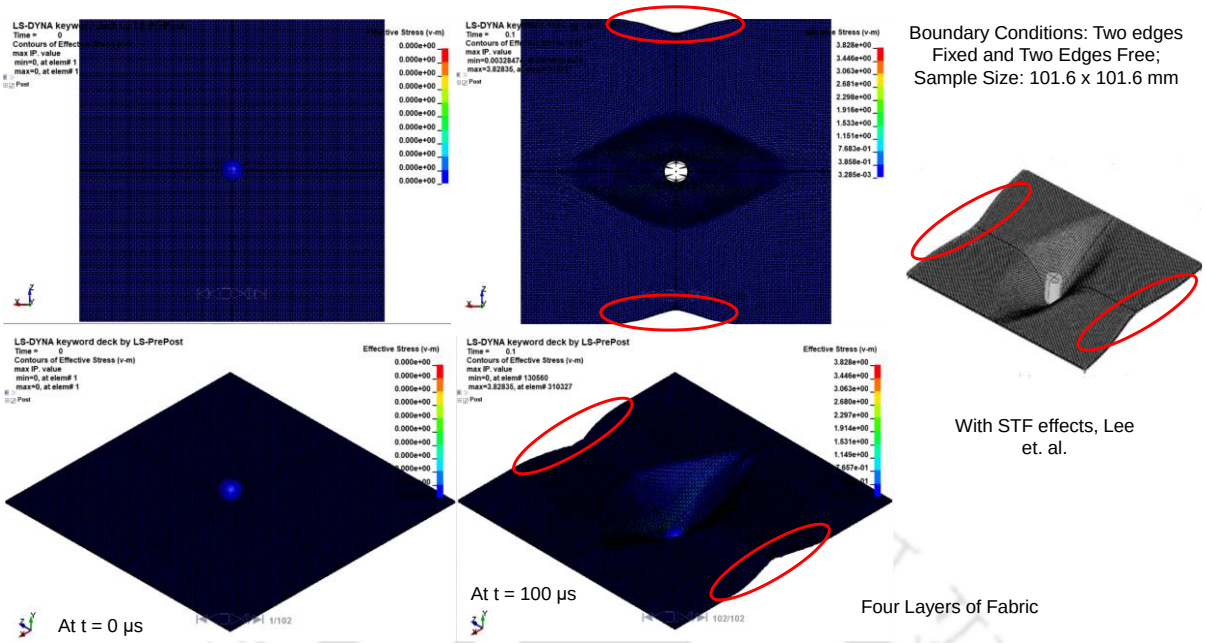

Figure 6-5 A graphic representation of model validation of STF treated fabric using friction-based model

Table 6-3 Experimental results of four layers of STF treated fabric under spherical rigid projectile of mass 5.52 gm and diameter 7.62 mm (Lee & Kim, 2012)

Initial Velocity (m/s)	Residual Velocity (m/s)	K. E. Dissipation (J)
102	47.90	20.32
151	108.54	27.92
214	179.49	34.01
242	214.06	32.31
269	243.16	33.28
280	254.68	32.37
316	300.77	24.70
385	374.75	17.04

The numerical model is validated using experimental results from (Lee & Kim, 2012). The experimental results used to compare both models are tabulated in Table 6-3.

Table 6-4 Results from friction-based models of STF treated fabric under spherical rigid projectile of mass 5.52 gm and diameter 7.62 mm

Initial Velocity (m/s)	**Residual Velocity (m/s)**	**K. E. Dissipation (J)**	**Absolute Error Residual velocity (m/s)**	**Absolute Error Dissipated energy (J)**
102.00	-9.35	28.47	57.25	8.15
151.00	14.61	62.34	93.93	34.42
214.00	175.92	40.98	3.57	6.97
242.00	213.05	36.35	1.01	4.04
269.00	254.25	21.30	11.09	11.98
280.00	266.53	20.32	11.85	12.05
316.00	308.18	13.46	7.41	11.24
385.00	380.45	9.62	5.7	7.42
Coefficient of variance (COV) of errors			140%	79%

Table 6-5 Results from MM-ALE based models of STF treated fabric under spherical rigid projectile of mass 5.52 gm and diameter 7.62 mm

Initial Velocity (m/s)	Residual Velocity (m/s)	K. E. Dissipation (J)	Absolute Error Residual velocity (m/s)	Absolute Error Dissipated energy (J)
102.00	33.51	25.62	14.39	5.3
151.00	111.19	28.81	2.65	0.89
214.00	185.31	31.62	5.82	2.39
242.00	217.06	31.59	3	0.72
269.00	249.23	28.27	6.07	5.01
280.00	260.45	29.16	5.77	3.21
316.00	299.72	27.67	1.05	2.97
385.00	369.77	31.74	4.98	14.7
Coefficient of variance (COV) of errors			74%	102%

The error for both models is calculated and given in Table 6-4 and Table 6-5. The MM-ALE based model is accurately capturing ballistic performance of the STF treated fabric. The coefficient of variance (COV) is a statistical measure of the relative dispersion of data points in a data series around the mean. Furthermore, the COV for both models is computed using the error vales from all projectile velocities. The computed COV for friction-based model and MM-ALE based model is given along with Table 6-4 and Table 6-5 respectively. Based on comparison of COV, the MM-ALE based model is predicting ballistic parameter accurately as compared to friction-based model for a very wide range of velocity. Further, a graphical comparison of ballistic performance of STF treated fabric using both models is also shown in Figure 6-6, Figure 6-7, Figure 6-8, and Figure 6-9. The friction-based model is fairly accurate for mid-range of initial projectile velocities while it produces poor results at low and high velocities. The reason for this deviation could be the use of same inter-yarn coefficients of friction for all initial projectile velocities. Furthermore, the prediction of ballistic performance

using friction-based model shows over rigid behavior at lower velocities and under rigid behavior at higher velocities. The unrealistic high value of inter-yarn coefficient of friction at low velocities restrict the movement of yarns at cross-over and hence predicts over rigid behavior. However, at higher velocities the premature failure of yarns took place due to inter-yarn coefficient of friction value higher than the optimum coefficient of friction. The high inter-yarn coefficient of friction restricts the movement of yarns and hence the stresses will be concentrated due to hinderance in the propagation of strain wave. Moreover, the viscous damping is neglected in the friction models and hence the under rigid behavior is obtained in these models.

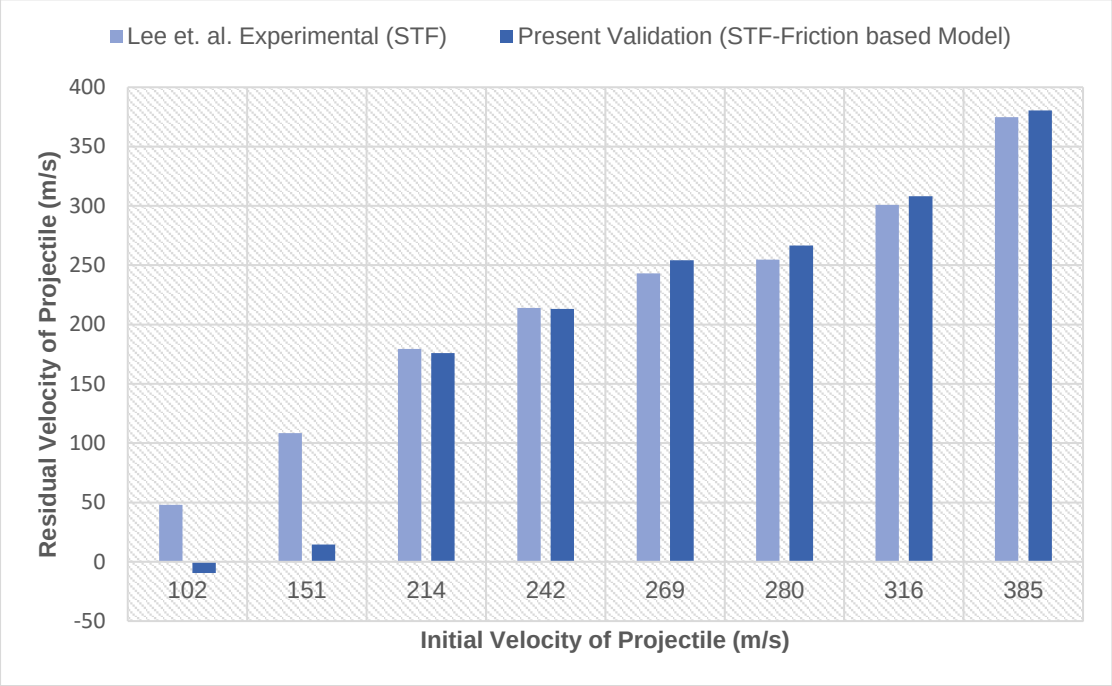

Figure 6-6 A graphic comparison of residual velocity of a projectile for STF impregnated fabric from a model based on inter-yarn friction and experimental values.

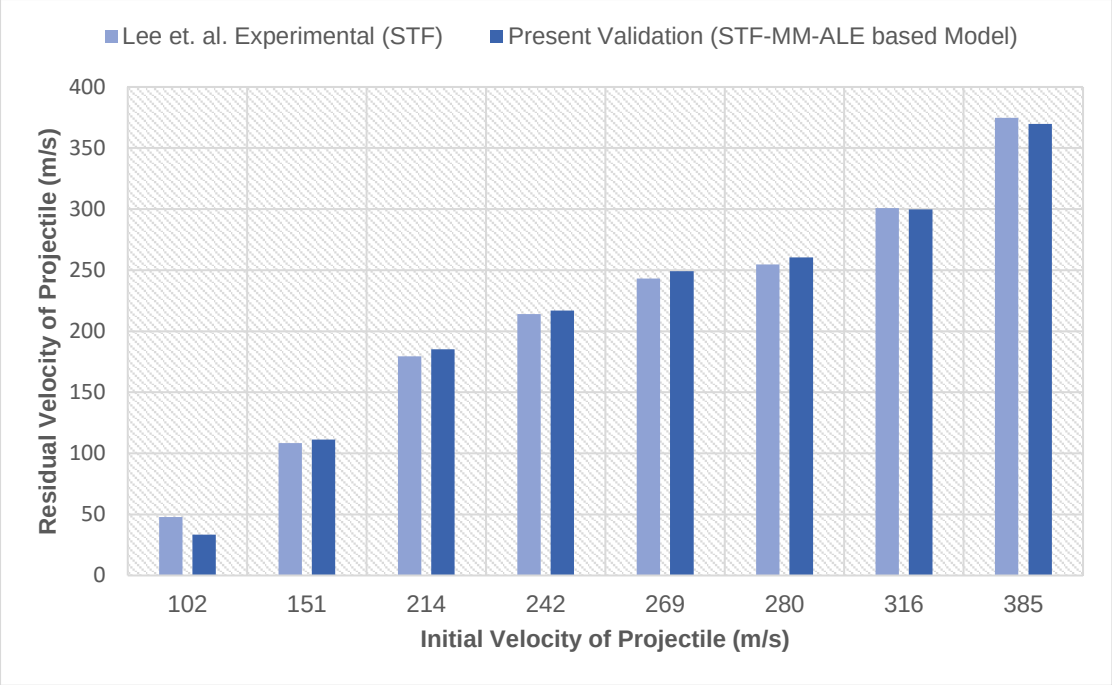

Figure 6-7 A graphic comparison of residual velocity of a projectile for STF impregnated fabric from a model based on MM-ALE technique and experimental values.

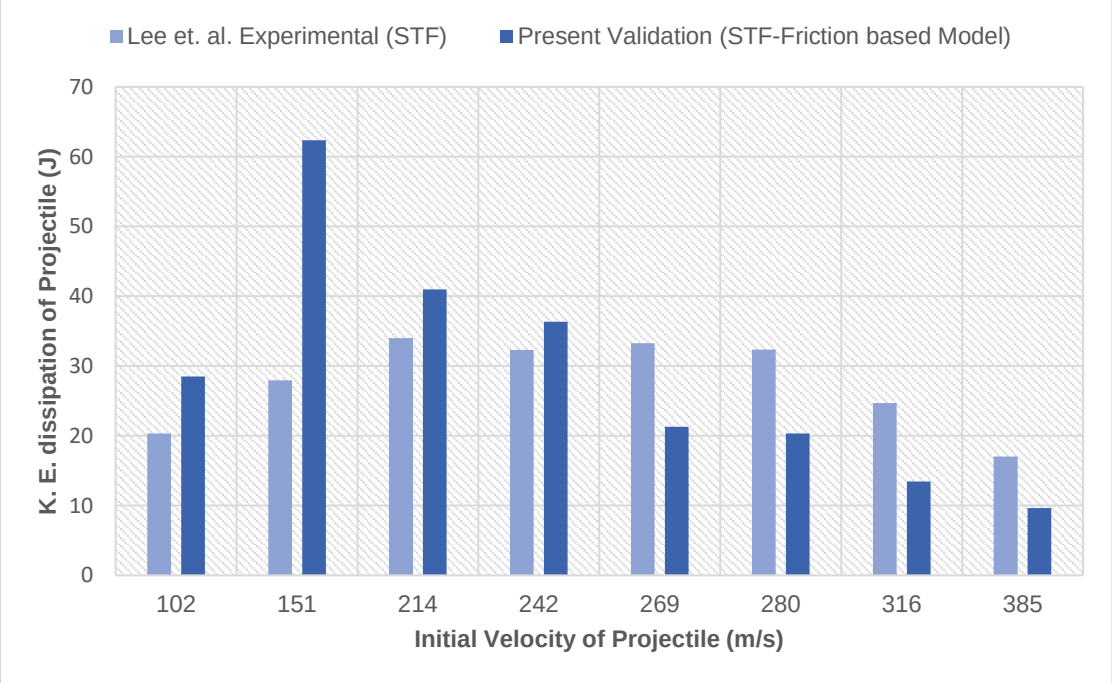

Figure 6-8 A graphic comparison of dissipated kinetic energy of a projectile for STF impregnated fabric from a model based on inter-yarn friction and experimental values.

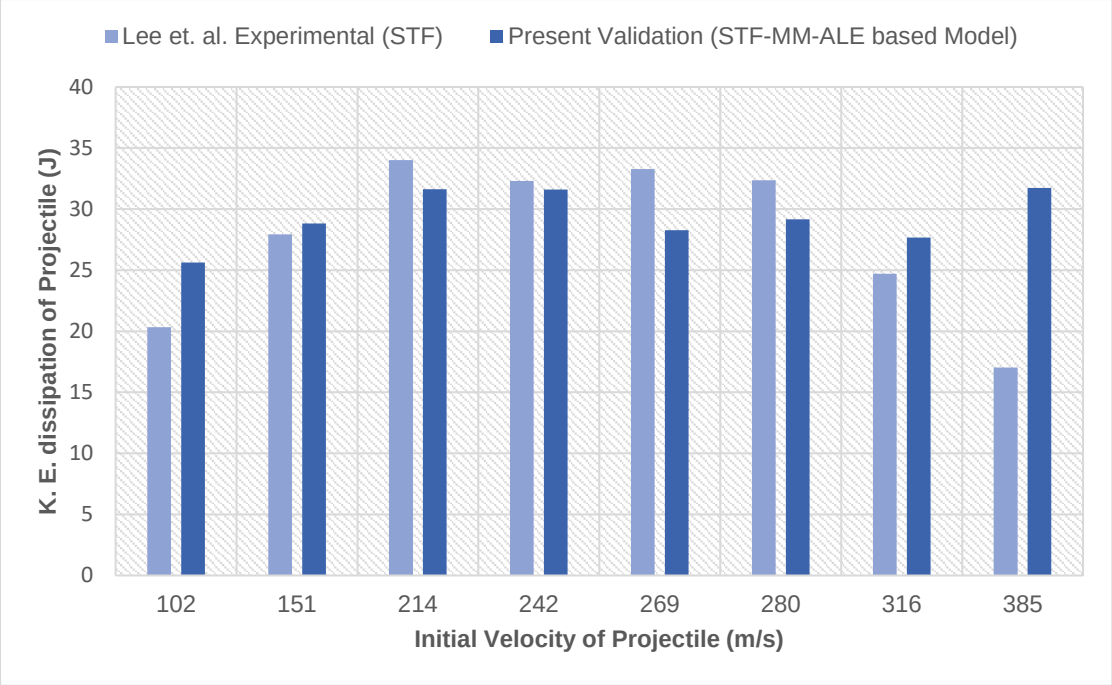

Figure 6-9 A graphic comparison of dissipated kinetic energy of a projectile for STF impregnated fabric from a model based on MM-ALE technique and experimental values.

6.3.3 Ballistic performance of STF impregnated multi-layer fabric system using MM-ALE approach

In the previous section friction and MM-ALE based models are compared and shown that the MM-ALE based model is found suitable for wide range of initial projectile velocities. The objective of this thesis is to present the design guidelines and methodology for ballistic threats BR I, IIA. II, and IIIA conforming to NIJ standards. The specification about these threats are given in Table 6-1. The initial velocities of these projectile are very high and hence the MM-ALE based technique should be adopted to predict the ballistic response of STF treated fabric system. Based on the rationale, the MM-ALE method is adopted to subsequently predict the ballistic response of STF treated fabric under the impact of projectile given in Table 6-1. The variation in the parameter of STF treated fabric is as such number of fabric layers, and type of STF sample. The physical properties of STF treated fabric sample is computed and given in Table 6-6. These properties will be used to compare the ballistic performance of STF treated fabric sample. Particularly, areal density of each sample will be used to normalize the kinetic energy dissipation to provide an insight of the optimum ballistic performance of the system.

Table 6-6 Physical specification of STF treated high performance fabric sample

Fabric Layers	STF	Sample Total Area (mm^2)	Sample Total wt. (kg)	Sample Areal density (gm/cm^2)
4	1	2766.76	0.01135	0.41
4	4	2766.76	0.0116	0.42
4	8	2766.76	0.0116	0.42
4	12	2766.76	0.0116	0.42
8	1	2766.76	0.0227	0.82
8	4	2766.76	0.0232	0.84
8	8	2766.76	0.0232	0.84
8	12	2766.76	0.0232	0.84
12	1	2766.76	0.03405	1.23
12	4	2766.76	0.0348	1.26
12	8	2766.76	0.0348	1.26
12	12	2766.76	0.0348	1.26
16	1	2766.76	0.0454	1.64
16	4	2766.76	0.0464	1.68
16	8	2766.76	0.0464	1.68
16	12	2766.76	0.0464	1.68

Table 6-7 Results from MM-ALE based models of PEG 200 and 15 wt. % of Nano-silica STF treated fabric.

No. of Layers	Ballistic rating	Residual Velocity	K. E. Dissipated	Areal Density	E_diss/Areal density
4	I	280.44	39.97	0.41	97.488
8	I	70.01	136.96	0.82	167.024
12	I	10.23	143.20	1.23	116.423
16	I	-30.00	143.33	1.64	87.396
4	II A	318.86	59.38	0.41	144.829
8	II A	86.01	438.28	0.82	534.483
12	II A	16.03	466.84	1.23	379.541
16	II A	-22.15	467.86	1.64	285.28
4	II	352.40	49.92	0.41	121.756
8	II	91.25	514.29	0.82	627.187
12	II	35.10	542.70	1.23	441.219
16	II	10.40	547.20	1.64	333.659
4	III A	389.46	91.15	0.41	222.317
8	III A	97.21	740.08	0.82	902.536
12	III A	60.08	763.48	1.23	620.715
16	III A	35.03	772.98	1.64	471.329

The predicted results obtained from MM-ALE based numerical model of PEG 200 and 15 % wt. of nano-silica STF treated sample is presented in Table 6-7. Further, the variation of residual velocity of projectile for the PEG 200 and 15% wt. of nano-silica have been graphically shown in Figure 6-10. Furthermore, the residual velocity of the projectile is decreasing with

the increase in the number of fabric layers for specific rating of the projectile. However, the magnitude of decrease in the residual velocity of the projectile is dropping significantly with the increase in the number of fabric layers and follows asymptotic curve. This could be due to the restricted propagation of strain waves in multi-layer system and accumulation of stresses in the vicinity of the projectile hit area. Further, the Figure 6-10 also contains the trendline equation for residual velocity of projectiles which is used to calculate the required number of layers to stop the projectiles of designated ratings. Depending upon variation of residual velocity the normalization of dissipated kinetic energy is done and the variation of the normalized dissipated kinetic energy of the projectiles have been graphically shown in Figure 6-11.

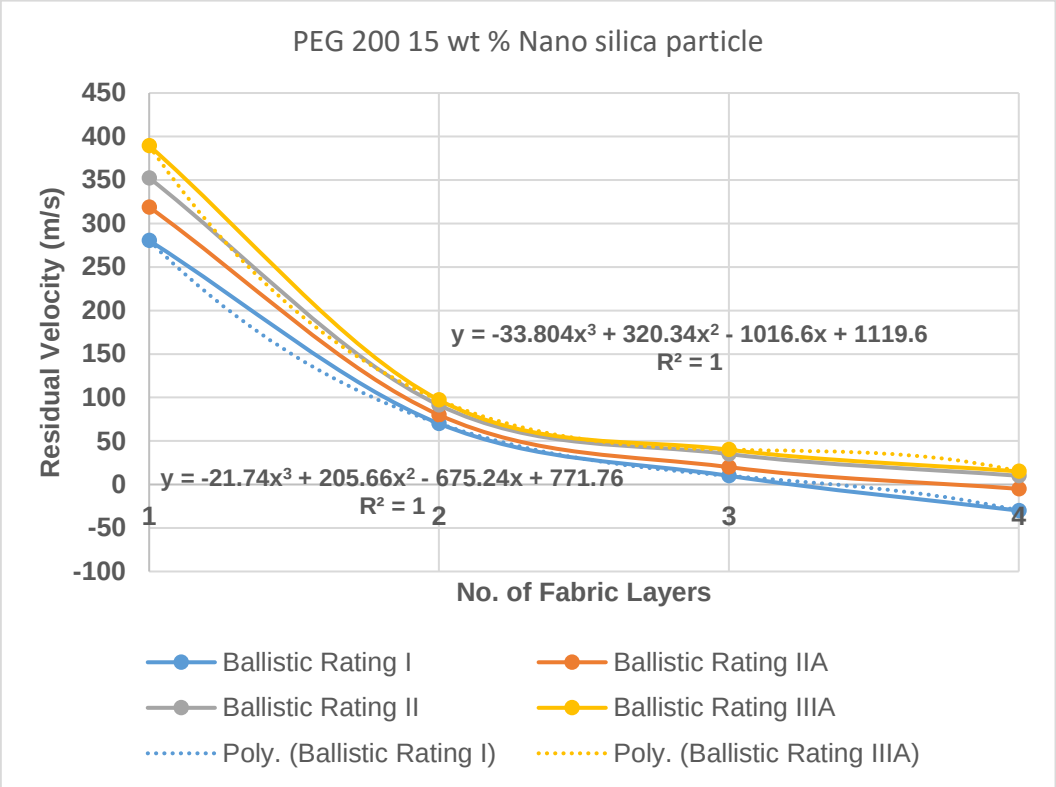

Figure 6-10 A graphic representation of variation of residual velocity of projectiles impacting multi-layer STF impregnated high performance fabric with STF sample having PEG 200 and 15 weight percent of nano silica under ballistic impact of different ballistic ratings.

The normalized dissipated kinetic energy increases with the increase in number of layers up to a critical layer and after onwards the dip is observed in the variation. The variation in the normalized dissipated kinetic energy will provide an insight about optimum design of STF treated fabric system respective to weight of the armour system.

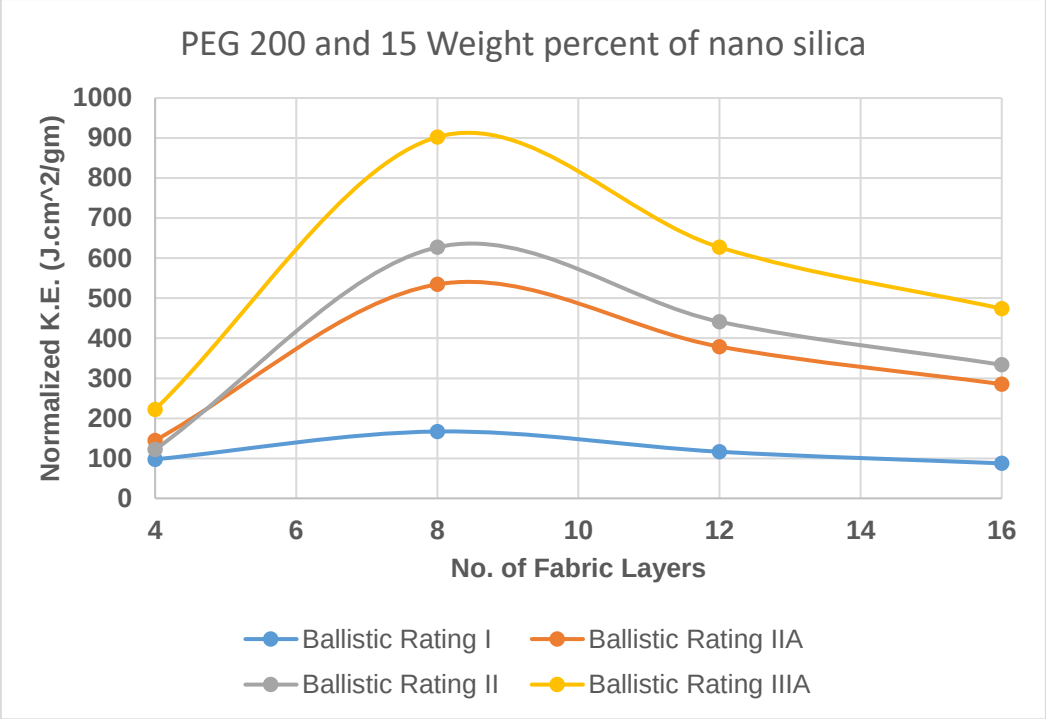

Figure 6-11 A graphic representation of variation of normalized dissipated kinetic energy of multi-layer STF impregnated high performance fabric with STF sample having PEG 200 and 15 weight percent of nano silica under ballistic impact of different ballistic ratings.

Table 6-8 Results from MM-ALE based models of PEG 200 and 30 wt. % of Nano-silica STF treated fabric.

No. of Layers	Ballistic rating	Residual Velocity	K. E. Dissipated	Areal Density	E_diss/Areal density
4	I	230.18	70.40	0.42	167.631
8	I	57.45	139.04	0.84	165.522
12	I	5.27	143.30	1.26	113.728
16	I	-32.31	143.33	1.68	85.315
4	II A	309.35	82.82	0.42	197.19
8	II A	77.22	444.01	0.84	528.584
12	II A	10.26	467.46	1.26	371
16	II A	-15.56	466.96	1.68	277.952
4	II	340.61	81.49	0.42	194.024
8	II	85.02	518.69	0.84	617.485
12	II	20.05	546.00	1.26	433.333
16	II	5.06	547.50	1.68	325.893
4	III A	391.40	87.77	0.42	208.976
8	III A	97.70	739.70	0.84	880.597
12	III A	41.35	771.16	1.26	612.029
16	III A	18.30	776.58	1.68	462.252

The predicted results obtained from MM-ALE based numerical model of PEG 200 and 30 % wt. of nano-silica STF treated sample is presented in Table 6-8. Further, the variation of residual velocity of projectile for the PEG 200 and 30% wt. of nano-silica have been graphically shown in Figure 6-12. Furthermore, the residual velocity of the projectile is decreasing with

the increase in the number of fabric layers for specific rating of the projectile. However, the magnitude of decrease in the residual velocity of the projectile is dropping significantly with the increase in the number of fabric layers and follows asymptotic curve. This could be due to the restricted propagation of strain waves in multi-layer system and accumulation of stresses in the vicinity of the projectile hit area. Further, the Figure 6-12 also contains the trend equation for residual velocity of projectiles which is used to calculate the required number of layers to stop the projectiles of designated ratings. Depending upon variation of residual velocity the normalization of dissipated kinetic energy is done and the variation of the normalized dissipated kinetic energy of the projectiles have been graphically shown in Figure 6-13.

Similar to earlier case, the normalized dissipated kinetic energy increases with the increase in number of layers up to a critical layer and after onwards the dip is observed in the variation. Further, the variation in the normalized dissipated kinetic energy will provide an insight about optimum design of STF treated fabric system respective to weight of the armour system.

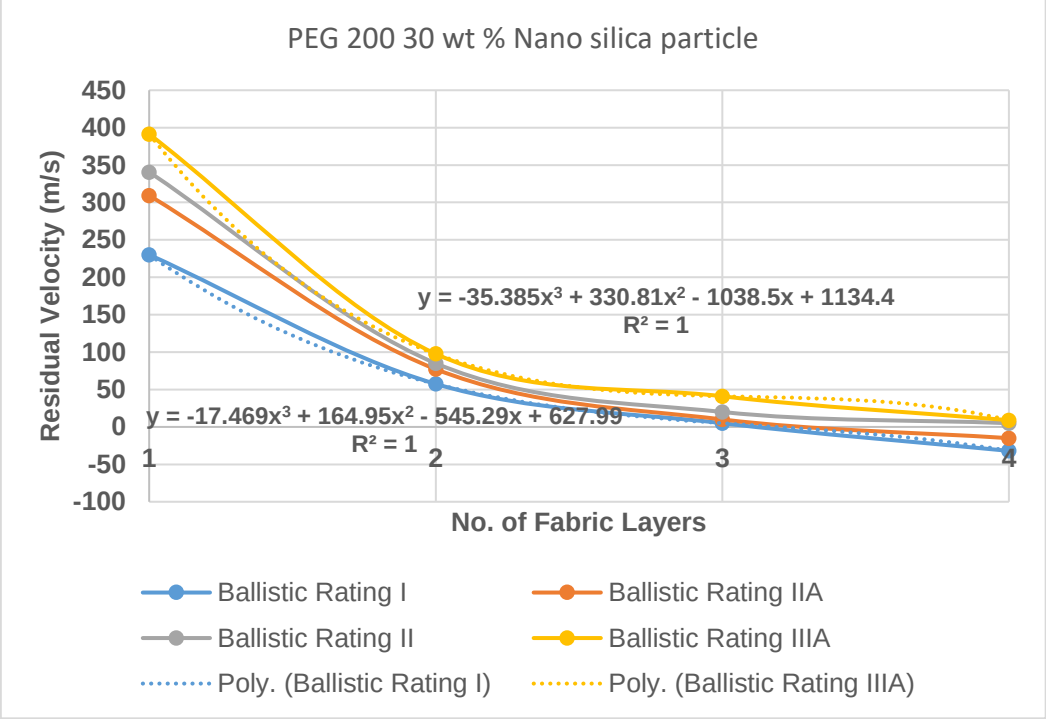

Figure 6-12 A graphic representation of variation of residual velocity of projectiles impacting multi-layer STF impregnated high performance fabric with STF sample having PEG 200 and 30 weight percent of nano silica under ballistic impact of different ballistic ratings.

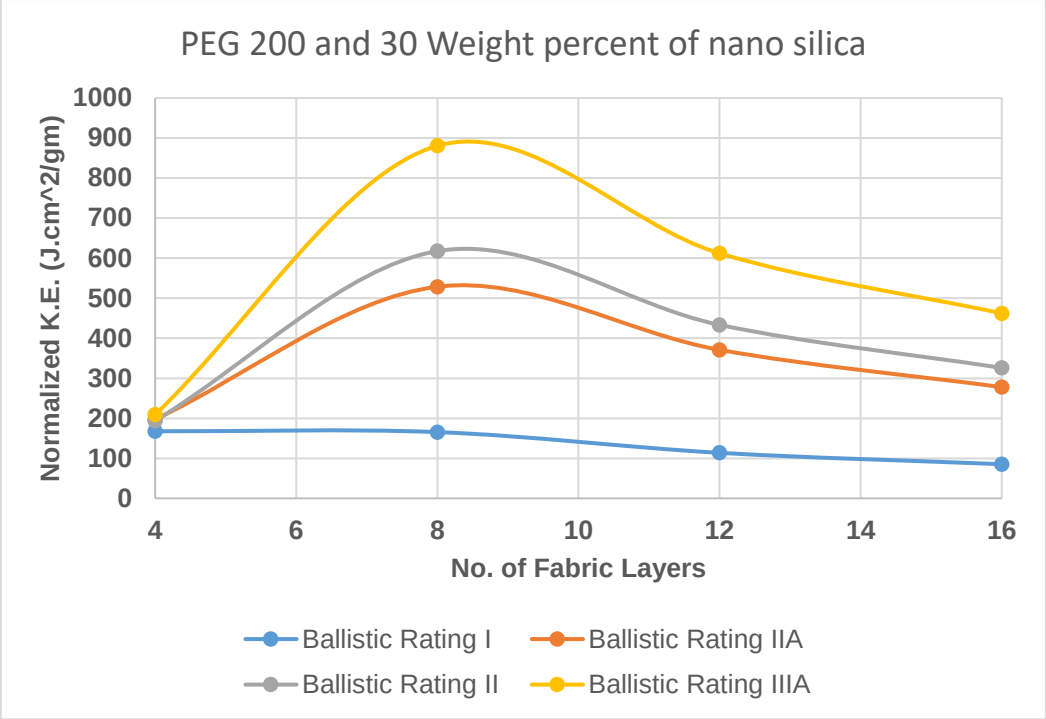

Figure 6-13 A graphic representation of variation of normalized dissipated kinetic energy of multi-layer STF impregnated high performance fabric with STF sample having PEG 200 and 30 weight percent of nano silica under ballistic impact of different ballistic ratings.

Table 6-9 Results from MM-ALE based models of PEG 300 and 30 wt. % of Nano-silica STF treated fabric.

No. of Layers	Ballistic rating	Residual Velocity	K. E. Dissipated	Areal Density	E_diss/Areal density
4	I	259.13	54.20	0.42	129.043
8	I	64.68	137.89	0.84	164.156
12	I	8.12	143.25	1.26	113.688
16	I	-26.15	143.33	1.68	85.315
4	II A	-12.35	76.48	0.42	182.095
8	II A	-7.88	443.60	0.84	528.094
12	II A	-0.03	467.46	1.26	371
16	II A	-15.07	466.96	1.68	277.952
4	II	-40.26	83.55	0.42	198.929
8	II	84.93	518.75	0.84	617.557
12	II	18.18	546.30	1.26	433.575
16	II	5.29	547.50	1.68	325.893
4	III A	391.42	87.75	0.42	208.929
8	III A	97.7	739.70	0.84	880.594
12	III A	40.01	771.48	1.26	612.286
16	III A	18.03	776.58	1.68	462.252

The predicted results obtained from MM-ALE based numerical model of PEG 300 and 30 % wt. of nano-silica STF treated sample is presented in Table 6-9. Further, the variation of residual velocity of projectile for the PEG 300 and 30% wt. of nano-silica have been graphically shown in in Figure 6-14. Furthermore, the residual velocity of the projectile is decreasing with

the increase in the number of fabric layers for specific rating of the projectile. However, the magnitude of decrease in the residual velocity of the projectile is dropping significantly with the increase in the number of fabric layers and follows asymptotic curve. This could be due to the restricted propagation of strain waves in multi-layer system and accumulation of stresses in the vicinity of the projectile hit area. Further, the Figure 6-14 also contains the trend equation for residual velocity of projectiles which is used to calculate the required number of layers to stop the projectiles of designated ratings. Depending upon variation of residual velocity the normalization of dissipated kinetic energy is done and the variation of the normalized dissipated kinetic energy of the projectiles have been graphically shown in Figure 6-15.

Similar to earlier case, the normalized dissipated kinetic energy increases with the increase in number of layers up to a critical layer and after onwards the dip is observed in the variation. Further, the variation in the normalized dissipated kinetic energy will provide an insight about optimum design of STF treated fabric system respective to weight of the armour system.

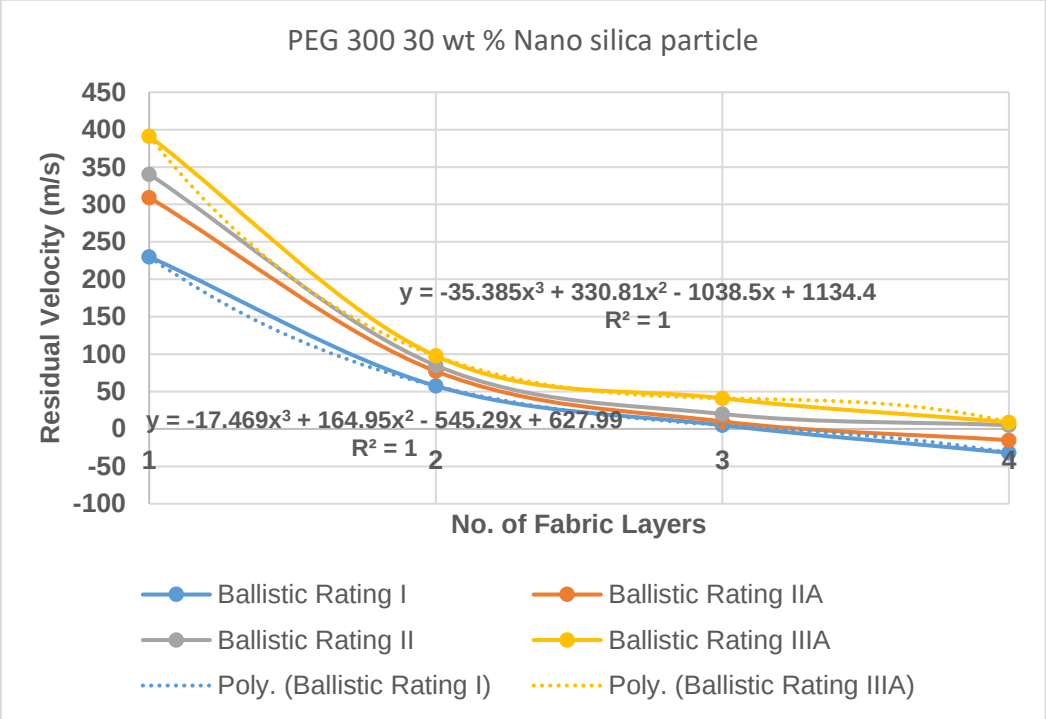

Figure 6-14 A graphic representation of variation of residual velocity of projectiles impacting multi-layer STF impregnated high performance fabric with STF sample having PEG 300 and 30 weight percent of nano silica under ballistic impact of different ballistic ratings.

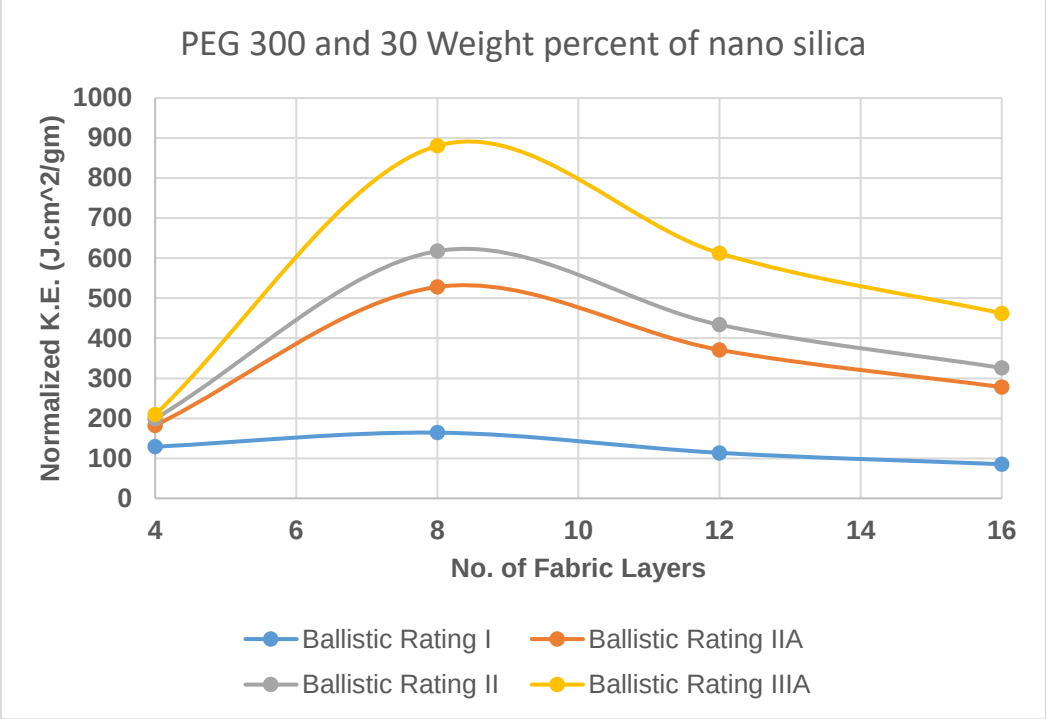

Figure 6-15 A graphic representation of variation of normalized dissipated kinetic energy of multi-layer STF impregnated high performance fabric with STF sample having PEG 300 and 30 weight percent of nano silica under ballistic impact of different ballistic ratings.

Table 6-10 Results from MM-ALE based models of PEG 400 and 30 wt. % of Nano-silica STF treated fabric.

No. of Layers	Ballistic rating	Residual Velocity	K. E. Dissipated	Areal Density	E_diss/Areal density
4	I	241.65	66.30	0.42	157.857
8	I	60.32	138.60	0.84	165
12	I	6.12	143.28	1.26	113.715
16	I	-28.14	143.33	1.68	85.315
4	II A	310.43	81.16	0.42	193.238
8	II A	77.49	443.84	0.84	528.382
12	II A	10.23	467.44	1.26	370.985
16	II A	-15.28	466.93	1.68	277.932
4	II	336.84	92.62	0.42	220.524
8	II	84.08	519.32	0.84	618.241
12	II	18.24	546.27	1.26	433.547
16	II	5.39	547.48	1.68	325.883
4	III A	391.42	87.73	0.42	208.881
8	III A	97.71	739.69	0.84	880.585
12	III A	40.16	771.43	1.26	612.245
16	III A	18.18	776.56	1.68	462.237

The predicted results obtained from MM-ALE based numerical model of PEG 400 and 30 % wt. of nano-silica STF treated sample is presented in Table 6-10. Further, the variation of residual velocity of projectile for the PEG 400 and 30% wt. of nano-silica have been graphically shown in Figure 6-16. Furthermore, the residual velocity of the projectile is

decreasing with the increase in the number of fabric layers for specific rating of the projectile. However, the magnitude of decrease in the residual velocity of the projectile is dropping significantly with the increase in the number of fabric layers and follows asymptotic curve. This could be due to the restricted propagation of strain waves in multi-layer system and accumulation of stresses in the vicinity of the projectile hit area. Further, the Figure 6-16 also contains the trend equation for residual velocity of projectiles which is used to calculate the required number of layers to stop the projectiles of designated ratings. Depending upon variation of residual velocity the normalization of dissipated kinetic energy is done and the variation of the normalized dissipated kinetic energy of the projectiles have been graphically shown in Figure 6-17.

Similar to earlier case, the normalized dissipated kinetic energy increases with the increase in number of layers up to a critical layer and after onwards the dip is observed in the variation. Further, the variation in the normalized dissipated kinetic energy will provide an insight about optimum design of STF treated fabric system respective to weight of the armour system.

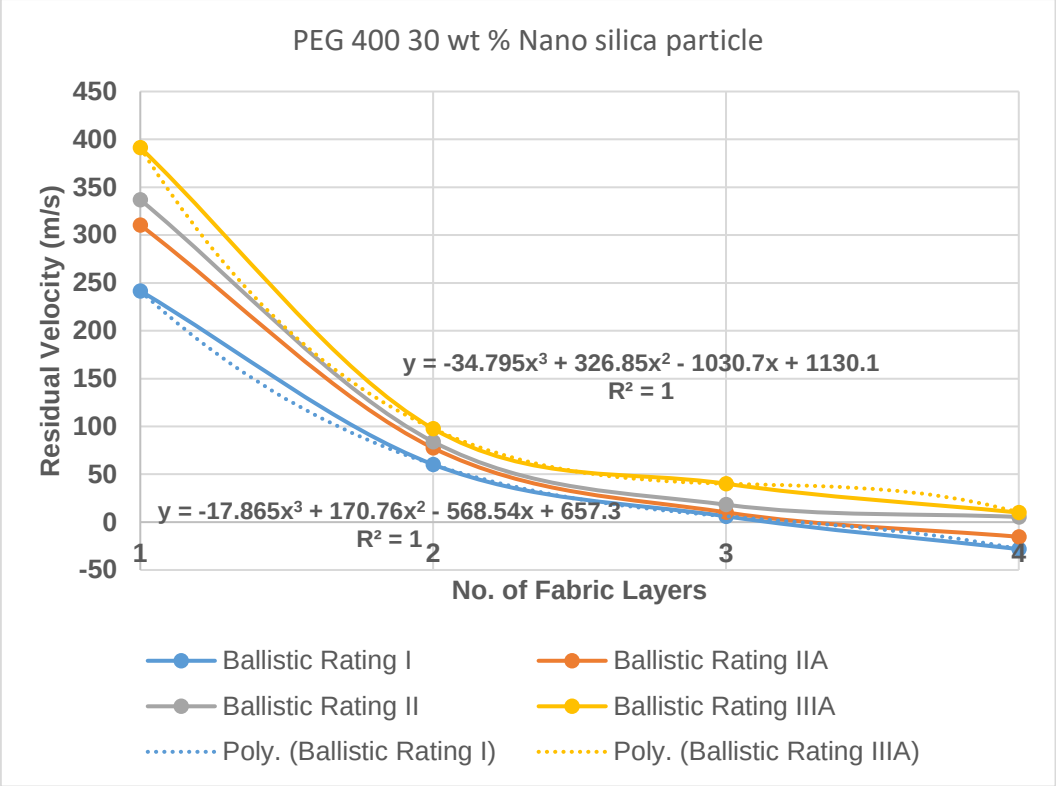

Figure 6-16 A graphic representation of variation of residual velocity of projectiles impacting multi-layer STF impregnated high performance fabric with STF sample having PEG 400 and 30 weight percent of nano silica under ballistic impact of different ballistic ratings.

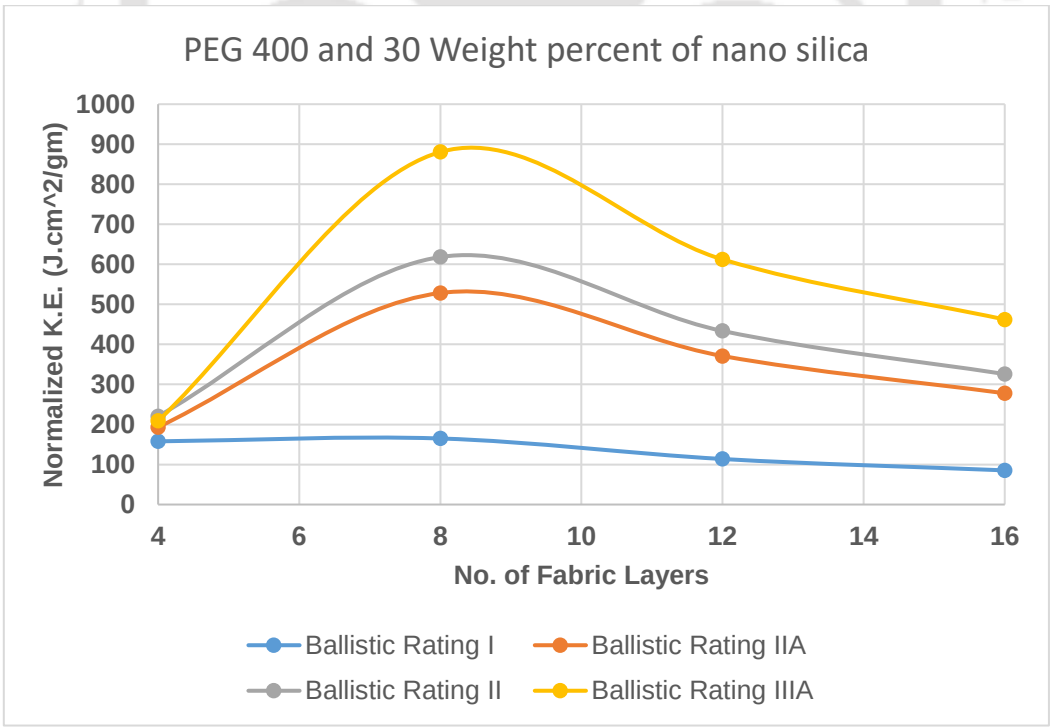

Figure 6-17 A graphic representation of variation of normalized dissipated kinetic energy of multi-layer STF impregnated high performance fabric with STF sample having PEG 200 and 30 weight percent of nano silica under ballistic impact of different ballistic ratings.

Collectively, the number of layers required to stop bullet of Ballistic Rating (BR) I and IIA is 16 while very high number of layers are required to stop the projectile for ballistic rating II and IIIA. The efficiency in terms of energy dissipation per areal density is higher for 8 layers of fabric system as compared to others. The energy dissipation per areal density is increases when number of fabric layer is increases and reaches to an optimum level when the number of fabric layer is 8 in all cases.

6.4 Conclusion

In this chapter a new approach to study the ballistic behavior of STF impregnated fabric is proposed. The MM-ALE approach is an integration of neat fabric models and STF models. The advantage of MM-ALE based approach lies in its neat and simple procedure as compared to its counterpart friction-based model. In this approach, only rheological data of STF sample and inter-yarn friction of neat fabric is required whereas in friction-based models, the inter-yarn friction for STF impregnated fabric is required. The limitation of friction based itself lies in the determination of friction using semi-empirical approach where the inter-yarn coefficients of friction at different pull out speed need to be incorporated which is impossible in reality. This limitation is overcome by modelling STF and fabric both using MM-ALE based modelling strategies. The MM-ALE approach produces better results at different velocities than friction-based models. Basically, the MM-ALE based modelling strategy considers the modelling of coupled STF model (ALE formulation) along with the fabric model (Lagrange formulation). The modelling of fabric and STF is detailed discussed in Chapter 3 and Chapter 5 respectively. The developed modelling strategy is validated using experimental data and produces very close results. The COV of errors from validated friction and MM-ALE based model is also compared and MM-ALE technique is found most suitable for further evaluation of ballistic performance of the STF treated fabric. Moreover, In the direction of achieving the objective of this research, an accurate and efficient modelling is developed which is used to obtain result for the different variation of the configuration of STF along with the variation in the heavy ballistic loadings of much higher class and clear up the gap by taking the soft armour to take much more heaver impacts. The predicted results from MM-ALE models shows that there is significant increase in the ballistic performance of the multi-layered fabric system. However, the quantum of enhancement is dropped significantly with the increase in the number of fabric layers. Further, the MM-ALE model is used to study the confinement effect on the ballistic performance of the STF encapsulated bubble wrap configurations and this study is presented in Chapter 7.

7 Numerical evaluation of ballistic performance of shear thickening fluid encapsulated in bubble wrap configuration

7.1 Introduction

The utilization of Shear Thickening Fluid (STF) in the field of ballistics is an emerging and effective method along with the already available materials used in this application. A lot of research has been carried out by using the STF with the Kevlar fibers and other materials in the field of armory, by composition variation along with its percentage variation. Both numerical and experimental studies have been made to evaluate the performance (Hasanzadeh, Mottaghitalab et al., 2017; Hassan et al., 2010; Park et al., 2015; Sen et al., 2019; Wetzel et al., 2004). The different composition of STF itself along with various methodologies for improving the performance of the STF as a shear thickener when any perturbation /dynamic force is applied on it and its utilization as an energy absorbent material is investigated to realize its full potential. Previous Chapter presented the detailed analysis, discussion, and limitations of the STF treated fabric system under ballistic impact. The main drawback of the STF treated fabric system is premature failure of fabric yarn for STF having better rheological properties. The premature failure of yarns restricts the optimum viscous damping of STF.

As per the research carried out, STF is traditionally used along with some other materials. Till date, most of the research focusses primarily on the development of better quality of STF. What is still lacking is the innovative use of STF as a stand-alone or combined mechanism for effective ballistic protection. One such potential of STF is to work as an energy absorbing material through viscous damping. The investigation in the mechanism of STF at varying shear strain rate is described on the basis of following theories:

- Formation of hydro-clusters of colloidal Nano-particles of silica, and
- Increase in contact forces between particles due to instabilities arising in the vicinity of nano-particles and STF due to application of high shear strain rate.

Both theories further indicate that there is likely chance of improved performance through optimal viscous damping in confined STF. This research targets to achieve this aim of utilizing the full potential of STF as an energy absorbing material during the ballistic impact. The STF will be used to arrest the effect of the impact due to a bullet by its Non-Newtonian behavior which is engaged at a high strain rate event. The STF has capability to significantly improve the performance of high strength fibers which are already in use in this application.

As such a novel bubble wrap configuration encapsulating the STF is proposed which acts like a great energy bubble. Furthermore, encapsulation preserves the rheological properties of STF for longer period and there is significant improvement in impact resistance as reported by (Zhang et al., 2017). The configuration of STF encapsulated in bubble wrap configuration is shown in Figure 7-1.

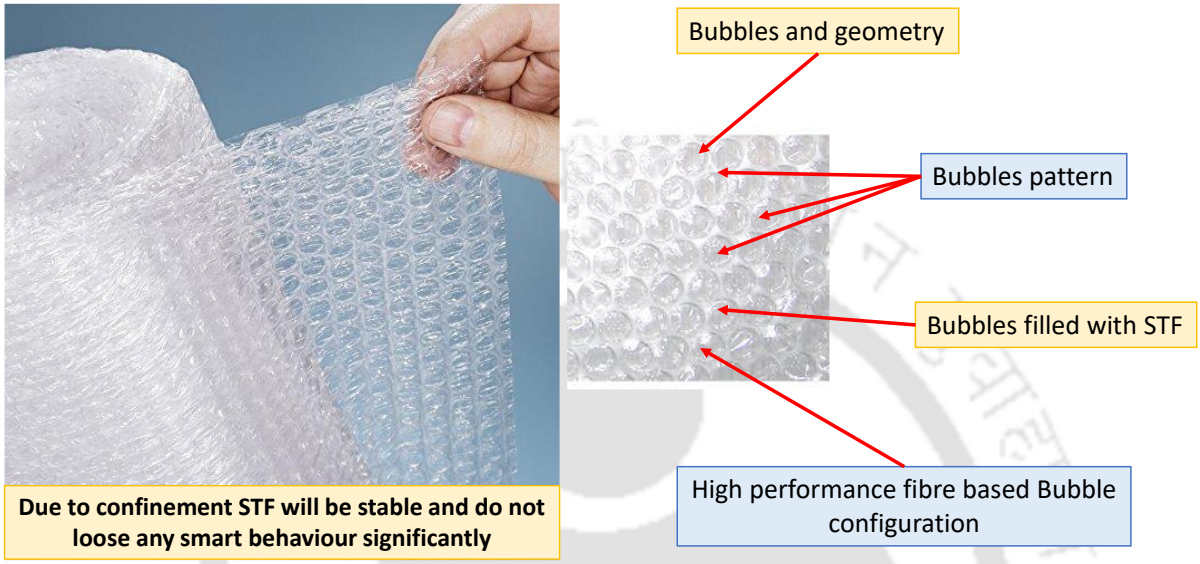

Figure 7-1 An overview of air bubble warp configuration used as an efficient energy absorbent.

On the basis of this configuration of STF, the numerical simulations are conducted. The simulations are done using the LS-DYNA software. The challenges that are encountered in the simulation of the numerical simulation were:

- Validating the material formulation of STF in LS-DYNA
- Casing of the STF, as it is a liquid material so that its behavior is not influenced by casing material.

The validation of the material formulation of STF with the experimental and numerical work has been carried out. The adopted material formulation was able to exhibit the property of STF with great accuracy. The second challenge was achieved by the use of bubble wrap made up of Low-Density Poly-Ethylene (LDPE). The LDPE bubble wraps has a negligible effect on the STF properties due to its inherent nature having low strength, high ductility and no energy absorption capacity. So, the effect of bubble casing on the behavior of STF under blasts and impacts loading has negligible effect. The absorption of energy during blast and impact events is due to its inherent capacity only. This bubble wrap configuration to explore the effect of confinement on STF.

The material formulation of LDPE was carried out by comparison with the established experimental work. After that, the encapsulated STF was simulated in the LDPE bubble wrap configuration. The contact interaction is also included in the model using the algorithm of LS-DYNA software. This resulted in a realistic simulation of the behavior of the STF under the dynamic loading having high shear rate due which is exhibited during a blast and impact event. The study can be further extended to the dependency of the bubble wrap configuration to various shaped like cuboidal, cubical etc. and the effect of this on the behavior of the total sheet of bubble wrap with STF within it. The effectiveness of STF in energy absorption during ballistic event is evaluated to mitigate the shock waves generated. This opens up the gateway of implementation of STF in the field of defense and mitigate the effect of ballistic explosion and impact.

7.2 Numerical Modelling

The numerical modelling of the STF encased in the bubble wrap configuration involves modelling of the STF, bubble wrap, the ballistic projectile and simulate the interaction between the STF, bubble wrap, and ballistic projectile. Adopting the similar methodology for the modelling of Kevlar fibers and STF impregnated on it using the MM-ALE approach which is detailed in Chapter 6, the modelling of STF is done using Eulerian approach and the bubble wrap is modelled with the Lagrangian approach. The simulation is done using LS-DYNA software. The numerical simulation is further extended to encompass various layers of the STF-bubble wrap sheet to analyze the behavior and effects of various layers in energy absorption. The ballistic projectile is simulated and its velocity is varied in different simulations as to test the extent of the usage of the STF in bubble wrap configuration. The subsequent sub-sections discuss the modelling techniques to simulation the behavior of STF encapsulated bubble wrap configuration.

7.2.1 SPH formulation of shear thickening fluid

The modelling of STF using ALE approach is adopted as detailed in and presented in Chapter 5. The developed model was implemented to study the effect of impregnation of STF into high performance dry fabric under ballistic impact. The commercial LS-DYNA solver has limited application in case of MM-ALE approach due to its stability issues at higher deformation rate. The MM-ALE approach yielded unstable results during simulation of STF encapsulated in confined structural environment under very high strain-rate. The instabilities

were counteracted using mesh free techniques without compromising the complexity and physics of the problem. There are several mesh free techniques available in LS-DYNA and a Lagrangian approach based Smoothed Particle Hydrodynamics (SPH) has been selected to model the STF. The coupled FEM-SPH method is adopted to model the confined fluid-structural interaction. The fluid part will be modelled using Smoothed Particle Hydrodynamics (SPH) and coupled to Lagrangian based structural (bubble wrap) part which is modelled based on Finite Element Method (FEM). The SPH formulation of STF is performed using SECTION_SPH card in LS-DYNA. In SPH, the field variables are represented using kernel function which is also known as kernel approximation. The basic objective of these kernel functions is to represent realistic field variables for contemplate particle as well as the space between neighborhood particles. This process in SPH is known as smoothening of the field variable. In the current numerical simulation cubic spline kernel function (smoothening function) is used to represent the field variables.

7.2.2 Formulation of bubbles and bubble container

The bubbles are modelled in the shape of cylinders in LS-DYNA. The sheet is divided into small cylindrical capsules that holds the STF material. As discussed above, the bubble containers are designed based on the Lagrangian approach and the interaction of the STF and the bubble wrap is also modelled. The containers are modelled as a shell element. The important aspect of the modelling is to adopt a material formulation which represents the realistic behavior of the bubble wrap. Based on the validation from the previous experiments, the material formulation of Linear Piecewise Elastic present in MAT_24 card in LS-DYNA is used to simulate the bubble contained made of Low-Density Poly-Ethylene (LDPE).

The modelling of the STF follows the formulation developed in Chapter 5. The STF is filled up in the bubble container as shown in Figure 7-2. The projectile is modelled following the formulation developed in Chapter 6.

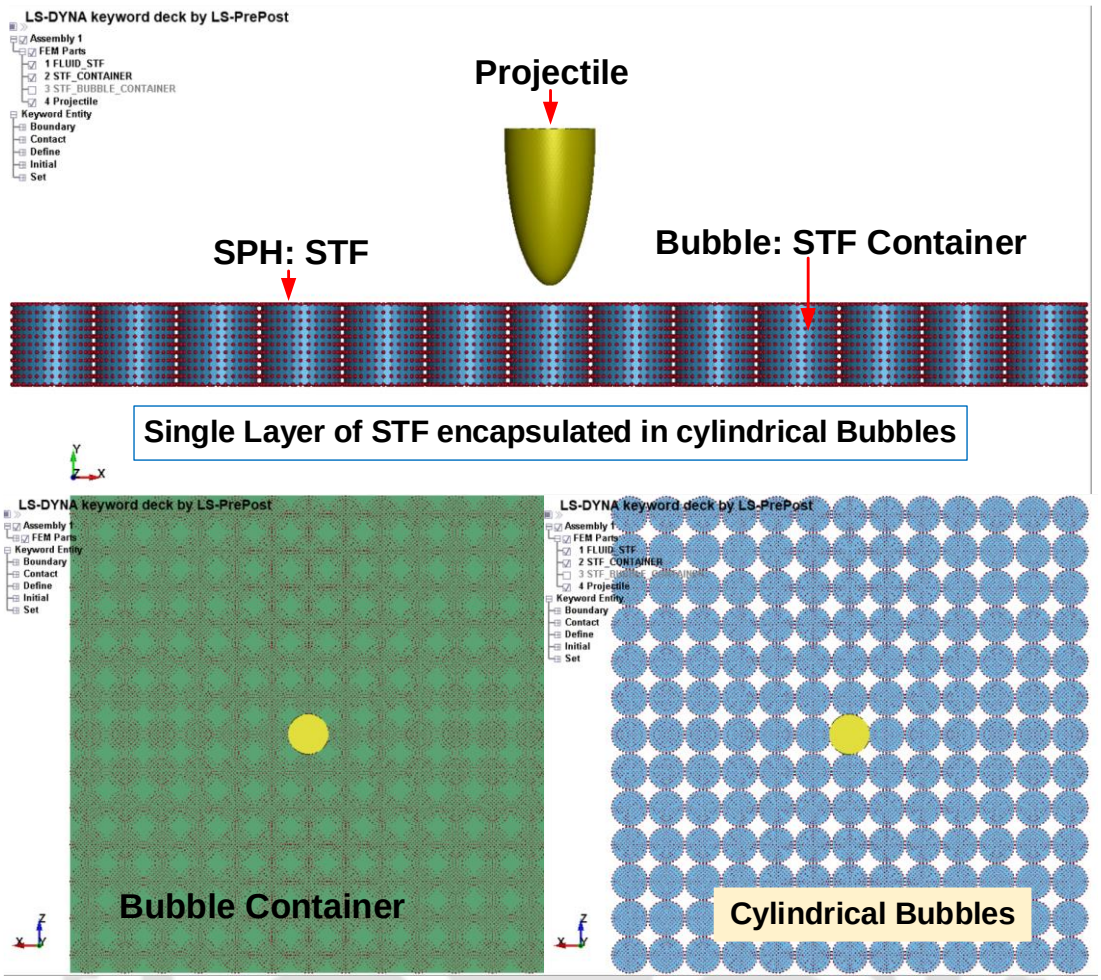

Figure 7-2 A graphic representation of coupled SPH-FE model of bubble wrap encapsulated STF configuration.

7.2.3 SPH to SHELL Contact

In the classic SPH technique a laborious composition of boundary particles and ghost points is normally adopted. In LS-DYNA, this method is circumvented and the software allows mesh-based and mesh-free methods to co-exist and interact in one simulation. Since the SPH particles are not interconnected, only one-way type of contact definitions is applicable in which the SPH is always defined to be the slave and the elements are defined to be the master. The interaction between the SPH and other elements is defined using penalty-based contact algorithms. An appropriate contact type is the simple *CONTACT_AUTOMATIC_NODES_TO_SURFACE card, where the slave nodes are checked for penetration through the master surface. When a node is in contact with the surface, a restoring force is applied to prevent further penetration. This force is proportional to the penetration distance into the shell or solid element and acts in the direction normal to the master surface. The restoring force is defined by:

$$\boldsymbol{f} = \boldsymbol{k} \times \boldsymbol{d} \times \boldsymbol{n} \qquad (7\text{-}1)$$

In this equation, d is the penetration distance, n is the surface normal vector and k is a penalty factor, comparable to a spring constant. The constant k should be set large to minimize penetration. The CONTACT_AUTOMATIC_NODES_TO_SURFACE card includes SPH as slave part and structural container (FEA) as master part.

7.3 Results and discussion

The outcome of the STF encapsulated in LDPE bubble warp is discussed in this section. One of the main concerns which effects the result is the sloshing phenomenon where the effect of impact on the confined fluid is main concern. The fluid undergoes very high deformation rate due to very high characteristic strain rate under external threat. This will be exhibited by STF encapsulated with shear thickening fluid under ballistic impact. The ballistic performance of STF in an encapsulated configuration is numerically simulated using coupled FEM-SPH method. Based on the methodology discussed above, the different simulations are done after varying the velocity of the projectile, the type of the STF used and the number of bubble wraps with STF in it. The projectile dimensions, shape and velocities are according to the ballistic rating as per NIJ standard and briefly presented in Table 6-1. The variation in the STF is shown Table 7-1.

Table 7-1 Physical specification of STF encapsulated in bubble wrap configuration sample

No. of Layers	STF Sample no.	Sample Total Area (mm^2)	Sample Total wt. (kg)	Sample Areal density (gm/cm^2)
1	1	4556.25	0.0259	0.57
1	4	4556.25	0.0272	0.6
1	8	4556.25	0.0272	0.6
1	12	4556.25	0.0272	0.6
2	1	4556.25	0.0518	1.14
2	4	4556.25	0.0544	1.19
2	8	4556.25	0.0544	1.19
2	12	4556.25	0.0544	1.19
3	1	4556.25	0.0777	1.71
3	4	4556.25	0.0816	1.79
3	8	4556.25	0.0816	1.79
3	12	4556.25	0.0816	1.79
4	1	4556.25	0.1036	2.27
4	4	4556.25	0.1088	2.39
4	8	4556.25	0.1088	2.39
4	12	4556.25	0.1088	2.39

The projectile characteristics including variation in the velocity is described and presented in the Chapter 6. The ballistic results from numerical models is normalized w.r.t. areal density of the models. The areal density of the sample models is calculated and presented in Table 7-1. The mass of different STF is varying as their weight percent of silica nano-particle and molecular weight of PEG is varying. The samples of STF and their constituents are discussed

and presented in Chapter 5. The total 4 out of 12 variants of STF is used to study the ballistic behavior. The STF sample no. 1 consists of PEG 200 and 15 weight percent of nano silica, further the STF sample no. 4, 8, and 12 consists of 30 weight percent each of nano silica and PEG 200, PEG 300, and PEG 400 respectively. Based on these variations, the numerical investigation of single and multi-layered bubble wrap filled with shear thickening fluid is carried out and the results obtained have been presented in the Table 7-2,

Table 7-3,

Table 7-4, and

Table 7-5. The results reported in this study are residual velocity of the projectile, kinetic energy of the projectile conforming to NIJ standards. Areal density of samples has been used to normalize the parameters which is used to characterize and standardize the proposed STF encapsulated bubble wrap configuration.

Table 7-2 Results from MM-ALE based models of PEG 200 and 15 wt. % of Nano-silica STF encapsulated in cylindrical bubble.

No. of Layers	Ballistic rating	Residual Velocity	K. E. Dissipated	Areal Density	E_diss/Areal density
1	I	326.356	4.83	0.57	8.474
2	I	268.265	49.735	1.14	43.627
3	I	220.514	80.077	1.71	46.829
4	I	181.262	100.579	2.27	44.308
1	II A	338.083	16.144	0.57	28.323
2	II A	280.609	158.378	1.14	138.928
3	II A	232.906	256.363	1.71	149.92
4	II A	193.312	323.866	2.27	142.672
1	II	363.71	18.46	0.57	32.386
2	II	301.516	183.952	1.14	161.361
3	II	249.956	297.688	1.71	174.087
4	II	207.214	375.849	2.27	165.572
1	III A	433.503	26.225	0.57	46.009
2	III A	359.374	261.325	1.14	229.232
3	III A	297.921	422.896	1.71	247.308
4	III A	246.977	533.933	2.21	241.599

Table 7-3 Results from MM-ALE based models of PEG 200 and 30 wt. % of Nano-silica STF encapsulated in cylindrical bubble.

No. of Layers	Ballistic rating	Residual Velocity	K. E. Dissipated	Areal Density	E_diss/Areal density
1	I	318.72	11.234	0.6	18.723
2	I	207.168	87.497	1.19	73.527
3	I	130.516	121.146	1.79	67.679
4	I	79.615	135.051	2.39	56.507
1	II A	330.24	37.11	0.6	61.85
2	II A	214.656	289.035	1.19	242.887
3	II A	135.233	400.192	1.79	223.571
4	II A	82.492	446.124	2.39	186.663
1	II	355.2	42.932	0.6	71.553
2	II	230.88	334.378	1.19	280.99
3	II	145.454	462.973	1.79	258.644
4	II	88.727	516.11	2.39	215.946
1	III A	423.36	60.989	0.6	101.648
2	III A	275.184	475.019	1.19	399.176
3	III A	173.366	657.701	1.79	367.431
4	III A	105.753	733.189	2.39	306.774

Table 7-4 Results from MM-ALE based models of PEG 300 and 30 % wt. STF encapsulated in cylindrical bubble.

No. of Layers	Ballistic rating	Residual Velocity	K. E. Dissipated	Areal Density	E_diss/Areal density
1	I	317.06	12.606	0.6	21.01
2	I	199.7478	91.422	1.19	76.825
3	I	121.846158	123.991	1.79	69.269
4	I	71.88923322	136.573	2.39	57.144
1	II A	328.52	41.642	0.6	69.403
2	II A	206.9676	302.002	1.19	253.783
3	II A	126.250236	409.588	1.79	228.82
4	II A	74.48763924	451.15	2.39	188.766
1	II	353.35	48.175	0.6	80.292
2	II	222.6105	349.378	1.19	293.595
3	II	135.792405	473.842	1.79	264.716
4	II	80.11751895	521.925	2.39	218.379
1	III A	421.155	68.438	0.6	114.063
2	III A	265.32765	496.329	1.19	417.083
3	III A	161.8498665	673.142	1.79	376.057
4	III A	95.49142124	741.45	2.39	310.23

Table 7-5 Results from MM-ALE based models of PEG 400 and 30 wt. % of Nano-silica STF encapsulated in cylindrical bubble.

No. of Layers	Ballistic rating	Residual Velocity	K. E. Dissipated	Areal Density	E_diss/Areal density
1	I	315.4	13.971	0.6	23.285
2	I	195.548	93.58	1.19	78.639
3	I	117.3288	125.395	1.79	70.053
4	I	68.050704	137.271	2.39	57.436
1	II A	327.832	43.449	0.6	72.415
2	II A	203.25584	308.092	1.19	258.901
3	II A	121.953504	413.853	1.79	231.203
4	II A	70.73303232	453.331	2.39	189.678
1	II	351.5	53.391	0.6	88.985
2	II	217.93	357.626	1.19	300.526
3	II	130.758	479.209	1.79	267.715
4	II	75.83964	524.593	2.39	219.495
1	III A	419.832	72.888	0.6	121.48
2	III A	260.29584	506.908	1.19	425.973
3	III A	156.177504	680.358	1.79	380.088
4	III A	90.58295232	745.103	2.39	311.759

The ballistic performance of the different samples of bubble wrap configurations under projectile impact of BRs I, II A, II, and III A were systematically compared. From the results presented in Table 7-2, Table 7-3, Table 7-4, and Table 7-5, it is observed that with increase in the number of layers, the energy absorption has increased. In order to do the optimum light-

weight design, the absorbed kinetic energy by ballistic armour should be normalized to the areal density of the sample. The normalized dissipated kinetic energy gives the estimate of the amount of kinetic energy absorbed per unit areal density of the sample.

As the projectile velocity increase, the absorption energy is also increasing which clearly indicates the efficacy of STF as a potential energy absorbing material. While comparing the results of different STF material composition, there are very slight changes observed in the energy absorption among STF sample no 4, 8, and 12 while there are significant changes observed from STF sample no. 1 as compared to others. The STF sample 1 consists of 15 weight percent of silica where other samples is having 30 weight percent of silica. The significant change in the energy absorption between 1 and other is due to difference in the fraction of silica particle in the STF. This shows that no matter what is the polyethylene glycol (PEG) of the STF, the energy absorption very much depends on the applied shear rate on it for the same fraction of silica particle. The areal density is directly related to the number of layers and the volume of the STF, clearly showing that with the increase in the density, the absorbed energy also shows an increasing trend in all the STF samples. From the individual comparisons in the Tables, for example, all the elements of II, it is observed that the energy absorption has only varied to the very small extent which can be taken as negligible.

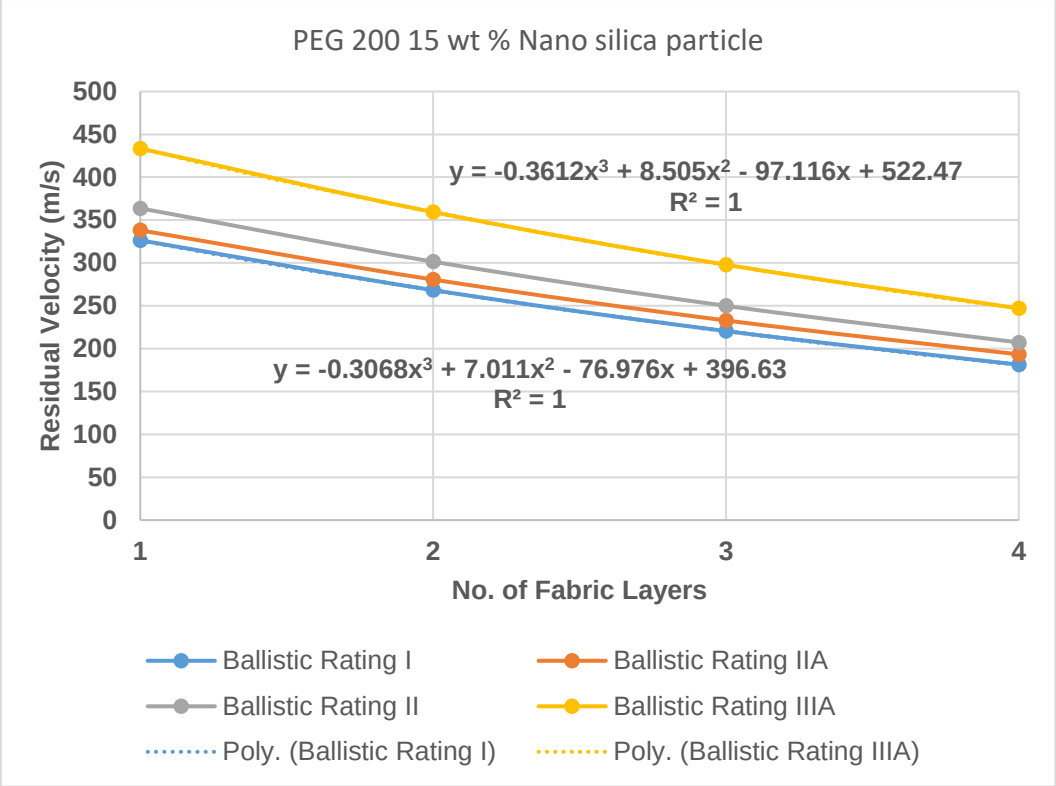

Figure 7-3 A graphic representation of variation of residual velocity of multi-layer STF encapsulated with STF sample no. 1 inside bubble wrap configuration under ballistic impact of different ballistic ratings.

The residual velocity of multi-layer STF encapsulated bubble wrap configuration for STF having PEG 200 and 15 weight percent of silica particle under different ratings of projectile is graphically shown in Figure 7-3. It shows that for all projectiles there is decrease in the residual velocity of the projectile while increasing number of encapsulated layers. The similar kind of trend is found in all projectile ratings. The trend of residual velocity upon varying number of layers is cubic polynomial and the equation for two ballistic projectile ratings I and IIIA case is shown in Figure 7-3. The estimated number of layers required to stop from penetration is calculated using trend equation for the two cases and it was found that 11 layers of bubble wrap configuration filled with STF sample 1 and 12 layers of the same will be required for projectile having rating I and IIIA respectively.

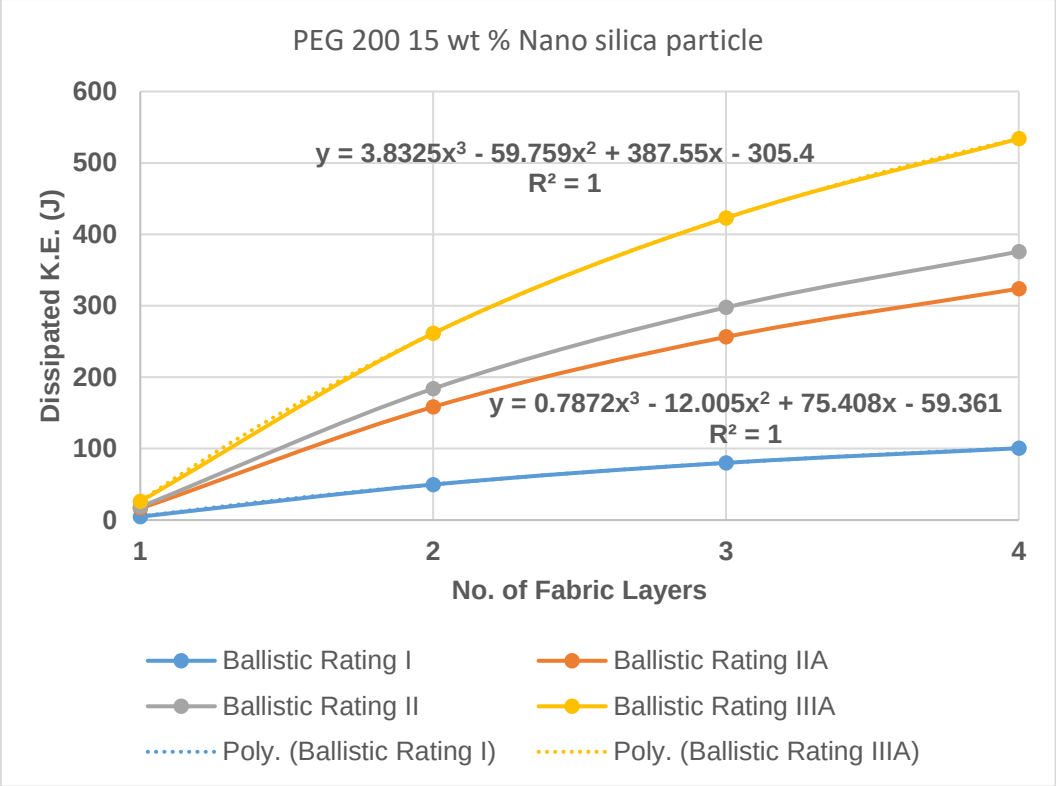

Figure 7-4 A graphic representation of variation of dissipated kinetic energy of multi-layer STF encapsulated with STF sample no. 1 inside bubble wrap configuration under ballistic impact of different ballistic ratings.

Similarly, graphic representation for dissipated kinetic energy is also shown in Figure 7-4. The dissipated kinetic energy by the STF encapsulated test sample is increasing with the increase in number of layers. The kinetic energy absorbed by the STF encapsulated sample follows cubic polynomial trend and the equation for BR I and IIIA is shown in Figure 7-4.

The dissipated kinetic energy is increasing but to measure the efficacy reference to the mass of the sample, dissipated kinetic energy is normalized to the related mass parameters by dividing to the areal density of the sample. The performance of bubble wrap configuration is further compared using normalized dissipated kinetic energy. The normalized dissipated kinetic energy for PEG 200 and 15 weight percent of nano-silica is compared by varying the number of layers. There is increase in the normalized kinetic energy when the layers of bubble wrap configuration are increasing and after a particular number of layers it becomes constant. It is evident from Figure 7-5 that after second layer of bubble wrap configuration the normalized dissipated kinetic energy is constant. Such behavior is observed for all projectile ratings and the only difference is the number of layers required to achieve constant normalized dissipated kinetic energy. By using Figure 7-5, we can estimate the number of layers required for the optimum ballistic performance of the bubble wrap configurations.

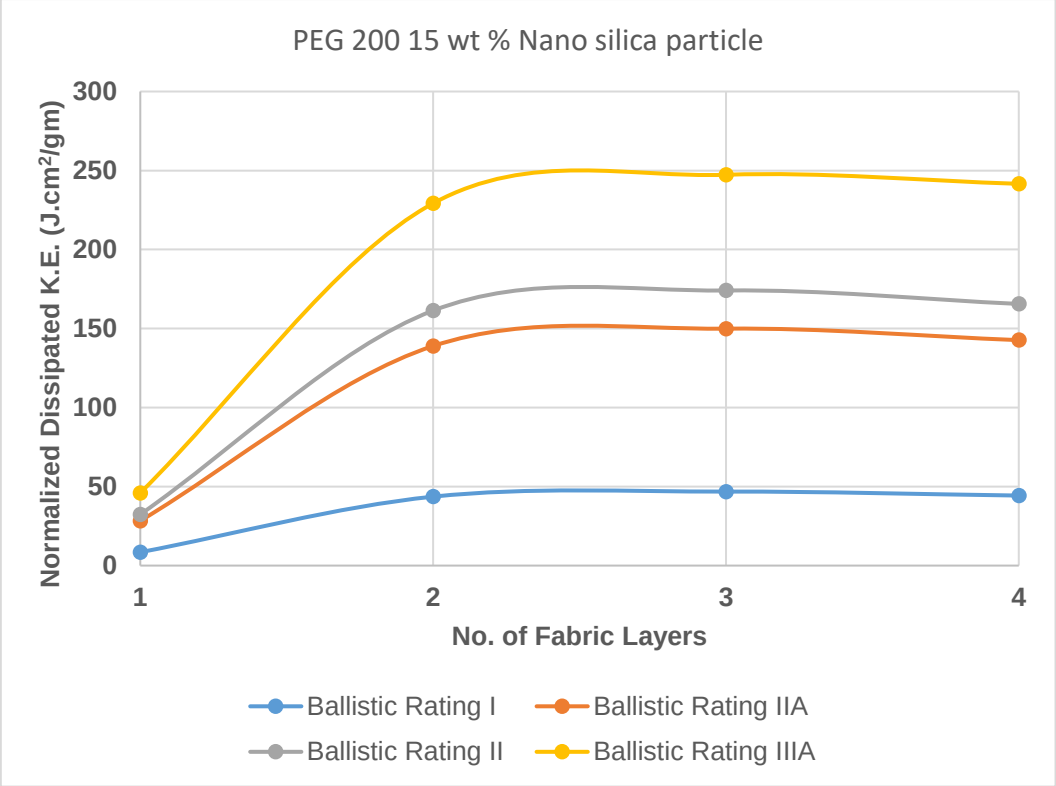

Figure 7-5 A graphic representation of variation of normalized dissipated kinetic energy of multi-layer STF encapsulated with STF sample no. 1 inside bubble wrap configuration under ballistic impact of different ballistic ratings.

The residual velocity of multi-layer STF encapsulated bubble wrap configuration for STF having constituents PEG 200 and 30 weight percent of silica particle under different ratings of projectile is graphically shown in Figure 7-6. A similar behavior is observed as compared to STF of constituents PEG 200 and 15 weight percent of silica particle. It shows that for all projectiles there is a decrease in the residual velocity of the projectile while increasing number of encapsulated layers. The similar kind of trend is found in all projectile ratings. The trend of residual velocity upon varying number of layers is cubic poly-fit and the equation for two ballistic projectile ratings I and IIIA case is shown in Figure 7-6. The estimated number of layers required to stop from penetration is calculated using trend equation for the two cases and it was found that 7 layers of bubble wrap configuration filled with STF sample 1 is required for both projectiles having rating I and IIIA. It is observed that while increasing the weight percent of nano silica particle there is enhancement in the ballistic performance of the STF encapsulated bubble wrap configuration. The rheological properties of STF having PEG 200 and different weight percent of the silica is shown in Figure 5-3 and from that it is concluded that the enhancement in the ballistic performance of the STF sample 4 is due to the enhanced rheological properties of the STF having PEG 200 and 30 weight percent

of nano-silica. The critical shear strain rate is lower and critical dynamic viscosity is higher for the STF sample having higher weight percent of the silica particle in the same molecular weight of the polyethylene glycol. Similarly, graphic representation for dissipated kinetic energy is shown in Figure 7-7. The dissipated kinetic energy by the STF encapsulated test sample is increasing with the increase in number of layers for STF having PEG 200 and 30 weight percent. The kinetic energy absorbed by the STF encapsulated sample follows cubic polynomial trend and the equation for BR I and III A is shown in Figure 7-7. On similar basis the variation of projectile's residual velocity of STF encapsulated bubble wrap configuration consisting 30 weight percent of nano silica and PEG 300, and PEG 400 is graphically shown in Figure 7-9 and Figure 7-12 respectively. A similar observation is noted for these STF samples. The only difference observed is that there is no significant improvement in the ballistic performance of the sample having same fraction of silica particles and different molecular weight of the polyethylene glycol (PEG). The kinetic energy of STF samples having PEG 300 and PEG 400 with same silica fraction is graphically shown in Figure 7-10, and Figure 7-13 respectively. The normalized kinetic energy of STF samples having PEG 300 and PEG 400 with same silica fraction is graphically shown in Figure 7-11, and Figure 7-14 respectively. A similar observation is drawn for these STF samples as STF of having PEG 200 and 30 percent weight fraction of silica particle.

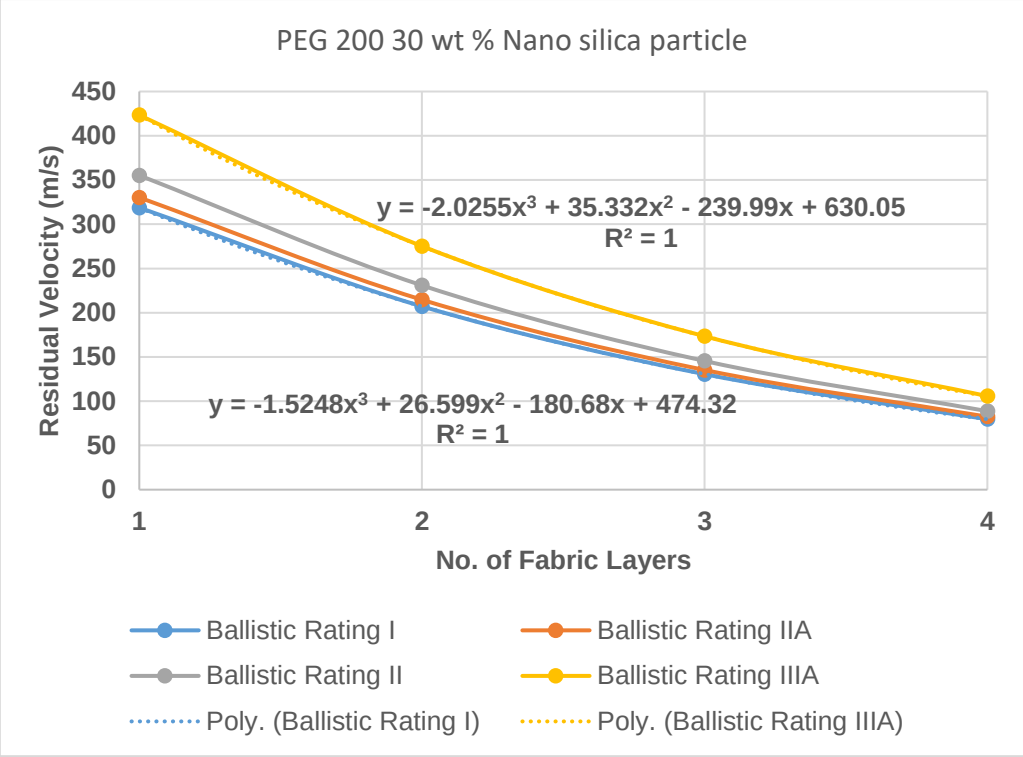

Figure 7-6 A graphic representation of variation of residual velocity of multi-layer STF encapsulated with STF sample no. 4 inside bubble wrap configuration under ballistic impact of different ballistic ratings.

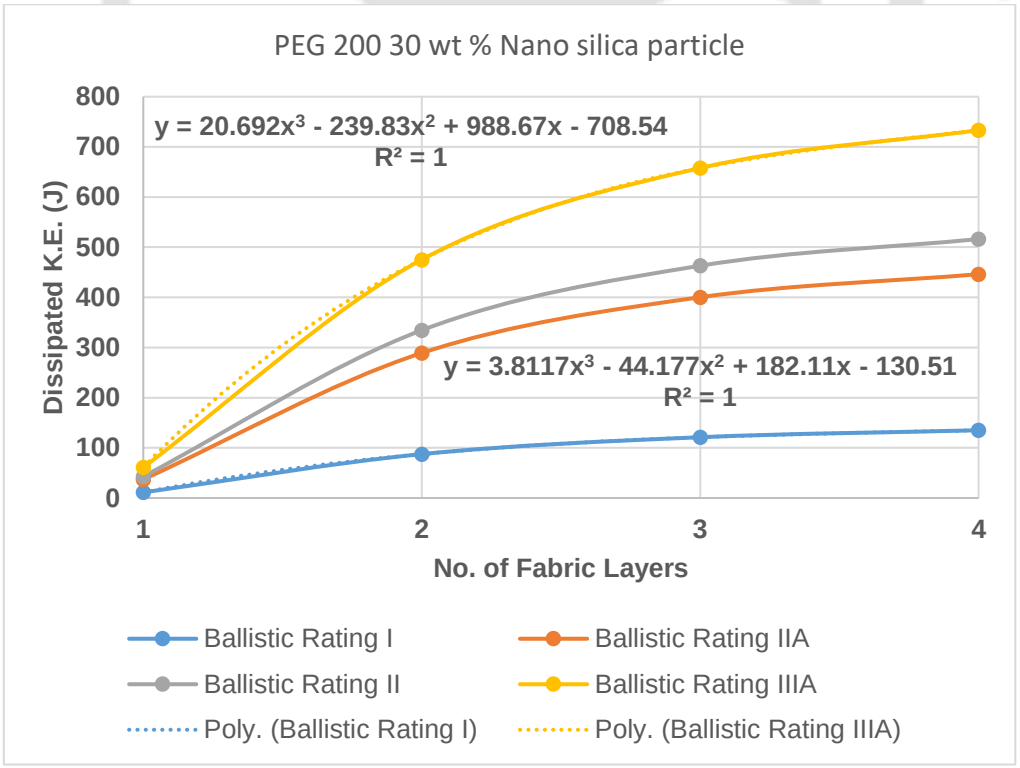

Figure 7-7 A graphic representation of variation of dissipated kinetic energy of multi-layer STF encapsulated with STF sample no. 4 inside bubble wrap configuration under ballistic impact of different ballistic ratings.

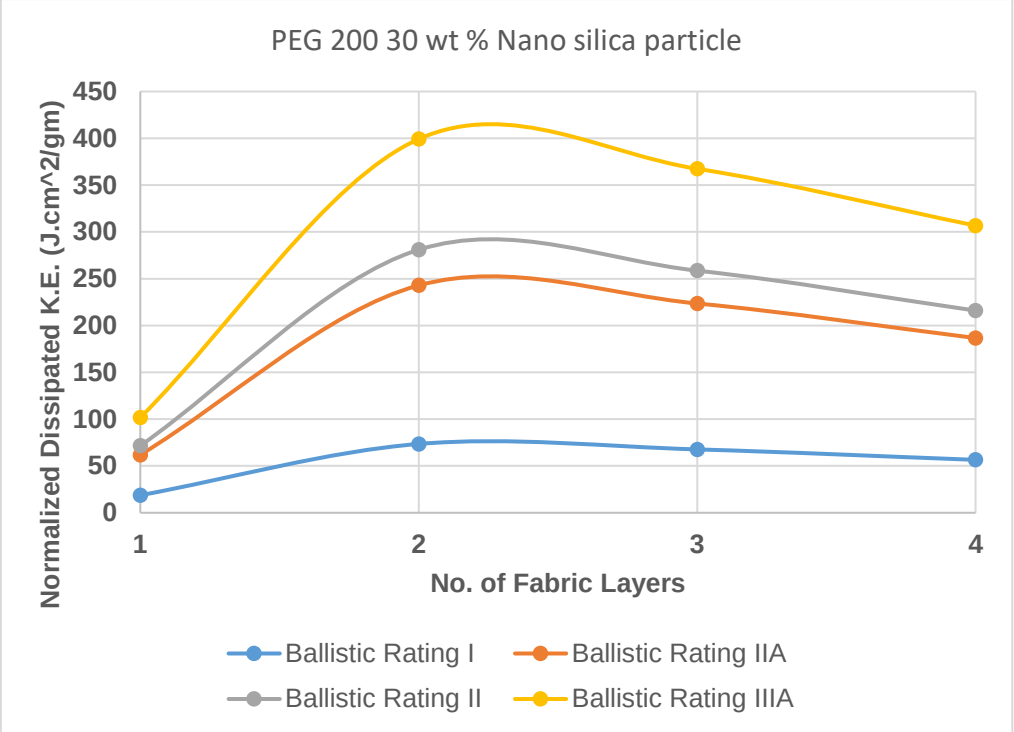

Figure 7-8 A graphic representation of variation of normalized dissipated kinetic energy of multi-layer STF encapsulated with STF sample no. 4 inside bubble wrap configuration under ballistic impact of different ballistic ratings.

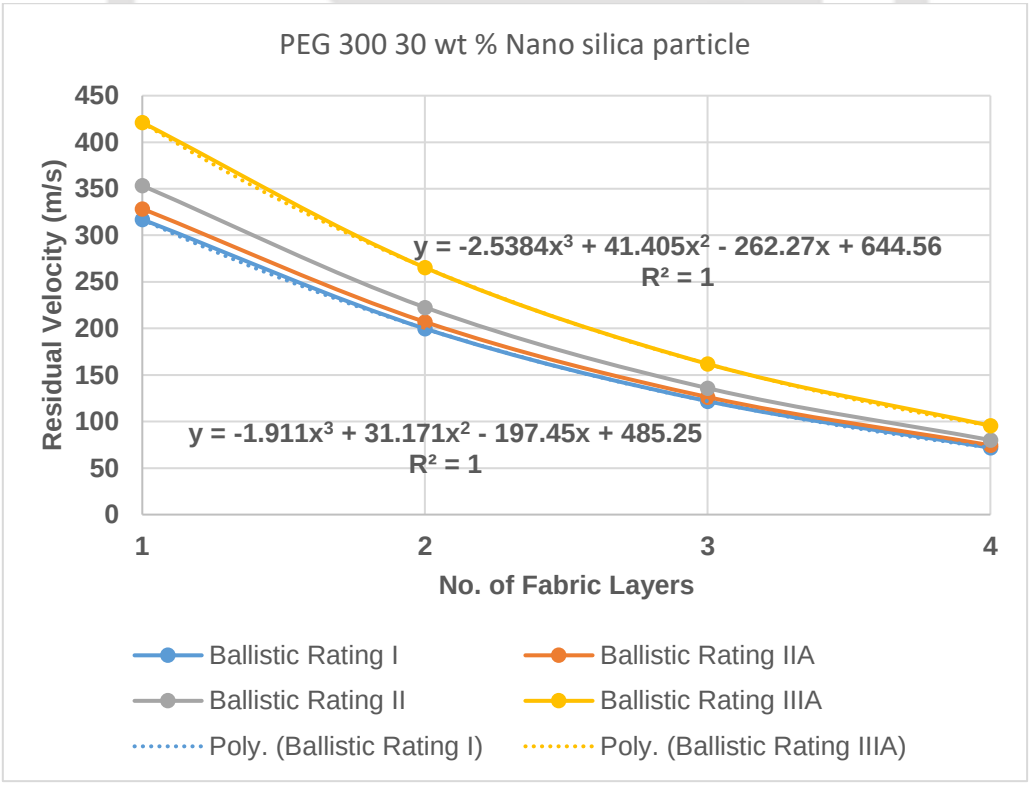

Figure 7-9 A graphic representation of variation of residual velocity of multi-layer STF encapsulated with STF sample no. 8 inside bubble wrap configuration under ballistic impact of different ballistic ratings.

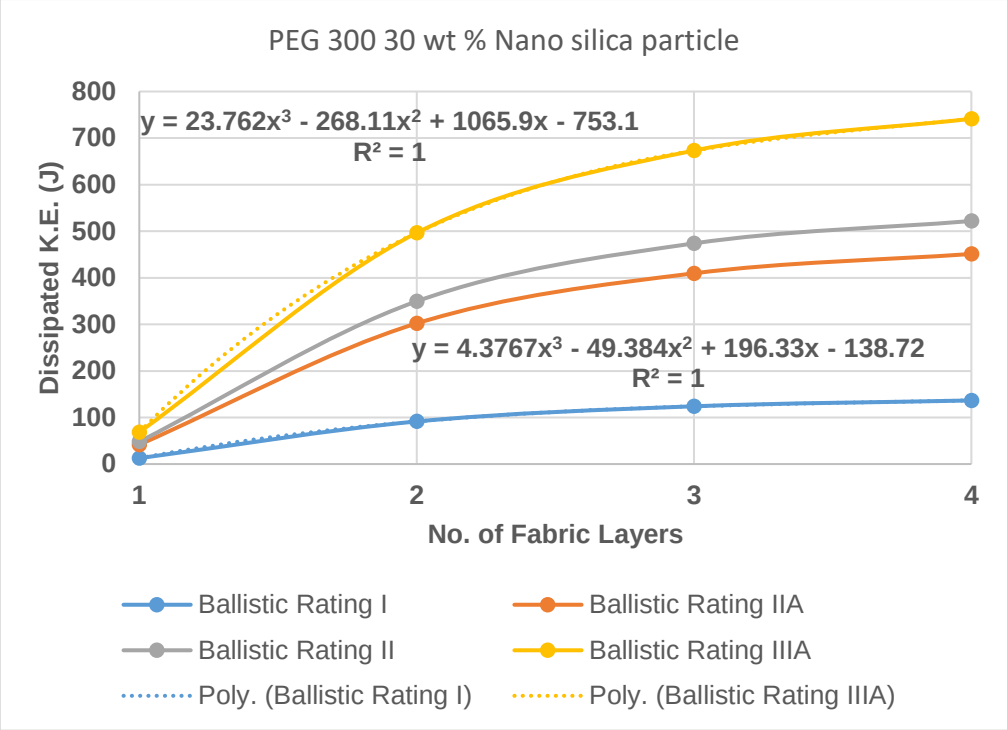

Figure 7-10 A graphic representation of variation of dissipated kinetic energy of multi-layer STF encapsulated with STF sample no. 8 inside bubble wrap configuration under ballistic impact of different ballistic ratings.

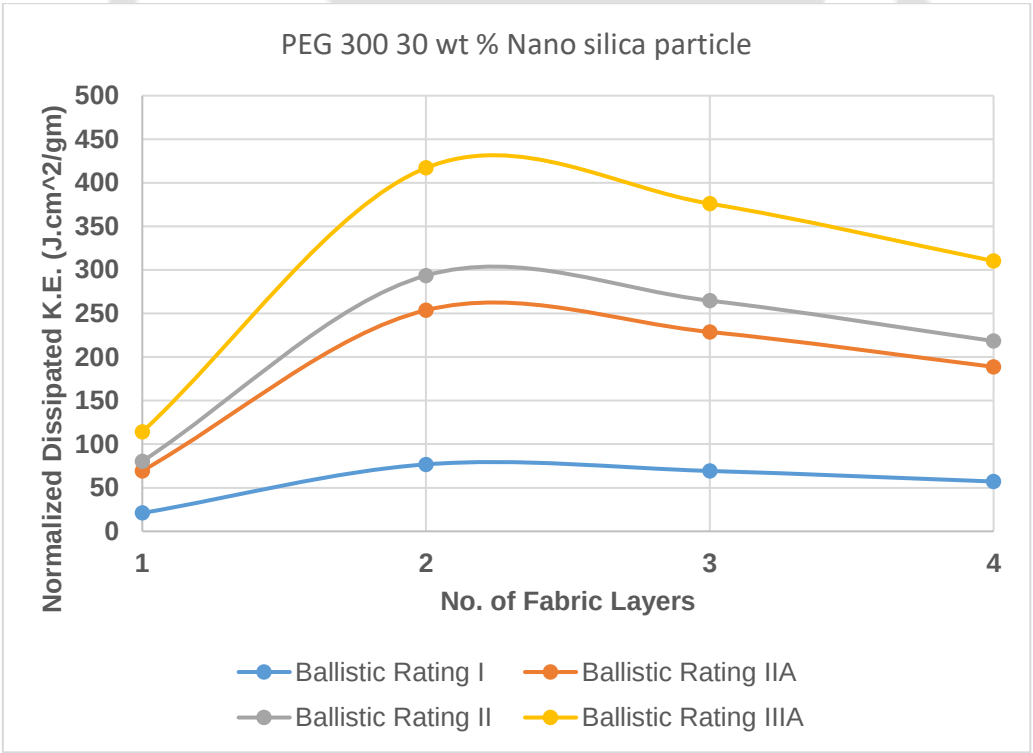

Figure 7-11 A graphic representation of variation of normalized dissipated kinetic energy of multi-layer STF encapsulated with STF sample no. 8 inside bubble wrap configuration under ballistic impact of different ballistic ratings.

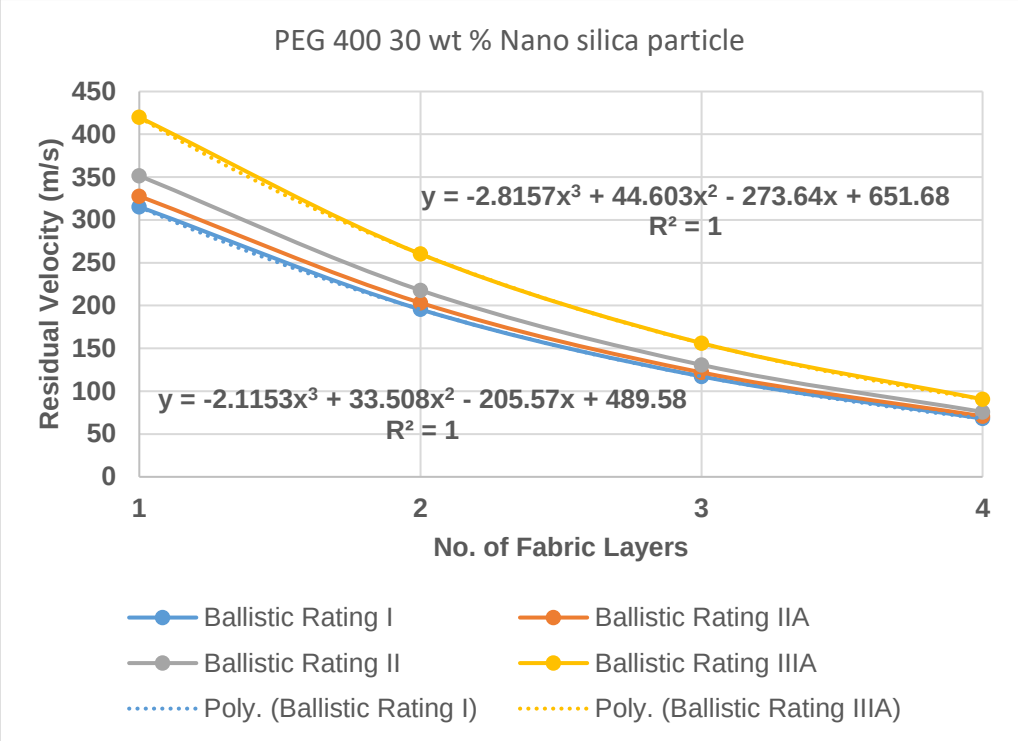

Figure 7-12 A graphic representation of variation of residual velocity of multi-layer STF encapsulated with STF sample no. 12 inside bubble wrap configuration under ballistic impact of different ballistic ratings.

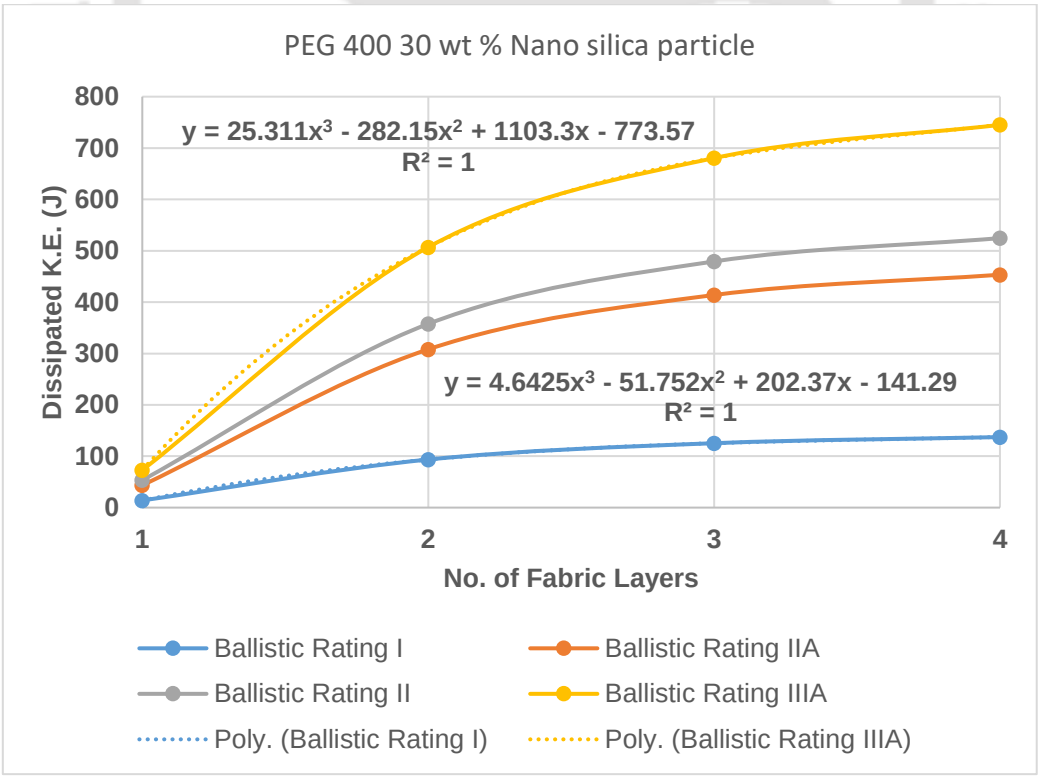

Figure 7-13 A graphic representation of variation of dissipated kinetic energy of multi-layer STF encapsulated with STF sample no. 12 inside bubble wrap configuration under ballistic impact of different ballistic ratings.

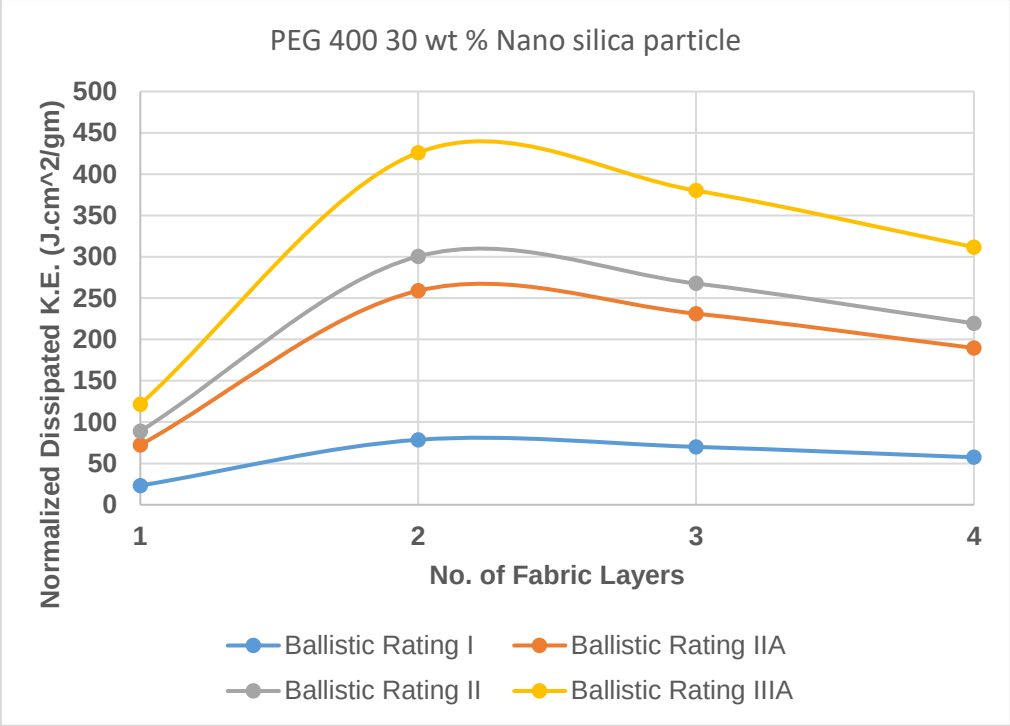

Figure 7-14 A graphic representation of variation of normalized dissipated kinetic energy of multi-layer STF encapsulated with STF sample no. 12 inside bubble wrap configuration under ballistic impact of different ballistic ratings.

7.4 Conclusion

This chapter presents a new configuration to harness the smart behavior of STF. The new proposed configuration is based on confinement of shear thickening fluid within negligible strength but highly flexible made of Low-Density Poly-Ethylene (LDPE) material. The present investigation considers only uniform placement of cylindrical shape bubbles. The bubble wrap configuration is filled with STF. From the above results, it is concluded that the variation in the type of the STF and its composition hardly effects the results of the energy absorption. It only varies with the density of the bubble wrap with the STF and the impact velocity of the projectile. There is an increasing trend in all the cases of energy absorption with the density of the bubble wrap capsule. With the increase in the amount of STF, the net area is less which results in more energy absorption capacity in that particular area. The results show a promising trend in the direction of utilizing STF as an energy absorbing material in the field of blast and ballistics to mitigate the effect of generated shockwaves. The objective of developing a novel configuration by using STF encapsulated in a bubble wrap configuration is established in this Chapter. A light-weight and flexible Smart thickening fluid based Ultra Resistant Adaptive Kinematic Soft Human Armour (SURAKSHA) is achieved as per NIJ standards.

8 Guidelines for Design and Development of Ballistic Body Armour

The aim of this Chapter is to formulate the design guidelines for the development of Smart thickening fluid based Ultra Resistant Adaptive Kinematic Soft Human Armour (SURAKSHA) based on the findings of the current work. The developed design guidelines will help in arriving the proper configuration of the ballistic body armour. It serves as a design aid for application of the developed methodology to design and develop the bullet proof armour as per the required demand. The developed design guidelines are formulated based on the existing standards. This helps in achieving the objective of development of ballistic body armour as per the requirement and standards.

8.1 Existing guidelines and test methods in design and development of body armour

The existing guidelines for the development of body armour is investigated in this section. These existing guidelines were formulated to use the research done in the area of body armour and make it commercially viable for filed implementation. Every country has developed some standards on this front so that the proper safety measures are always achieved as any negligence can cost someone's life and it also makes the country stronger in terms of defense capability. In order to keep the test procedure same, the methodologies of the testing conducted is also provided so that there is a uniform testing done to check the adequacy of the armour. Such guidelines and methodologies provide the opportunity of putting up industries in this direction for commercialization, as already have been there in some countries. This will enhance the productivity and fulfilment of demand with ease in application due to already existing safety and utility guidelines. The guidelines will be discussed in the following sub-section so that the proposed design and methodologies are safe and effective in mass manufacturing of the proposed bullet proof armour along with the fulfilment of the desired requirement.

8.1.1 NIJ Guidelines for bullet proof armour

NIJ has rated the bullet proof armour types into 6 categories based on the type and number of impacts it can take without any penetration. The following table discuss about the NIJ guidelines and the required methodology in testing in detail.

Table 8-1 NIJ guidelines for rating bullet proof armour

Armour type	Test Ammunition	Nominal bullet mass	Required bullet velocity	Required hits per armour	Penetration permitted
I	22 LHRV Lead	2.6g	320±12m/s	5	0
	38 special RN Lead	10.2g	259±15m/s	5	0
II-A	357 Magnum JSP	10.2g	381±15m/s	5	0
	9mm FMJ	8.0g	332±12m/s	5	0
II	357 Magnum JSP	10.2g	425±15m/s	5	0
	9mm FMJ	8.0g	358±12m/s	5	0
III-A	44 Magnum lead SWC	15.5g	426±15m/s	5	0
	9mm FMJ	8.0g	426±15m/s	5	0
III	7.62mm 308 Winchester FMJ	9.7g	838±15m/s	5	0
IV	30-06 AP	10.8g	868±15m/s	1	0

8.1.2 UL 752 – (Standard for Bullet-Resisting Equipment) guidelines

Some of the guidelines given by the United States for the development of any bullet proof equipment are given in this standard. The criteria is fixed based upon the testing standard adopted. This includes the shot space which is to be kept constant at 4.5-inch square. The range in all the test methodologies is kept at 15 ft on a sample size of 12 x 12 inch. The witness plate is made up of 0.125-inch-thick corrugated cardboard which is kept at a distance of 18 inches from the target. It is used to divide a single category into its by-parts based on whether the witness plate is required in the procedure or not as discussed in Table 8-2.

Table 8-2 UL 752 Ballistic standards

UL-Level	**Projectile Caliber**	**Cartridge type**	**Velocity Range (ft/sec)**	**Shot spacing**	**No. of shots**	**Witness Plate (Yes/No)**	**Penetration**
3 (Part 1)	0.44 magnum	240 grain SWC	1350-1485	4.5-inch triangle	3	yes	0
3 (Part 2)	0.44 magnum	240 grain SWC	1350-1485	1.25 – 1.75 inch	2	no	0
3 (Part 3)	0.44 magnum	240 grain SWC	1350-1485	-	1	no	0
4 (Part 1)	0.30 30-06	180 grain JSP	2540-2790	-	1	yes	0
4 (Part 2)	0.30 30-06	180 grain JSP	2540-2790	-	1	no	0
5 (Part 1)	0.30 7.62 NATO	150 grain FMJ	2750-3025	-	1	yes	0
5 (Part 2)	0.30	150 grain FMJ	2750-3025	-	1	no	0

		7.62 NATO							
4, (Part 1A)	5	12 gauge 2 ¾ inch	437	grain slug	1585-1743.5	-	1	yes	0
4, (Part 1B)	5	12 gauge 2 ¾ inch	437	grain slug	1585-1743.5	-	1	no	0
4, (Part 2A)	5	12 gauge 2 ¾ inch Mag.	650	grain #00 Buck	1200-1320	-	1	yes	0
7		0.223 5.56 NATO	55	grain FMJ	3080-3388	4.5 in. square	5	yes	0

8.2 Proposed guidelines for SURAKSHA

The developed Smart thickening fluid based Ultra Resistant Adaptive Kinematic Soft Human Armour (SURAKSHA) will be evaluated on the basis of the standard guidelines that have been discussed above. It will help in arriving at the configuration required for achieving the desired level of safety as per the stated guidelines. On the basis of this, Smart thickening fluid based Ultra Resistant Adaptive Kinematic Soft Human Armour (SURAKSHA) can be developed which will eventually help in the mass production at an industrial scale. The energy/ momentum of the impact is a common quantity which will be used as a basis for the comparison of different configurations. The following tables from Table 8-3 to Table 8-11 presents results of different configurations comprising of Kevlar (neat), Kevlar with STF and bubble wrap as per the existing guidelines.

Table 8-3 Ballistic rating for neat Kevlar fiber

Neat Kevlar (No. of layers) 30x30 fabric set	**NIJ rating**	**UL 752 level**
4	Unrated Performance	Unrated Performance
8	Underrated Performance	Underrated Performance
12	Underrated Performance	Underrated Performance
16	I	Underrated Performance

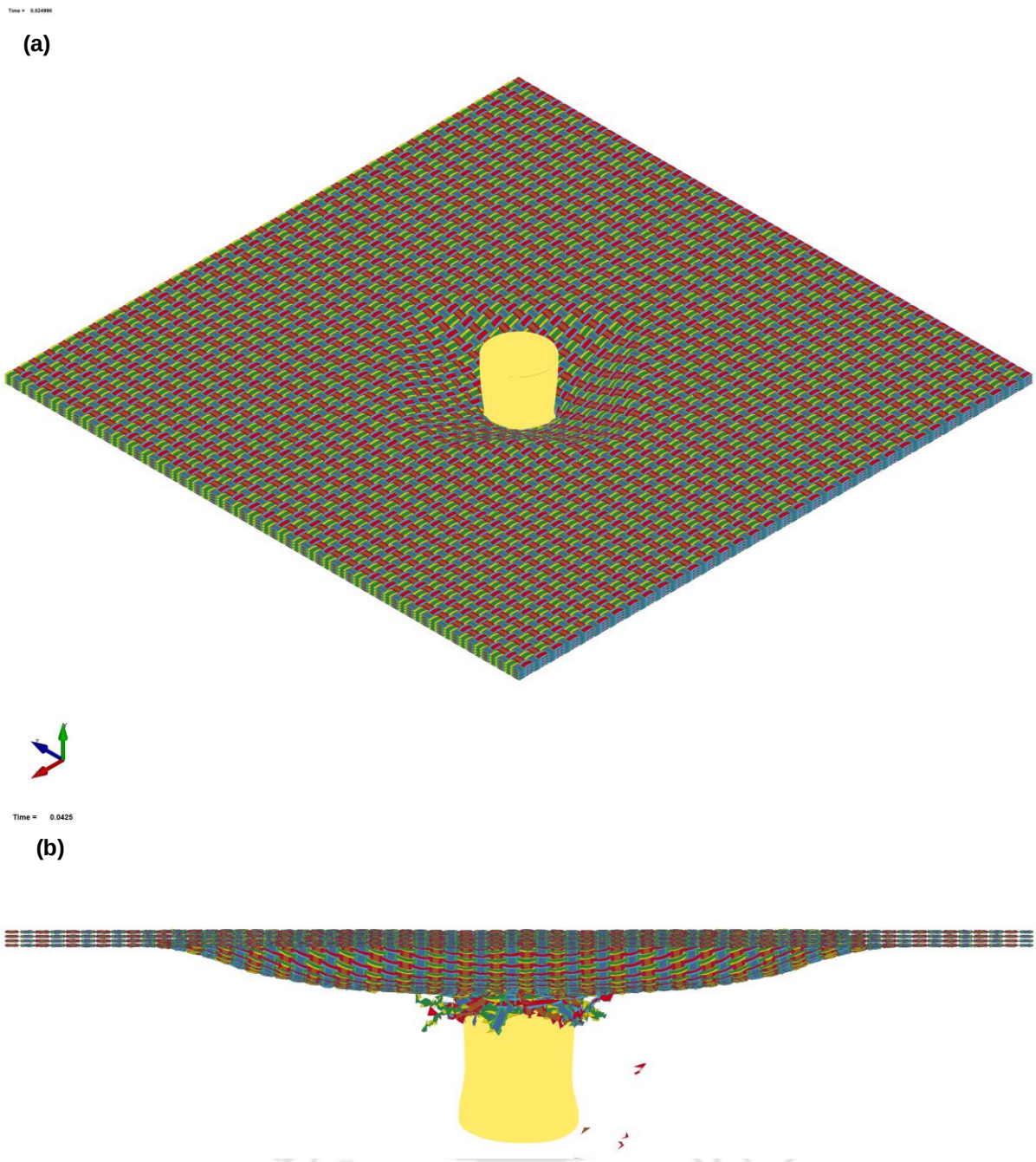

Figure 8-1 The penetration of neat multi-layer fabric system under ballistic impact comprised of bullet having BR I (a) Isometric view and (b) Front View of the multi-layer fabric system

In the neat Kevlar configuration, it is observed that in order to achieve the desired level of standards, the number of layers in the body armour needs to be increased, thus increasing the bulkiness of the armour along with the weight. The number of layers tested indicates the necessity of an upgrade in Kevlar to enhance its performance along with reducing the areal density of the armour. With these many layers, the armour is restricted for encountering very light impact blows only including the blow from knives or other very low velocity sharp objects. It might not be that effective from the blow of blunt heavy objects. In Table 8-4, Kevlar

with STF is discussed. The results clearly indicate the effectiveness of STF in improving the ballistic rating of the armour. The penetration model of neat multi-layer fabric system is shown in Figure 8-1. The projectile of rating BR I is fully penetrating the multi-layer fabric system. Table 8-4 provides the ballistic performance of STF treated fabric having STF sample comprised of PEG 200 and 15 wt. % of nano-silica. The treated multi-layer fabric system shows the improved ballistic behavior as compared to the neat multi-layer fabric system. However, there performance is not significantly improved to qualify for certain ratings up to 8 layers of treated fabric system. The ballistic behavior of 12 layer of treated fabric is improved in such a way that it qualifies for BR I rating.

Table 8-4 Ballistic rating for Kevlar with STF (PEG 200 and 15% nano silica)

Kevlar (No. of layers) 30x30 fabric set	**NIJ rating**	**UL 752 level**
4	Underrated Performance	Underrated Performance
8	Underrated Performance	Underrated Performance
12	I	3 (part 3)
16	I	3 (part 3)

The penetration of STF treated sample consisting PEG 200 and 15 wt. % treated four-layer fabric system is shown in Figure 8-2. The full penetration of the STF treated multi-layer fabric system is observed. There is a significant piercing of the deformable bullet. The extent of damage has propagated to the larger area of the fabric system. This indicates that the STF system is supporting the propagation of strain wave resulting from the ballistic impact to the larger area.

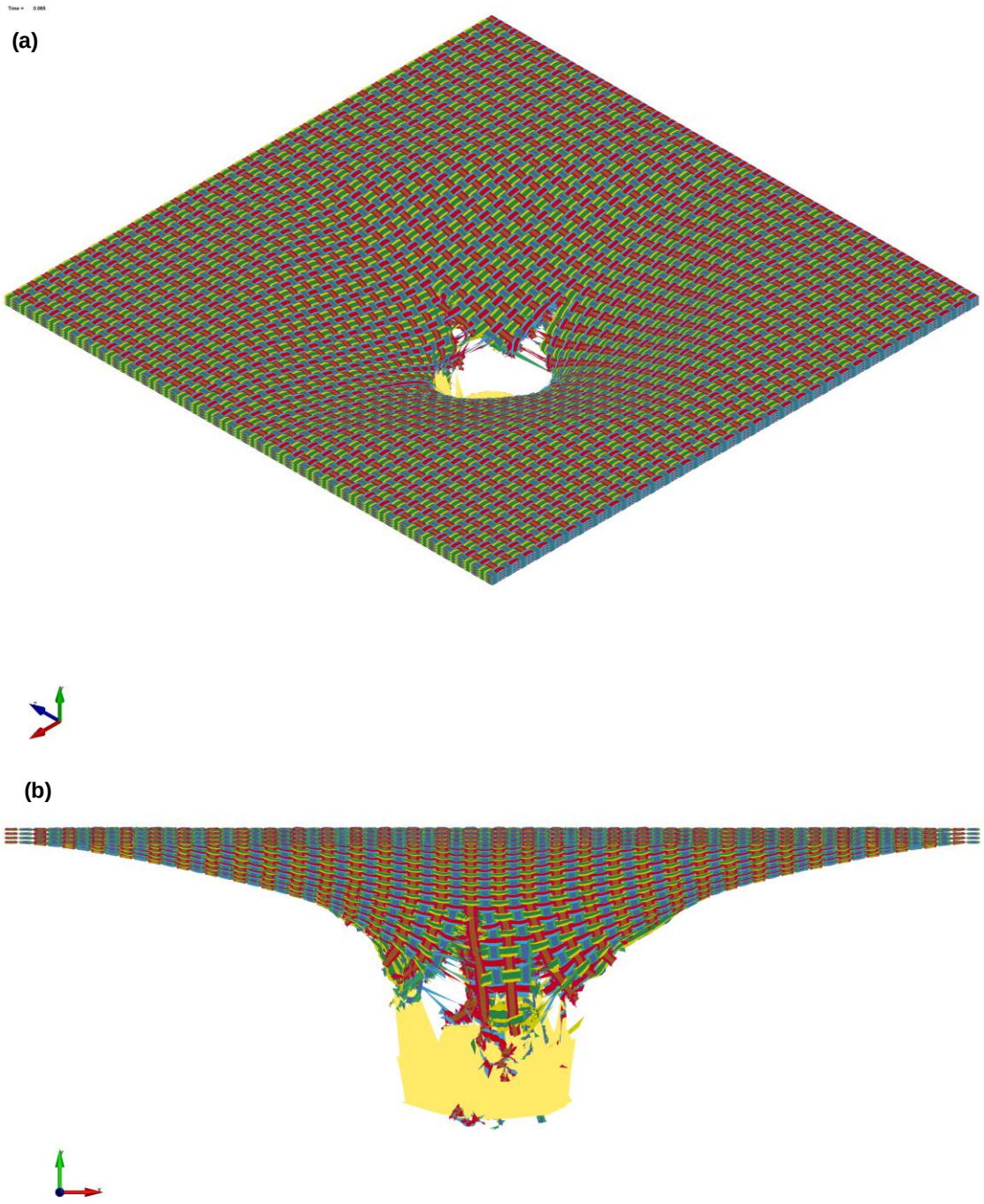

Figure 8-2 The penetration of PEG 200 and 15 wt. % STF sample treated multi-layer fabric system under ballistic impact comprised of bullet having BR I (a) Isometric view and (b) Front View of the multi-layer fabric system

Table 8-5 presents the ballistic rating of STF treated multi-layer fabric system for STF sample PEG 200 and 30 wt.% of nano-silica. The four-layer fabric system correspond to the BR I as per NIJ rating while there is no rating due to underperformance of the armour system for UL 752 level. Further, eight layers conform to BR IIA as per NIJ standards while the same is conforming to unrated as per UL 752 level. The rest of the multi-layer STF treated fabric

system conforms to BR II according to NIJ standards and as per UL 752 level the ratings are 3 (part 3), 3 (part 2), and 3 (part 2) for 8, 12 and 16 layers respectively for STF treated fabric system.

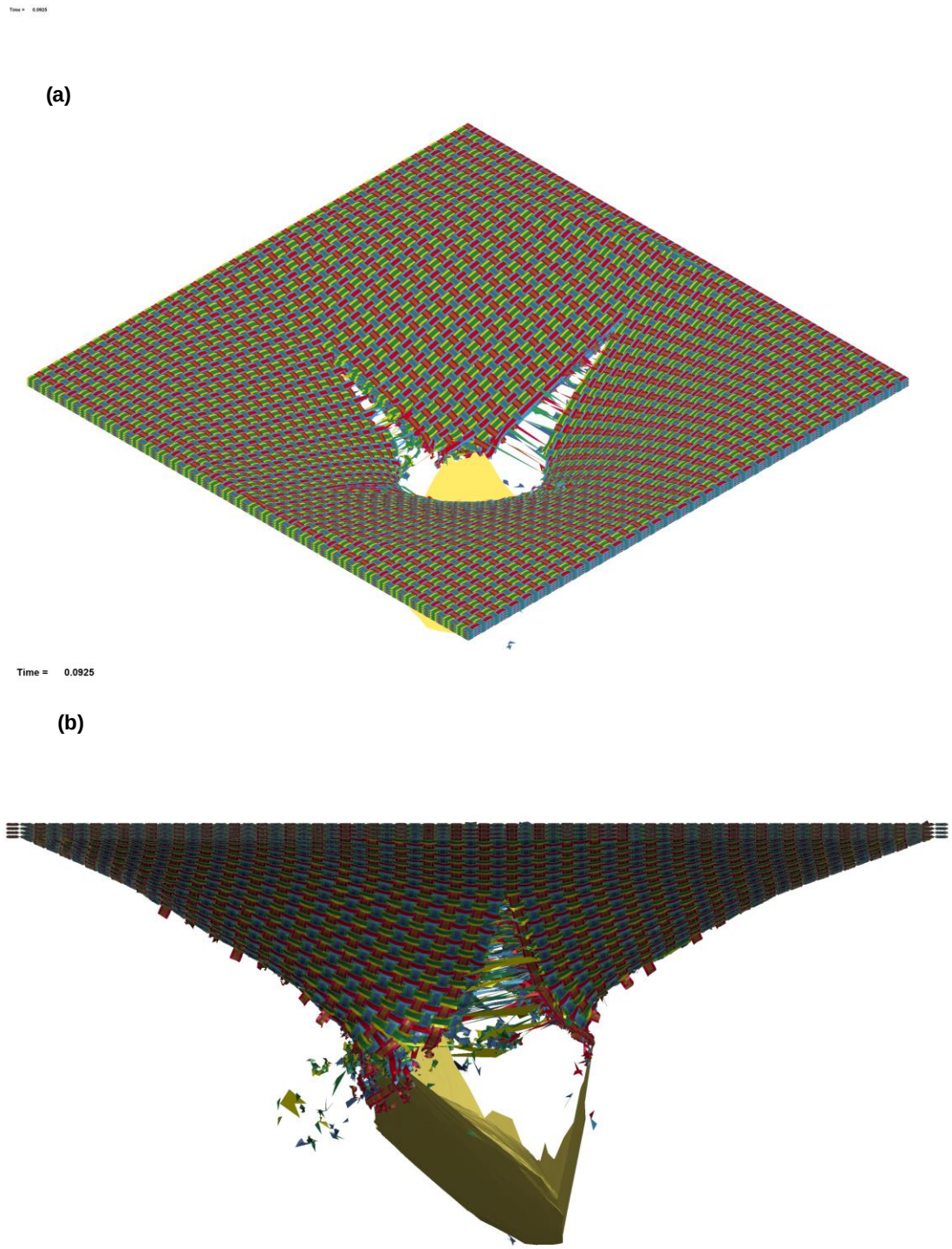

Figure 8-3 The penetration of PEG 200 and 30 wt. % STF sample treated multi-layer fabric system under ballistic impact comprised of bullet having BR I (a) Isometric view and (b) Front View of the multi-layer fabric system

The penetration of STF treated sample consisting of PEG 200 and 30 wt. % treated four-layer fabric system is shown in Figure 8-3. The extent of damage is propagating to the larger area of the treated fabric system. This shows that the STF is providing greater resistance towards the penetration of the overall system. The bullet is significantly piercing while interacting to the armour system. This is due to more resistance provided due to enhanced rheometric properties of the STF.

Table 8-5 Ballistic rating for Kevlar with STF (PEG 200 and 30% nano silica)

Kevlar (No. of layers) 30x30 fabric set	**NIJ rating**	**UL 752 level**
4	Underrated Performance	Unrated Performance
8	Underrated Performance	Underrated Performance
12	II A	3 (part 2)
16	II A	3 (part 2)

Table 8-6 presents the ballistic rating of STF treated multi-layer fabric system for STF sample PEG 300 and 30 wt.% of nano-silica. The four-layer fabric system correspond to the BR I as per NIJ rating while there is no rating due to underperformance of the armour system for UL 752 level. Eight layers conform to BR IIA as per NIJ standards while the same is conforming to (3 part 3) as per UL 752 level. Twelve layers conforms to IIA as per NIJ and 3 (part 3) as per UL 752 level. The rest of the multi-layer STF treated fabric system conforms to BR II according to NIJ standards and as per UL 752 level the ratings are 3 (part 3). The penetration of STF treated sample consisting of PEG 300 and 30 wt. % treated four-layer fabric system is shown in Figure 8-4. The extent of damage is propagating to the larger area of the treated fabric system. This shows that the STF is providing greater resistance towards the penetration of the overall system. The bullet is significantly piercing while interacting to the armour system. This is due to more resistance provided due to enhanced rheometric properties of the STF.

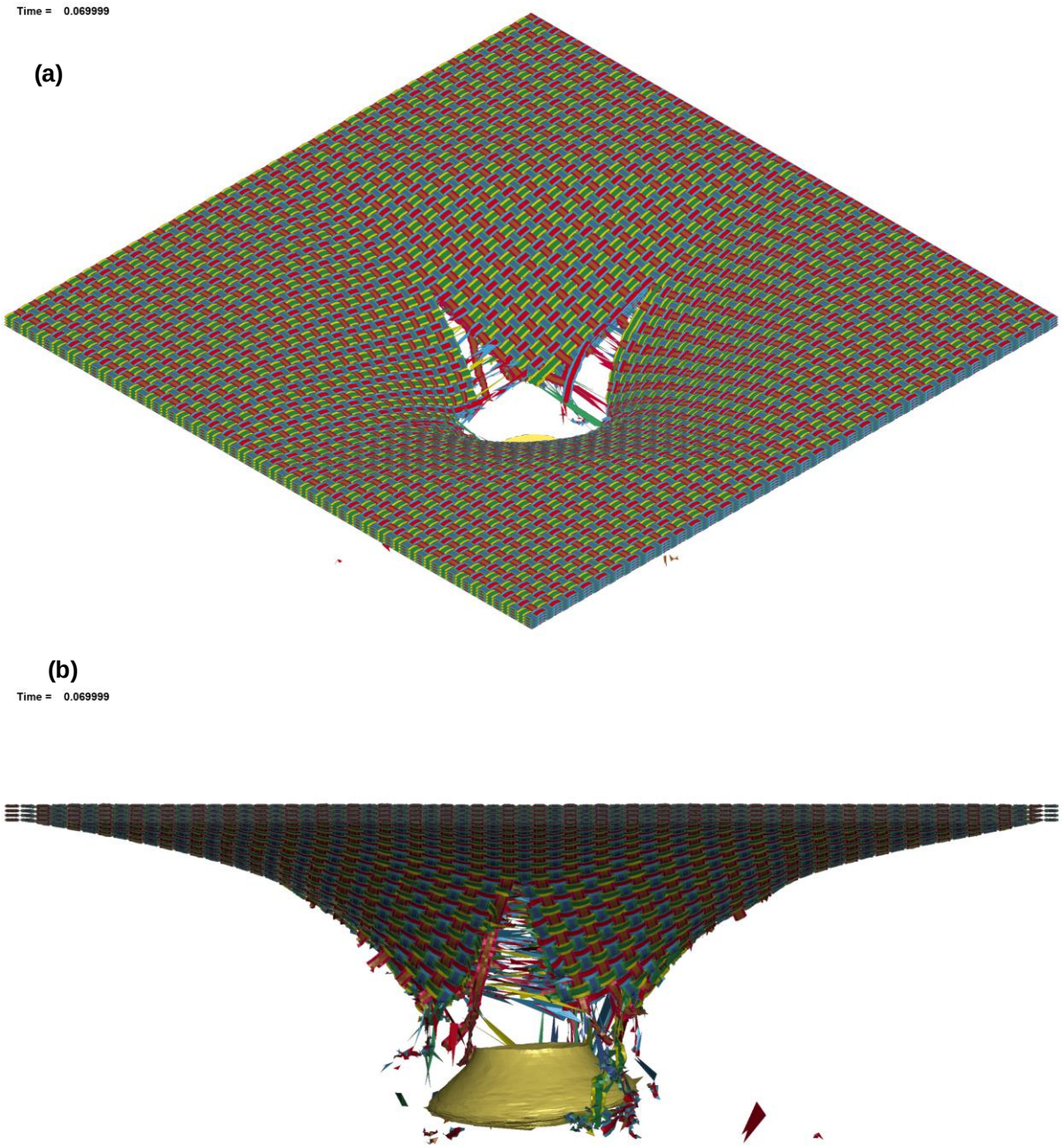

Figure 8-4 The penetration of PEG 300 and 30 wt. % STF sample treated multi-layer fabric system under ballistic impact comprised of bullet having BR I (a) Isometric view and (b) Front View of the multi-layer fabric system

Table 8-6 Ballistic rating for Kevlar with STF (PEG 300 and 30% nano silica)

Kevlar (No. of layers) 30x30 fabric set	**NIJ rating**	**UL 752 level**
4	Underrated Performance	Unrated Performance
8	Underrated Performance	Underrated Performance
12	II A	3 (part 3)
16	II A	3 (part 2)

Table 8-7 presents the ballistic rating of STF treated multi-layer fabric system for STF sample PEG 400 and 30 wt.% of nano-silica. The four-layer fabric system correspond to the BR I as per NIJ rating while there is no rating due to underperformance of the armour system for UL 752 level. Eight layers conform to BR IIA as per NIJ standards while the same is conforming to (3 part 3) as per UL 752 level. Twelve layers conforms to IIA as per NIJ and 3 (part 3) as per UL 752 level. The rest of the multi-layer STF treated fabric system conforms to BR II according to NIJ standards and as per UL 752 level the ratings are 3 (part 3). The penetration of STF treated sample consisting PEG 400 and 30 wt. % treated four-layer fabric system is shown in Figure 8-5. The extent of damage is propagating to the larger area of the treated fabric system. This shows that the STF is providing greater resistance towards the penetration of the overall system. The bullet is significantly piercing while interacting to the armour system. This is due to more resistance provided due to enhanced rheometric properties of the STF.

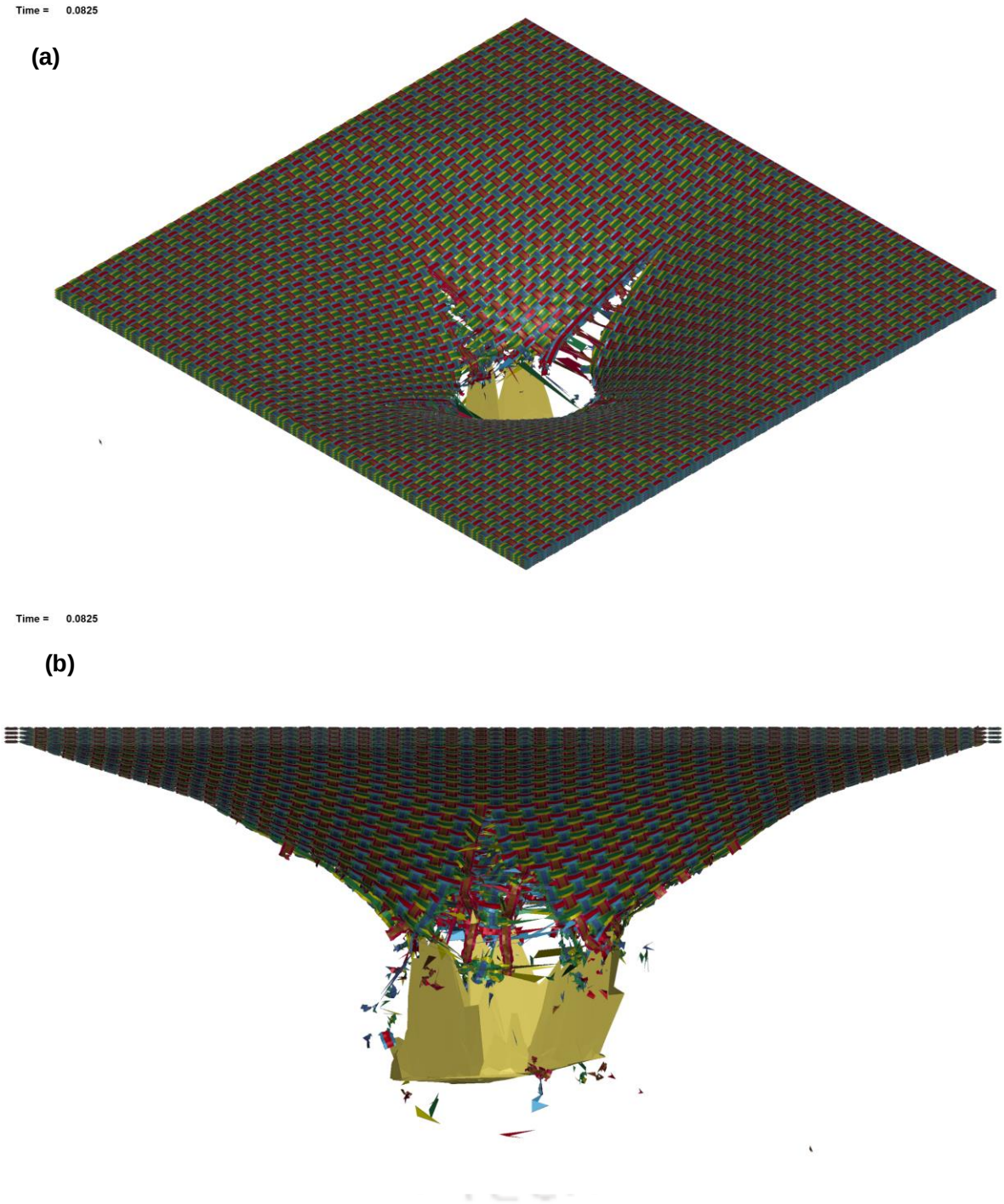

Figure 8-5 The penetration of PEG 400 and 30 wt. % STF sample treated multi-layer fabric system under ballistic impact comprised of bullet having BR I (a) Isometric view and (b) Front View of the multi-layer fabric system

Table 8-7 Ballistic rating for Kevlar with STF (PEG 400 and 30% nano silica)

Kevlar (No. of layers) 30x30 fabric set	**NIJ rating**	**UL 752 level**
4	Underrated Performance	Underrated Performance
8	Underrated Performance	Underrated Performance
12	II A	3 (part 3)
16	II A	3 (part 2)

The efficacy of the developed Smart thickening fluid based Ultra Resistant Adaptive Kinematic Soft Human Armour (SURAKSHA) is discussed and highlighted in the previous Chapters 7. In this section the development guidelines will be presented. The achieved ballistic ratings as per the existing standards are given in the Table 8-8 to Table 8-11.

Table 8-8 Ballistic rating of bubble wrap encapsulated with STF (PEG 200 and 15% nano silica)

No. of bubble wrap layers	**NIJ rating**	**UL 752 level**
1	Unrated Performance	Unrated Performance
2	Unrated Performance	Unrated Performance
3	Unrated Performance	Unrated Performance
4	Unrated Performance	Unrated Performance

Table 8-9 Ballistic rating of bubble wrap encapsulated with STF (PEG 200 and 30% nano silica)

No. of bubble wrap layers	**NIJ rating**	**UL 752 level**
1	Unrated Performance	Unrated Performance
2	Unrated Performance	Unrated Performance
3	I	Unrated Performance
4	I	Unrated Performance

Table 8-10 Ballistic rating of bubble wrap encapsulated with STF (PEG 300 and 30% nano silica)

No. of bubble wrap layers	NIJ rating	UL 752 level
1	Underrated Performance	Underrated Performance
2	Underrated Performance	Underrated Performance
3	I	Underrated Performance
4	I	Underrated Performance

Table 8-11 Ballistic rating of bubble wrap encapsulated with STF (PEG 400 and 30% nano silica)

No. of bubble wrap layers	NIJ rating	UL 752 level
1	Underrated Performance	Underrated Performance
2	Underrated Performance	Underrated Performance
3	Underrated Performance	Underrated Performance
4	I	Underrated Performance

The results from the Table 8-8 to Table 8-11 are used to achieve the required level of ballistic rating. A design methodology is proposed in Table 8-12 to arrive at the suitable configuration of Smart thickening fluid based Ultra Resistant Adaptive Kinematic Soft Human Armour (SURAKSHA). The different parameters for configuration such the amount of PEG, its type, Number of Kevlar fiber layers, Number of bubble wrap layers can be evaluated by using the results from Table 8-12 as per the desired rating. This paves the way for making the Smart thickening fluid based Ultra Resistant Adaptive Kinematic Soft Human Armour (SURAKSHA) a feasible product as the demand and the capacity are presented in a single applicable Table. This will also help in achieving the economy for developing SURAKSHA. Subsequently, the number of layers required to stop the designated projectile ratings the developed equation for residual velocity of the projectile is used. The number of layers required to stop the designated projectile ratings is given in Table 8-12 and Table 8-13 for STF

impregnated multi-layer fabric system and for multi-layer STF encapsulated bubble wrap configuration respectively.

Table 8-12 Number of layers respective to the ballistic performance of STF impregnated fabric system (SURAKSHA A)

V(m/s) / *M (gm)*		**I**	**II A**	**II**	**III A**
		332	**344**	**370**	**441**
I	**2.6**	16			
II A	**8**		16		
II	**8**			20	
III A	**8**				24

Table 8-13 Number of layers respective to the ballistic performance of STF encapsulated bubble wrap configuration (SURAKSHA B)

V(m/s) / *M (gm)*		**I**	**II A**	**II**	**III A**
		332	**344**	**370**	**441**
I	**2.6**	12 (STF_01)			
II A	**8**		7 (STF_04,08,12)		
II	**8**			7 (STF_04,08,12)	
III A	**8**				7 (STF_04,08,12)

The numerical simulation of multi-layer fabric system is conducted to evaluate the penetration of the 18-layer fabric system. The projectile is non-penetrating the for the proposed armour configuration. The numerical model of 18-layer projectile system is as shown in Figure 8-6.

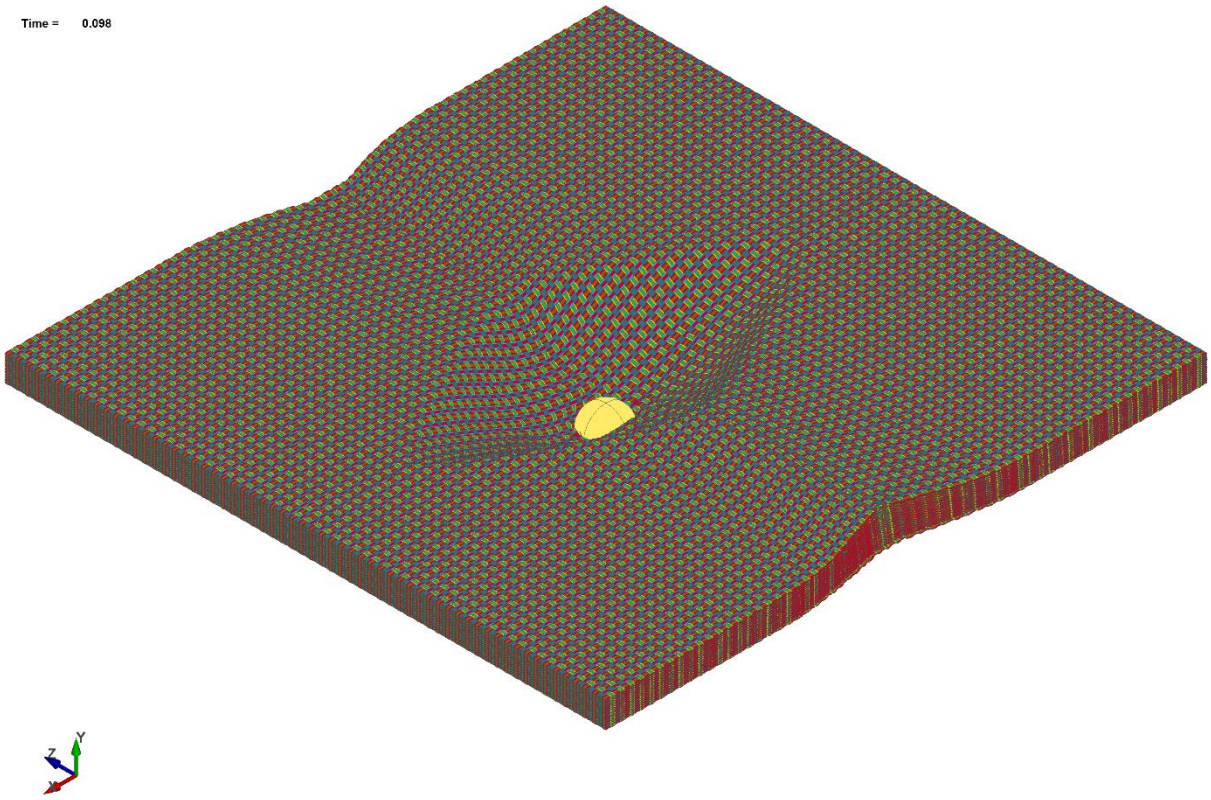

Figure 8-6 A graphic representation of numerical model of 18-layer fabric system

8.3 Methodology for designing a light weight bullet proof armour

On the basis of the requirement of the SURAKSHA i.e., the level of safety required to be achieved based on the standards, the design guideline is proposed in the following steps as stated below:

8.3.1 Guidelines for SURAKSHA A

1) Define the level of bullet proof armour as per user requirement and the standard followed (NIJ/ UL 752).
2) Based on this, select the number of Kevlar layers, the type of STF and its percentage on the basis of availability.
3) Prepare the STF as per the level of armour protection following the methodology discussed in Chapter 5 . The rheological data (a curve of dynamic viscosity vs shear strain rate) of the designated STF samples is selected from the database or determined experimentally.

4) Based on prepared STF sample/ selected from the database, ballistic performance of the multi-layer either we can confirm/select number of layers of STF treated fabric system from Table 8-12.
5) If the type of material of fabric, and STF sample will be different from the designated attributes of the armour system then the design will be governed by combination of said constituent followed by numerical analysis using methodology mentioned in Chapter 6 for STF impregnated fabric system.
6) Based on the numerical analysis the constituents of body armour such as type of fabric layer, Type of STF sample, will be selected.
7) Further, to synthesis the STF impregnated fabric system apply the STF on the Kevlar layers uniformly throughout. The application of STF should be such that the Kevlar fibres are surface saturated.
8) The Kevlar layers are to be winded using the double winder as to keep the yarn fibers intact in tension from all four sides.
9) Make sure that the edges of the fibers are secured with a help of selvage.

An extra protective layer of a water-resistant material is provided over the SURAKSHA A configuration to protect it from extreme weather conditions and water.

8.3.2 Guidelines for SURAKSHA B

1) Define the level of bullet proof armour as per user requirement and the standard followed (NIJ/ UL 752).
2) Based on this, select the number of bubble wrap configuration layers, the type of STF and its percentage on the basis of availability.
3) Prepare the STF as per the level of armour protection following the methodology discussed in Chapter 5 . The rheological data (a curve of dynamic viscosity vs shear strain rate) of the designated STF samples is selected from the database or determined experimentally.
4) Based on prepared STF sample/ selected from the database, the ballistic performance of the multi-layer either we can confirm/select the number of layers of STF encapsulated bubble wrap configuration system from Table 8-13.
5) If the type of bubble wrap configuration, material of bubble wrap, and STF sample will be different from the designated attributes of the armour system then the design will be governed by combination of said constituent followed by numerical analysis using

methodology mentioned in Chapter 7 for STF encapsulated bubble wrap configuration respectively.

6) Based on the numerical analysis the constituents of body armour such as number of required layers, type of STF sample, and bubble wrap configuration including its material and geometric shape will be selected.
7) An extra protective layer of a water-resistant material is provided over the bubble wrap jacket to protect it from extreme weather conditions and water.

Additional points to be kept in mind:

- The jacket should not exceed 5kg in total as our aim to target light weight bullet proof armour.
- A prior testing is required for the level of armour to be targeted and one level above it. No penetration should be there in the level that is targeted and no penetration in one shot of the higher impact level.

Testing standards should be followed as per the standards followed. The aim of development of design guidelines for the development of Smart thickening fluid based Ultra Resistant Adaptive Kinematic Soft Human Armour (SURAKSHA A and B) is achieved in this research. The detailed configuration is developed as per standard ballistic scenarios.

9 Conclusions, Limitations, and Future work

This Chapter details the salient finding of the present research and provide new ideas for the future work. In order to develop lightweight, flexible ballistic body armour Shear thickening based body armour has been investigated under ballistic impact from projectiles conforming to NIJ standards. The performance of the proposed ballistic armour SURAKSHA consists of multi-layer STF impregnated fabric and STF encapsulated in bubble wrap have been studied. The ballistic performance of neat fabric is evaluated and validated through experimental results. The mechanical properties of fabric fiber are taken from open literature. The validated model considers the following parameter viz. yarn density, yarn crimp of plain weave fabric, inter-yarn friction. These parameters are important to characterize the ballistic performance of the fabric. The present model considers yarn as continuum body by neglecting filament and fiber level modelling. Due to this, the accuracy of the model decreases but the deviation in the results are within the limit of 5 %. Another important parameter is inter-yarn friction which is incorporated through contact models. The inter-yarn friction is implemented using Mohr-Coulomb friction model. The coefficients of inter-yarn fabric for neat fabric is taken from the open literature. During ballistic impact, the idealization of boundary condition is very difficult and hence for the simplicity, the two-side fixed and two opposite side free boundary condition is adopted in the present model of neat fabric. Ballistic impact is a localized phenomenon and hence the role of boundary condition is minimal. However, the effect of boundary condition on the ballistic performance of the fabric is not nullified. The ballistic performance of simulated neat fabric is in good agreement with the experimental results for initial projectile velocity which is varying from 82 to 389 m/s. It is observed from the simulations done that STF significantly improves the ballistic performance of the STF treated fabric.

For evaluation of the ballistic performance of the STF treated fabric, friction-based model is used and extended to study the efficacy of the model for STF treated fabric configuration. The research found that there are limitations in the friction-based models. The friction-based model predicts accurate results for mid-range of the projectile velocities. But, it fails to produce accurate results at lower and higher projectile velocities. Such discrepancies are due to modelling approach of STF using friction-based model. The friction-based model enhances the inter-yarn coefficient of friction from neat state to STF treated state of the fabric. Generally, literature reports that the coefficient of friction is predicted using semi-empirical

approach for neat as well as STF treated fabric. The steps in semi-empirical approach are as follows: (1) experimental establishment of force-displacement relationship using pull-out experiments and subsequently, (2) numerical validation of pullout test by changing coefficient of friction. The force-displacement relation is established at a specific pull-out speed and hence the co-efficient of friction will be valid for that specific speed only. But, ballistic impact is having varying speed of the projectile. Moreover, STF shows rheological properties depending upon the shear strain rate and hence due to varying speed of the projectile the STF mechanism will be also different. These limitations are well discussed in appropriate Chapters in this research.

The current study shows that the ballistic performance of the fabric will be optimum in terms of residual velocity and kinetic energy of the projectile at a critical coefficient. This observation is highlighting the issue with friction-based models as they fail to capture the effect of STF and hence they cannot be used to study the exact behavior of STF impregnated with fabric. Moreover, many researchers have taken very high coefficients of friction which will predict at par ballistic performance of STF treated fabric but they certainly fail to capture the behavior and effect of STF on the fabric. In view of these limitations, a novel MM-ALE method to simulate ballistic performance of the STF impregnated fabric has been proposed and implemented. In MM-ALE method, STF, fabric and the interaction of STF and fabric is modelled. The STF is modelled using ALE formulation while fabric is modelled as Lagrangian formulation. The coupling between STF and fabric is provided using CONSTRAINED_LAGRANGE_IN_SOLID by defining coupling direction as normal compression only. The interface between STF and fabric is modelled as no slip wall condition and it is achieved by defining very high friction value between them. The variation of pressure due to change in volume is modelled using EOS_LINEAR_POLYNOMIAL. The current study only considers volumetric change in the STF upon application of normal loading and hence only bulk modulus is defined in the EOS card. The MM-ALE based model produces results which is well in agreement with the experimental results for wide range of projectile velocity. The developed STF model is found promising to replicate the STF impregnation of fabric. The developed MM-ALE based model is used to predict the ballistic response of STF treated multi-layer fabric system. The ballistic response is evaluation for projectile conforming to NIJ standards and having used to rate armour system as BR I, BR IIA, BR II, and BR IIIA.

The developed STF model has been implemented to study the impact behavior of confined STF encapsulated in bubble made of polyethylene under projectile rating of BR I, BR

IIA, BR II, and BR IIIA. The new proposed configuration is based on confinement of shear thickening fluid within negligible strength but highly flexible made of material Low Density Poly-Ethylene (LDPE). The present investigation considers only uniform placement of cylindrical shape bubbles. The bubble wrap configuration is filled with shear thickening fluid. From the results, it is concluded that the variation in the type of the STF and its composition hardly effects the results of the energy absorption. It only varies with the density of the bubble wrap with the STF and the impact velocity of the projectile. There is an increasing trend in all the cases of energy absorption with the density of the bubble wrap capsule as expected. This is due to the fact that the more amount of STF will result in less amount of area, thereby having more energy absorption capacity in that particular area. The results pave way for the utilization of STF as an efficient energy absorbing material in the field of blasts and ballistic impact to mitigate the shockwaves.

The following were achieved in this thesis:

- A novel MM-ALE method to simulate ballistic performance of the STF impregnated fabric and such system has been developed. The MM-ALE approach of modelling can be used to simulate the STF effect using rheological data.
- A numerical framework based on modelling of shear thickening fluid is developed to analyses the ballistic behavior of STF impregnated fabric under impact having ballistic rating conforming to NIJ standards.
- A numerical framework is developed to analyses the ballistic performance of STF encapsulated in the bubble wrap under impact having ballistic rating conforming to NIJ standards.
- A design methodology and development guidelines are formulated to develop lightweight and flexible armour.
- **The aim of development of design guidelines for the development of Smart thickening fluid based Ultra Resistant Adaptive Kinematic Soft Human Armour (SURAKSHA A and B) is achieved in this research. The detailed configuration is developed as per standard ballistic scenarios.**

9.1 Limitations

The current study presents the design and development methodologies for soft armour made of high-performance fabric and bubble wraps. The study basically presents a numerical

framework which may be used to design and develop soft body armour. The numerical modelling involves modelling of fabric, bubble wrap, STF, and coupled models with other constituent material. In the entire modelling the base model of the fabric, model of yarn is continuum based 4-noded shell elements. Further, the strain rate independent material model is used and there is probability that the same model will be not valid for low and very high velocity of the projectile. Further, coupled STF-fabric model is based on MM-ALE technique. Since MM-ALE based approach uses empirical rheometric data, the model may produce inaccurate results at very high projectile velocity. This will be due to limitations of the rheometer which will be not able to characterize STF at very shear strain rate. Furthermore, the accuracy of MM-ALE based STF treated fabric depend upon interaction of STF and neat fabric as the adopted fabric model is at yarn level it is not able to capture the effect of STF on filament of the yarn and may produce inaccurate results. The current study mainly focuses on two boundary conditions viz. two side fixed and clamped boundary condition, there will be always scope for the change in prediction of the ballistic behavior of the fabric depending upon different boundary conditions and hence this study should be extended on other boundary conditions.

9.2 Future work

Based on these findings, the following works may be carried out in the future:

- The statistical performance optimization studies can be carried using developed STF model to determine the ballistic limit of armour.
- Study the effect of confinement on STF on numerous types of micro-configurations of bubble on its ballistic performance.
- Study the effect of STF impregnation of different types of architecture of fabric using MM-ALE approach.
- Study the effect of carbon Nano-tube and graphene fillers on rheological, ballistic impact, and electrical properties of shear thickening fluid in the development of smart ballistic human armour.
- Study the ballistic impact performance of STF impregnated into stochastic auxetic foam structures.

Based on above proposed futuristic work, the findings of the study could be applied to design and development of prototype of smart and intelligent ballistic body armour system like the shown armour system in Figure 9-1.

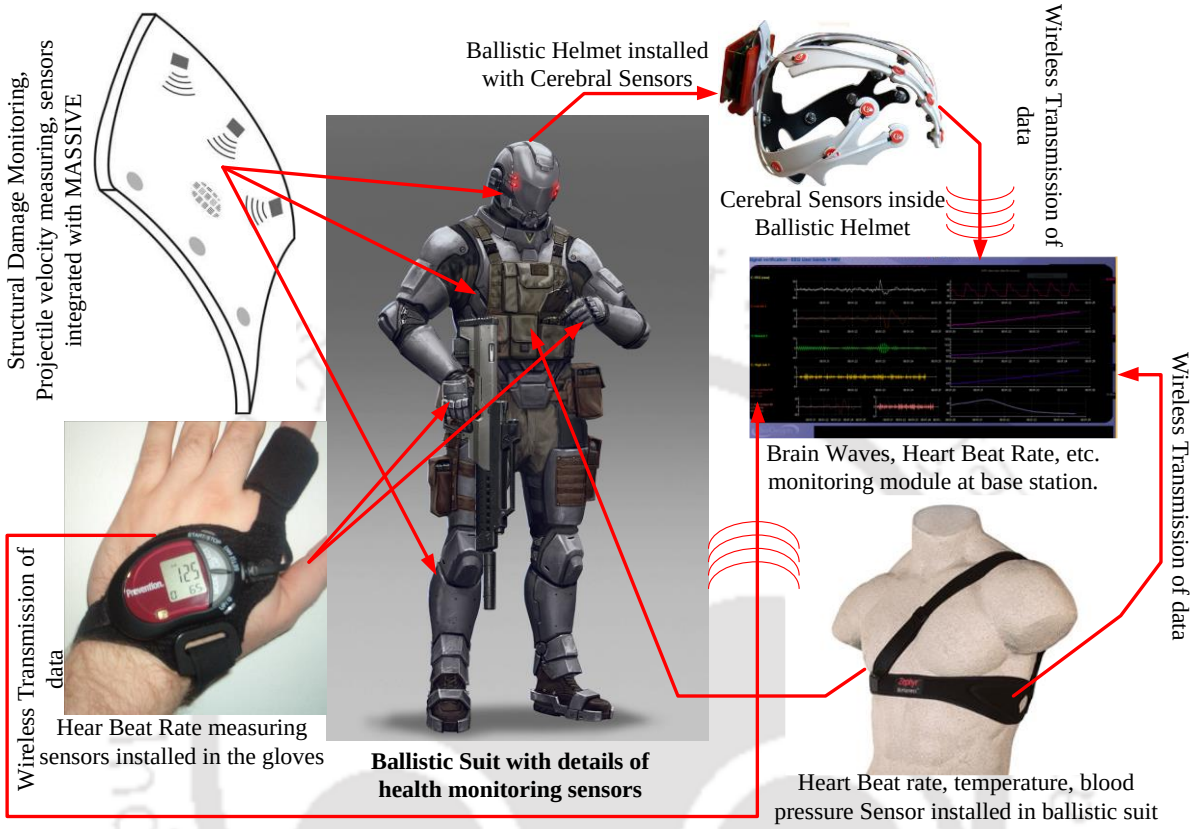

Figure 9-1 Futuristic smart and intelligent ballistic body armour

REFERENCES

Ågårdh, L. (1997). Fe-Modeling of Fibre Reinforced Concrete Slabs Subjected to Blast Load. *Le Journal de Physique IV*, *07*(C3), C3-723. https://doi.org/10.1051/JP4:19973123

Anderson, K. J. (1992). Bulletproof Materials. *MRS Bulletin*, *17*(4), 72–75. https://doi.org/10.1557/s0883769400041166

Aradian, A., & Cates, M. E. (2005). Instability and spatiotemporal rheochaos in a shear-thickening fluid model. *EPL (Europhysics Letters)*, *70*(3), 397. https://doi.org/10.1209/EPL/I2005-10011-9

Arora, S., Laha, A., Majumdar, A., & Butola, B. S. (2017). Prediction of rheology of shear thickening fluids using phenomenological and artificial neural network models. *Korea-Australia Rheology Journal 2017*, *29*(3), 185–193. https://doi.org/10.1007/S13367-017-0019-X

Arora, S., Majumdar, A., & Butola, B. S. (2020). Soft armour design by angular stacking of shear thickening fluid impregnated high-performance fabrics for quasi-isotropic ballistic response. *Composite Structures*, *233*(November 2019), 111720. https://doi.org/10.1016/j.compstruct.2019.111720

Arriaga, A., Pagaldai, R., Zaldua, A. M., Chrysostomou, A., & O'Brien, M. (2010). Impact testing and simulation of a polypropylene component. Correlation with strain rate sensitive constitutive models in ANSYS and LS-DYNA. *Polymer Testing*, *29*(2), 170–180. https://doi.org/10.1016/J.POLYMERTESTING.2009.10.007

Bajaj, P., & Sriram. (1997). Ballistic protective clothing: An overview. *Indian Journal of Fibre & Textile Research*, *22*, 274–291. http://nopr.niscair.res.in/handle/123456789/19236

Barauskas, R., & Abraitienė, A. (2007). Computational analysis of impact of a bullet against the multilayer fabrics in LS-DYNA. *International Journal of Impact Engineering*, *34*(7), 1286–1305. https://doi.org/10.1016/j.ijimpeng.2006.06.002

Bazhenov, S. (1997). Dissipation of energy by bulletproof aramid fabric. *Journal of Materials Science*, *32*(15), 4167–4173. https://doi.org/10.1023/A:1018674528993

Bisagni, C., & Pigazzini, M. S. (2018). Modelling strategies for numerical simulation of aircraft ditching. *International Journal of Crashworthiness*, *23*(4), 377–394. https://doi.org/10.1080/13588265.2017.1328957

Blanc, G. Le, Adoum, M., & Users, V. L. (2005). External blast load on structures–Empirical approach. *5th European LS-DYNA Users Conference*, 12. https://www.dynalook.com/conferences/european-conf-2005/Leblanc.pdf

Boersma, W. H., Laven, J., & Stein, H. N. (1992). Viscoelastic properties of concentrated shear-thickening dispersions. *Journal of Colloid and Interface Science*, *149*(1), 10–22. https://doi.org/10.1016/0021-9797(92)90385-Y

Bridgens, B. N., & Gosling, P. D. (2008). A Predictive Fabric Model for Membrane Structure Design. In E. Oñate & B. Kröplin (Eds.), *Textile Composites and Inflatable Structures II* (pp. 35–50). Springer Netherlands. https://doi.org/10.1007/978-1-4020-6856-0_3

Briscoe, B. J., & Motamedi, F. (1990). Role of Interfacial Friction and Lubrication in Yarn and Fabric Mechanics. *Textile Research Journal*, *60*(12), 697–708. https://doi.org/10.1177/004051759006001201

Briscoe, B. J., & Motamedi, F. (1992). The ballistic impact characteristics of aramid fabrics: The influence of interface friction. *Wear*, *158*(1–2), 229–247. https://doi.org/10.1016/0043-1648(92)90041-6

Cannon, L. (2001). Behind Armour Blunt Trauma - an emerging problem. *Journal of the Royal Army Medical Corps*, *147*(1), 87 LP – 96. https://doi.org/10.1136/jramc-147-01-09

Cao, S., Chen, Q., Wang, Y., Xuan, S., Jiang, W., & Gong, X. (2017). High strain-rate dynamic mechanical properties of Kevlar fabrics impregnated with shear thickening fluid. *Composites Part A: Applied Science and Manufacturing*, *100*, 161–169. https://doi.org/10.1016/J.COMPOSITESA.2017.04.015

Challenge. (2020, February 6). *HIGHLY RECYCLABLE CONTENT BUBBLE WRAP COMES TO CHALLENGE*. https://challengepackaging.co.uk/highly-recyclable-content-bubble-wrap-comes-to-challenge/

Chatla, P. (2012). *LS-Dyna for Crashworthiness of Composite Structures*.

Cheng, M., Chen, W., & Weerasooriya, T. (2005a). Mechanical properties of Kevlar® KM2 single fiber. *Journal of Engineering Materials and Technology, Transactions of the ASME*, *127*(2), 197–203. https://doi.org/10.1115/1.1857937

Cheng, M., Chen, W., & Weerasooriya, T. (2005b). Mechanical Properties of Kevlar® KM2 Single Fiber. *Journal of Engineering Materials and Technology*, *127*(2), 197.

https://doi.org/10.1115/1.1857937

Chu, T. L., Ha-Minh, C., & Imad, A. (2016). A numerical investigation of the influence of yarn mechanical and physical properties on the ballistic impact behavior of a Kevlar KM2® woven fabric. *Composites Part B: Engineering*, *95*, 144–154. https://doi.org/10.1016/J.COMPOSITESB.2016.03.018

Clements, F. E., & Mahfuz, H. (2007). ENHANCING THE STAB RESISTANCE OF FLEXIBLE BODY ARMOR USING FUNCTIONALIZED SIO 2 NANOPARTICLES. *16TH INTERNATIONAL CONFERENCE ON COMPOSITE MATERIALS*, 1–11.

Crouch, I. G. (2019). Body armour – New materials, new systems. *Defence Technology*, *15*(3), 241–253. https://doi.org/10.1016/J.DT.2019.02.002

Cunnif, P. M. (1992). *An Analysis of the System Effects in Woven Fabrics Under Ballistic Impact*. https://apps.dtic.mil/dtic/tr/fulltext/u2/a273891.pdf

Cunniff, P. (1999). Dimensionless parameters for optimization of textile-based body armor systems. *Proceedings of the 18th International Symposium on Ballistics*, 1303–1310.

Cunniff, P. M., & Auerbach, M. A. (2002). High performance "M5" fiber for ballistics/structural composites. *23rd. Army Science Conference*, 1–8. http://scholar.google.com/scholar?hl=en&btnG=Search&q=intitle:HIGH+PERFORMANCE+?+M5+?+FIBER+FOR+BALLISTICS+/+STRUCTURAL+COMPOSITES#0

David, N. V., Gao, X.-L., & Zheng, J. Q. (2009). Ballistic Resistant Body Armor: Contemporary and Prospective Materials and Related Protection Mechanisms. *Applied Mechanics Reviews*, *62*(5), 050802. https://doi.org/10.1115/1.3124644

Dong, Z., & Sun, C. T. (2009). Testing and modeling of yarn pull-out in plain woven Kevlar fabrics. *Composites Part A: Applied Science and Manufacturing*, *40*(12), 1863–1869. https://doi.org/10.1016/j.compositesa.2009.04.019

Duan, Y., Keefe, M., Bogetti, T. A., & Cheeseman, B. A. (2005a). Modeling friction effects on the ballistic impact behavior of a single-ply high-strength fabric. *International Journal of Impact Engineering*, *31*(8), 996–1012. https://doi.org/10.1016/j.ijimpeng.2004.06.008

Duan, Y., Keefe, M., Bogetti, T. A., & Cheeseman, B. A. (2005b). Modeling the role of friction during ballistic impact of a high-strength plain-weave fabric. *Composite Structures*, *68*(3), 331–337. https://doi.org/10.1016/j.compstruct.2004.03.026

Duan, Y., Keefe, M., Bogetti, T. A., Cheeseman, B. A., & Powers, B. (2006). A numerical investigation of the influence of friction on energy absorption by a high-strength fabric subjected to ballistic impact. *International Journal of Impact Engineering*, *32*(8), 1299–1312. https://doi.org/10.1016/j.ijimpeng.2004.11.005

Duan, Y., Keefe, M., Bogetti, T. A., & Powers, B. (2006). Finite element modeling of transverse impact on a ballistic fabric. *International Journal of Mechanical Sciences*, *48*(1), 33–43. https://doi.org/10.1016/j.ijmecsci.2005.09.007

Fahool, M., & Sabet, A. R. (2016). Parametric study of energy absorption mechanism in Twaron fabric impregnated with a shear thickening fluid. *International Journal of Impact Engineering*, *90*, 61–71. https://doi.org/10.1016/j.ijimpeng.2015.11.016

Franz, U., & Graf, O. (n.d.). *Accurate and Detailed LS-DYNA FE Models of the US-and EUROSID: A Review of the German FAT Project*.

Funk, N., Vera, M., Szewciw, L. J., Barthelat, F., Stoykovich, M. P., & Vernerey, F. J. (2015). Bioinspired Fabrication and Characterization of a Synthetic Fish Skin for the Protection of Soft Materials. *ACS Applied Materials & Interfaces*, *7*(10), 5972–5983. https://doi.org/10.1021/acsami.5b00258

Ge, J., Tan, Z., Li, W., & Zhang, H. (2017). The rheological properties of shear thickening fluid reinforced with SiC nanowires. *Results in Physics*, *7*, 3369–3372. https://doi.org/10.1016/j.rinp.2017.08.065

Gill, V. (2010). *Liquid armour "can stop bullets" - BBC News*. Science & Environment. https://www.bbc.com/news/10569761

Grujicic, M., Bell, W. C., Arakere, G., He, T., Xie, X., & Cheeseman, B. A. (2010). Development of a Meso-Scale Material Model for Ballistic Fabric and Its Use in Flexible-Armor Protection Systems. *Journal of Materials Engineering and Performance*, *19*(1), 22–39. https://doi.org/10.1007/s11665-009-9419-5

Grujicic, M., Hariharan, A., Pandurangan, B., Yen, C.-F., Cheeseman, B. A., Wang, Y., Miao, Y., & Zheng, J. Q. (2012). Fiber-Level Modeling of Dynamic Strength of Kevlar® KM2 Ballistic Fabric. *Journal of Materials Engineering and Performance*, *21*(7), 1107–1119. https://doi.org/10.1007/s11665-011-0006-1

Gürgen, S. (2020a). Numerical modeling of fabrics treated with multi-phase shear thickening

fluids under high velocity impacts. *Thin-Walled Structures*, *148*, 106573. https://doi.org/10.1016/J.TWS.2019.106573

Gürgen, S. (2020b). Numerical modeling of fabrics treated with multi-phase shear thickening fluids under high velocity impacts. *Thin-Walled Structures*, *148*(November 2019), 106573. https://doi.org/10.1016/j.tws.2019.106573

Gürgen, S., & Kuşhan, M. C. (2017). The ballistic performance of aramid based fabrics impregnated with multi-phase shear thickening fluids. *Polymer Testing*, *64*, 296–306. https://doi.org/10.1016/J.POLYMERTESTING.2017.11.003

Gürgen, S., Kuşhan, M. C., & Li, W. (2017). Shear thickening fluids in protective applications: A review. *Progress in Polymer Science*, *75*, 48–72. https://doi.org/10.1016/j.progpolymsci.2017.07.003

Gürgen, S., & Sofuoğlu, M. A. (2020). Integration of shear thickening fluid into cutting tools for improved turning operations. *Journal of Manufacturing Processes*, *56*, 1146–1154. https://doi.org/10.1016/J.JMAPRO.2020.06.012

Ha-Minh, C., Imad, A., Boussu, F., Kanit, T., & Crépin, D. (2012). Numerical study on the effects of yarn mechanical transverse properties on the ballistic impact behaviour of textile fabric. *The Journal of Strain Analysis for Engineering Design*, *47*(7), 524–534. https://doi.org/10.1177/0309324712457901

Hasanzadeh, M., Mottaghitalab, V., Rezaei, M., & Babaei, H. (2017a). Numerical and experimental investigations into the response of STF-treated fabric composites undergoing ballistic impact. *Thin-Walled Structures*, *119*, 700–706. https://doi.org/10.1016/J.TWS.2017.07.020

Hasanzadeh, M., Mottaghitalab, V., Rezaei, M., & Babaei, H. (2017b). Numerical and experimental investigations into the response of STF-treated fabric composites undergoing ballistic impact. *Thin-Walled Structures*, *119*, 700–706. https://doi.org/10.1016/J.TWS.2017.07.020

Hassan, T. A., Rangari, V. K., & Jeelani, S. (2010). Synthesis, processing and characterization of shear thickening fluid (STF) impregnated fabric composites. *Materials Science and Engineering A*, *527*(12), 2892–2899. https://doi.org/10.1016/j.msea.2010.01.018

Hazell, P. J. (2016). *Armour: materials, theory, and design*.

http://search.ebscohost.com/login.aspx?direct=true&scope=site&db=nlebk&db=nlabk&AN=1022192

Hogg, P. J. (2006). Composites in armor. *Science (New York, N.Y.)*, *314*(5802), 1100–1101. https://doi.org/10.1126/science.1131118

Horsfall, I. (2012). Key issues in body armour: threats, materials and design. *Advances in Military Textiles and Personal Equipment*, 3–20. https://doi.org/10.1533/9780857095572.1.3

Huo, J. L., Sun, F., Li, T. T., Shiu, B. C., Lou, C. W., & Lin, J. H. (2020). Preparation and properties of shear thickening fluid (STF) capsule filled graded buffer composites. *Journal of Materials Research and Technology*, *9*(5), 10982–10990. https://doi.org/10.1016/j.jmrt.2020.07.106

Ibrahim, Y. Y. H. (2012). *Auxetic Polyurethane Foam (Fabrication, Properties and Applications)*. https://inis.iaea.org/collection/NCLCollectionStore/_Public/46/131/46131661.pdf?r=1&r=1

Ivanov, I., & Tabiei, A. (2004). Loosely woven fabric model with viscoelastic crimped fibres for ballistic impact simulations. *International Journal for Numerical Methods in Engineering*, *61*(10), 1565–1583. https://doi.org/10.1002/nme.1113

Ivanov, I., & Tabiet, A. (2002). Flexible woven fabric micromechanical material model with fiber reorientation. *Mechanics of Advanced Materials and Structures*, *9*(1), 37–51. https://doi.org/10.1080/153764902317224860

Jacobs, M. J. N., & Van Dingenen, J. L. J. (2001). Ballistic protection mechanisms in personal armour. *Journal of Materials Science*, *36*(13), 3137–3142. https://doi.org/10.1023/A:1017922000090

Joselin, R., & Wilson, W. J. (2014). Investigation on impact strength properties of kevlar fabric using different shear thickening fluid composition. *Defence Science Journal*, *64*(3), 236–243. https://doi.org/10.14429/dsj.64.7322

Khodadadi, A., Liaghat, G. H., Sabet, A. R., Hadavinia, H., Aboutorabi, A., Razmkhah, O., Akbari, M., & Tahmasebi, M. (2017). Experimental and numerical analysis of penetration into Kevlar fabric impregnated with shear thickening fluid:

Https://Doi.Org/10.1177/0892705717704485, *31*(3), 392–407. https://doi.org/10.1177/0892705717704485

Khodadadi, A., Liaghat, G. H., Sabet, A. R., Hadavinia, H., Aboutorabi, A., Razmkhah, O., Akbari, M., & Tahmasebi, M. (2018). Experimental and numerical analysis of penetration into Kevlar fabric impregnated with shear thickening fluid. *Journal of Thermoplastic Composite Materials*, *31*(3), 392–407. https://doi.org/10.1177/0892705717704485

Khodadadi, A., Liaghat, G., Vahid, S., Sabet, A. R., & Hadavinia, H. (2019). Ballistic performance of Kevlar fabric impregnated with nanosilica/PEG shear thickening fluid. *Composites Part B: Engineering*, *162*, 643–652. https://doi.org/10.1016/J.COMPOSITESB.2018.12.121

Kirkwood, J. E., Kirkwood, K. M., Lee, Y. S., Ronald G. Egres, J. R., Wagner, N. J., & Wetzel, E. D. (2004). Yarn Pull-Out as a Mechanism for Dissipating Ballistic Impact Energy in Kevlar® KM-2 Fabric: Part II: Predicting Ballistic Performance. *Textile Research Journal*, *74*(11), 939–948. https://doi.org/10.1177/004051750407401101

Kirkwood, K. M., Kirkwood, J. E., Lee, Y. S., Egres, R. G., Wagner, N. J., & Wetzel, E. D. (2004). Yarn Pull-Out as a Mechanism for Dissipating Ballistic Impact Energy in Kevlar® KM-2 Fabric: Part I: Quasi-Static Characterization of Yarn Pull-Out. *Textile Research Journal*, *74*(10), 920–928. https://doi.org/10.1177/004051750407401012

Klöppel, T., Liebold, C., & Haufe, A. (2013). *Recent developments for process simulations of composite structures in LS-DYNA.*

Laha, A., & Majumdar, A. (2016). Interactive effects of p-aramid fabric structure and shear thickening fluid on impact resistance performance of soft armor materials. *Materials & Design*, *89*, 286–293. https://doi.org/10.1016/J.MATDES.2015.09.077

Lane, R. A. (2005). High Performance Fibers for Personnel and Vehicle Armor Systems. *Advanced Materials and Processes Technology Information Analysis Center (AMPTIAC)*, 3–9. http://amptiac.alionscience.com/quarterlyhttp://amptiac.alionscience.com/quarterly

Larsen, B., Netto, K., & Aisbett, B. (2011). The Effect of Body Armor on Performance, Thermal Stress, and Exertion: A Critical Review. *Military Medicine*, *176*(11), 1265–1273. https://doi.org/10.7205/MILMED-D-10-00470

Lee, B.-W., & Kim, C.-G. (2012). Computational analysis of shear thickening fluid

impregnated fabrics subjected to ballistic impacts. *Advanced Composite Materials*, *21*(2), 177–192. https://doi.org/10.1080/09243046.2012.690298

Lee, B.-W., Kim, I., & Kim, C.-G. (2009). The influence of the particle size of silica on the ballistic performance of fabrics impregnated with silica colloidal suspension. *Journal of Composite Materials*, *43*(23), 2679–2698. https://doi.org/10.1177/0021998309345292

Lee, B. W., & Kim, C. G. (2012). Computational analysis of shear thickening fluid impregnated fabrics subjected to ballistic impacts. *Http://Dx.Doi.Org/10.1080/09243046.2012.690298*, *21*(2), 177–192. https://doi.org/10.1080/09243046.2012.690298

Lee, Y. S., Wetzel, E. D., & Wagner, N. J. (2003). The ballistic impact characteristics of Kevlar® woven fabrics impregnated with a colloidal shear thickening fluid. *Journal of Materials Science*, *38*(13), 2825–2833. https://doi.org/10.1023/A:1024424200221

Liu, P., Zhu, D., Yao, Y., Wang, J., & Bui, T. Q. (2016). Numerical simulation of ballistic impact behavior of bio-inspired scale-like protection system. *Materials & Design*, *99*, 201–210. https://doi.org/10.1016/J.MATDES.2016.03.040

Liu, X., Huo, J. L., Li, T. T., Peng, H. K., Lin, J. H., & Lou, C. W. (2019). Investigation of the shear thickening fluid encapsulation in an orifice coagulation bath. *Polymers*, *11*(3), 1–13. https://doi.org/10.3390/polym11030519

Majumdar, A., Butola, B. S., & Srivastava, A. (2013). Optimal designing of soft body armour materials using shear thickening fluid. *Materials & Design*, *46*, 191–198. https://doi.org/10.1016/J.MATDES.2012.10.018

Matthew, C. (2016). *Army Plans to Field New Protective Vest, Armored Shirt in 2019*. Military.Com. https://www.military.com/daily-news/2016/02/11/army-plans-to-field-new-protective-vest-armored-shirt-in-2019.html/amp

Meng, J., Zhang, P., & Wang, S. (2016). Recent progress of abrasion-resistant materials: learning from nature. *Chemical Society Reviews*, *45*(2), 237–251. https://doi.org/10.1039/C5CS00459D

Messiry, M. El. (2014). Investigation of Puncture Behaviour of Flexible Silk Fabric Composites for Soft Body Armour. *Fibres and Textiles in Eastern Europe*, *5*(107), 71–76.

Mirrahimi, A. H., Hasanzadeh, M., Mottaghitalab, V., & Sharma, P. (2017). Numerical Modelling of Ballistic Impact on HMPP Woven Fabric Impregnated with Shear-thickening Fluids. *Procedia Engineering*, *173*, 73–76. https://doi.org/10.1016/J.PROENG.2016.12.031

Montanarelli, N., Hawkins, C. E., Goldfarb, M. A., & Ciurej, T. F. (1973). *Protective Garments for Public Officials*. https://apps.dtic.mil/sti/citations/ADA089163

Nayak, N., Banerjee, A., & Sivaraman, P. (2013). Ballistic impact response of ceramic-faced aramid laminated composites against 7.62 mm armour piercing projectiles. *Defence Science Journal*, *63*(4), 369–375. https://doi.org/10.14429/dsj.63.2616

NIJ 0108.01. (1985). *Ballistic Resistant Protective Materials*.

NIJ Selection and Application Guide-0101.06. (2014). *Selection & Application Guide 0101.06 to Ballistic-Resistant Body Armor*. http://www.ojp.usdoj.gov

NIJ Standard-0101.06. (2008). Ballistic Resistance of Personal Body Armor. In *NIJ Standards* (p. 89). https://doi.org/10.1017/CBO9781107415324.004

Nilakantan, G., & Gillespie, J. W. (2012). Ballistic impact modeling of woven fabrics considering yarn strength, friction, projectile impact location, and fabric boundary condition effects. *Composite Structures*, *94*(12), 3624–3634. https://doi.org/10.1016/j.compstruct.2012.05.030

Nilakantan, G., Keefe, M., Bogetti, T. A., Adkinson, R., & Gillespie, J. W. (2010). On the finite element analysis of woven fabric impact using multiscale modeling techniques. *International Journal of Solids and Structures*, *47*(17), 2300–2315. https://doi.org/10.1016/J.IJSOLSTR.2010.04.029

Nilakantan, G., Keefe, M., Bogetti, T. A., & Gillespie, J. W. (2010). Multiscale modeling of the impact of textile fabrics based on hybrid element analysis. *International Journal of Impact Engineering*, *37*(10), 1056–1071. https://doi.org/10.1016/j.ijimpeng.2010.04.007

Nilakantan, G., Wetzel, E. D., Bogetti, T. A., & Gillespie, J. W. (2013). A deterministic finite element analysis of the effects of projectile characteristics on the impact response of fully clamped flexible woven fabrics. *Composite Structures*, *95*, 191–201. https://doi.org/10.1016/J.COMPSTRUCT.2012.07.023

O'Donnell, R. G. (1992). *Calculation of the Energy of Elastic Deformation of Kevlar Backing*

Plates for Ceramic Armours. https://apps.dtic.mil/sti/citations/ADA250129

Ortiz, C., & Boyce, M. C. (2008). Bioinspired Structural Materials. *Science*, *319*(5866), 1053–1054. https://doi.org/10.1126/science.1154295

Park, Y., Kim, Y., Baluch, A. H., & Kim, C. G. (2015a). Numerical simulation and empirical comparison of the high velocity impact of STF impregnated Kevlar fabric using friction effects. *Composite Structures*, *125*, 520–529. https://doi.org/10.1016/j.compstruct.2015.02.041

Park, Y., Kim, Y. H., Baluch, A. H., & Kim, C. G. (2015b). Numerical simulation and empirical comparison of the high velocity impact of STF impregnated Kevlar fabric using friction effects. *Composite Structures*, *125*, 520–529. https://doi.org/10.1016/J.COMPSTRUCT.2015.02.041

Polanco, M., Kellas, S., & Jackson, K. (n.d.). *Evaluation of Material Models within LS-DYNA ® for a Kevlar/Epoxy Composite Honeycomb*.

Prabhu, T. A., & Singh, A. (2021). Effect of carrier fluid and particle size distribution on the rheology of shear thickening suspensions. *Rheologica Acta*, *60*(2–3), 107–118. https://doi.org/10.1007/s00397-021-01257-5

Priyanka, P., Dixit, A., & Mali, H. S. (2019). High strength Kevlar fiber reinforced advanced textile composites. *Iranian Polymer Journal 2019 28:7*, *28*(7), 621–638. https://doi.org/10.1007/S13726-019-00721-7

Ramadhan, A. A., Talib, A. R. A., Rafie, A. S. M., & Zahari, R. (2013). High velocity impact response of Kevlar-29/epoxy and 6061-T6 aluminum laminated panels. *Materials & Design*, *43*, 307–321. https://doi.org/10.1016/J.MATDES.2012.06.034

Rao, M. P., Duan, Y., Keefe, M., Powers, B. M., & Bogetti, T. A. (2009). Modeling the effects of yarn material properties and friction on the ballistic impact of a plain-weave fabric. *Composite Structures*, *89*(4), 556–566. https://doi.org/10.1016/J.COMPSTRUCT.2008.11.012

Ren, X., Das, R., Tran, P., Ngo, T. D., & Xie, Y. M. (2018). Auxetic metamaterials and structures: a review. *Smart Materials and Structures*, *27*(2), 023001. https://doi.org/10.1088/1361-665X/aaa61c

Rizzo, F., Pinto, F., & Meo, M. (2020). Investigation of Silica-Based Shear Thickening Fluid

in Enhancing Composite Impact Resistance. *Applied Composite Materials*, *27*(3), 209–229. https://doi.org/10.1007/s10443-020-09805-7

Roylance, D., Chammas, P., Ting, J., Chi, H., & Scott, B. (1995). *Numerical Modeling Of Fabric Impact*.

Sen, S., Jamal M, N. Bin, Shaw, A., & Deb, A. (2019). Numerical investigation of ballistic performance of shear thickening fluid (STF)-Kevlar composite. *International Journal of Mechanical Sciences*, *164*(September), 105174. https://doi.org/10.1016/j.ijmecsci.2019.105174

Souli, M., Sofiane, Y., & Olovsson, L. (2008). ALE and Fluid/Structure Interaction in LS-DYNA. *American Society of Mechanical Engineers, Pressure Vessels and Piping Division (Publication) PVP*, *485*(PART 1), 181–187. https://doi.org/10.1115/PVP2004-2870

Srivastava, A., Majumdar, A., & Butola, B. S. (2012). Improving the Impact Resistance of Textile Structures by using Shear Thickening Fluids: A Review. *Critical Reviews in Solid State and Materials Sciences*, *37*, 115–129. https://doi.org/10.1080/10408436.2011.613493

Tan, V. B. C., Tay, T. E., & Teo, W. K. (2005). Strengthening fabric armour with silica colloidal suspensions. *International Journal of Solids and Structures*, *42*(5), 1561–1576. https://doi.org/10.1016/j.ijsolstr.2004.08.013

Tanov, R., & Tabiei, A. (2002). Computationally Efficient Micromechanical Models for Woven Fabric Composite Elastic Moduli. *Journal of Applied Mechanics*, *68*(4), 553. https://doi.org/10.1115/1.1357516

Ternik, P., Marn, J., & Žunič, Z. (2006). Non-Newtonian fluid flow through a planar symmetric expansion: Shear-thickening fluids. *Journal of Non-Newtonian Fluid Mechanics*, *135*(2–3), 136–148. https://doi.org/10.1016/J.JNNFM.2006.01.003

Tian, T., Peng, G., Li, W., Ding, J., & Nakano, M. (2015). Experimental and modelling study of the effect of temperature on shear thickening fluids. *Korea-Australia Rheology Journal*, *27*(1), 17–24. https://doi.org/10.1007/S13367-015-0003-2

TM 5 1300. (1990). *Structures to Resist the Effects of Accidental Explosions*.

TM 5 855. (1986). *Design & analysis of hardened structures to conventional weapons effects*.

Headquarters, Dept. of the Army [Washington, D.C.].

Vesenjak, M., Matthaei, S., Mu¨llerscho¨n, H., & Ren, Z. (2008). Fluid Models in LS-DYNA and Their Interaction With a Structure in Dynamic Simulations. *American Society of Mechanical Engineers, Pressure Vessels and Piping Division (Publication) PVP*, *4*, 199–203. https://doi.org/10.1115/PVP2005-71557

Wagner, N. J., Kalman, D. P., Schein, J. B., Houghton, J. M., Laufer, C. H. N., Wetzel, E. D., & Wagner, N. J. (2007). *Polymer dispersion based shear thickening fluid-fabrics for protective applications Molecular Simulations of the Amorphous Polymers View project Modelling the rheology of complex suspensions View project POLYMER DISPERSION BASED SHEAR THICKENING FLUID-FAB* (pp. 3–7). https://www.researchgate.net/publication/267771188

Wang, L., Du, Z., Fu, W., & Wang, P. (2021). Study of mechanical property of shear thickening fluid (STF) for soft body-armor. *Materials Research Express*, *8*(4). https://doi.org/10.1088/2053-1591/abf76a

Wang, X., Zhang, J., Bao, L., Yang, W., Zhou, F., & Liu, W. (2020). Enhancement of the ballistic performance of aramid fabric with polyurethane and shear thickening fluid. *Materials and Design*, *196*. https://doi.org/10.1016/j.matdes.2020.109015

Wang, Y., Miao, Y., Huang, L., Swenson, D., Yen, C.-F., Yu, J., & Zheng, J. Q. (2016a). Effect of the inter-fiber friction on fiber damage propagation and ballistic limit of 2-D woven fabrics under a fully confined boundary condition. *International Journal of Impact Engineering*, *97*, 66–78. https://doi.org/10.1016/J.IJIMPENG.2016.06.007

Wang, Y., Miao, Y., Huang, L., Swenson, D., Yen, C. F., Yu, J., & Zheng, J. Q. (2016b). Effect of the inter-fiber friction on fiber damage propagation and ballistic limit of 2-D woven fabrics under a fully confined boundary condition. *International Journal of Impact Engineering*, *97*, 66–78. https://doi.org/10.1016/j.ijimpeng.2016.06.007

Wegst, U. G. K., Bai, H., Saiz, E., Tomsia, A. P., & Ritchie, R. O. (2015). Bioinspired structural materials. *Nature Materials*, *14*(1), 23–36. https://doi.org/10.1038/nmat4089

Wei, M., Lin, K., & Guo, Q. (2018). Modeling mechanical properties of a shear thickening fluid damper based on phase transition theory. *EPL (Europhysics Letters)*, *121*(5), 50001. https://doi.org/10.1209/0295-5075/121/50001

Wetzel, E. D., Lee, Y. S., Egres, R. G., Kirkwood, K. M., Kirkwood, J. E., & Wagner, N. J. (2004a). The Effect of Rheological Parameters on the Ballistic Properties of Shear Thickening Fluid (STF)-Kevlar Composites. *AIP Conference Proceedings*, *712*(1), 288–293. https://doi.org/10.1063/1.1766538

Wetzel, E. D., Lee, Y. S., Egres, R. G., Kirkwood, K. M., Kirkwood, J. E., & Wagner, N. J. (2004b). The Effect of Rheological Parameters on the Ballistic Properties of Shear Thickening Fluid (STF)-Kevlar Composites. *AIP Conference Proceedings*, *712*(1), 288–293. https://doi.org/10.1063/1.1766538

Wu, J., Qin, Z., Qu, L., Zhang, H., Deng, F., & Guo, M. (2019). Natural hydrogel in American lobster: A soft armor with high toughness and strength. *Acta Biomaterialia*, *88*, 102–110. https://doi.org/10.1016/J.ACTBIO.2019.01.067

Yan, Q., & Ho, P. (2018). *Introduction to LS-PrePost* (pp. 1–138). LSTC.

Yeh, S.-K., Lin, J.-J., Zhuang, H.-Y., Chen, Y.-C., Chang, H.-C., Zheng, J.-Y., Yang, L.-Y., Lee, K.-C., Chen, Y.-L., & Rwei, S.-P. (2019). Light shear thickening fluid (STF)/Kevlar composites with improved ballistic impact strength. *Journal of Polymer Research*, *26*(6), 155. https://doi.org/10.1007/s10965-019-1811-8

Yen, C.-F. (n.d.). *7 th International LS-DYNA Users Conference Penetration/Explosive BALLISTIC IMPACT MODELING OF COMPOSITE MATERIALS*.

Yurgartis, S. W., Morey, K., & Jortner, J. (1993). Measurement of yarn shape and nesting in plain-weave composites. *Composites Science and Technology*, *46*(1), 39–50. https://doi.org/https://doi.org/10.1016/0266-3538(93)90079-V

Zaera, R., Sánchez-Sáez, S., Pérez-Castellanos, J. L., & Navarro, C. (2000a). Modelling of the adhesive layer in mixed ceramic/metal armours subjected to impact. *Composites Part A: Applied Science and Manufacturing*, *31*(8), 823–833. https://doi.org/10.1016/S1359-835X(00)00027-0

Zaera, R., Sánchez-Sáez, S., Pérez-Castellanos, J. L., & Navarro, C. (2000b). Modelling of the adhesive layer in mixed ceramic/metal armours subjected to impact. *Composites Part A: Applied Science and Manufacturing*, *31*(8), 823–833. https://doi.org/10.1016/S1359-835X(00)00027-0

Zeng, X. S., Shim, V. P. W., & Tan, V. B. C. (2005). Influence of boundary conditions on the

ballistic performance of high-strength fabric targets. *International Journal of Impact Engineering*, *32*(1–4), 631–642. https://doi.org/10.1016/J.IJIMPENG.2005.06.011

Zeng, X. S., Tan, V. B. C., & Shim, V. P. W. (2006). Modelling inter-yarn friction in woven fabric armour. *International Journal for Numerical Methods in Engineering*, *66*(8), 1309–1330. https://doi.org/10.1002/nme.1596

Zhang, D. N., Shangguan, Q. Q., Xie, C. J., & Liu, F. (2015). A modified Johnson–Cook model of dynamic tensile behaviors for 7075-T6 aluminum alloy. *Journal of Alloys and Compounds*, *619*, 186–194. https://doi.org/10.1016/J.JALLCOM.2014.09.002

Zhang, H., Zhang, X., Chen, Q., Li, X., Wang, P., Yang, E. H., Duan, F., Gong, X., Zhang, Z., & Yang, J. (2017). Encapsulation of shear thickening fluid as an easy-to-apply impact-resistant material. *Journal of Materials Chemistry A*, *5*(43), 22472–22479. https://doi.org/10.1039/c7ta04904h

Zhao, Q., He, Y., Yao, H., & Wen, B. (2018). Dynamic performance and mechanical model analysis of a shear thickening fluid damper. *Smart Materials and Structures*, *27*(7), 75021. https://doi.org/10.1088/1361-665X/AAC23F

Zhu, D., Zhang, X., Ou, Y., & Huang, M. (2016). Experimental and numerical study of multi-scale tensile behaviors of Kevlar® 49 fabric: *Http://Dx.Doi.Org/10.1177/0021998316671573*, *51*(17), 2449–2465. https://doi.org/10.1177/0021998316671573

Publications and conferences

- **Kumar S.**, and Sharma H., Performance characterization of bubble wrap encapsulated smart thickening fluid based ultra-Resistant adaptive kinematic human armour (Submitted, International Journal of Impact Engineering, ISSN: 0734-743X)
- **Kumar S.**, Saxena S., and Sharma H., Ballistic performance assessment of smart thickening fluid based ultra-Resistant adaptive kinematic human armour using numerical framework (Submitted, Journal of Composite Structures, ISSN: 0263-8223)
- **Kumar S.**, Saxena S., and Sharma H., Ballistic performance evaluation of the high-performance fabric due to inter-yarn friction (Under review, Journal of Pract. Period. Struct. Des. Constr., ASCE, ISSN (online): 1943-5576)
- **Kumar S.**, Saxena S., and Sharma H., Blast and heavy impact simulating mechanism for blast resistant design and validation of structures (Under review, Journal of Pract. Period. Struct. Des. Constr., ASCE)
- Umesh, R., **Kumar S.**, and Sharma, H. "Progress and Evolution in Fatigue studies of Advanced Composite Materials" **Second ASCE conference on CRSIDE 2020.**
- Umesh, R., **Kumar S.**, and Sharma, H. "Blast Induced Brain Traumatic Injury: Current progress and challenges" **6th national symposium on shock waves 2020**, IIT Madras.
- Jaswanth G., **Kumar S.**, Kumar A., and Sharma H., "Numerical technique for prestressing post-tensioning members subjected to missile impact load," **Proceedings of ICCMS 2019**, IIT Mandi, India
- Jaswanth G., **Kumar S.**, and Sharma H., "Impact testing Facility: BHISM for Performance-based Blast Resistant Design of Reinforced Concrete (RC) Structures," ***Procedia Engineering, IMPLAST 2016*** IIT Delhi.
- **Kumar S.**, and Sharma H., "Development of BHISM for Performance-based Blast Resistant Design of Reinforced Concrete (RC) Structures," **Proceedings of ICCMS 2016**, IIT Bombay, India.

Patents

1) Patent Title: A BLAST SIMULATOR FOR TESTING OF SPECIMENS OF VARIABLE DIMENSIONS

Authors: Hrishikesh Sharma and Suman Kumar, INDIAN INSTITUTE OF TECHNOLOGY, GUWAHATI, India

Indian Patent No. IN201831017926A, Filing Date: 2018-05-12, Publishing Date: 2019-11-15, **International Patent No:** WO2019220302A1, Filing Date: 2019-05-13, Publishing Date: 2019-11-21

2) Patent Title: BAMBOO FOR CONSTRUCTION OF FRANGIBLE STRUCTURES FOR AVIATION INDUSTRY

Authors: Hrishikesh Sharma and Suman Kumar, INDIAN INSTITUTE OF TECHNOLOGY GUWAHATI, India A K Sharma and D S Gariya, AIRPORTS AUTHORITY OF INDIA , **Indian Patent No.** IN201831024409A, Filing Date: 2018-06-29, Publishing Date: 2020-01-03, **International Patent No:** WO2020003020A1, Filing Date: 2019-05-15, Publishing Date: 2020-01-02